SYNTHESIS OF FUNCTIONALIZED CATIONIC GLYCOLIPIDS FOR TARGETED DRUG DELIVERY

GOH EAN WAI

FACULTY OF SCIENCE
UNIVERSITY OF MALAYA
KUALA LUMPUR

2019

SYNTHESIS OF FUNCTIONALIZED CATIONIC GLYCOLIPIDS FOR TARGETED DRUG DELIVERY

GOH EAN WAI

THESIS SUBMITTED IN FULFILMENT OF THE REQUIREMENTS FOR THE DEGREE OF DOCTOR OF PHILOSOPHY

DEPARTMENT OF CHEMISTRY
FACULTY OF SCIENCE
UNIVERSITY OF MALAYA
KUALA LUMPUR

2019

UNIVERSITY OF MALAYA

ORIGINAL LITERARY WORK DECLARATION

Name of Candidate: **GOH EAN WAI**

Matric No: **SHC 140065**

Name of Degree: **DOCTOR OF PHILOSOPHY**

Title of Thesis ("this Work"):

SYNTHESIS OF FUNCTIONALIZED CATIONIC GLYCOLIPIDS FOR TARGETED DRUG DELIVERY

Field of Study: **ORGANIC CHEMISTRY**

I do solemnly and sincerely declare that:

(1) I am the sole author/writer of this Work;
(2) This Work is original;
(3) Any use of any work in which copyright exists was done by way of fair dealing and for permitted purposes and any excerpt or extract from, or reference to or reproduction of any copyright work has been disclosed expressly and sufficiently and the title of the Work and its authorship have been acknowledged in this Work;
(4) I do not have any actual knowledge nor do I ought reasonably to know that the making of this work constitutes an infringement of any copyright work;
(5) I hereby assign all and every rights in the copyright to this Work to the University of Malaya ("UM"), who henceforth shall be owner of the copyright in this Work and that any reproduction or use in any form or by any means whatsoever is prohibited without the written consent of UM having been first had and obtained;
(6) I am fully aware that if in the course of making this Work I have infringed any copyright whether intentionally or otherwise, I may be subject to legal action or any other action as may be determined by UM.

Candidate's Signature Date:

Subscribed and solemnly declared before,

Witness's Signature Date:

Name:

Designation:

SYNTHESIS OF FUNCTIONALIZED CATIONIC GLYCOLIPIDS FOR TARGETED DRUG DELIVERY

ABSTRACT

Amphiphilic glycolipids are known for their role in cellular recognition processes. This has created interest in using their assemblies, particularly vesicles, as drug carriers, because their strong intermolecular hydrogen bonding ensures high stability. Introduction of biological recognition domains onto the vesicular surface enables a targeting delivery of drugs to specific cells. This prevents unwanted interaction between the drug and non-target cells, thus minimizing drug's side effects. A series of functionalized glycolipids carrying CLICK functionality was prepared, which renders a bioconjugation opportunity with suitable antigens or targeting ligands under mild conditions. To ensure coupling efficiency, an ethylene oxide spacer was introduced between the CLICK functionality and the sugar head group to provide flexibility to the anchor. The incorporation of a quaternary ammonium cation, based on the Menshutkin reaction, gave rise to cationic character of the glycolipids. The electrostatic repulsion between these cations increased the hydrophilic surface area, thereby leading to an increased curvature in the assemblies and resulting in the formation of micellar aggregates in water instead of vesicles. All glycolipids exhibited very similar assembly behaviour, despite differing in the position of the functionalized linker on the sugar head group. Application of the compounds as co-surfactant for vesicle preparation furnished uniformly small-sized and stable vesicles, as indicated by their zeta potential.

Keywords: cationic glycolipids, CLICK, surfactant assembly, vesicle, drug delivery.

SINTESIS SEBATIAN GLIKOLIPID KATIONIK YANG DIFUNGSIKAN UNTUK PENGHANTARAN UBAT BERSASAR

ABSTRAK

Glikolipid yang bersifat *amphiphilic* dikenali dengan peranannya dalam proses pengecaman sel. Ini telah mencetuskan minat terhadap penggunaan perhimpunannya, terutamanya vesikel sebagai pembawa ubat atas sebab kestabilannya yang tinggi, disebabkan oleh pengikatan hidrogen antara molekul yang kuat. Pengenalan domain pengecaman biologi pada permukaan vesikel mengizinkan sistem penghantaran ubat yang menyasar, khususnya ke sel sasaran. Dengan itu, interaksi antara ubat dengan sel bukan sasaran dapat dielakan dan kesan sampingan ubat juga dapat dikurangkan. Satu siri glikolipid yang mengandungi fungsi KLIK telah dihasilkan dan ia telah mewujudkan peluang untuk biokonjugasi dengan antigen atau ligan yang menyasar dalan keadaan tindak balas yang sederhana. Untuk memastikan gandingan yang lebih efisien, penjarak berasaskan etilena oksida telah diperkenalkan di antara kefungsian KLIK dengan bahagian karbohidrat, supaya fleksibiliti dapat dibekalkan kepada sauh tersebut. Pencatuman kation ammonium kuaternan berdasarkan tindak balas *Menshutkin* telah menimbulkan sifat kationik dalam sebatian glikolipid tersebut. Penolakan elektrostatik antara kation ini telah meningkatkan luas permukaan hidrofilik dan menyebabkan kelengkungan dalam struktur perhimpunan glikolipid, serta mengakibatkan pembentukan agregat misel, bukannya vesikel di dalam air. Semua sebatian glikolipid mempamerkan perilaku perhimpunan yang agak sama, walaupun berbeza dalam kedudukan penyambung yang berfungsi di bahagian karbohidrat. Penggunaan sebatian glikolipid sebagai surfaktan sampingan telah pun berjaya menghasilkan vesikel yang bersaiz kecil dan stabil, dibuktikan melalui pengukuran potensi zeta tersebut.

Kata kunci: kationik glikolipid, KLIK, penghimpunan surfaktan, vesikel, penghantaran ubat.

ACKNOWLEDGEMENTS

This study would not have been possible without the help and support of several special people. Therefore, I would like to take this opportunity to thank those who assisted me throughout my study.

First and foremost, I would like to express my heartfelt gratitude to my supervisor Associate Professor Dr. Thorsten Heidelberg for his invaluable guidance, support and expertise throughout my PhD journey. Special thanks to Dr. Rusnah Syahila Binti Duali Hussen for her expert advices on this project. I also gratefully appreciate assistance and support from my friends, Dr. Mojtaba Tabandeh, Ng Su-Han, Olla Hassan Saleh Sharhan, Dr. Chong Kam Weng, Dr. Ng Zoe Yi and Joanne Yeap Soon Yee.

To my family, thank you for encouraging and supporting me in all my pursuits. I am especially grateful to my parents for showing faith in me and giving me liberty to follow my dreams. Also, great thanks to my sister and brother for their constant support through the ups and downs during my study.

Lastly, the financial support from University of Malaya in a form of scholarship (SBUM) is also gratefully acknowledged.

TABLE OF CONTENTS

LIST OF FIGURES

LIST OF SCHEMES

LIST OF TABLES

LIST OF SYMBOLS AND ABBREVIATIONS

°C	:	Degree Celsius
ζ	:	Zeta potential
Å	:	Angstrom
Ac	:	Acetate
ACN	:	Acetonitrile
Aq	:	Aqueous
a.u.	:	Atomic unit
$BF_3 \cdot OEt_2$	:	Boron trifluoride etherate
Bn	:	Benzyl
bs	:	Broad singlet
CAC	:	Critical aggregation concentration
Conc.	:	Concentrated
CAPB	:	Cocamidopropyl betaine
CPP	:	Critical packing parameter
CTAB	:	Cetyltrimethylammonium bromide
d	:	Doublet
dd	:	Doublet of doublet
DDS	:	Drug delivery system
DMF	:	N, N-dimethylformamide
DTAB	:	Dodecyltrimethylammonium bromide
EO	:	Ethylene glycol
Equiv	:	Equivalent
Ga	:	Gauge
IL	:	Ionic liquid

IR	:	Infrared
LC	:	Liquid crystal
m	:	Multiplet
N	:	Normality
NBS	:	N-bromosuccinimide
NCS	:	N-chlorosuccinimide
NMR	:	Nuclear magnetic resonance
OPM	:	Optical polarizing microscopy
PBS	:	Phosphate buffered saline
Pd/C	:	Palladium on activated charcoal
PLG	:	Pyrene-labelled glycolipid
PPh_3	:	Triphenyl phosphine
PPTS	:	Pyridinium *p*-toluenesulphonate
Py	:	Pyrene
*p*TsOH	:	Para-toluenesulphonic aicd
Rf	:	Retention factor
s	:	Singlet
SDS	:	Sodium dodecyl sulphate
t	:	Triplet
TBAB	:	Tetra-n-butylammonium bromide
TEA	:	Triethylamine
TFA	:	Trifluoroacetic acid
THF	:	Tetrahydrofuran
TLC	:	Thin layer chromatography
Ts	:	Tosyl
ZP	:	Zeta potential

LIST OF APPENDICES

CHAPTER 1: INTRODUCTION

1.1 Introduction

Side-effects of drugs result from undesirable interactions between the drugs and non-target cells that share similar biochemical processes with the target cell. They have become a major factor that narrows their therapeutic window and limits their clinical use (Botchkarev, 2003; Ramirez *et al.*, 2009). One common example is observed in the use of cytostatic drug in chemotherapy, which actively interferes the proliferation process of fast growing cells, particularly the cancerous cells (Schirrmacher, 2019). However, due to the lack of its targeting property, the drug also targets the other fast-growing healthy cells, like hair follicle cells.

The use of targeting vesicles is one promising drug delivery method to overcome the aforementioned problem. Their unique bilayer structures allow encapsulation of both lipophilic and hydrophilic active ingredients and avoids damage the drug by the biological defensive system (Elizondo *et al.*, 2011). Besides, the presence of specific biological recognition domain on the vesicular surface through introduction of the antigens or targeting ligands, enables an antigen receptor-mediated drug delivery system that prevents unwanted drug interaction with the non-targets, thus minimizing its side effects.

Carbohydrate-based surfactants or glycolipids, have gained growing interest for use in vesicle preparation, as they are biodegradable and biocompatible materials that can be derived from natural resources (Bazito & El Seoud, 2001; Esmaeilian *et al.*, 2018). In comparison with the phospholipid-based liposomes, which are the most investigated drug carriers (Allen & Cullis, 2013; Li *et al.*, 2015), glycolipid vesicles are more stable towards oxidation and hydrolysis (Grit & Crommelin, 1993; Akbarzadeh *et al.*, 2013). The polyhydroxyl head group of glycolipids not only contributes in the formation of stable assemblies, owing to their strong intermolecular hydrogen bonding (Li *et al.*, 2014;

Salman *et al.*, 2016), but also enables functionalization on the carbohydrate component (Dimakos & Taylor, 2018). Particularly interesting is the introduction of a functionality, which serves as docking site for bioconjugation with antigens or targeting ligands on vesicles, thus furnishing a biological recognition domain on a drug carrier to achieve receptor-antigen mediated targeted drug delivery. Thereby it minimizes side-effects of drugs by preventing unwanted interactions with non-target cells and significantly increases the drug concentration at the target site (Jones, 1994; Lukyanov *et al.*, 2004).

Clustering of the docking sites on a vesicular surface can restrain an efficient bioconjugation. This can be avoided by introducing ionic charges on the functionalized glycolipids that exhibit intermolecular electrostatic repulsion, thereby maintaining a reasonable distance between docking sites on the vesicular assembly. Besides, their ionic repulsion promotes the distribution of surfactants during vesicle formulation, thereby furnishing smaller-sized vesicles that can pass through small blood vessels (Bnyan *et al.*, 2018).

1.2 Objectives of Study

The objectives of this study are:

1. to synthesize and functionalize glycolipids with CLICK functionality.
2. to investigate the assembly and surface behaviour of functionalized glycolipids.
3. to investigate and characterize the vesicles formed by applying functionalized glycolipids as co-surfactants.

CHAPTER 2: LITERATURE REVIEW

2.1 Drug Delivery

2.1.1 Problems of Conventional Drugs

Concerning enteral and parenteral drug administration, the drug efficiency is strongly depending on its bioavailability. This is mainly governed by two factors, *i.e.* permeability and solubility of the drug. As the human body comprises of around 70 % water, low drug solubility in water will result in low dissolution rate, thereby impeding the rate of drug absorption. As a result, a higher drug dosage may be required in order to achieve the remedial effect (Jain *et al.*, 2015). Different approaches have been developed to resolve the drug solubility issue, such as ionization of drug molecules into salt (Agharkar *et al.*, 1976). Yet, there remains disadvantages, like instability of the drug salt and low dissolution rate due to the common-ion effect (Waterman *et al.*, 2002; Serajuddin, 2007). Moreover, these strategies are all still unable to achieve a high drug's efficacy, owing to their low capability of localizing and concentrating the drugs at the tissue of interest. This limitation has then fostered the efforts to develop suitable drug delivery systems to minimize side effects of the drug, on the other hand maximize this therapeutic effect on the target cells.

2.1.2 Concept of Drug Delivery

Drug delivery is a process whereby pharmaceutically active agents are administered to humans to achieve therapeutic effects (Maiti & Sen, 2017). Drug delivery system is a formulation applied to introduce a drug into the human body while maintaining its high efficacy by controlling the rate and location of its release (Allen & Cullis, 2004). This process typically involves administration and release of the therapeutic ingredients, followed by their transport across the biological membrane (Jain, 2008).

Advances in biotechnology and nanotechnology research have produced a great variety of novel drug delivery systems, in particular nano-scaled drug carriers to entrap drugs, thus providing protection for the drug throughout the delivery process (Jiang *et al.*, 2007). The remarkably small-sized drug carriers ensure access across biological barriers that are usually impermeable for big sized particulates (Lockman *et al.*, 2002). Some drug carriers, *e.g.* vesicles are able to undergo membrane fusion to release the active ingredients into the target cells owing to their similar bilayer structures (Yang *et al.*, 2016; Oshima & Sumitomo, 2017). The desirable pharmacokinetic of drugs can also be altered and adjusted by a modification of the surface of drug carriers, in order to meet the criteria of safe and effective therapy (Nguyen *et al.*, 2016).

2.1.3 Vesicular Drug Delivery

Vesicles are highly ordered assemblies, which result from self-assembling ability of amphiphiles in water, and consist of one or more lipid bilayers (Jain *et al.*, 2014). Generally, vesicles are classified according to the number of lamellae and their sizes, into small unilamellar vesicles (SUVs), multilamellar vesicles (MLVs) and large unilamellar vesicles (LUVs) as shown in **Figure 2.1**. They can be differentiated based on electron microscopy and dynamic light scattering (Hallett *et al.*, 1991; Pencer & Hallett, 2003; Bibi *et al.*, 2011; Ahmed *et al.*, 2015).

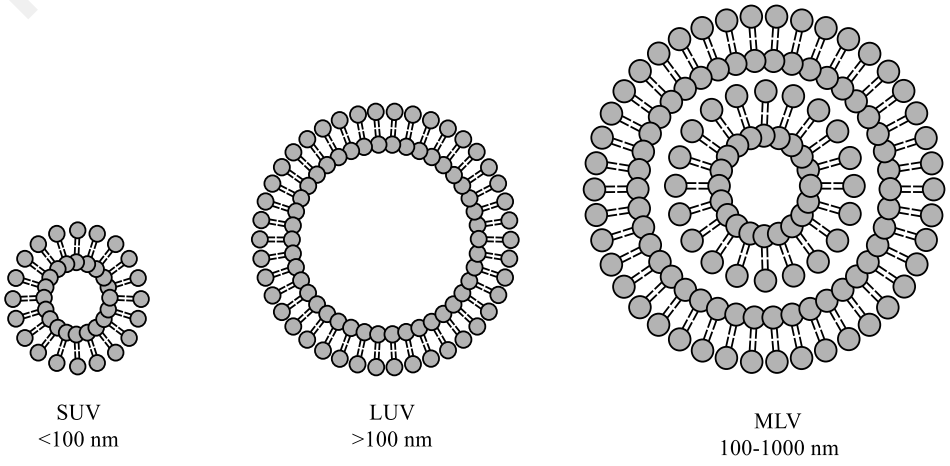

Figure 2.1: Vesicles of different diameter sizes and number of lamellae.

Vesicles have been gaining interest for application as drug carriers, owing to their unique bilayer structures that provide environments for the encapsulation of both lipophilic and hydrophobic drug molecules. They also serve as a protective layer to prevent and delay the metabolism of the drug, thereby improving the drug bioavailability at the target site (Jain *et al.*, 2014; Kalpesh *et al.*, 2014).

In search of a more efficient drug delivery system, surface modification of vesicles is usually targeted as the strategy to improve their physiological properties (Torchilin, 2006). Drug carriers are usually recognized as "foreign particles" and easily destroyed by the immune system. A strategy was found to improve the stability of vesicles by coating its surface. For example, vesicles coated with polyethylene glycol or polymeric glycolipids, like acylated chitosan were found to exhibit prolonged circulation time in blood, due to the increased hydrophilicity on the vesicular surface resulting from the polymeric coating. This prevents undesirable interactions between the vesicles and blood proteins like opsonins, which would possibly eliminate the vesicles by phagocytosis (Senior *et al.*, 1991; Allen, 1994; Roos *et al.*, 2004; Immordino *et al.*, 2006).

Visualization of the drug carriers in a biological system is also crucial, because it allows evaluation of the drug delivery efficiency based on the bio-distribution and target accumulation of the drug carriers. Gamma-scintigraphy and magnetic resonance are examples of the most commonly used medical imaging modalities. They apply a contrast agent that absorbs irradiations strongly, thus enhancing the radiopacity in the target tissue. Vesicles loaded or labelled with paramagnetic or radioactive contrast agents were found not only useful for the visualization of tissue which is rich in macrophages but they also demonstrated high efficiency in targeting regional lymph nodes (Patel *et al.*, 1984; Unger *et al.*, 1989; Phillips *et al.*, 2000; Cai *et al.*, 2011).

2.1.4 Targeting Vesicular Drug Delivery

Targeted drug delivery was introduced by Paul Ehrlich (Ehrlich, 1960) who referred antibodies as "magic bullets" that selectively target the disease-causing organisms, consequently enabling selective delivery of the toxin to the organism (Tan & Grimes, 2010; Kamboj *et al.*, 2013). Unlike the conventional drug delivery system, targeted drug delivery allows site-specific delivery of medication through recognition and interaction of the drug carriers with the target cells (Poste & Kirsh, 1983; Mishra *et al.*, 2016). This approach not only provides a better drug efficacy, but also avoids the uptake of drug by non-target cells, thus minimizing the side-effects of drug that appear as one of the major drawbacks in the conventional drug delivery system. As illustrated in **Figure 2.2**, passive and active targeting are the two most commonly known strategies in drug targeting delivery. The former is commonly referred as Enhanced Permeability and Retention effect, which is based on the drug accumulation at the target sites (Nichols & Bae, 2014), whereas, active targeting involves specific ligand-receptor interaction between drug carriers and target cells (Poste & Kirsh, 1983; Mishra *et al.*, 2016). This can be achieved by coupling the carriers with specific targeting ligands or antigens. The latter enable the selective binding of the carrier to the specific surface molecule on the target cell, such as receptors, followed by the release of the active ingredients through biological active transport or membrane fusion. For example, the glycoprotein transferrin was employed as targeting ligand on the vesicular surface for selective delivery of drug to tumour cells (Hatakeyama *et al.*, 2004).

Despite the presence of targeting ligands, non-specific adsorption of the vesicles to other cells, especially reticuloendothelial cells, appears to be another barrier preventing vesicles from reaching the target site. This led to the suggestion of multifunctional drug carriers with combined properties as shown in **Figure 2.3**. The idea was clearly demonstrated by Lukyanov and his co-workers, who created vesicles exhibiting both long

circulating and targeting properties and used them for selective delivery of doxorubicin to tumour cells (Lukyanov *et al.*, 2004). However, in some cases polymeric coating precluded the releasing of the drug at the target cells. Consequently, it requires the introduction of a labile linkage, such as ester between the vesicular surface and the polymer, to facilitate detachment of the latter in response to particular stimuli, such as pH changes (Roux, Francis*, et al.*, 2002; Roux, Stomp*, et al.*, 2002).

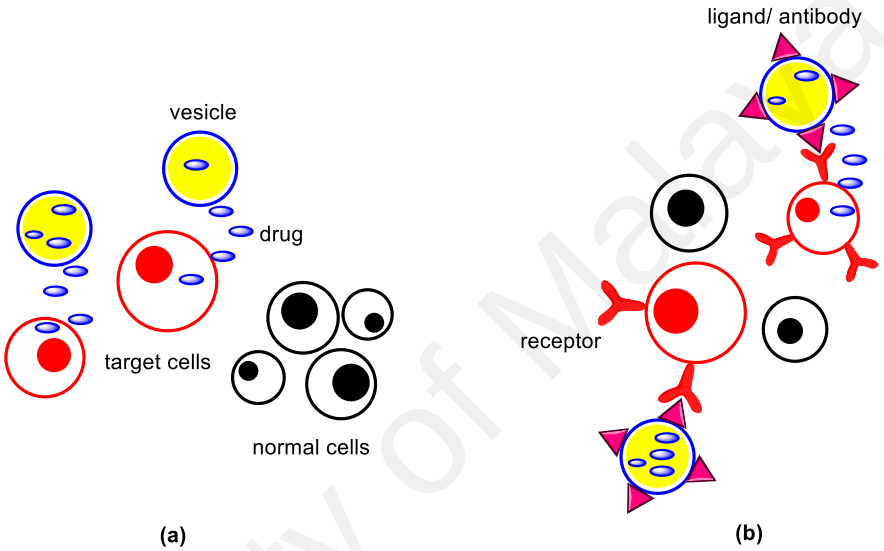

Figure 2.2: Schematic illustration of (a) passive targeting and (b) active targeting.

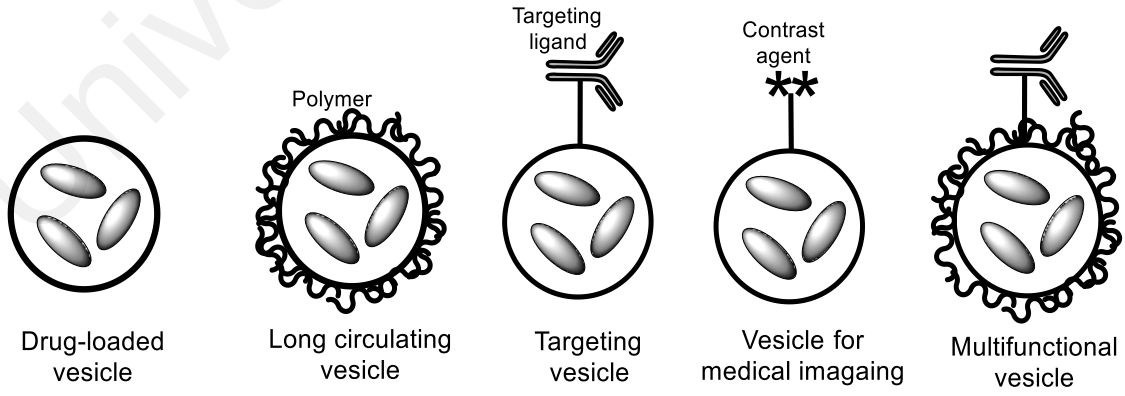

Figure 2.3: Surface modification of vesicles.

2.2 Surfactants, Self-assemblies and Vesicles

2.2.1 Microseparation Creates Assemblies

Classical assemblies result from their closest packing, in which the elongated and linear molecules that resemble a rod-like structure, are closely packed in an ordered way. They exhibit liquid-like fluidity owing to their intramolecular mobility, caused by the rotational freedom around the molecular axes (Demus, 1994). Glycolipid-based assemblies, on the other hand, originate from microphase separation of two incompatible molecular regions, *i.e.* the hydrophilic (polar) sugar head group and the lipophilic (non-polar) chain of a glycolipid molecule (Vill & Hashim, 2002; Goodby *et al.*, 2006; Hashim *et al.*, 2018). These two domains segregate from one another; while the sugar units are interacting by hydrogen bonding, van der Waals forces dominate the lipophilic chains region. The driving force of the separation is the optimization of hydrogen bonding, which would be distributed without domain separation and it is known as the hydrophobic effect (Lindman, 2002; Maibaum *et al.*, 2004).

2.2.2 Assembly Types and Geometry

The critical packing parameter (CPP) was introduced by Israelachvili to explain the geometry of self-assembled structures formed by amphiphiles based on their molecular shape (Cullis *et al.*, 1986; Israelachvili, 1992). It takes into account the volume of the hydrophobic region (v), the effective interphase area of the hydrophilic domain (a_o) and the length of the fully extended hydrophobic chain (l_c) as shown in the following equation (Israelachvili, 1992; Butt *et al.*, 2003).

$$\mathrm{CPP} = \frac{v}{a_0 l_c} \tag{2.1}$$

As illustrated in **Table 2.1**, amphiphiles with a CPP less than 1/3 resemble conical shapes that prefer to form micelles. To maximize the overall packing, these ball-shaped micelles can be arranged in a cubic face-centred lattice, thereby leading to the formation

of a discontinuous cubic phase. Another type of cubic phase is the bicontinuous cubic phase, in which a continuous bilayer separates the space into two continuous and intertwined networks (Sakya *et al.*, 1997; Takeuchi *et al.*, 2016). Glycolipid bicontinuous cubic mesophases are rarely found in a thermotropic system, but commonly developed at the borderline between the lamellar and hexagonal phases in a lyotropic system. The bicontinuous cubic phase is attributed with biological relevance, especially for membrane fusion processes (Nieva *et al.*, 1995; Demurtas *et al.*, 2015) and sustainable drug delivery (Rizwan *et al.*, 2010). This explains the great interest that it receives for pharmaceutical applications, like for sustained drug delivery systems (Shah *et al.*, 2001; Chen *et al.*, 2014; Nazaruk *et al.*, 2015). Amphiphilic molecules with a CPP value between 1/3 and 1/2 usually adopt a truncated cone-liked shape, resulting in stacking of these molecules in a hexagonal array reflecting the hexagonal or columnar phase. This phase is also of great interest for drug delivery applications. (Manaia *et al.*, 2015).

When the CPP falls between 1/2 and 1, a balance is achieved between the hydrophilic and hydrophobic regions, thus the amphiphiles resemble rod-like shapes that preferably form a planar bilayer or the lamellar phase. The bilayer-based lamellar assembly provides high potential for the formation of vesicles, which allow drug uptake by the target cell via a membrane fusion process (Cevc & Richardsen, 1999; Demé *et al.*, 2002). The previously discussed LC phases are all normal types, whereas inverse LC phases are formed only if the CPP is greater than 1 as shown in **Figure 2.4** and **Table 2.1**. This type of molecule forms a structure in which the inner discontinuous region consists of hydrophilic head groups, while the hydrophobic chains form the outer continuous domain layer of the aggregate.

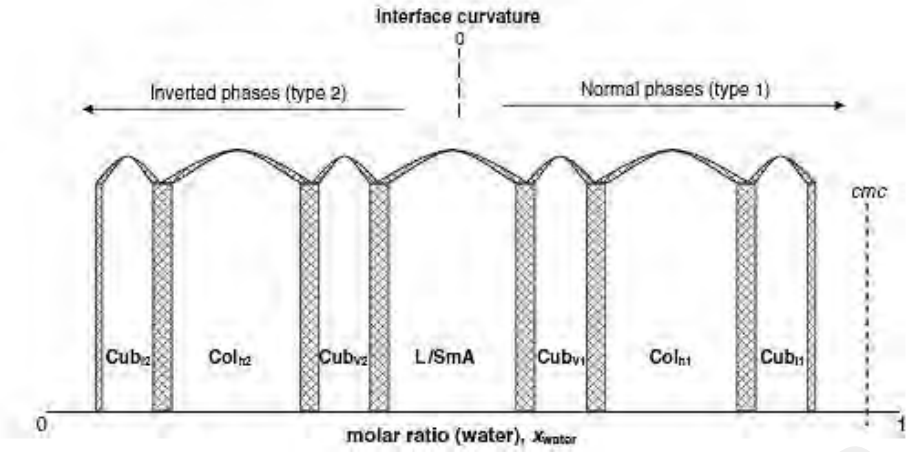

Figure 2.4: Types of lyotropic LCs.

Table 2.1: Relation between CPP and packing structure.

		Packing shape	Structure formed	
Micelle	CPP ≤ 1/3	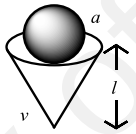	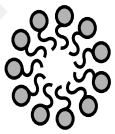	Sphere
	1/3< CPP ≤ 1/2	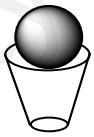	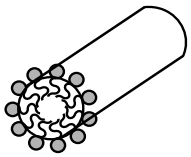	Cylinder
Liquid crystal	CPP ≤ 1/3	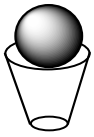	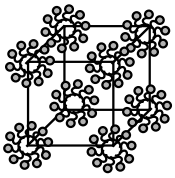	Discontinuous cubic
	1/3< CPP ≤ 1/2	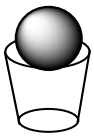	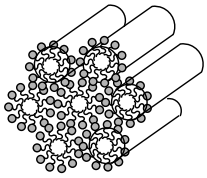	Hexagonal
	1/2< CPP ≤ 1		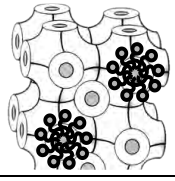	Bicontinuous cubic

Table 2.1, continued

Liquid crystal	CPP ≈1	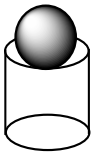	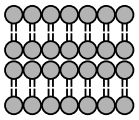	Lamellar
	1 < CPP	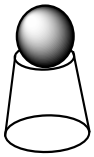	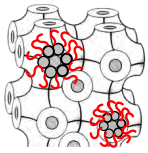	Inversed bicontinuous cubic
			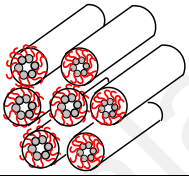	Inversed hexagonal
			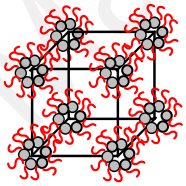	Inversed discontinuous cubic
Inversed micelle	1 < CPP	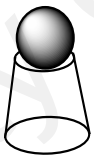	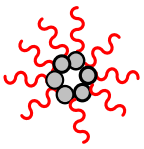	Sphere

2.2.3 Liquid Crystal

A liquid crystal (LC) is a liquid-like matter possessing remaining degrees of orientational order similar to a crystalline solid. It was discovered by the botanist Friedrich Reinitzer in the year 1888. During his experiments on a cholesterol-based material he observed two melting points, which later being classified as the melting and clearing point respectively (Reinitzer, 1888). The intermediate state after the first melting appeared as a cloudy liquid and was termed as liquid crystal by the physicist Otto Lehmann (Lehmann, 1889; An *et al.*, 2016).

LCs are categorized into two main groups, *i.e.* thermotropic and lyotropic LCs. The former is formed by pure compounds upon change of temperature, while the latter is developed owing to the strong interaction of molecules with a solvent. For glycolipids, this is usually water, which can lead to an increased cross-sectional area of the hydrophilic sugar head groups owing to hydration based on strong hydrogen bonding with water molecules (Goodby *et al.*, 2014; Garidel *et al.*, 2015). Amphiphilic glycolipids are able to show both thermotropic and lyotropic LCs, thus they are also known as amphotropic compounds (Demus, 1994; Tschierske, 2002; Hashim *et al.*, 2018). Although the assembly geometries are very similar, different nomenclatures are applied for thermotropic and lyotropic LCs, as listed in the **Table 2.2** (Luzzati & Husson, 1962; Brooks *et al.*, 2011).

Table 2.2: Nomenclature of thermotropic and lyotropic mesophases.

Thermotropic		Lyotropic	
Bicontinuous cubic	Cub_{bi}	Bicontinuous cubic	Normal, V_1 Inverse, V_2
Discontinuous cubic	Cub_{dis}	Discontinuous cubic	Normal, I_1 Inverse, I_2
Columnar	Col	Hexagonal	Normal, H_1 Inverse, H_2
Smectic A	S_A	Lamellar	L_α
Smectic C	S_C	Gel	L_β
Isotropic	Iso	Micellar	Normal, L_1 Inverse, L_2

Determination and characterization of LC phases involve several physical techniques, such as differential scanning calorimetry (DSC), which provides information about phase transition and related enthalpy changes, small-angle X-ray scattering (SAXS), by which the types of LCs can be identified based on the scattering patterns, and

optical polarizing microscopy (OPM) (Garidel *et al.*, 2015; An *et al.*, 2016). The latter was employed in this study for identifying the anisotropic LC phases exhibited by the glycolipids. Anisotropic LC shows birefringent property, which refers to its ability to refract the incident light (in a direction different to the LC's optical axis) into two different directions, thus leading to a texture that can be seen under the microscope (An *et al.*, 2016).

Glycolipids self-assemble into various LC phases, such as hexagonal or columnar phases and lamellar or smectic phases. They are typically birefringent and form characteristic textures under the polarizing microscope (Saupe, 1977; Hindi, 2016). Amongst them, cubic phases are not birefringent and hence are observed as a dark band owing to their isotropic behaviour (Garidel *et al.*, 2015). However, they exhibit higher viscosity than the usual isotropic liquids.

2.2.4 Vesicles Formulation Strategies

A variety of methods to prepare vesicles has been introduced since the first reported lipid-based vesicle (Bangham *et al.*, 1965). The shape of the vesicles in terms of sizes and number of lamellae depend on the method of preparation. MLVs are easiest to prepare; simple hydration of a thin lipid film deposited on the wall of a round bottom flask with aqueous buffer can provide the vesicles. To obtain smaller sized MLVs, techniques such as membrane filtration (Olson *et al.*, 1979; Tamba *et al.*, 2011) that separates the giant lipid vesicles and vigorous shearing using a vortex stirrer can be applied. However, MLVs usually show lower encapsulation capacity than unilamellar vesicles of comparable size due to their multi-bilayer structures (Szoka & Papahadjopoulos, 1980; Xu *et al.*, 2012).

Unilamellar vesicles can be obtained by breaking down the structure of MLVs with the aid of mechanical forces, such as sonication. Yet, the use of sonication can cause

lipid degradation and metal contamination from the sonicator's probe tip (Varshosaz *et al.*, 2003). Therefore, several other methods have been introduced to address the aforementioned problems. For example, French press extrusion is a non-destructive method, whereby SUVs are produced by injecting a lipid suspension through a small orifice under high pressure (Hamilton *et al.*, 1980; Wagner & Vorauer-Uhl, 2011). Ethanol injection is another approach based on solvent dispersion. It involves injection of an ethanolic lipid solution into an aqueous phase through a small needle hole (Batzri & Korn, 1973). This method appears to be relatively simple and fast for vesicle preparation in laboratory scale, compared to others, *e.g.* the detergent removal method (Kagawa & Racker, 1966; Schurtenberger *et al.*, 1984; Schubert, 2003). Whereas, LUVs are formed based on the fusion of SUVs through a freezing-thawing process (Pick, 1981; Traïkia *et al.*, 2000).

2.2.5 Classification of Surfactants

Surfactants are amphiphiles that can reduce the interfacial surface tension, like interface between air and a liquid. They are classified according to their hydrophilic domain as shown in **Figure 2.5**.

Non-ionic surfactants carry no electrical charge. Their hydrophilicity is due to the presence of highly polar groups, such as polyols. Unlike for ionic surfactants, assemblies of non-ionic surfactants are stable towards pH changes and resistant to water hardness deactivation (Danby *et al.*, 2018). For example, esters of long chain fatty acid are edible and they possess good emulsifying properties, which making them useful emulsifiers in food and pharmaceutical industries (Spernath *et al.*, 2002). Alkyl glycoside is another example of non-ionic surfactants, which has been used for drug carriers owing to its biocompatibility (Kiwada, Niimura, Fujisaki*, et al.*, 1985; Aulmann & Sterzel, 1997).

Anionic surfactants possess negatively charged hydrophilic groups, such as carboxylate ($-COO^-$), sulphate ($-SO_4^{2-}$) and sulphonate ($-SO_3^-$). They are the most economic surfactants (Butt *et al.*, 2003) and are commonly used in cleanser or detergent formulation, owing to their good foaming and cleaning properties (Draelos, 2018). However, anionic surfactants are unstable below pH 7, where the anionic head groups are prone to be acidified, thus losing their ionic character. The most common examples are sodium dodecyl sulphate (SDS) and sodium stearate.

Cationic surfactants are usually amines or ammonium salts. Unlike anionic surfactants, cationic surfactants are ineffective agents for cleansing purpose (St. Laurent *et al.*, 2007), but they are used as oral disinfectants, antiseptics and sanitizers (Madunić-Čačić *et al.*, 2008), owing to their good bactericidal properties (Kamboj *et al.*, 2012; Inácio *et al.*, 2016). Most of the cationic surfactants are sensitive towards high pH, except for quaternary ammonium salts (Rosen, 2004), such as N-alkyltrimethylammonium chlorides and N-alkylimidazoline that are used as emulsifiers in acidic emulsions (Porter, 1991; Barney *et al.*, 2006).

Zwitterionic surfactants bear both negative and positive charges at their isoelectic points. They show anionic properties at high pH and cationic properties at low pH. The negative part is either a carboxylate or sulphate, while the positive part is made of an ammonium cation. Zwitterionic surfactants, such as betaines and N-alkyl amino acids, are frequently used in personal care products, like shampoos, owing to their mild characteristics, like low skin and eye irritation (Trüeb, 2007; Tadros, 2014).

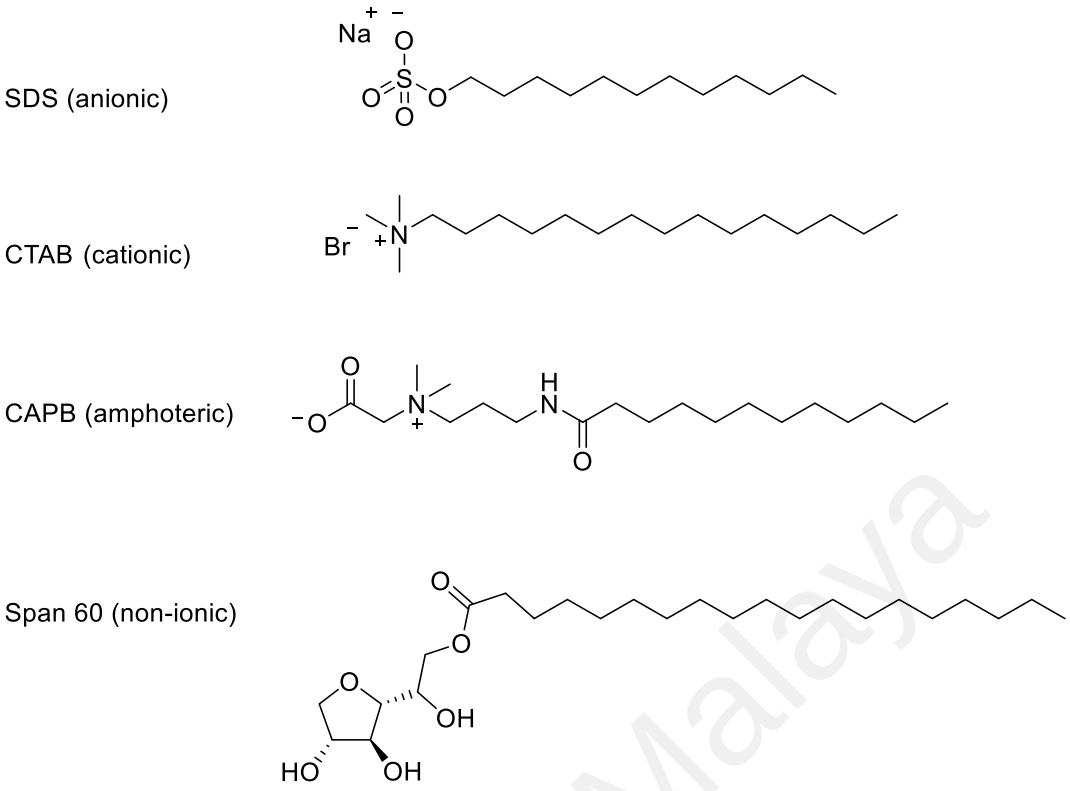

Figure 2.5: Four major types of surfactants.

2.3 Glycolipids

Glycolipids are carbohydrate-based surfactants that belong to the glycoconjugate family, comprising of other biogenic substances, such as glycoproteins, glycopeptides, lipopolysaccharides and peptidoglycans. Their peculiar amphiphilic structure allows them to self-assemble into supramolecular complexes, like micelles, based on the hydrophobic effect (Dowhan *et al.*, 2008). Glycolipids can be classified in many different ways, yet the primary way is based on the aglycon or the lipid part. As shown in **Figure 2.6**, glycolipids attached to a glycerol backbone belong to glycoglycocerolipids, while those with sphingosine or ceramide are classified as glycosphingolipids (Kopitz, 2009). Glycophospholipids are phosphorylated diglycerides in which the phosphoric acid is also esterified with the anomeric hydroxyl group of a carbohydrate (Takahashi *et al.*, 2012).

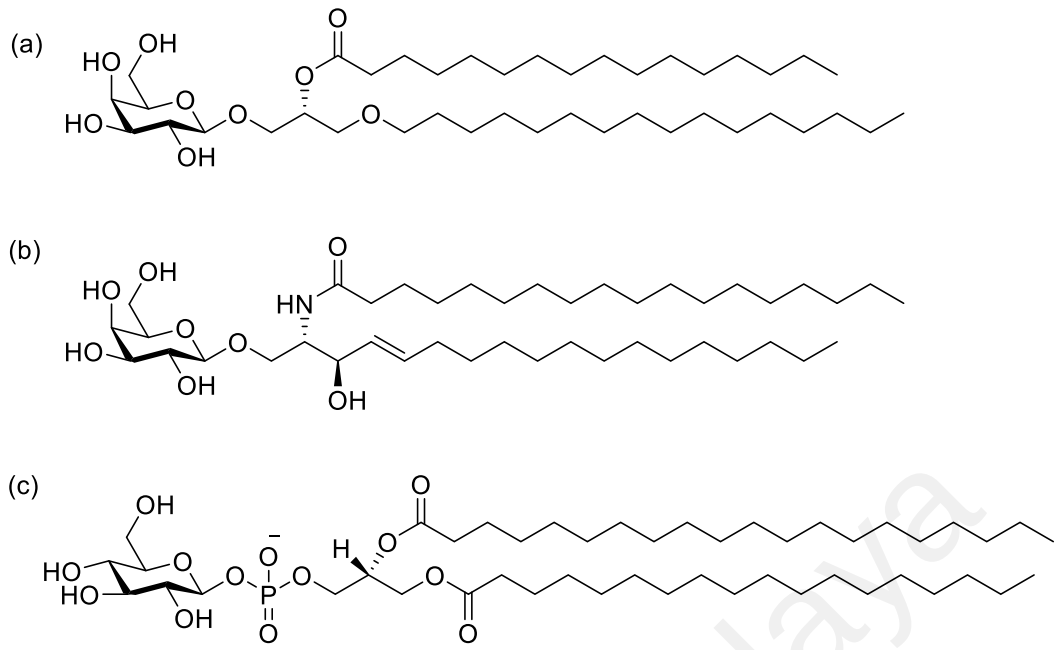

Figure 2.6: (a) Glycoglycocerolipid, (b) glycosphingolipid and (c) glycophospholipid.

Alkyl glycoside are synthetic glycolipids, in which a hydrophobic alkyl chain is attached to the reducing end of a carbohydrate. Industrial manufacture of alkyl glycosides usually results in a complex mixture of alkyl mono-, di- or oligoglycosides, therefore they are also known as alkyl polyglucosides (APGs). Alkyl glycosides have been used for various surfactant applications owing to their good surface active properties and high stability towards hydrolysis, especially in basic media (von Rybinski & Hill, 1998; El-Sukkary *et al.*, 2009). The first alkyl glucoside of simple structure was reported by Emil Fischer around the year 1900. He and Helferich successfully synthesized the first long-chain glucosides (Fischer, 1893; Fischer & Helferich, 1911).

2.3.1 Classification of Glycosides

Chemical syntheses of glycosides typically involve a nucleophilic reaction at the activated anomeric centre of sugar (Brito-Arias, 2007; Nicotra *et al.*, 2007). The type of nucleophiles, also termed as aglycone, determines the glycoside formed. They are classified according to the atom that is attached to the sugar; there are four types, referring to *N*-, *C*-, *O*- and *S*-glycosides. Examples of glycosides are shown in **Figure 2.7**.

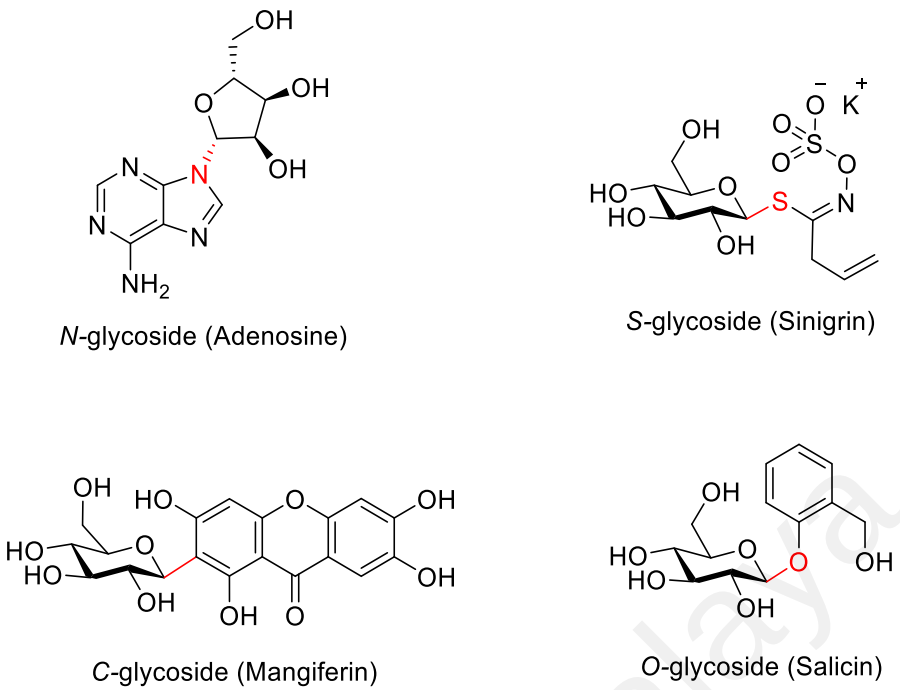

Figure 2.7: Examples of natural occurring glycosides.

O-glycosides are widely distributed in plants as secondary metabolites (Singh, 2016), *e.g.* flavonol glycosides, while nucleosides are well-known examples of *N*-glycosides that are essential building blocks of many biomolecules, such as DNA and RNA(Shabarova & Bogdanov, 1994; Boschi-Muller & Motorin, 2013). *C*- and *S*-glycosides are relatively rare compared to the others. Yet, they have been gaining increasing interest for potential application as glycomimetic or anticancer drugs, owing to their metabolic stability (Driguez, 1998; Buqui *et al.*, 2015) and anticancer properties (Herscovici *et al.*, 1991; Talalay, 1999; Sánchez-Fernández *et al.*, 2010). However, both *C*- and *S*-glycosides are not suitable for this study in view of the chemical stability of the C-C and C-S linkages, which affects the biodegradability of the glycolipids.

2.3.2 Biological Functions of Glycolipids

Significant developments in glycolipid research have revealed the crucial roles of glycolipids in many life processes. For example, monogalactosyldiacylglycerol (MGDG),

found abundantly in the thylakoid membrane of all photosynthesis performing organisms, stabilizes and maintains the flexibility of quinone, an essential electron receptor for the photosynthesis process (Dowhan *et al.*, 2008). On the other hand, glycopeptidolipids (GPL), a structural element found in the cell wall of mycobacteria, are responsible for preserving its rigidity (Brandenburg & Holst, 2015).

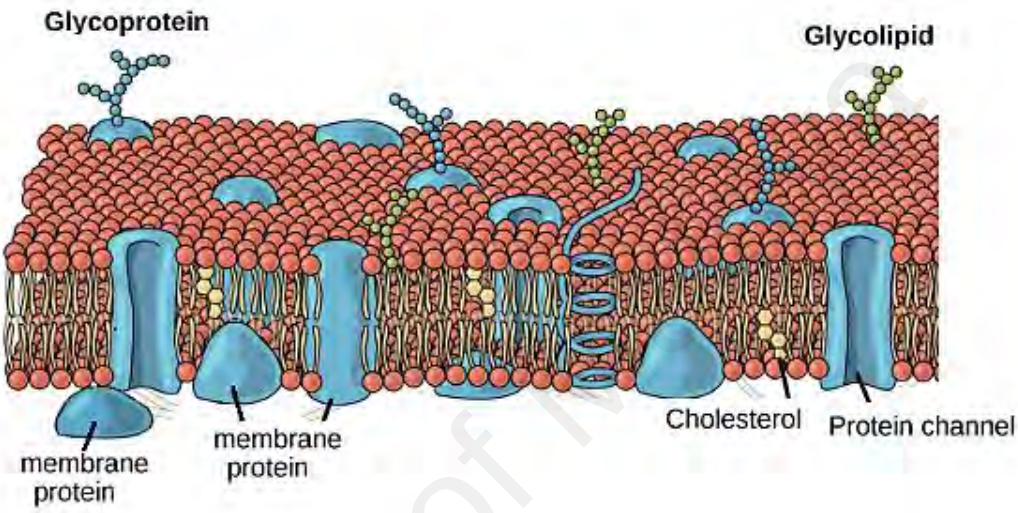

Figure 2.8: Fluid mosaic model of plasma membrane. Modified from: https://tophat.com/marketplace/science-&-math/biology/textbooks/oer-openstax-biology-openstax-content/79/4108

Figure 2.8 shows the orientation of glycolipid in the membrane bilayer, in which the amphiphilic structure is responsible for the extracellular facing carbohydrate while the lipid chain is embedded in the membrane bilayer, thereby building the glycocalyx, a common protective layer found in most bacteria (Merrill *et al.*, 2007). Another type of glycolipid, glucosylceramides, is found profusely in the skin and is vital to maintain the water permeability (Squier *et al.*, 1991).

Besides the significant contribution in structural support as the lipid component of the plasma membrane, recent studies have also revealed the active involvement of glycolipids in various cellular functions, such as signal transduction, modulation of immune system and cellular interaction. This was particularly observed in the studies of

T-cell activation mechanism, which involves the interaction between bacterial glycolipids and CD1, a major histocompatibility complex protein. This complex is then bound to T-cell receptor and triggers the corresponding immune responses (Moody & Besra, 2001).

The assembly of glycosphingolipids (GSLs) within the cell membrane forms lipid rafts' microdomains, which act as specific target sites for various transmembrane proteins and regulate the activity of raft proteins (Lucero & Robbins, 2004). In addition, GSL microdomain was found involving in signal transduction at the cell surface, through binding of specific ligand to the domain, thereby causing structural changes across the cell membrane. This induces the activity of intracellular signal transducers and likely triggers intracellular signalling cascades, thereby resulting in regulation of cellular events, such as cell proliferation, differentiation and apoptosis (Simons & Toomre, 2000).

2.3.3 Glycolipids for Drug Delivery

Glycolipids have been gaining increasing interest as material for drug delivery, replacing commonly used surfactants, like ethylene oxide based surfactants and phospholipids, because they are competitively amphiphilic, biodegradable and biocompatible. Unlike liposomes by phospholipids, glycolipid based assemblies are more stable due to the presence of hydroxyl groups that contribute in forming attractive hydrogen bonding with the neighbouring carbohydrate head groups, and their biological roles in cellular communication and recognition can also be adopted to promote bioadhesion of the carriers in drug delivery (Brandley & Schnaar, 1986; Faivre & Rosilio, 2010). In addition, the presence of the unsaturated bond in the fatty acid renders the phospholipid susceptible to oxidation, which potentially leads to a structural disruption of the liposome (Araseki *et al.*, 2002). Remarkably, glycolipid-based drug carriers have also shown higher encapsulation efficiency and better stability in plasma solution than

liposomes (Kiwada, Niimura, Fujisaki*, et al.*, 1985; Faivre & Rosilio, 2010; Salim *et al.*, 2015).

Glycolipids exhibit effective surface properties that can be varied by altering the hydrophobic chain length and the number of carbohydrate moieties. In view of their noteworthy lyotropic properties, glycolipids have been specially designed and modified to give interesting self-assemblies that lead to the formation of nanostructured particles or micro-emulsions, which have potential to be used for drug delivery purpose (Uchegbu & Vyas, 1998; Abd-Elbary *et al.*, 2008; Faivre & Rosilio, 2010). A remarkable research work by Lee and his colleagues has even demonstrated that glycolipids based micro-emulsions not only showed better drug solubilization, but also induced less pain upon injection in comparison with the other commercially available dosage forms (Lee *et al.*, 2002).

Besides of their application as drug carriers, glycolipids have been used as targeting ligands for surface modification of the drug carriers to promote specific interactions with the target cells or tissues. For instance, mannosylated liposome, formulated by Minakshi Grag, was used for targeted delivery of stavudine, a common drug used for treating human immunodeficiency virus (HIV) via specific protein-carbohydrate interaction. This formulation has shown improved cell uptake and increased mean residence time of the drug, thereby reducing the required drug dosage and minimizing side effects of the drug (Garg *et al.*, 2006). The distinctly high uptake and retaining of galactose in liver was also used as a measure for hepatocytes-targeted drug delivery by applying alkyl galactoside based vesicles (Kiwada, Niimura, & Kato, 1985; Coelho *et al.*, 2015).

2.4 Synthesis of Glycolipids

Biological glycolipids are produced based on a highly stereospecific enzymatic reactions and their isolation process is usually tedious. Considering the high manufacturing cost of natural glycolipids, alkyl glycosides, which are much more easily accessible based on organic synthesis, are more practical base material for the current study.

2.4.1 Glycosylation

A glycoside is a cyclic acetal, in which an aglycone moiety is bound to the anomeric centre of a sugar. The chemical procedure involved is known as glycosylation. In biological systems, enzymes, typically glycosyltransferases mediate the glycolipid biosynthesis by attaching glycans to other organic molecules, such as ceramides (Malhotra & Kumar, 2010). There is a few classes of glycosides, yet only *O*-linked glycosides will be discussed based on the target of this research.

The very first chemical glycosylation was reported in year 1879 by an organic chemist named Michael Arthur who successfully demonstrated an anomeric substitution on a glycopyranosyl halide to an aryl glycoside, as shown in **Scheme 2.1** (Michael, 1881).

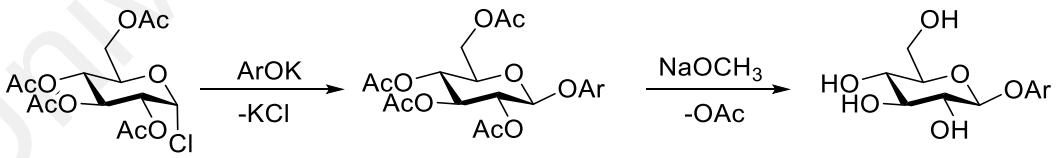

Scheme 2.1: Michael glycosylation.

In 1893, Emil Fischer established a very distinct synthetic approach, which applied unprotected monosaccharides as the starting materials. The reaction was carried out under harsh acidic conditions in the presence of excess alcohol as glycosyl acceptors

to furnish a complex mixture of pyranosides and furanosides, as illustrated in **Scheme 2.2** (Fischer, 1893; Fischer & Beensch, 1894; Bishop & Cooper, 1962). His findings inspired the use of hydroxyl protecting groups to prevent interconversion between furanosides and pyranosides during the glycosylation.

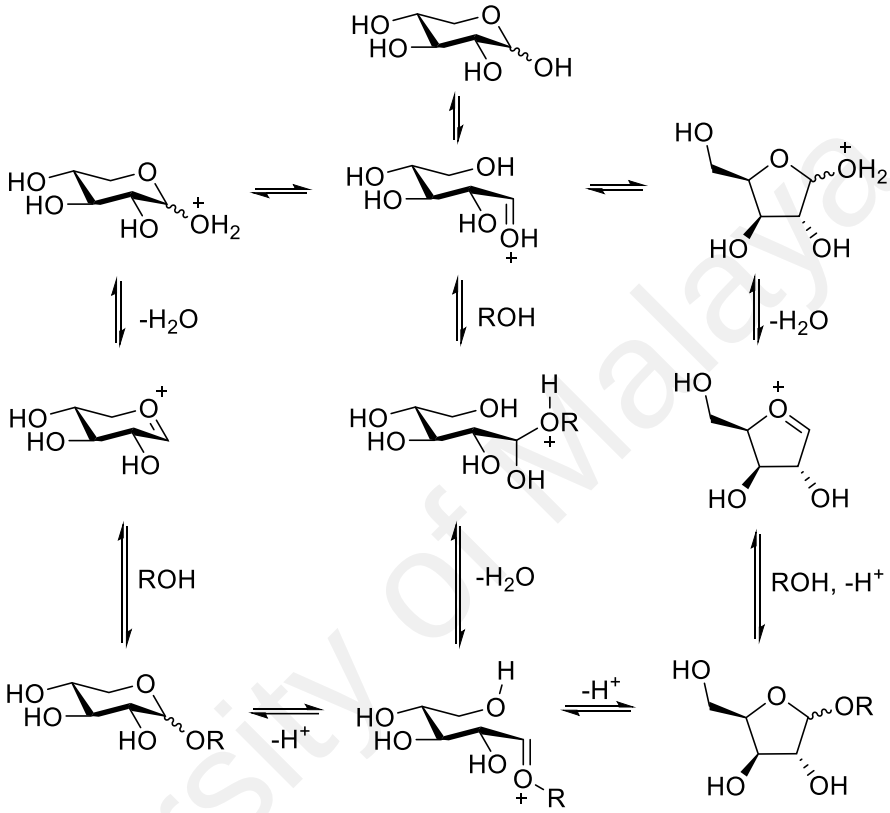

Scheme 2.2: Fischer glycosylation.

In 1901, Koenigs and Knorr reported another approach of chemical glycosylation, whereby glycosyl halides were reacted with glycosyl acceptors in the presence of silver carbonate or silver oxide as scavenger for the hydrogen halide by-product (Koenigs & Knorr, 1901). The Koenigs-Knorr glycosylation usually showed a complete inversion of the anomeric configuration in the product and the reaction was hence assumed to proceed via Walden inversion *i.e.* a concerted nucleophilic substitution mechanism as indicated in **Scheme 2.3**.

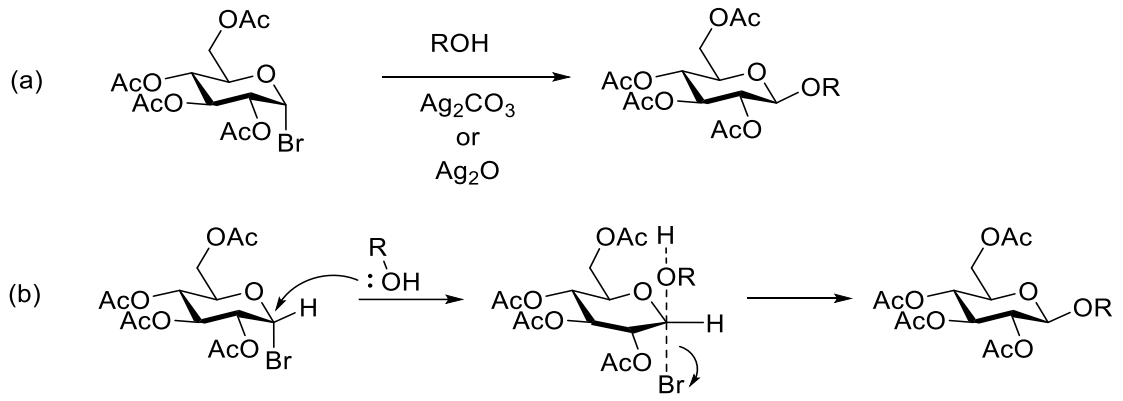

Scheme 2.3: (a) Koenigs-Knorr glycosylation; (b) Walden inversion.

However, further mechanistic studies by Pigman and Isbell rejected the Walden mechanism. Instead the inversion of the anomeric configuration was attributed to the participation of a neighbouring group effect at position C-2. Either a normal glycoside or an orthoester can be obtained, depending on the experimental conditions employed for the glycosylation reaction as illustrated in **Scheme 2.4** (Isbell, 1940).

A variety of glycosylation reactions applying various activated glycosyl donors, such as thioglycosides (Veeneman *et al.*, 1990; Krag *et al.*, 2010), glycosyl trichloroacetimidates (Schmidt & Michel, 1980; Minamikawa *et al.*, 1994; Das & Mukhopadhyay, 2016) and n-pentenyl glycosides (Mootoo *et al.*, 1988; Fraser-Reid *et al.*, 1993; Cristobal Lopez *et al.*, 1995; López *et al.*, 2007) has been reported. Ester glycosylation (**Scheme 2.5**) is amongst the most commonly used method to prepare glycoside. It employs an anomeric acetate as the glycosyl donor and a Lewis acid catalyst, such as borontrifluoride to furnish both α- and β-anomeric glycosides. The ratio of which can be controlled based on the catalyst used and the reaction time (Lemieux & Shyluk, 1953; von Minden *et al.*, 2000; Milkereit *et al.*, 2005).

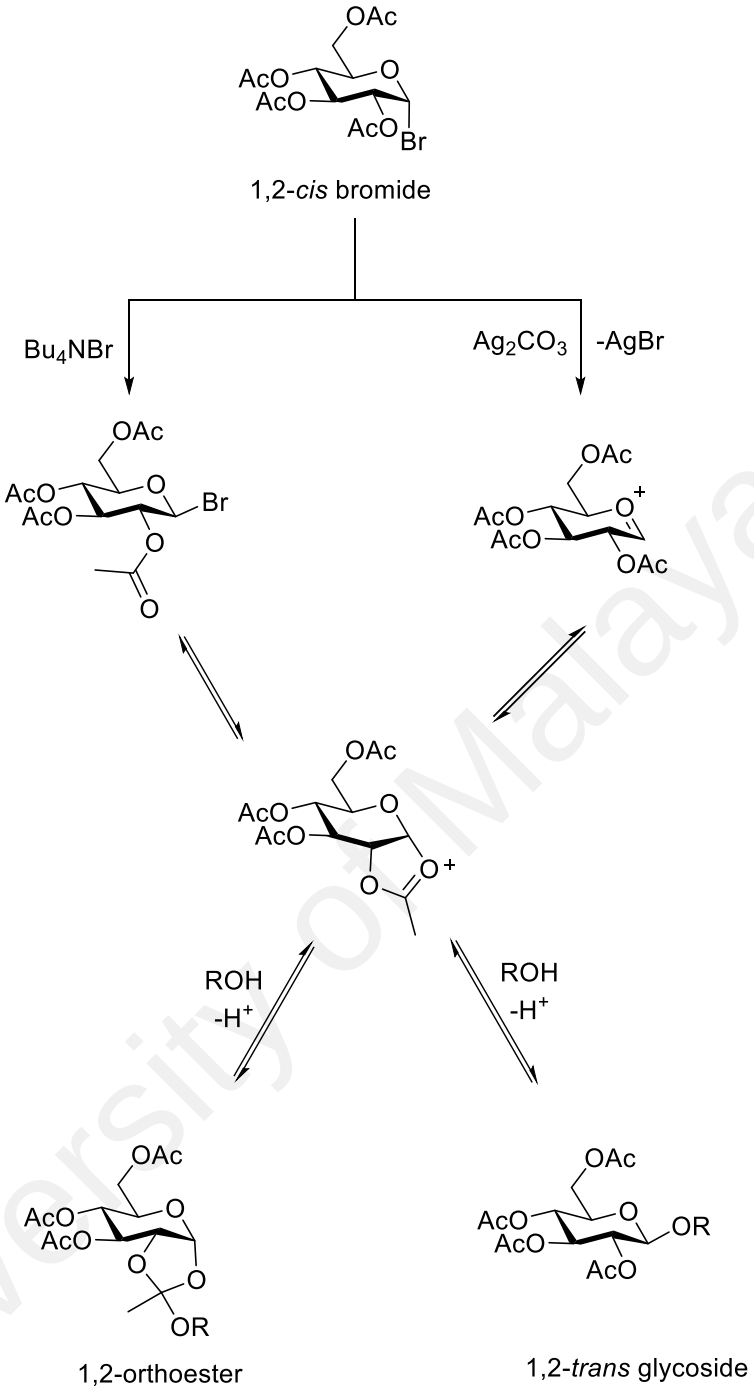

Scheme 2.4: Neighbouring group effect.

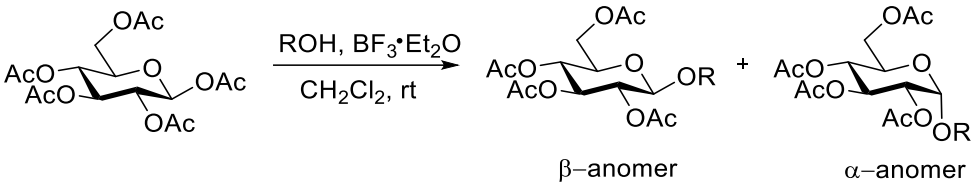

Scheme 2.5: Ester glycosylation.

Further studies on the anomeric reactivity revealed an unconventional inclination towards formation of the α–anomeric product due to the anomeric effect, which can be explained in terms of dipole moments. The anomeric C-O bond of the β-anomer is in equatorial orientation, as depicted in **Figure 2.9**. The lone pairs of electrons on the ring oxygen and the anomeric C-O bond add up to a large dipole moment, which destabilizes the β-anomer. In the α -anomer, the two dipole moments partially compensate each other, resulting in a more favourable small dipole moment (Mydock & Demchenko, 2010).

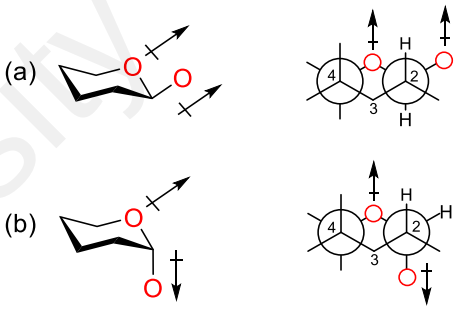

Figure 2. 9: Anomeric effect.

2.4.2 Protecting Group Strategies

Regioselectivity has always been a great challenge in carbohydrate chemistry, due to the presence of several hydroxyl groups of different reactivity that necessitates the application of suitable protecting group strategies to inhibit the participation of non-target hydroxyl groups. Differences in the reactivity of the hydroxyl groups form the basis of regioselective protections, such as the formation of a benzylidene acetal selectively

blocking the OH-groups at C-4 and C-6 of a glucopyranose. Listed below are the protecting group strategies that have been applied throughout the syntheses.

2.4.2.1 Ester (Acetate)

Acetic acid ester is one of the most commonly used protecting groups in carbohydrate chemistry. Acetates are frequently applied on free sugars to provide a blocking of all alcoholic hydroxyl groups, while activating the anomeric carbon at the same time. Treatment with acetic anhydride and sodium acetate as buffer at reflux condition preferably produces the β-anomer as depicted in **Scheme 2.6**. This is due to the fast mutarotation between the α - and β-anomeric free sugars at elevated temperature, in which the latter is more nucleophilic owing to the less hindered equatorial position (Davis & Fairbanks, 2002).

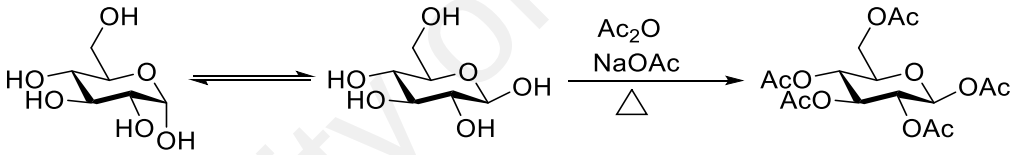

Scheme 2.6: Preparation of β-D-glucose pentaacetate.

A mild approach to introduce an acetate at a complex carbohydrate precursor applies acetic anyhydride in pyridine at room temperature (Rye & Withers, 2002) as shown in **Scheme 2.7**.

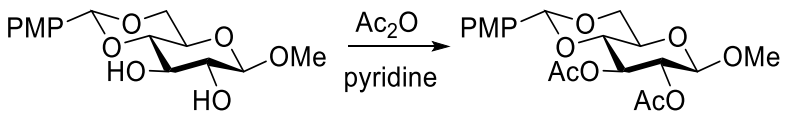

Scheme 2.7: Acetylation of sugar hydroxyl groups.

Acetates are easily removed by transesterification based on the Zemplén procedure (Zemplén & Kunz, 1924; Ren *et al.*, 2015) which employs basic conditions. However, the high reactivity of acetates still limits their application for protection purpose.

2.4.2.2 Acetal (Benzylidene)

As shown in **Scheme 2.8**, selective protection of the 4- and 6- hydroxyl groups of aldopyranosides can be achieved by formation of a cyclic benzylidene acetal using benzaldehyde or one of its acyclic acetals under acid-catalyzed condition (Coterón *et al.*, 1996). Unlike isopropylidene acetals, which typically favour 5-membered rings, benzylidene acetals prefer the formation of a 6-membered ring, in which the bulky phenyl group adopts the equatorial position to prevent any unfavourable 1,3-diaxial interactions (Lindhorst, 2000; Davis & Fairbanks, 2002).

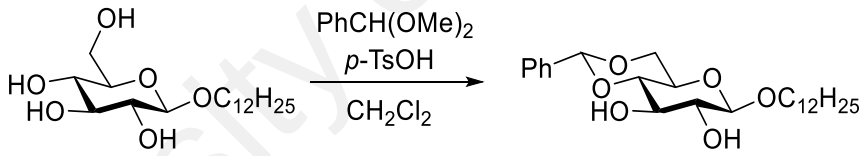

Scheme 2.8: Synthesis of 4,6-*O*-benzylidene.

Benzylidene acetal can be readily cleaved under acidic condition or by hydrogenation (Coterón *et al.*, 1996; Santra *et al.*, 2013). A selective opening of benzylidene acetal also provides a regioselective benzylation on either the 4- or 6-hydroxyl group, depending on the substituents and the reagents used as shown in **Scheme 2.9** and **2.10** (Lee, Zulueta*, et al.*, 2011; Ohlin *et al.*, 2011).

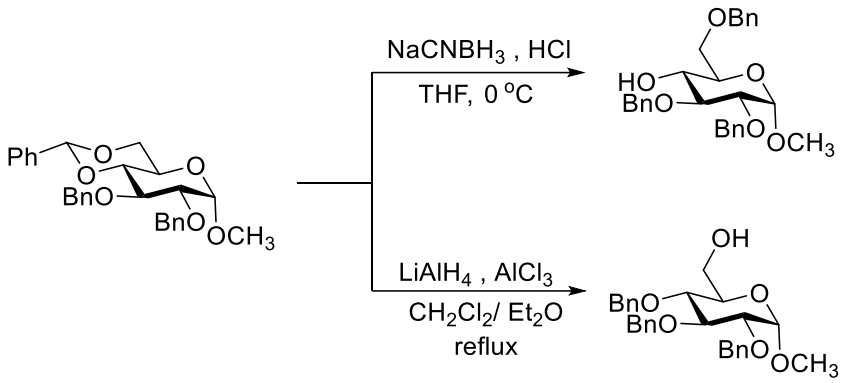

Scheme 2.9: Selective reduction opening of benzylidene acetal.

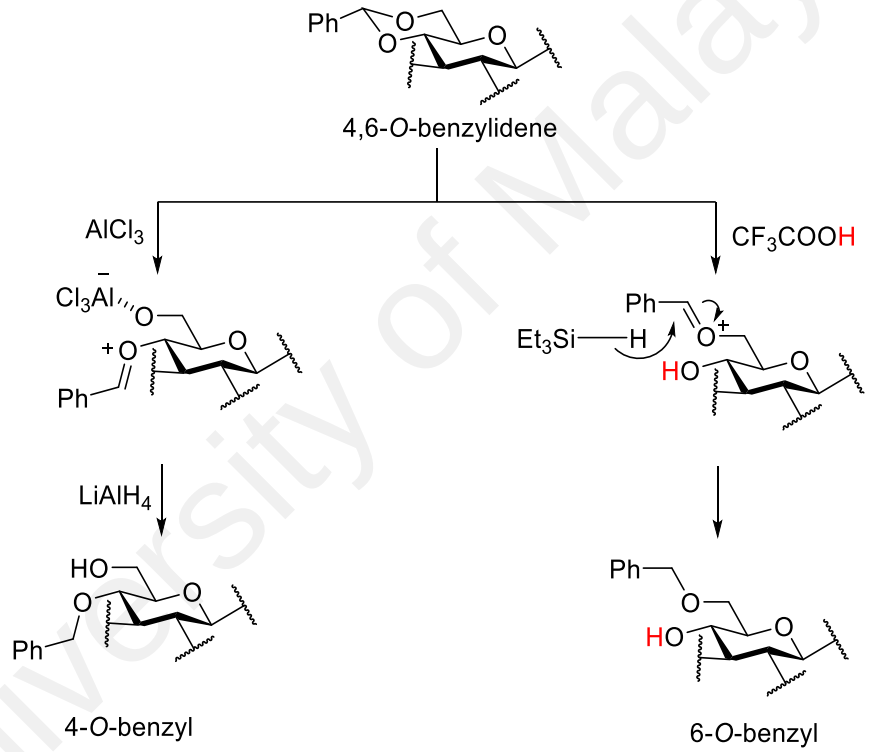

Scheme 2.10: Proposed mechanism of selective opening of 4,6-*O*-benzylidene.

2.4.2.3 Benzyl Ether

Sugar hydroxyl group can be protected as benzyl ethers. They are formed by converting the hydroxyl group to an alkoxide anion with a suitable base, *e.g.* sodium hydride, followed by a S_N2 substitution on a benzyl halide. An example is shown in **Scheme 2.11** (Konda *et al.*, 2014).

The benzyl ether protecting group is highly stable towards both base and acid, but can readily be cleaved under a mild condition by catalytic hydrogenation, requiring the use of palladium on carbon as the catalyst (Röhrling *et al.*, 2002), as illustrated in **Scheme 2.12**. Selective benzylation is typically achieved through regioselective opening of an intermediate cyclic acetal, as previously discussed in section **2.4.2.2**.

Scheme 2.11: Benzylation of 2- and 3-hydroxyl groups.

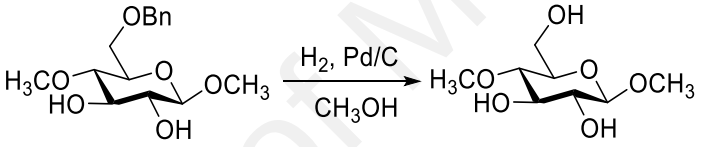

Scheme 2.12: Hydrogenolysis of benzyl ether.

2.4.2.4 Imine

In an amino sugar, the amino group can be protected as an imine through the Schiff base reaction with an aldehyde as shown in **Scheme 2.13**. The imine is labile under acidic condition, which enables a selective deprotection of an acetylated sugar compound as illustrated in **Scheme 2.14**.

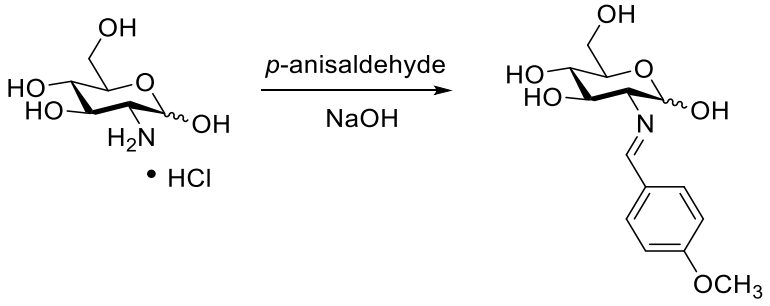

Scheme 2.13: An imine protecting group results from a Schiff base reaction.

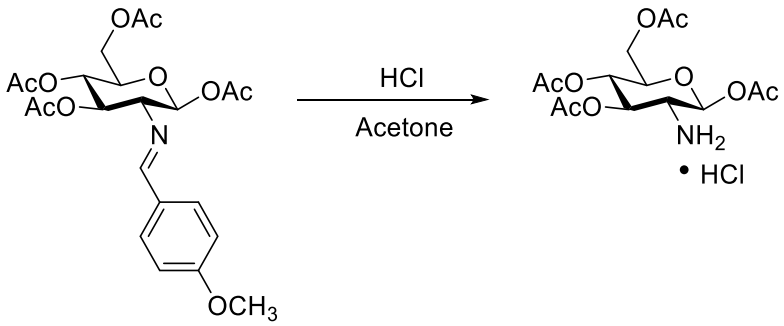

Scheme 2.14: Removal of the imine protecting group.

2.4.3 Functionalization of Glycolipids

The targeted functionalized glycolipid resulted from a coupling reaction between functionalized linkers and glycolipid cores. The compounds carry two key features: one is its CLICK functionality that acts as docking site for targeting ligands or antigens on the vesicle stage; the second is the positive charge of the imidazolium cation, which gives rise to intermolecular ionic repulsion. The latter feature is crucial for the formation of uniformly small-sized vesicles and preventing clustering of the docking sites on the vesicle membrane as well. The imidazolium cations were synthesized based on the Menshutkin reaction, involving the quaternization of the heterocyclic amine by treatment with an alkyl halide (Menschutkin, 1890a, 1890b). As illustrated in **Scheme 2.15**, the lone pair at N-1 is unavailable for nucleophilic attack, because it is part of the aromatic system, whereas the lone pair at N-3 is free to attack the electrophilic carbon of alkyl halide as nucleophile, thus resulting in a very stable imidazolium salt owing to its high degree of symmetry (Duffin, 1964). To ensure efficient couplings, alkyl chlorides were avoided in this study due to their low reactivity (Larsen & Kraus, 1954).

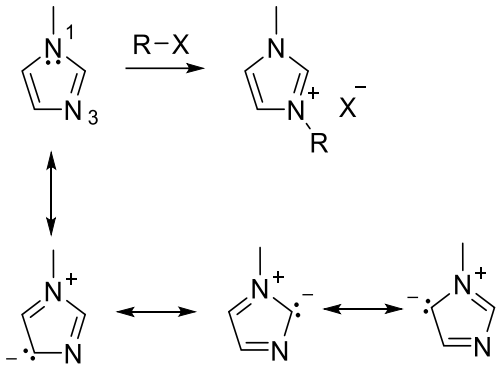

Scheme 2.15: Quaternization of N-alkylimidazole and its resonance structures.

2.5 Imidazolium Cation and Coupling Strategies

2.5.1 Imidazolium Ionic Liquids

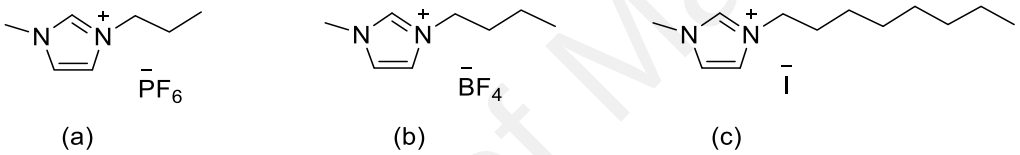

Figure 2.10: Examples of simple imidazolium-based ionic liquids.

As shown in **Figure 2.10** are examples of imidazolium-based ionic liquids (ILs), which generally defined as salts consisting of imidazolium cations and inorganic anions, which are liquids at room temperature (Seddon *et al.*, 2000). Their unusual physical state compared to the other ionic compounds, is attributed to the molecular symmetry distortion caused by the uncommon hydrogen bond between the cation and the anion, bulkiness of the anion, asymmetrical charge distribution in the cation and rotational freedom, thus preventing intermolecular packing and leading to a liquid state (Noack *et al.*, 2010). They have been widely used as "green solvent", in replacement of the typical organic solvents due to their negligible vapour pressure (Wasserscheid *et al.*, 2002). Detailed biological studies on imidazolium-based ILs have also provided some scientific insights into their

antibacterial, antifungal and anticancer activities, which would be an additional advantage for drug delivery application (Docherty & Kulpa, 2005; Malhotra & Kumar, 2010).

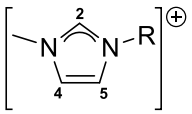

Figure 2.11: General denotation of 1-alkyl-3-methylimidazolium cation.

As shown in **Figure 2.11**, the C_2 hydrogen atom of an imidazolium cation is susceptible forming hydrogen bonding with an anion. This interaction is found mildly orientation dependent in contrast to the conventional hydrogen bonding. Yet it still causes a significant downfield shift on the C_2 proton (Bonhôte *et al.*, 1996; Tsuzuki *et al.*, 2007). The signal of the C_2 proton usually appears as a small and broad peak in the ^{1}H-NMR spectrum recorded in a protic NMR solvent, such as CD_3OD. This is due to the substantial acidity of C_2 proton that readily undergoes H/ D-chemical exchange with the protic solvent (Balme & Lederer, 1994) as shown in the following **Scheme 2.16**.

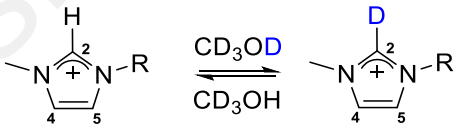

Scheme 2.16: H/ D-chemical exchange process.

2.5.2 CLICK Chemistry- an Approach for Bioconjugation

CLICK chemistry was firstly introduced by K. B. Sharpless in 2001 to define those modular and stereospecific reactions, which are wide in scope, give very high yields, produce by-products that can be readily eliminated by non-chromatographic procedures and can be carried out under easy reaction conditions without or with only benign solvents (Kolb *et al.*, 2001). It involves the formation of new carbon-heteroatom

bonds with fast reaction completion owing to high thermodynamic driving force. Generally, CLICK reactions cover the following classes of chemical transformations:

- 1,3-dipolar cycloaddition reactions
- Diels-Alder reactions
- nucleophilic reactions which comprise ring opening reactions
- non-aldol typed carbonyl reactions
- addition reactions to carbon-carbon multiple bonds

The Huisgen 1,3-dipolar cycloaddition appears to be the most noteworthy among all the CLICK reactions. It unites a 1,3-dipole (an azide) with a dipolarophile (an alkyne), generating a five membered heterocycle in a concerted approach. The original Huisgen 1,3-dipolar cycloaddition was found inappropriate for application on delicate biomaterials due to its harsh reaction conditions and because it usually furnishes a mixture of regioisomers (Huisgen, 1963), as depicted in **Scheme 2.17**.

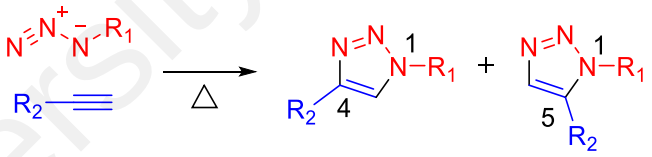

Scheme 2.17: Huisgen 1,3-dipolar cycloaddition.

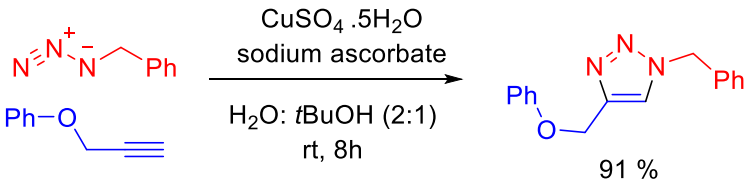

Scheme 2.18: CuAAC reaction

However, Rostovtsev *et al.* have introduced the Copper(I)-catalyzed Azide-Alkyne Cycloaddion (CuAAc), a modified Huisgen reaction, which employs terminal alkynes and azides together with a Cu (I) catalyst, as shown in **Scheme 2.18**. The

catalyzed reaction is highly regiospecific and produces only 1,4-disubstituted 1,2,3-triazoles in very high yields. The proposed mechanism is shown in **Scheme 2.19** (Worrell *et al.*, 2013).

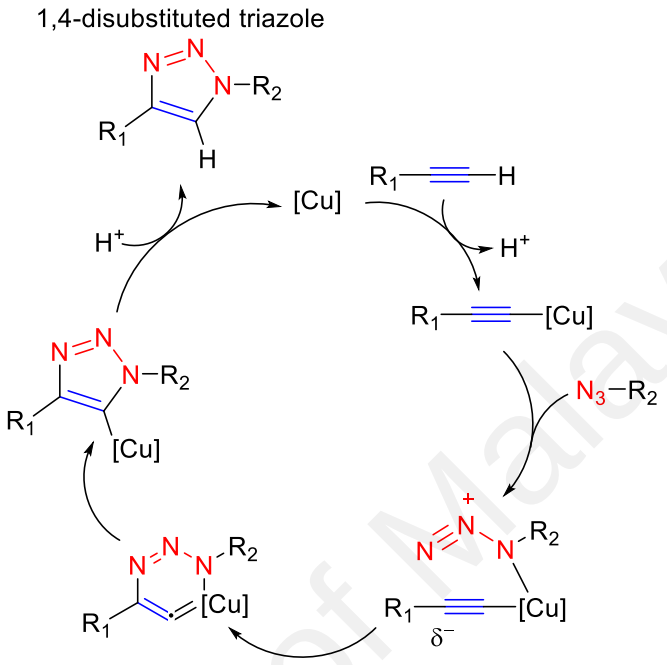

Scheme 2.19: Proposed mechanism for Cu (I)-catalyzed CLICK reaction

CLICK chemistry has been gaining a lot of interests as an efficient bioconjugation strategy that involves binding of synthetic labels to biomolecules, owing to its unique properties as listed below (Nwe & Brechbiel, 2009):

- it is bio-orthogonal
- proceeds irreversibly in water at neutral pH
- feasible at biocompatible temperatures (25 – 37 °C)
- no cytotoxic reagent is necessary
- it produces no cytotoxic byproducts

For example, Wang *et al.* coupled fluorescein-labelled Cowpea mosaic virus particles using a CLICK reaction in more than 95 % yield (Wang *et al.*, 2003). Deiters *et*

al. established a protein-encoding method, which fused the protein of yeast with either acetylene- or azide-bearing synthetic amino acids based on CLICK chemistry. Moreover, they also proved the possibility of incorporating organic dyes to the proteins by the same approach (Deiters *et al.*, 2003). Despite the concern that copper catalysis may be unsuitable for certain biological applications due to the toxicity of the metal, yet there is still a significant growing application of CLICK reaction in many research fields, especially in pharmaceutical and biomedical fields due to some remarkable biological activities of the triazoles, such as anti-HIV and antibacterial activities (Alvarez *et al.*, 1994; Docherty & Kulpa, 2005). In addition, the triazoles also exhibit extraordinary stability towards metabolic degradation.

CLICK reaction requires very mild reaction condition and it is water compatible, which avoids disturbing the vesicle assemblies, as well as prevents denaturation of the biological antigens during the bioconjugation reaction. Therefore it was targeted as the bioconjugation strategy for associating antigens or targeting ligands onto the vesicular surface in this study, as illustrated in **Figure 2.12**.

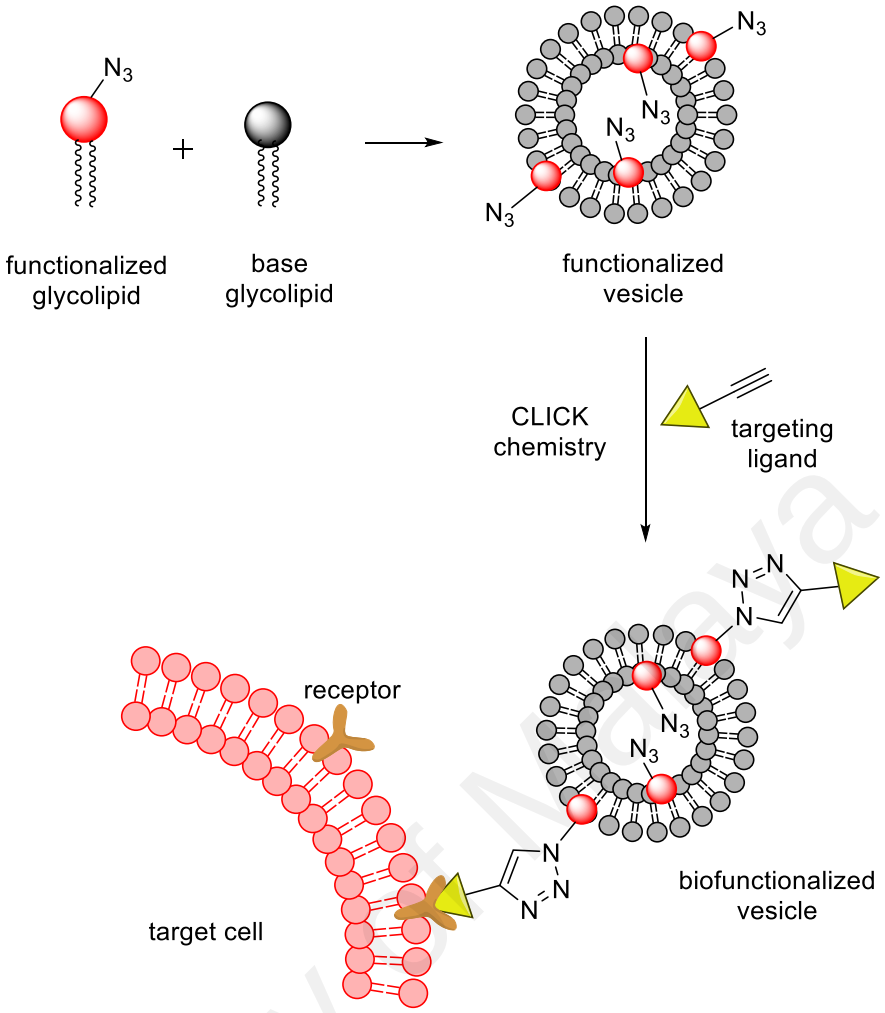

Figure 2.12: Targeting vesicle using functionalized glycolipids as co-surfactant.

CHAPTER 3: METHODOLOGY

3.1 Structure Characterization

3.1.1 NMR Spectroscopy

^{1}HNMR spectra provide information about the number of proton atoms, chemical environment and configuration of the investigated nuclei. The information can be extracted based on the analysis of signal integration, chemical shift, coupling pattern and coupling constants. The latter are particularly important for assigning the NMR signals of carbohydrate compounds. The value of a vicinal proton-proton coupling, $^{3}J_{H,H}$, greatly depends on the dihedral angle of the two C-H bonds as shown in **Figure 3.1**. Thereby it provides information on the spatial arrangement between the protons, which is the key in identifying the stereochemistry of carbohydrate compounds (Coxon, 2009). In pyranose, β-anomers display an axial-axial orientation of H-1 and H-2, reflecting a dihedral angle close to 180 °. The correlated coupling constant is around 8 Hz as shown in **Figure 3.2**, while the dihedral angle between an equatorial H-1 and an axial H-2 in α-anomers is around 60 °, leading to a coupling constant of around 4 Hz (Lindhorst, 2000).

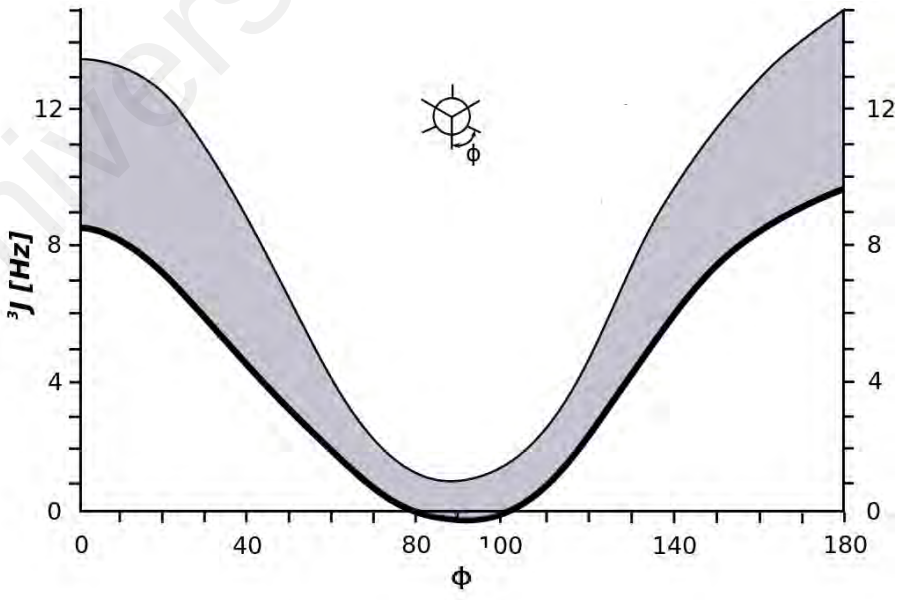

Figure 3.1: Karplus relation

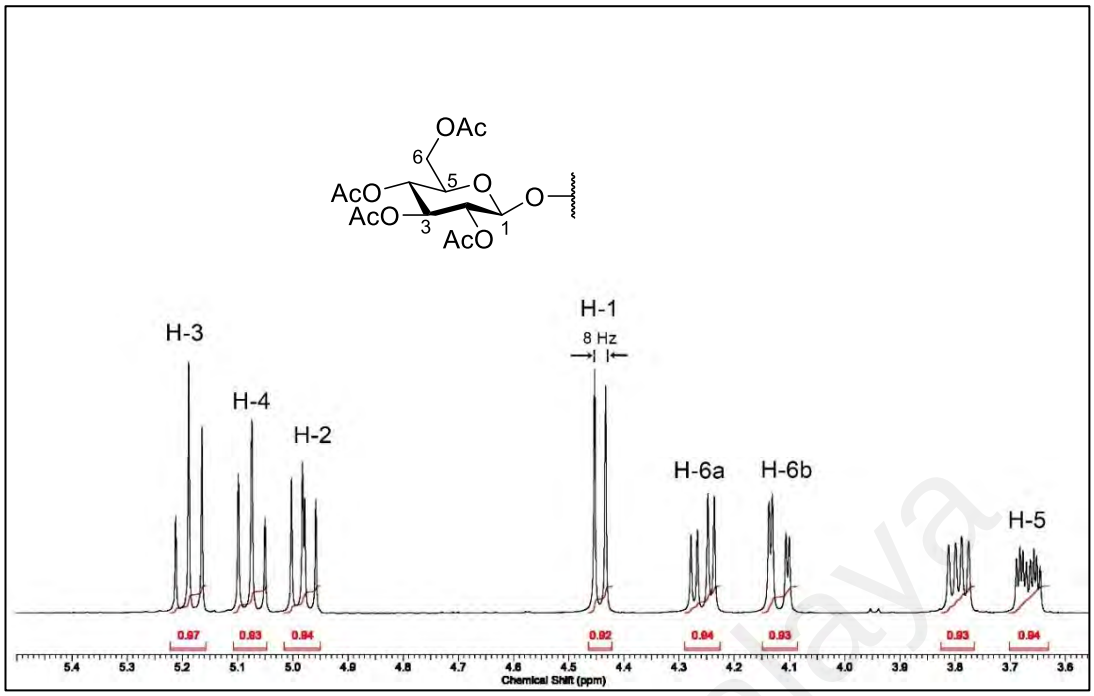

Figure 3.2: ^{1}H NMR spectrum.

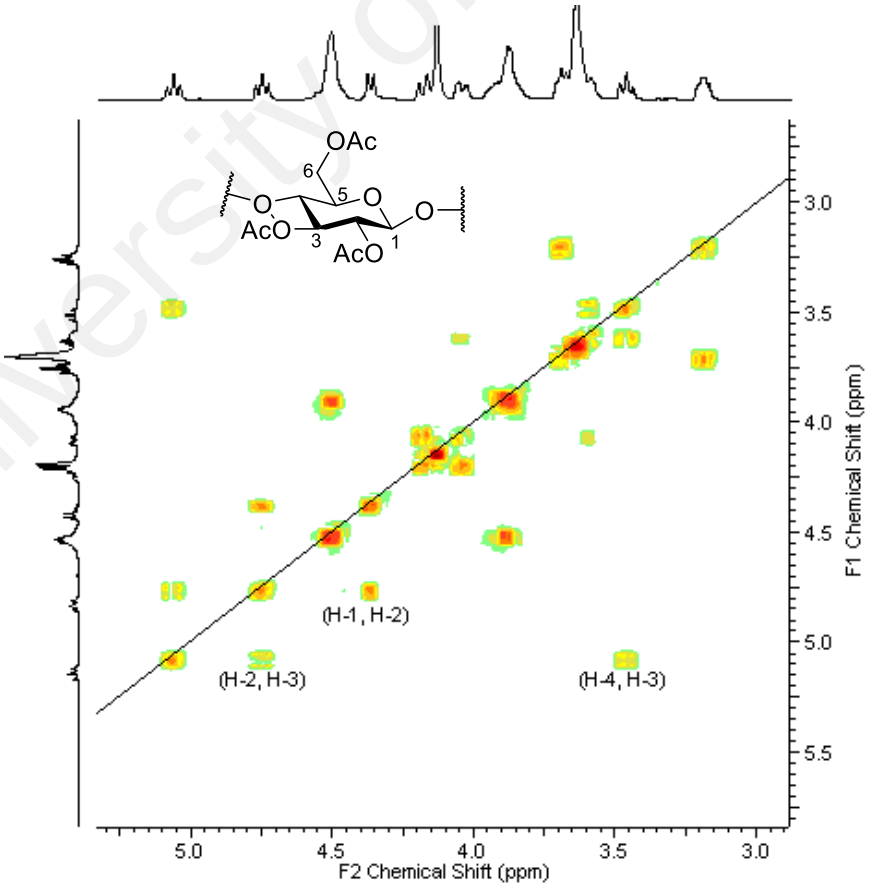

Figure 3.3: ^{1}H-^{1}H COSY spectrum.

However, there were some cases, where the ^{1}H NMR signals were found not well resolved or overlapped with other signals, causing difficulties in determination of the coupling constants. In these cases, a 2D NMR ^{1}H-^{1}H Correlation Spectroscopy (COSY) was employed to indicate which ^{1}H atoms are coupling with each other, as shown in **Figure 3.3**.

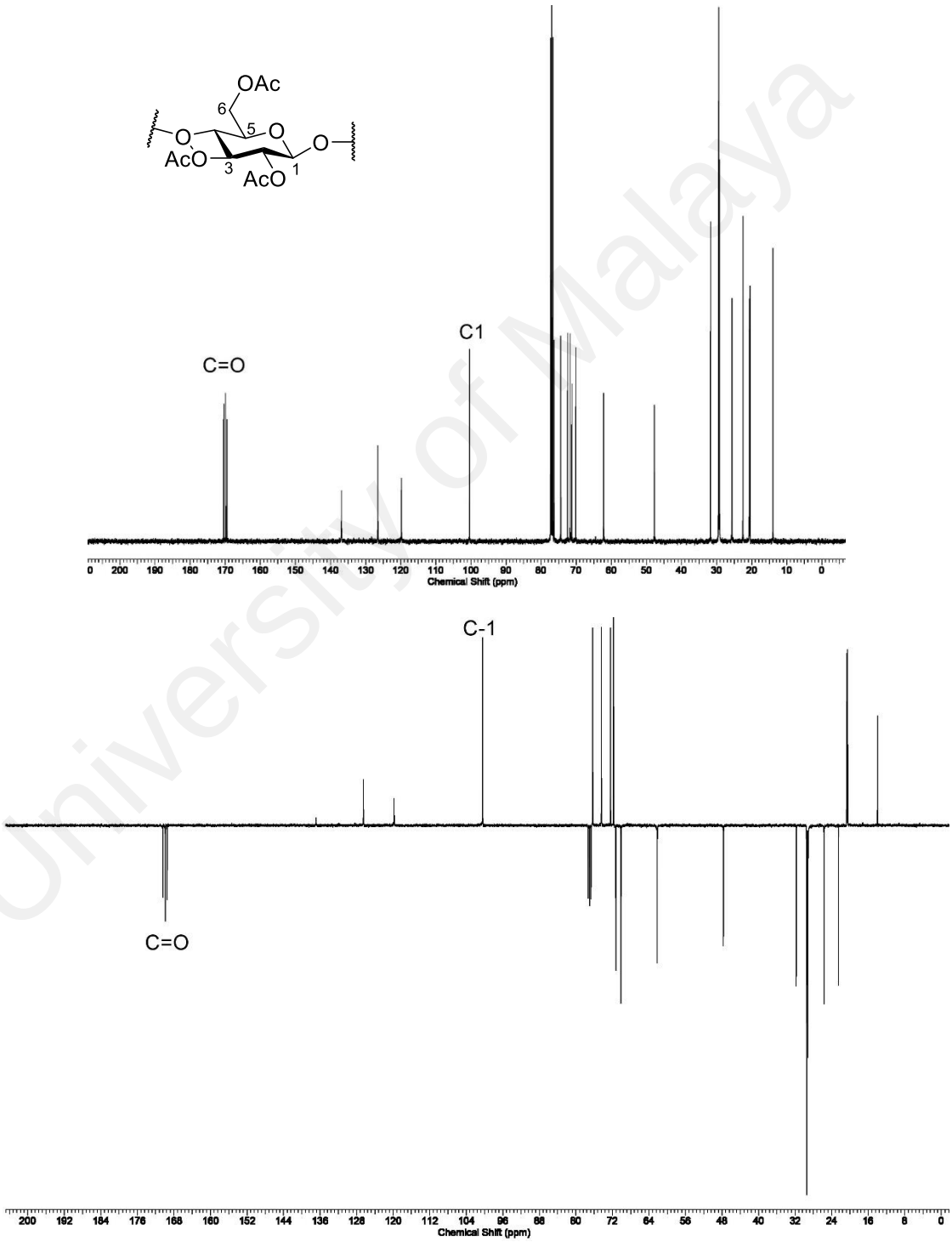

Figure 3.4: ^{13}C (top) and APT (bottom) NMR spectra.

A ^{13}C NMR spectrum shows all the carbon atoms in a compound, but it does not differentiate between quaternary carbon (C), methine (CH), methylene (CH_2) and methyl (CH_3) signals. Therefore, APT (Attached Proton Test) or PENDANT (Polarization Enhancement Nurtured during Attached Nucleus Testing) experiments, was applied instead, in which both CH and CH_3 will appear as positive signals, while C and CH_2 are negative signals in the spectrum, as illustrated in **Figure 3.4**. The assignments of carbon signals was based on 2D NMR Heteronuclear Single Quantum Coherence Spectroscopy (HSQC), which provides a correlation of carbons and their attached protons, as shown in **Figure 3.5**. As for compounds involving polycyclic aromatic rings, Heteronuclear Multiple Bond Correlation (HMBC) spectrum, as shown in **Figure 3.6** enables the correlation between carbons and protons that are separated by two to three bonds, was applied.

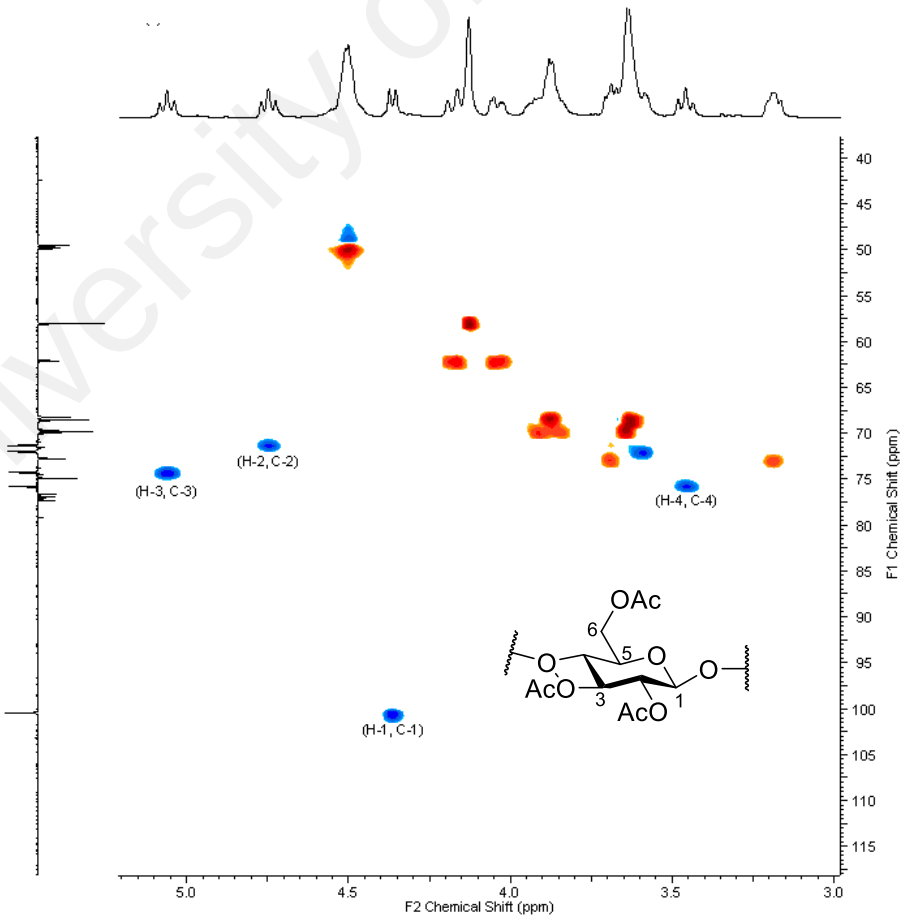

Figure 3.5: HSQC spectrum.

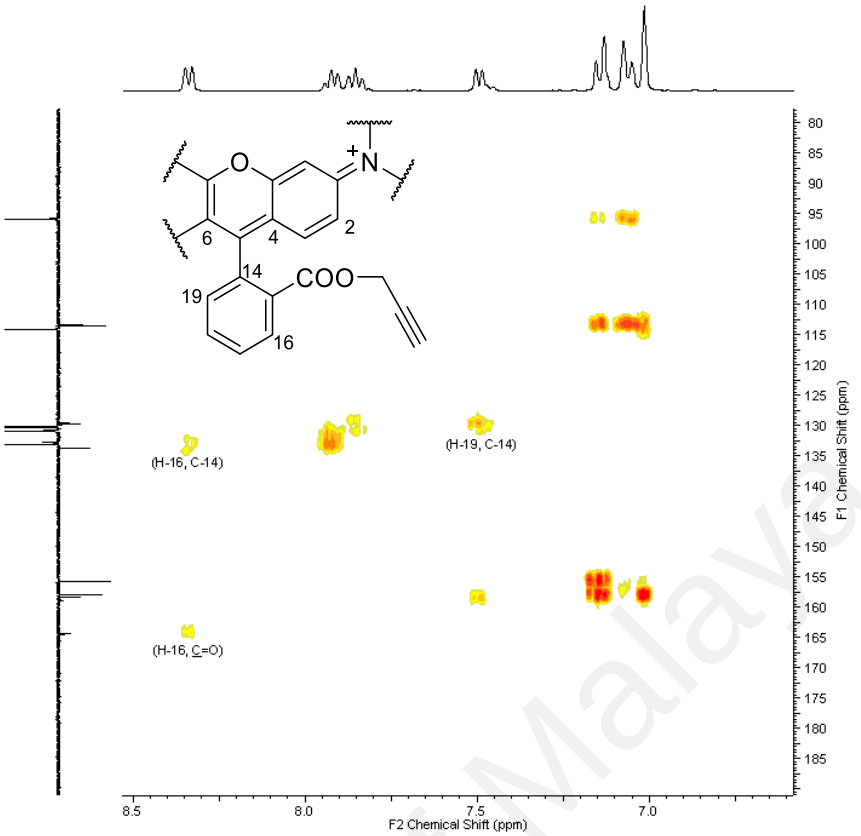

Figure 3.6: HMBC spectrum.

3.1.2 IR Spectroscopy

In this study, IR was applied to confirm the presence of azido groups, which appear as a strong peak at around 2100 cm^{-1}, as shown in **Figure 3.7**.

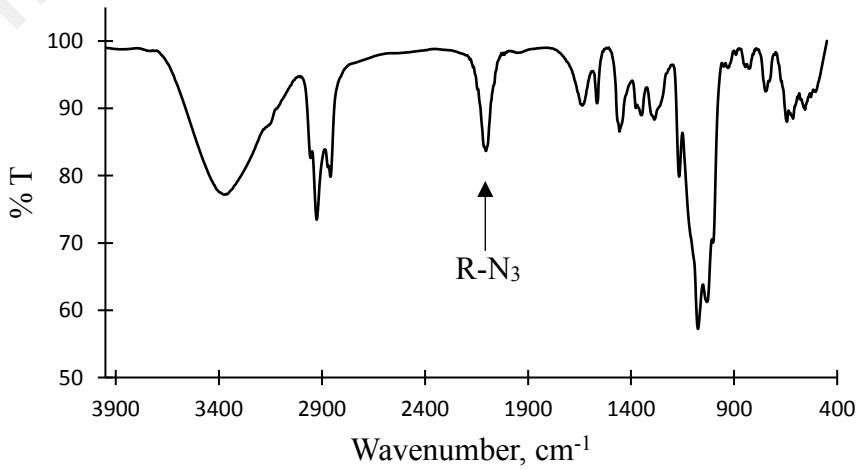

Figure 3.7: IR spectrum.

3.1.3 Mass Spectrometry

The compounds were dissolved in 1 mL of HPLC grade methanol and the respective HRMS (High Resolution Mass Spectra) were recorded by electrospray ionization based on time of flight measurements (TOF).

3.2 Physical Properties Investigations

3.2.1 Surfactant Assembly Behaviour

Surfactant solutions of different concentrations in water were prepared and their respective surface tension was measured in five replicates. The measurement was repeated until the statistical error was below 0.1 mN m^{-1}. The graph of surface tension versus logarithmic concentration was plotted and the critical aggregation concentration (CAC) was obtained from the intersection point of two regression lines reflecting the concentration dependent region and the concentration independent region. The surface area per molecule, A_{min} was calculated using the Gibbs adsorption isotherm based on equation 3.2, which explains the relation between surface area per molecule and surface excess concentration. The latter was determined based on equation 3.1 (Rosen & Kunjappu, 2012).

$$\Gamma_{max} = -\frac{10^{-3}}{2.303nRT}\left(\frac{\partial\gamma}{\partial log C}\right)_{max\ T} \tag{3.1}$$

$$A_{min} = \frac{10^{20}}{N\Gamma_{max}} \tag{3.2}$$

In these equations, Γ_{max} is the surface excess concentration, n is the factor depending on the valency of the ionic species, R is the universal gas constant, T is the absolute temperature, γ is the surface tension, C is the surfactant concentration, A_{min} is the molecular surface area and N is Avogadro's constant.

3.2.2 Optical Polarizing Microscopy

For the study of surfactant mixtures, the sample was prepared by dissolving the surfactants based on a desired ratio in methanol under sonication to ensure a uniform mixing. The solvent was then evaporated and the sample dried at high vacuum for several hours. Lyotropic behaviour of the surfactants was studied using a modified Amscope microscope with installed polarizers based on the water penetration method (Laughlin, 1992; von Minden *et al.*, 2000). A small amount of the surfactant was melted on a glass slide until it reached an isotropic phase. The sample was covered with a cover slip and a drop of solvent was placed at the edge of the cover slip to penetrate the sample by capillary force. The textures reflecting lyotropic phases were observed under the optical polarized microscope at room temperature (~25 $^{\circ}$C) at 50 x magnification.

3.2.3 Vesicle Preparation

The ethanol injection method was applied for the vesicle preparation (Jaafar-Maalej *et al.*, 2010). A mixture of surfactant and co-surfactant at the desired ratio was dissolved in ethanol (5 % of total volume) and rapidly injected into bulk water through a 25 Ga bevel tip needle at room temperature. The resulting dispersion was stirred for 10 minutes at room temperature to yield the vesicles. Samples applied concentration of 2 mM for the surfactants and a ratio of ethanol and water of 1: 19.

3.2.4 Vesicle Characterization

The vesicle sizes were measured based on dynamic light scattering (DLS) method, relying on a backscatter detection angle at 173°. Owing to Brownian motion, particles suspended in a liquid phase will experience different diffusing speed and it provides a fluctuation pattern of the scattered light. The size of particles can be determined from their translational diffusion coefficient based on Stoke-Einstein equation (Sutherland, 1905; Einstein, 1906; Bhattacharjee, 2016). The same instrument was used to determine

zeta potential, in a gold-plated electrode U-shaped cell. Zeta potential is the electrostatic potential measured at the surface of shear or slip surface in an electrical double layer. It is determined using electrophoresis, which involves migration of the charged particles towards the electrode of opposite charge when an electric field is applied. This gives information about the velocity of the particle in a unit of electric field, or the particle's electrophoretic mobility, which is related to the zeta potential according to the Henry's equation (Henry & Lapworth, 1931; Bhattacharjee, 2016).

3.2.5 Specific Optical Rotation

Chemical compounds were dissolved in either chloroform or methanol (10 mL), depending on the solubility and their respective specific optical rotations of the sugar compounds were determined according to the following equation:

$$[\propto]_D^{25} = \frac{\alpha}{lc} \qquad (3.3)$$

Where,

$\propto$ = measured rotation in degrees

l = path length in decimetres

c = concentration (g/ mL for pure liquid compound; g/100 mL for a solution

3.2.6 Fluorescence Calibration Curve

A stock solution of **R3** (10 μM) in methanol was prepared and used to prepare a series of solutions of different concentrations by dilution. A fluorescence calibration curve was obtained by plotting the measured fluorescence intensities of the solutions against the corresponding concentrations.

3.3 Molecular Modelling

Molecular structures were created in GaussView 5.0 and structural optimizations were carried out in Gaussian 9.0, using Density Functional Theory under B3LYP function with 6-31G + (d,p) basis set (Salman *et al.*, 2013; Bayach *et al.*, 2016).

3.4 General Synthetic Procedures

3.4.1 N-alkylation of Imidazole

Into a solution of imidazole in tetrahydrofuran, sodium hydride (60 % suspension in paraffin oil) was added. After an hour of stirring, alkyl halide was added under ice bath cooling and the mixture was subsequently refluxed overnight. The reaction was cooled to room temperature and quenched with methanol (3-5 mL). The solvent was evaporated at reduced pressure and the resulting residue was extracted with dichloromethane. The concentrated extract was subjected to column chromatography over silica gel (EtOAc: acetone= 8: 1 for compound **2a-c**) to give the alkylated imidazole. **Table 3.1** describes the molar equivalents of the reagents needed for the reaction (Xu *et al.*, 2009; Lee, Choi, *et al.*, 2011).

Table 3.1: Molar equivalents of the reagents

Reagent	Molar equivalent		
	Alkyl halide	Imidazole	Sodium hydride
Mono-halogenated	1	2	2.3
Dichloro compound	4	1	2

3.4.2 Azidation

A mixture of alkyl halide (1 equiv) and sodium azide (2 equiv) in dimethylformamide was heated to 80°C overnight and the solvent was subsequently evaporated at reduced pressure (Hanessian *et al.*, 1978; Lin *et al.*, 2011).

Alkyl imidazole: the residue was extracted with dichloromethane and insoluble solids were filtered off. The solvent was evaporated under reduced pressure to furnish the azido compound.

Sugar compound: the residue was taken up in dichloromethane and water. The organic layer was dried over magnesium sulphate and concentrated.

3.4.3 Peracetylation of Glucose

A suspension of sodium acetate (10 g) in acetic anhydride (100 mL) was heated to reflux. D-glucose (20 g) was added portionwise with continuous heating. The mixture was heated to 120 °C for another 1.5 hours after the sugar had completely dissolved. The mixture was cooled to room temperature and slowly poured into an iced water (1 L) with continuous stirring and left to warm to room temperature overnight. The resulting solid was collected by suction filtration and recrystallized from ethanol to obtain pure β-D-glucose pentaacetate as a white powder (Fischer, 1916; Chen *et al.*, 2016).

3.4.4 Sugar Ester Glycosylation

A solution of β- D- glucose pentaacetate (1 equiv) and long-chained alcohol (1.3 equiv) in dichloromethane was treated with boron trifluoride diethyl etherate (1.5 equiv) and stirred for 5 hours at room temperature. The reaction was washed successively with saturated sodium bicarbonate solution and water, and dried over magnesium sulphate. The crude product was subjected to column chromatography over silica gel to isolate the β-glucoside (Dahmén *et al.*, 1983).

3.4.5 Deacetylation

Acetylated glycoside was dissolved in methanol and a catalytic amount of sodium methoxide was added to obtain a basic medium. The mixture was stirred overnight at

room temperature. Amberlite 120 (H^+) was added to neutralize the basic medium. The resin was filtered off and solvent was evaporated to yield the glycoside (Ren *et al.*, 2015).

3.4.6 Selective Halogenation on Sugar C-6

Glycolipid (1 equiv) and triphenylphosphine (2 equiv) were dissolved in dimethylformamide. About 2-5 mL dimethylformamide was evaporated to remove water contents. The mixture was cooled to 0°C and subsequently N-bromosuccinimide or N-chlorosuccinimide (2 equiv) was added slowly. The mixture was then heated to 70 ° C for another two hours under nitrogen atmosphere and cooled to room temperature before the reaction was quenched by addition of methanol (10 mL). After evaporation of the solvent, the residue was distributed between dichloromethane and saturated sodium bicarbonate solution. The organic layer was dried over magnesium sulphate and concentrated to furnish the crude material, which was directly used for subsequent reaction (Hanessian *et al.*, 1972).

3.4.7 Acetylation of Sugar Compound

Into a solution of glycoside (1 equiv) in pyridine, acetic anhydride (2 equiv per hydroxyl group) was added slowly. The mixture was stirred at room temperature overnight. Pyridine was evaporated and the residue was taken up in dichloromethane and 2 N hydrochloric acid. The organic layer was washed with water and dried over magnesium sulphate. The concentrated crude product was chromatographed over silica gel to isolate the target compound (Ichikawa *et al.*, 1985; Taniguchi & Monde, 2012).

3.4.8 Benzylidenation

Into a suspension of glycoside (1 equiv) in dichloromethane, benzaldehyde dimethyl acetal (2.4 equiv) and *p*-toluenesulphonic acid monohydrate (100 mg) were added. The mixture was stirred at room temperature overnight. The reaction was washed with saturated sodium bicarbonate solution and water, dried over magnesium sulphate

and concentrated. The 4,6-*O*-benzylidene compound was obtained either by column chromatography or crystallization from hexane (Coterón *et al.*, 1996; Ito *et al.*, 2012).

3.4.9 Benzylation

To a solution of glycoside (1 equiv) in dimethylformamide, sodium hydride (60 % suspension in paraffin oil) (2 equiv per hydroxyl group) was added slowly. The mixture was stirred for an hour at room temperature. Benzyl bromide (1.5 equiv per hydroxyl group) was added dropwise at 0 °C and the mixture was warmed to room temperature and stirred overnight. The reaction was quenched by addition of methanol (10 ml) and the solvent was removed at reduced pressure. The resulting residue was distributed between dichloromethane and water. The organic layer was dried over magnesium sulphate and concentrated (Uzawa *et al.*, 2005).

3.4.10 Selective Opening of Benzylidene

A solution of 4,6-*O*- benzylidene compound (1 equiv) in dichloromethane was treated with activated 4 Å molecular sieves (2 g per 2 mmol of sugar compound) and stirred for 5 minutes. The mixture was cooled to 0 °C, followed by addition of triethylsilane (6 equiv) and trifluoroacetic acid (6 equiv). The reaction was stirred at room temperature overnight. The solid was filtered and the filtrate was washed successively with saturated sodium bicarbonate solution and water. The organic layer was dried over magnesium sulphate and concentrated under reduced pressure. Target compound was obtained by column chromatography over silica gel (Yoneda *et al.*, 2005; Kasuya *et al.*, 2007).

3.4.11 Hydrogenolysis of Benzyl Ether

Benzylated glycoside was dissolved in methanol (100 ml) and palladium on activated carbon (10 % Pd, oxidic form) (25-40 mg) was added. The mixture was placed under hydrogen atmosphere with stirring after addition of concentrated hydrochloric acid

(0.5-1 mL). The reaction was complete as indicated by TLC showing absence of starting material. The catalyst was filtered through a celite pad and the resulting filtrate was neutralized with sodium bicarbonate. The solvent was evaporated after filtering off the solid to give the crude product which was used for the next reaction without prior purification (Combs *et al.*, 1949; Röhrling *et al.*, 2002).

3.4.12 Catalytic Phase Transfer Alkylation

A solution of glycoside (1 equiv) in toluene was cooled in an ice bath. Tetra-n-butylammonium bromide (0.5-1 equiv) and aqueous solution of sodium hydroxide (50 % w/w) were added and the mixture was then stirred vigorously for 15 minutes. Tert-butylbromoacetate (1.5 equiv per hydroxyl group) was added slowly at 0 °C and vigorous stirring was continued. Methanol (10 mL) was added when the reaction was complete as indicated by TLC. The organic layer was isolated and concentrated. The crude material was subjected to the next reaction without prior purification (Dou *et al.*, 1977; Starks *et al.*, 1994; Sabah *et al.*, 2011).

3.4.13 Reduction of Ester

A solution of the ester (1 equiv) in tetrahydrofuran was cooled to 0 °C and lithium aluminium hydride (4 equiv per ester) was added slowly. The mixture was warmed to room temperature with continuous stirring until TLC indicated absence of the starting material. Water (1-2 mL) was added slowly and stirred for two minutes. White precipitates formed upon addition of aqueous solution of sodium hydroxide (15 % w/w) (1-2 mL). After five minutes, another 3 ml of water was added and stirring was continued for another 3 minutes. The white precipitate was filtered off and the filtrate was then concentrated. The residue was distributed between dichloromethane and water. The organic layer was dried over magnesium sulphate and concentrated to give the crude

product, which was directly used for the subsequent reaction (González-García *et al.*, 2003; Qabaja *et al.*, 2013).

3.4.14 Iodination of Primary Hydroxyl Group

Into a solution of glycoside (1 equiv) in toluene, iodine (1.5 equiv), triphenyphosphine (1.5 equiv) and imidazole (3 equiv) were added. The reaction was then heated to 50 °C until TLC indicated complete conversion of the starting material. After cooling to room temperature, the mixture was diluted with methanol to around 50 %. The solvent was evaporated and the residue was distributed between dichloromethane and aqueous solution of sodium thiosulphate (10 % w/w). The organic layer was washed with water and dried over magnesium sulphate. The remaining solvent was evaporated under reduced pressure and the resulting crude was used for the subsequent reaction without prior purification (Sletten & Liotta, 2006).

3.4.15 Quaternization of Alkyl Imidazoles

A solution of alkyl imidazole (1 equiv) and alkyl bromide (1 equiv) in xylene or toluene (3-5 mL) was heated to 130 °C for xylene or 90 °C for toluene with TLC monitoring. The solvent was evaporated when the reaction was complete to furnish the imidazolium compound.

3.4.16 CLICK Reaction

Into a micellar or vesicle dispersion containing azide-terminated functionalized glycolipids in water, alkyne terminated compound, copper (II) acetate (0.15 equiv) and sodium ascorbate (0.45 equiv) were added. The reaction was stirred at room temperature overnight.

CHAPTER 4: RESULTS AND DISCUSSION

4.1 Conceptual Design of a Vesicular Targeting Drug Delivery System

An antigen-receptor mediated targeted drug delivery system requires a biological recognition domain on the vesicular surface. This can be achieved through vesicle formulation using surfactant mixture containing both base and antigen-bearing glycolipids. However, random distribution of the surfactants during vesicle formation will result in the embedment of antigens inside the vesicle, where they are unable to interact with the receptors of the target cells. An alternative strategy can employ functionalized glycolipids as co-surfactant for vesicle preparation, as illustrated in **Figure 4.1**, which serve as docking sites for the antigens on the vesicular surface. This approach avoids the loss of precious antigen inside the vesicle and enables the use of same vesicles for diverse therapeutic applications simply by applying different antigens.

CLICK reaction was targeted for the bioconjugation of the functionalized vesicles with antigens owing to its high reaction efficiency and selectivity. Moreover, a CLICK reaction can proceed under mild reaction condition, which prevents subjecting the antigens to harsh reaction conditions, which may lead to denaturation. Its water compatibility also avoids the use of potentially problematic solvents. Therefore, glycolipids carrying CLICK functionality, referred to as "functionalized glycolipids" were prepared in this study.

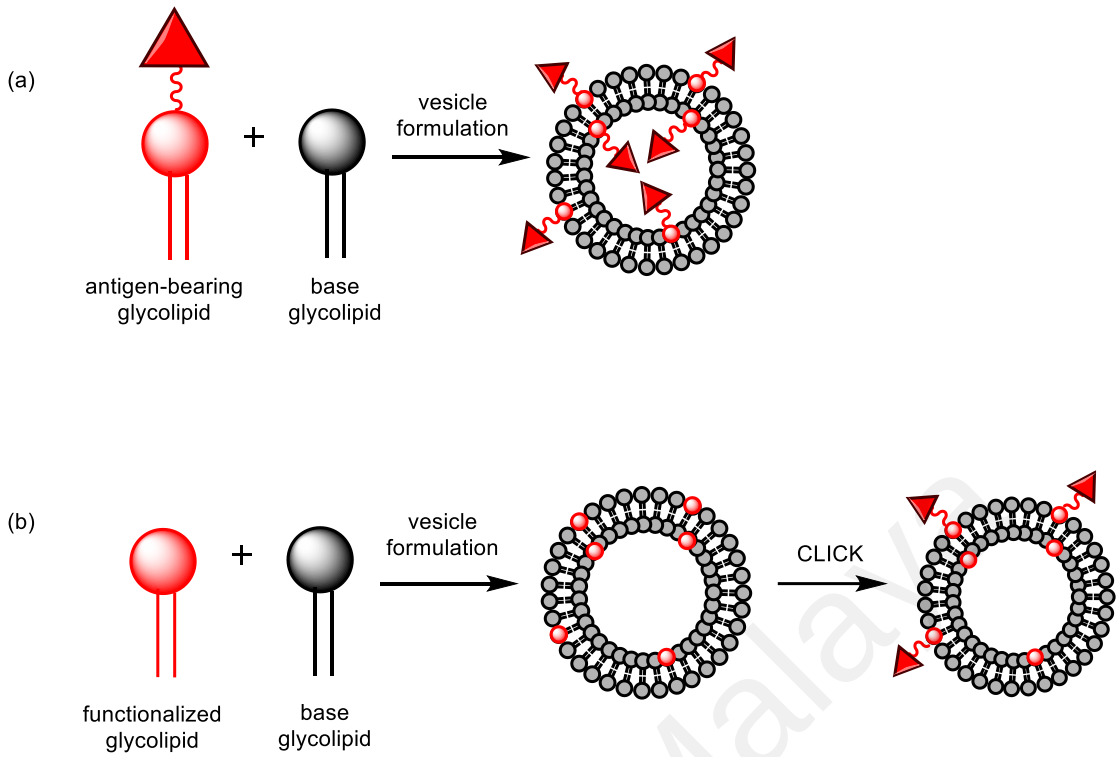

Figure 4.1: Approaches to prepare bio-functionalized vesicles.

The design of the functionalized glycolipid, comprising of a glycolipid core and a functionalized linker is depicted in **Figure 4.2**. A biantennary glycolipid was used as it mimics the structure of natural biosurfactants and its relatively larger hydrophobic volume favours the formation of the lamellar phase that highly potential to give rise to vesicular assemblies. The Guerbet alcohols used for glycosylation are commercially available as a racemic mixture, thus they gave rise to a diastereomeric mixture of the glycosides. The natural glycolipid (as shown in **Figure 2.6**) has a chiral centre, C-2 at the glycerol unit, which is attached to four significantly different substituents. On the other hand, the chiral centre at the hydrocarbon chain of Guerbet glycoside (as indicated in **Figure 4.2**) exhibits an almost identical local environment since it is attached to two alkyl chains that only differ by two carbon atoms. This is reflected in an almost identical ^{13}C NMR data for the two sub-chains. Thus, the stereochemical impact of the Guerbet

alcohols, particularly those of longer hydrocarbon chain, is assumed to be irrelevant for both biological and physicochemical properties.

A key feature in the functionalized linker is the CLICK functionality, which can be either an azide or a terminal alkyne that serves as docking site for the antigen. An ethylene oxide (EO) backbone was introduced as the spacer between the CLICK functionality and the sugar head group to provide flexibility to the anchor, thus facilitating an efficient bioconjugation reaction at the vesicle stage. The EO spacer was chosen because of its low toxicity and low immunogenicity (Powel, 1980; Yamaoka *et al.*, 1994). Besides, it does not exhibit significant influence on specific biological properties of pharmaceuticals (Zalipsky, 1995).

Another key feature is the imidazolium cation, which results from the Menshutkin reaction and provides cationic character to the functionalized glycolipid. Vesicles incorporating these functionalized glycolipids as co-surfactant are stable towards pH, as the quaternary ammonium cation is pH-insensitive (Gelardi *et al.*, 2016). During the vesicle formation, the electrostatic repulsion between the imidazolium cations maintains a reasonable distance between the glycolipids, thereby avoiding clustering of the docking sites on the vesicular surface, which otherwise could restrict the accessibility for the target cells. Besides, the use of ionic glycolipids furnishes smaller-sized vesicles, due to the ionic repulsion between the cationic surfactants that promotes the surfactant distribution during the injection (Varshosaz *et al.*, 2003; Israelachvili, 2011; Mak *et al.*, 2015; Bnyan *et al.*, 2018). Positive surface charge of the vesicles is expected to improve the interaction with target cells, which typically possess abundant negative surface charges, such as Gram-negative bacterial cells (Costerton *et al.*, 1974) and nuclei acid of negative nature (Yang *et al.*, 2014; Kasyanenko *et al.*, 2018).

To compare the effect of the position of the functionalized linker on the surfactant assembly behaviour, three different positions (C-1, C-4 and C-6) of the sugar head group were targeted as the functionalizing sites for the linkers in this study. This selection is based on their easy accessibility.

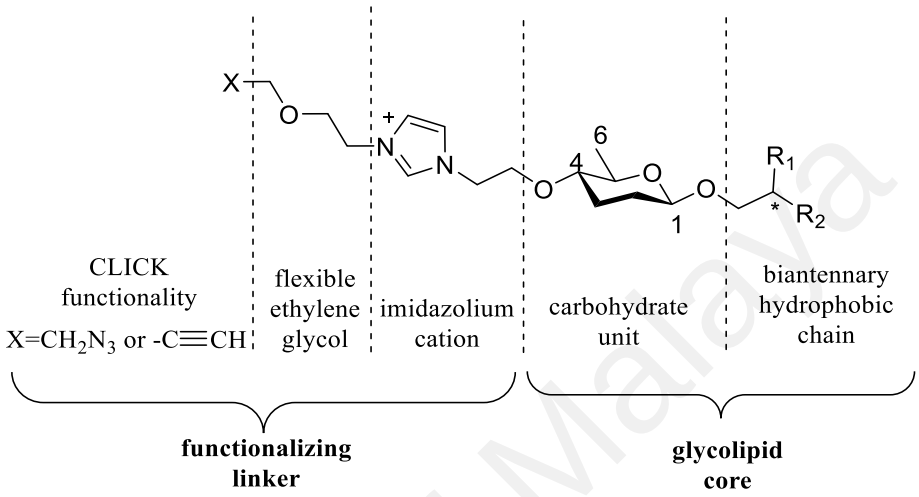

Figure 4.2: General structure of a C-4 functionalized glycolipid.

4.2 Synthesis of Functionalized Linkers

Each functionalized linker carries either a terminal alkyne or an azido group, which is the key element for the targeted biofunctionalization of vesicles through CLICK reaction. This approach requires a complementary functionalization of the antigens, as illustrated in **Figure 2.12**.

The synthetic scheme of azide terminated functionalized linkers is illustrated in **Scheme 4.2**. An imidazolate was generated through proton abstraction from the heterocyclic nitrogen by a strong base, sodium hydride, followed by a nucleophilic substitution with dichloro compounds (**1a-c**) respectively to yield the intermediates **2a-c**. Considering the competition between formations of the target compounds (**2a-c**) and bis-imidazole derivatives, excessive dichloro compounds (**1a-c**) were used to enhance the selectivity towards the target compounds without promoting the formation of

imidazolium cations, because the latter usually requires high temperature condition. Compound **1c** was prepared based on the reaction with thionyl chloride as shown in **Scheme 4.1**. Compound **1c** was used for the subsequent alkylation with the imidazolate without prior purification, which explains the lower percentage yield of compound **2c**, in comparison with the others. Lastly, azidation of the N-alkylated imidazoles furnished a series of azide-terminated linkers (**3a**-**3c**) in reasonably good yields.

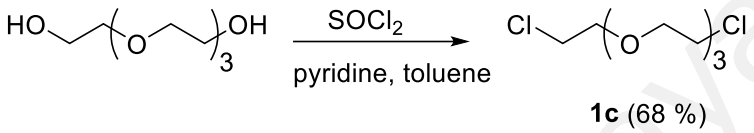

1c (68 %)

Scheme 4.1: Synthesis of **1c**.

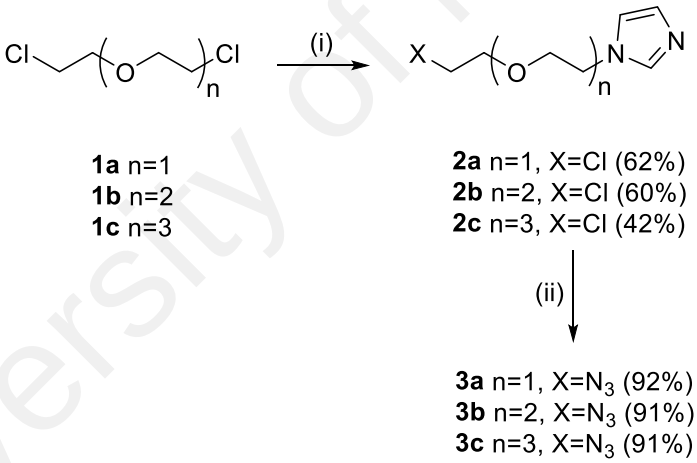

Scheme 4.2: Synthesis of azide-terminated linkers.

The azide-terminated functionalized linkers were meant for association with the halogen-bearing glycolipid core through the Menshutkin reaction. However, during the preparation of the O-4 modified glycolipid core, an N-alkyl imidazole was successfully incorporated instead of a halogen group owing to synthetic constraints (detailed discussion in section **4.3.2**). Therefore, a halogen-group was introduced onto the linker

as shown in **Scheme 4.3**. Unlike for the linkers in **Scheme 4.2**, terminal alkyne was used as biofunctionalization anchor to simplify the synthesis. Reaction of propargyl bromide with an ethylene oxide salt, obtained from the reaction between diethylene glycol and sodium hydride provided the linker. Excessive glycol was used to enhance the selectivity for the formation of mono-alkyne compound **4**. Since the tosylate ion is unsuitable for biological application, the remaining hydroxyl group was first converted to a tosylate and subsequently subjected to a nucleophilic exchange reaction (Finkelstein, 1910; Baughman *et al.*, 2004) to provide iodo-compound **6** in an overall yield of around 50 %.

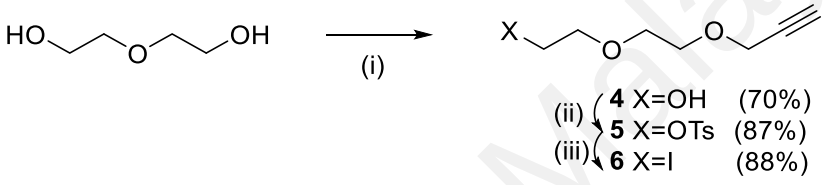

(i) NaH, propagyl bromide, THF; (ii) NaOH, TsCl, THF; (iii) NaI, acetone

Scheme 4.3: Synthesis of linker **6**.

4.3 Synthesis of Functionalized Glycolipids

The preparation of functionalized glycolipids involved association of functionalized linkers with glycolipid cores by the Menshutkin reaction, resulting in the formation of the imidazolium cation. Both ionic character and lack of molecular symmetry of functionalized glycolipids precluded the purification procedures by classic chromatographic techniques or crystallization. Therefore, the reaction was performed by applying both reactants at an exact ratio of 1: 1, with monitoring by TLC over time to prevent the materials from getting charred or burnt since high temperature condition was necessary for the reaction.

To study the effect of the position of the functionalized linker on the surfactant behaviour, three different positions (C-6, C-4 and C-1) of the glycolipid were targeted. In

order to achieve regioselective functionalization, the polyfunctionality of carbohydrate with its many hydroxyl groups necessitated the application of protecting group strategies.

4.3.1 Synthesis of C-6 Functionalized Glycolipids

The difference in reactivity between the primary hydroxyl group at C-6 and other secondary hydroxyl groups of the sugar head group enables a selective halogenation at C-6. As illustrated in **Scheme 4.4**, the synthesis started with an ester-based glycosylation of two commercial Guerbet alcohols (Hashim *et al.*, 2006). Subsequent selective bromination at C-6 of the glucosides, applied N-bromosuccinimide and triphenylphosphine, followed by an acetylation reaction to facilitate the purification for the products (**11**-**12**) by chromatography (Stanek, 1963). The bromination was performed under nitrogen atmosphere and provided a higher yield than the literature reported analogous transformation (Hanessian *et al.*, 1972).

Functionalization of the glucosides by quaternization of the alkyl imidazole required high temperature condition, therefore xylene was employed as the solvent (Maton *et al.*, 2015). Final deacetylation of the imidazolium compounds successfully furnished two series of C-6 functionalized glycolipids in an overall yield of about 40 % based on Guerbet glucoside (**9**, **10**).

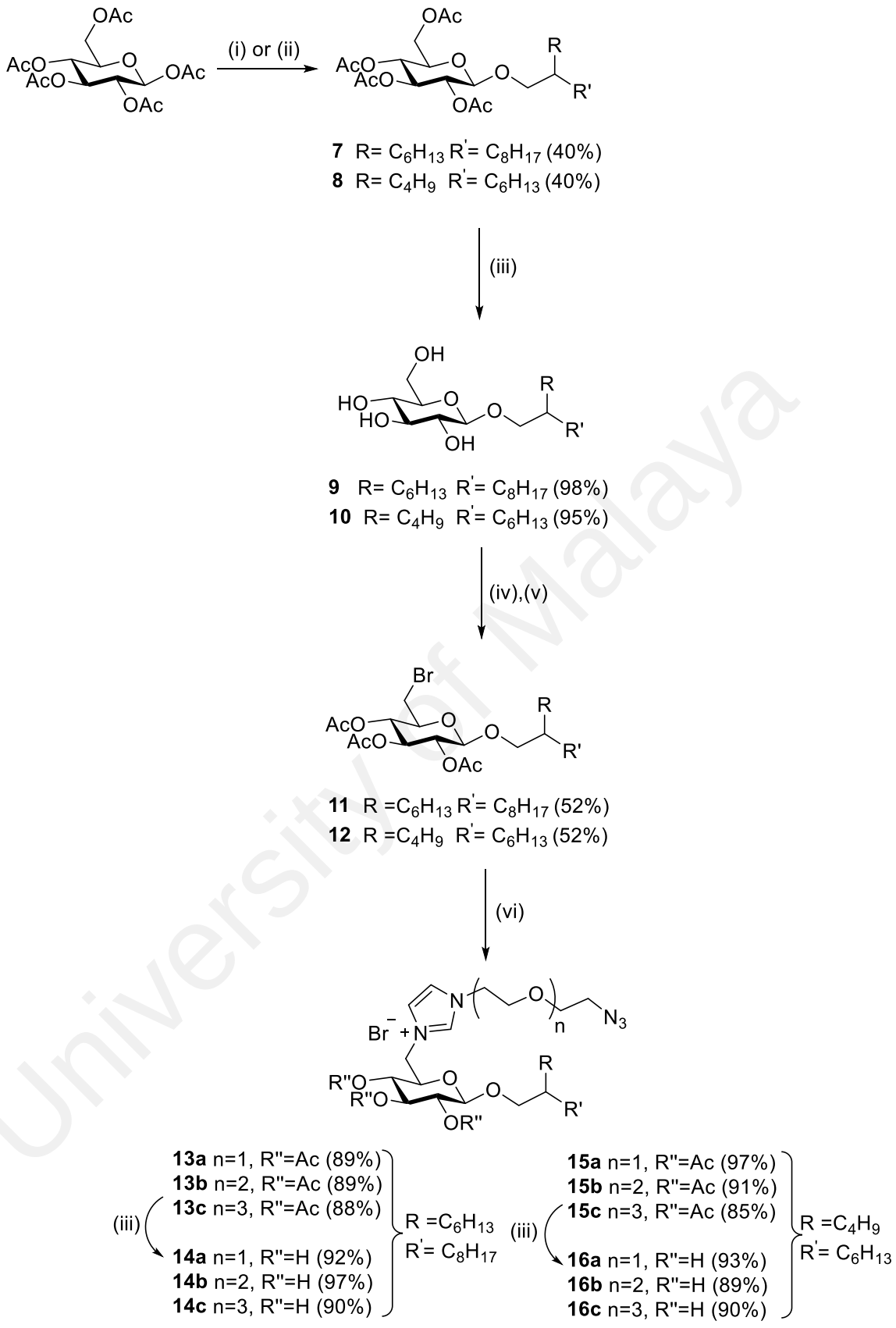

Scheme 4.4: Synthesis of C-6 functionalized glycolipids.

4.3.2 Synthesis of C-4 Functionalized Glycolipids

Straight chain glycolipid **18** was employed as a model compound for the preparation of C-4 functionalized glycolipids, as the synthesis involved intermediates that had been previously reported. Moreover, the intermediates were isolated based on easy extraction and crystallization procedures instead of chromatographic purification (Sabah *et al.*, 2011). As shown in **Scheme 4.5**, selective opening of the 4,6-*O*-benzylidene afforded compound **21** with a free hydroxyl group at C-4. Two different approaches, indicated as **(v)** and **(vi)** in **Scheme 4.5**, were applied. The former involved iodine complexation with the electron pair on the glucoside's O-4 in combination with a cyanoborohydride and provided a relatively lower yield (Rao *et al.*, 2010), compared to the latter approach, which applied triethylsilane and trifluoroacetic acid (Kasuya *et al.*, 2007).

Seeing that a halogen group was essential for associating the alkyl imidazole-based functionalized linkers with the glucoside, a few attempts to introduce bis-halogen- and bis-tosyl-terminated spacers with structures as shown in **Scheme 4.6** were carried out. Amongst them, only alkylation with spacer **23** proceeded based on TLC analysis, as illustrated in **Scheme 4.7**. Since the CLICK functionality is unstable towards hydrogenation, the benzyl groups of compound **24** were replaced with acetates in a 2-step sequence before introduction of the functionalized linker, but the yield was very low. Moreover, the subsequent Menshutkin reaction with linker **3a** was incomplete.

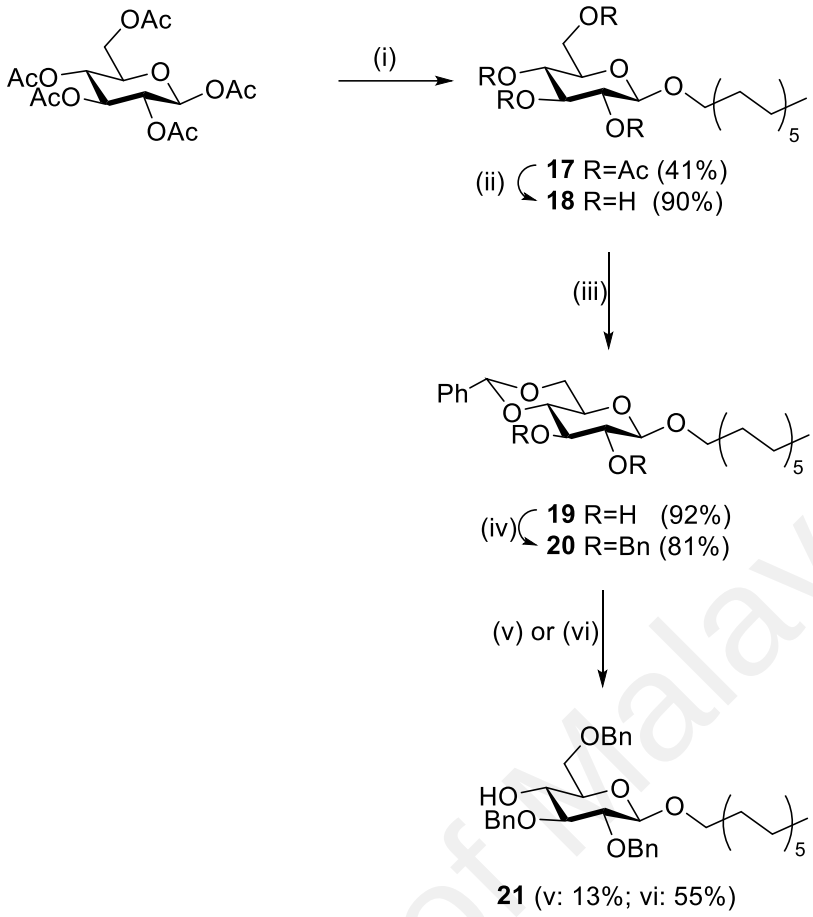

(i) 1-Dodecanol, $BF_3.OEt_2$, CH_2Cl_2; (ii) $NaOCH_3$, CH_3OH; (iii) $PhCH(OCH_3)_2$, *p*-TsOH,CH_2Cl_2; (iv) NaH, BnBr, DMF; (v) $NaCNBH_3$, I_2, CH_3CN; (vi) Et_3SiH, TFA, CH_2Cl_2.

Scheme 4.5: Synthesis of **21**.

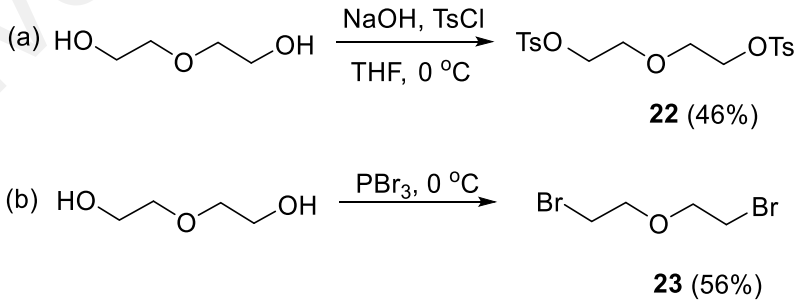

Scheme 4.6: Preparation of spacers **22** and **23**.

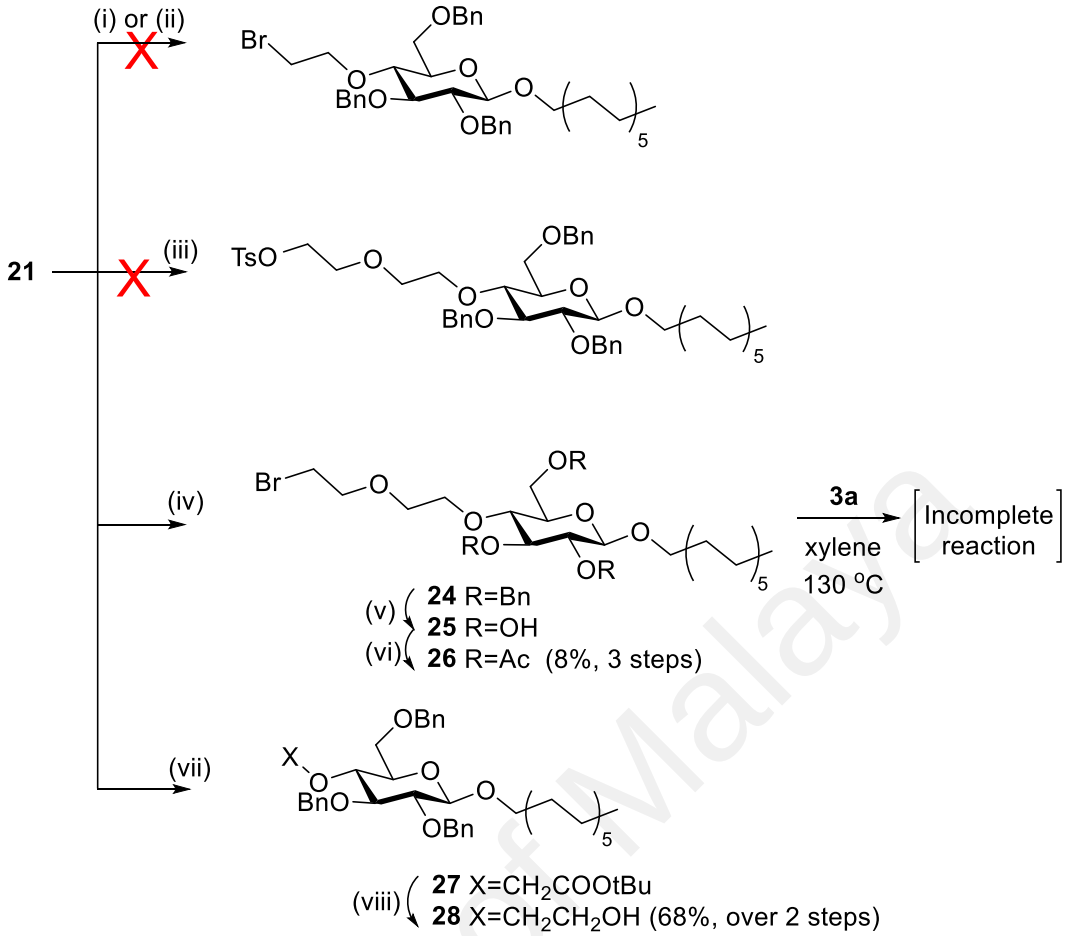

(i) Dibromoethane, toluene, 50 % NaOH (aq), TBAB; (ii) NaH, dibromoethane, DMF; (iii) **22**, toluene, 50 % NaOH (aq), TBAB; (iv) NaH, **23**, DMF; (v) H_2, Pd/C, CH_3OH; (vi) Ac_2O, pyridine; (vii) tert-butyl bromoacetate, toluene, 50 % NaOH (aq), TBAB; (viii) $LiAlH_4$, THF, 0°C.

Scheme 4.7: Different attempts at preparing the C-4 glycolipid cores.

The failures of the previously discussed alkylation might be due to low reactivity of the alkyl bromides. Consequently a more reactive, tert-butyl bromoacetate, was used and the tert-butyl ester was successfully introduced at O-4 of glucoside **21**, followed by a reduction to furnish a less hindered, primary alcohol in compound **27** in a reasonable yield, as depicted in **Scheme 4.7**.

Two strategies were attempted to convert this hydroxyl group into a halogen. As illustrated in **Scheme 4.8**, one involved tosylation of the hydroxyl group, followed by

conversion of benzyl ethers into acetates prior to an iodide exchange reaction. However, the compound resulted from acetylation of glucoside **30** was found missing tosyl group signals in the ^{1}H NMR spectrum. On the other hand, direct iodination of the hydroxyl group successfully produced iodo-sugar **32** in a good yield (Sletten & Liotta, 2006). The compound was subjected to a 2-step reaction to convert the benzyl ethers to acetates prior to functionalization. Unfortunately, the resulting compound missed the ^{13}C-I signal in the ^{13}C NMR spectrum. The result can be explained with the formation of a cyclic ether due to the favourable 6-membered ring during the acetylation, as illustrated in **Scheme 4.8**.

Multiple failures in producing a halogenated sugar unit led to a modified synthetic strategy, in which an imidazole-bearing sugar and a halogen-terminated linker (as discussed in **Scheme 4.3** of section **4.2**) were targeted. As a result, highly polar imidazole-bearing sugar compound **35** was successfully synthesized in a 3-step sequence, in an overall yield of 35 % based on **32**. Unlike the typical arrangement for hydrogenolysis of benzyl ethers, hydrochloric acid was used in this case instead of acetic acid to ensure acidic condition, considering the significant basicity of the alkyl imidazole compound.

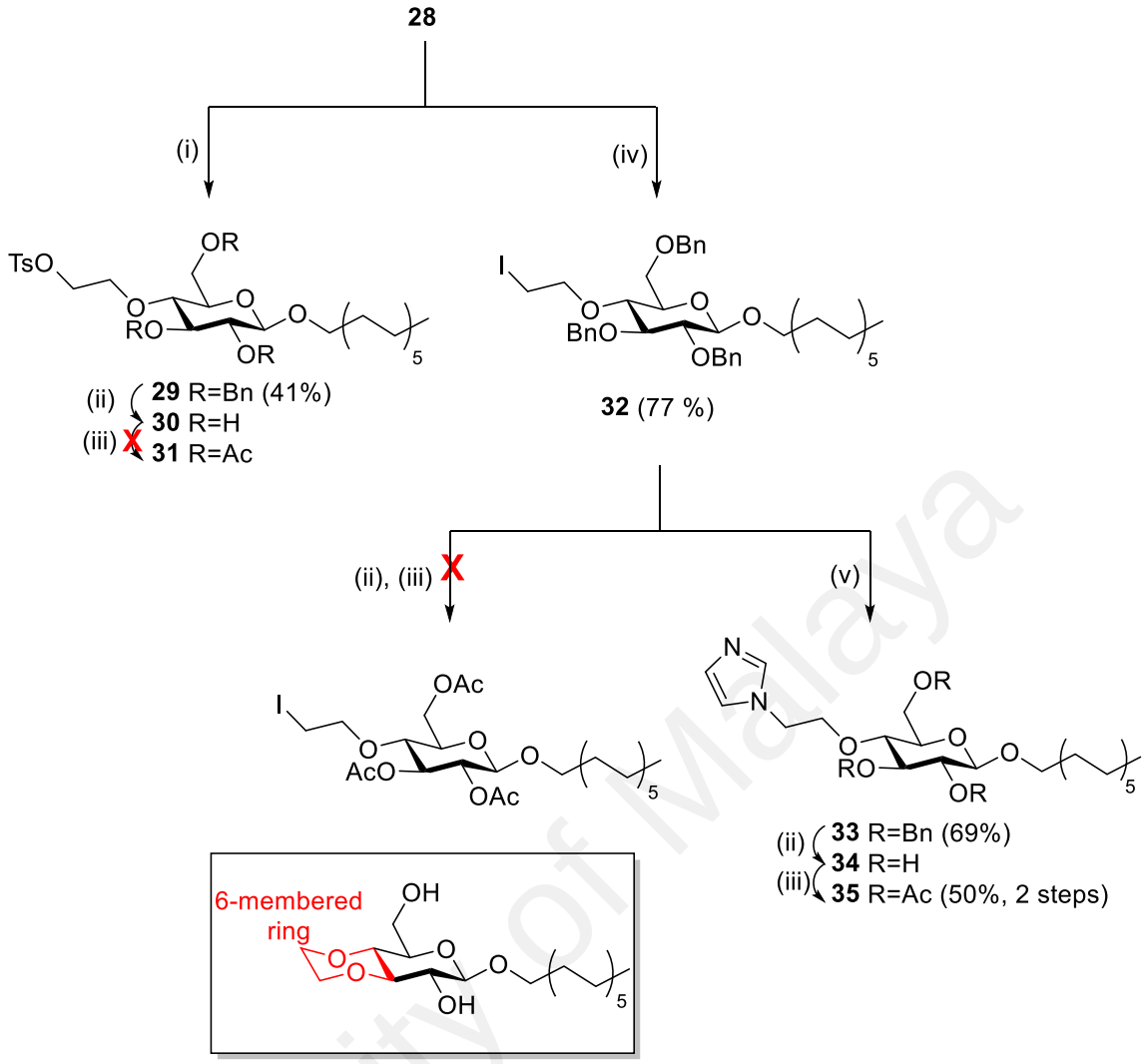

(i) NaOH, TsCl, THF, 0 °C; (ii) H_2, Pd/C, CH_3OH; (iii) Ac_2O, pyridine;
(iv) I_2, PPh_3, imidazole, toluene, 50 °C; (v) NaH, imidazole, THF, reflux.

Scheme 4.8: Preparation of the C-4 glycolipid core from **28**.

Functionalization of compound **35** with linker **6** employed similar reaction condition applied for preparation of the C-6 functionalized glycolipids. However, remaining starting material **35** in the TLC indicated an incomplete reaction. The appearance of a black product that poorly soluble in most of the organic solvents suggested decomposition of the linker.

Accordingly, milder reaction conditions were applied as shown in **Scheme 4.9**. Cationic acetylated sugar compound was successfully produced and subsequent deacetylation furnishing the C-4 functionalized glycolipid **37**.

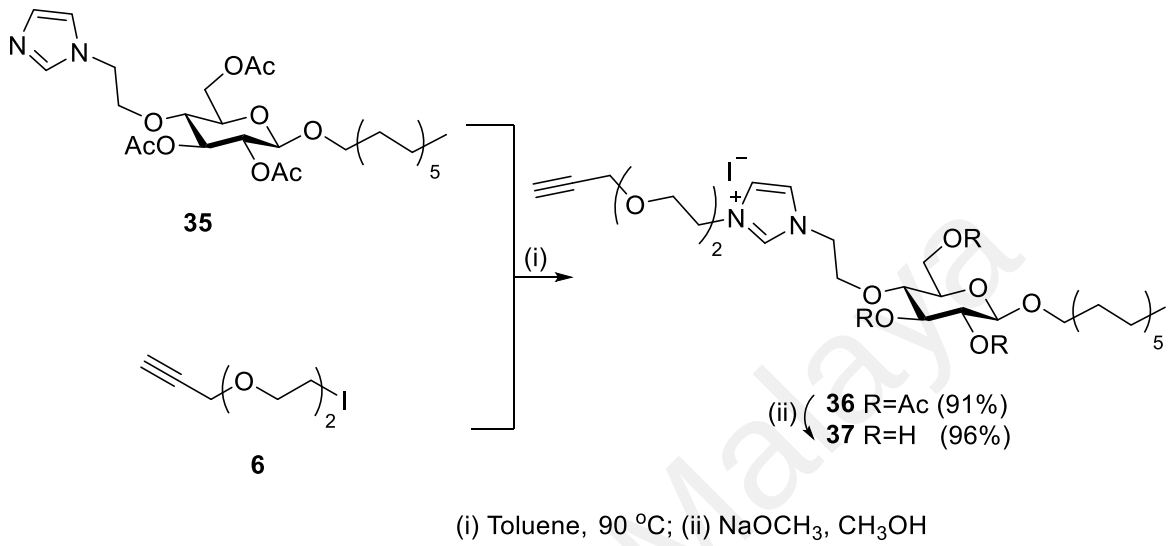

Scheme 4.9: Synthesis of C-4 functionalized glycolipid **37**.

The successful preparation of **37** led to synthesis of branched chain, C-4 functionalized glycolipids **48a** and **48b** following the same procedure, as summarized in **Scheme 4.10**.

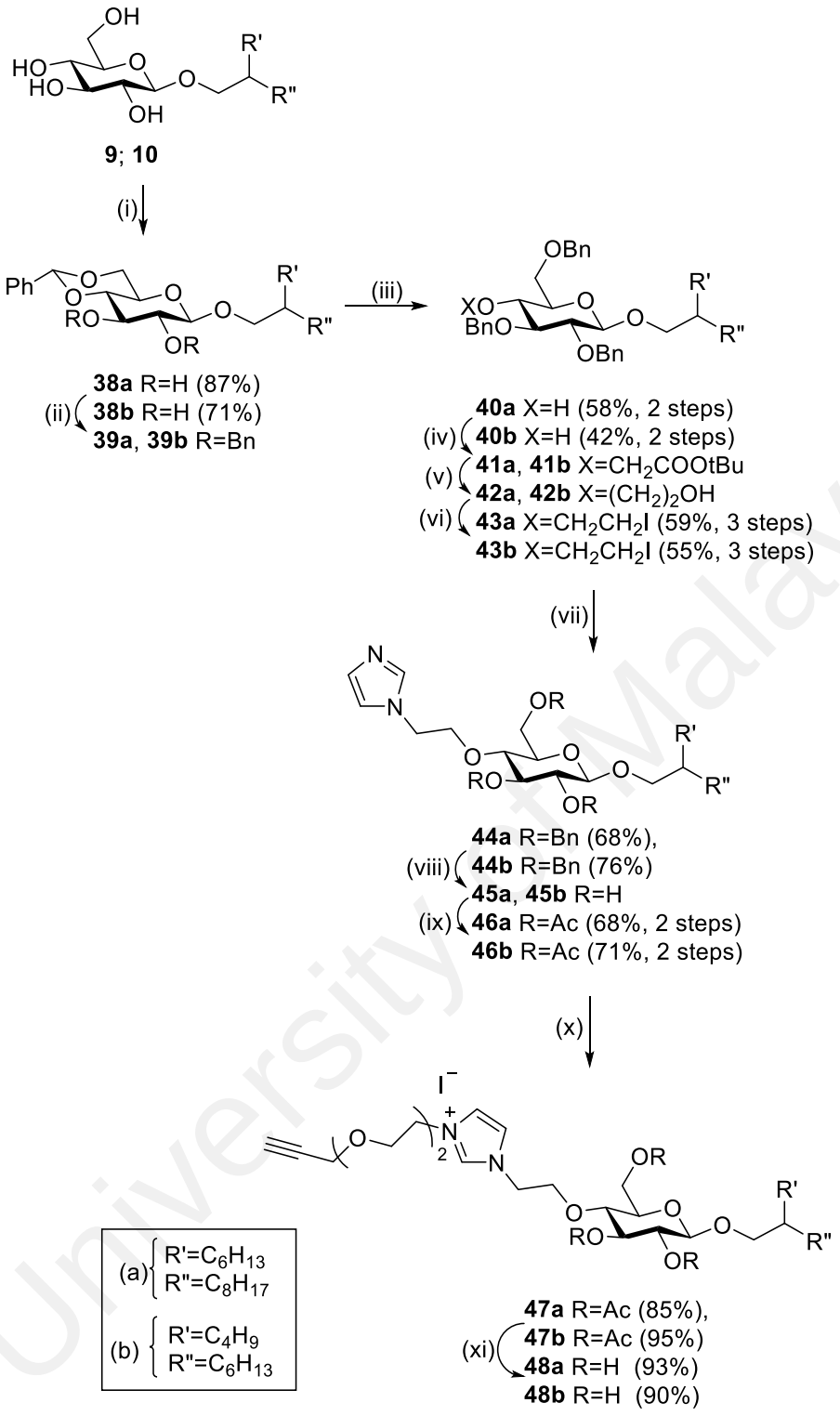

(i) $PhCH(OCH_3)_2$, *p*-TsOH, CH_2Cl_2; (ii) NaH, BnBr, DMF; (iii) Et_3SiH, TFA, CH_2Cl_2; (iv) tert-butyl bromoacetate, toluene, 50% NaOH (aq), TBAB; (v) $LiAlH_4$, THF, 0 ^oC; (vi) I_2, PPh_3, imidazole, toluene, 50 ^oC; (vii) NaH, imidazole, THF, reflux; (viii) H_2, Pd/C, CH_3OH; (ix) Ac_2O, pyridine; (x) **6**, toluene, 90 ^oC; (xi) $NaOCH_3$, CH_3OH.

Scheme 4.10: Synthesis of branched chain C-4 functionalized glycolipids.

4.3.3 Synthesis of C-1 Functionalized Glycolipids

The preparation of C-1 functionalized glycolipids involved functionalization at the anomeric center, while the hydrophobic chain was targeted to be introduced elsewhere, which made this synthesis challenging. Since position C-6 is easily accessible due to its higher reactivity compared to the other hydroxyl groups, it was aimed as the target site for attaching the hydrophobic domain by Staudinger coupling (Staudinger & Jules, 1919; Gololobov & Kasukhin, 1992; Salman *et al.*, 2014).

The overall synthetic scheme is illustrated in **Scheme 4.11**. Commercially available methyl-α-D-glucoside was used as starting material. A selective chlorination was performed using chlorinating agent, N-chlorosuccinimide and triphenylphosphine under nitrogen atmosphere (Hanessian *et al.*, 1972), followed by an acetylation to facilitate chromatographic purification of target compound **51**. Subsequent nucleophilic substitution with sodium azide furnished azido compound **52** in a very good yield. The reactivity of the anomeric centre improved by acetolysis of the methyl glucoside **52** (Guthrie & McCarthy, 1967) and the resulting α-anomer **53** was isolated by crystallization from ethanol (Combemale *et al.*, 2014).

An easy approach to introduce a halogen terminated aglycone unit at C-1 of **53** appeared to be an ester glycosylation using 2-chloroethanol. However, the reaction did not proceed as indicated by TLC. Thus, classic Fischer glycosylation was employed, which required deacetylation of **53** prior to acid catalyzed glycosylation with 2-chloroethanol (Fischer, 1893; Sani *et al.*, 2012). The resulting free glucoside underwent an acetylation to give less polar **56**, which was isolated as an anomeric mixture (α: β=3: 2) by chromatography in an overall yield of 61 % based on **54**. To avoid complication during structural elucidation, only the major α-anomer **57** was isolated after Staudinger coupling of glycoside **56** with palmitoyl chloride (Maunier *et al.*, 1997). The low reaction

yield reflects the molar ratio of anomeric pure **57** to anomeric mixture **56**. To ensure a more efficient quaternization with linker **3b**, the chloride was exchanged to an iodide. Complete conversion of the chloro group was indicated by the disappearance of ^{13}C-Cl (42.5 ppm) and emergence of new ^{13}C-I (1.6 ppm) signal in the ^{13}C NMR spectrum. Lastly, deacetylation of imidazolium compound **59** successfully produced the C-1 functionalized glycolipid **60** in an overall yield of 28 % based on **56**. The same synthetic procedure was carried out in attempt to produce a branched chain functionalized glycolipid as well. However, the isolation of intermediate **61** was unsuccessful, owing to its very similar Rf with the unreacted material **56** and other side-product, particularly the triphenyl phosphine oxide.

The use of triphenylphosphine in Staudinger coupling complicated the purification process of the resulting amide, owing to the side-product, triarylphosphine oxide, which shares a very similar Rf with the amide product. Therefore, another synthetic strategy was proposed, which involved glucosamine as an alternative starting material that enables the introduction of the hydrocarbon chain by acylation of the amino group at C-2, without the use of a phosphine reagent. As depicted in **Scheme 4.12** (red), the glucosamide **67** was firstly prepared by treating the commercially available glucosamine hydrochloride with a strong base to restore its basicity, followed by direct acylation with 2-hexyldecanoyl chloride (Boullanger *et al.*, 1987). The target compound **67** was obtained as a white solid by crystallization from diethyl ether, yet the yield was extremely low. Moreover, the purification procedure based on chromatography could not be carried out since the crude product was a complex mixture of many compounds, resulting from acylation of the hydroxyl groups as well. Accordingly, initial protection of the hydroxyl groups was performed as shown in **Scheme 4.12** (blue). Although additional synthetic steps were required, this approach appeared to be more efficient in comparison with the previous procedure. It gave a better overall yield of amide **67** and isolation of the

intermediates required simple crystallization. Detailed structural studies were avoided as the synthesis of **66** had been reported in the literature (Biswas *et al.*, 2017).

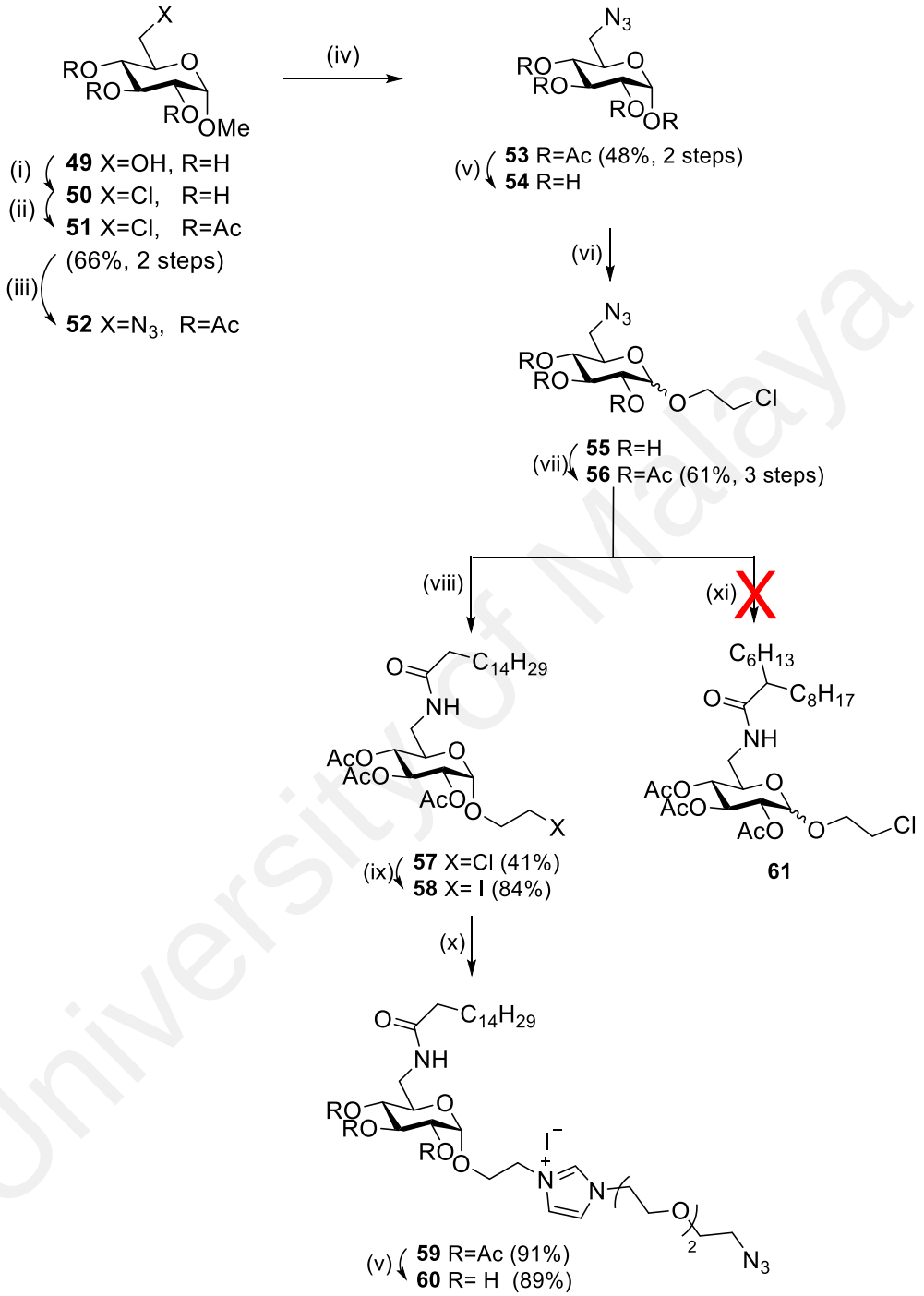

(i) NCS, PPh_3, DMF, 70 ^oC; (ii) Ac_2O, pyridine; (iii) NaN_3, DMF, 80 ^oC; (iv) Ac_2O:AcOH:H_2SO_4= 5:4:1, Ac_2O, 0 ^oC; (v) $NaOCH_3$, CH_3OH; (vi) 2-chloroethanol, H^+, 80 ^oC, 5h; (vii) Ac_2O, pyridine; (viii) palmitoyl chloride, PPh_3, CH_2Cl_2; (ix) NaI, acetone, reflux; (x) **3b**, toluene, 90 ^oC; (xi) 2-hexyldecanoyl chloride, PPh_3, CH_2Cl_2.

Scheme 4.11: Synthesis of C-1 functionalized glycolipid.

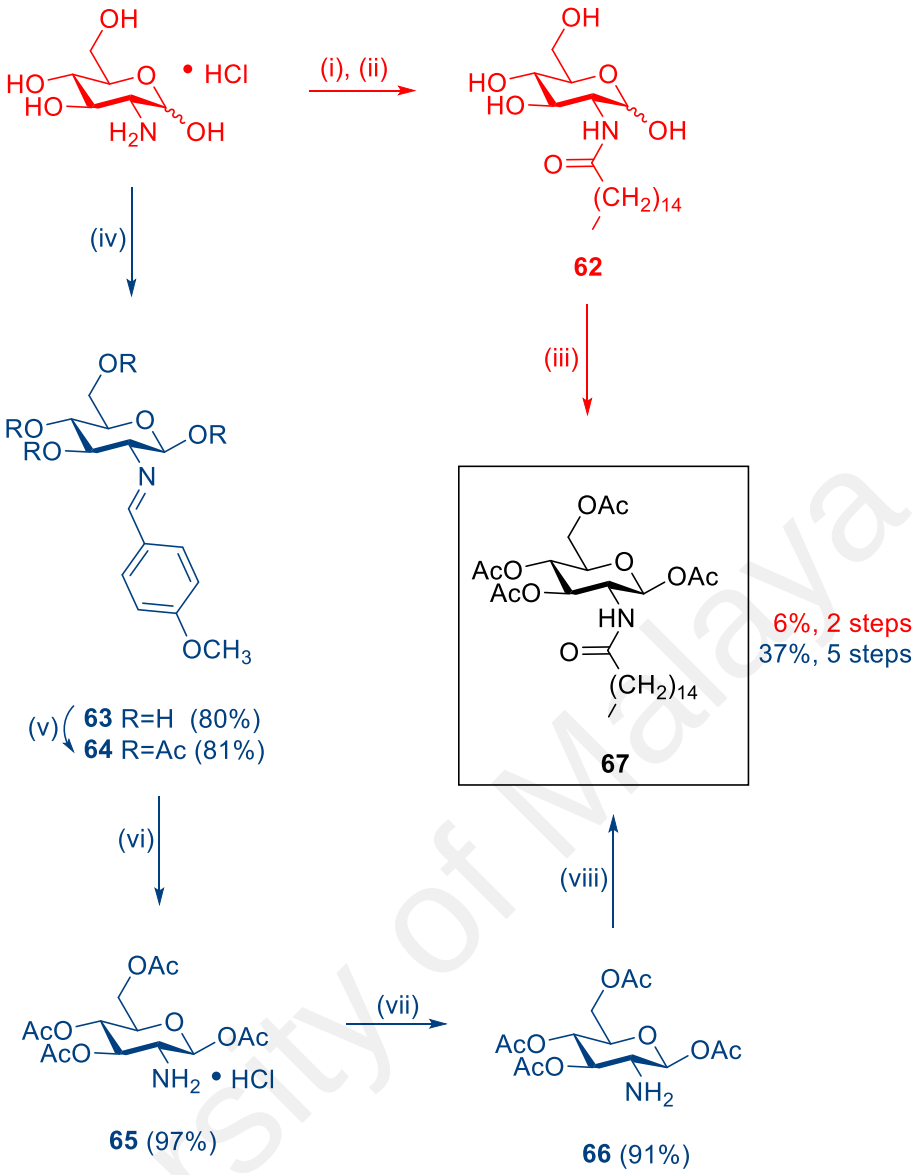

(i) $NaOCH_3$, CH_3OH; (ii) palmitoyl chloride, Et_3N; (iii) Ac_2O, pyridine; (iv) *p*-anisaldehyde, 1 M NaOH (aq); (v) Ac_2O, pyridine; (vi) 5 M HCl, acetone; (vii) 1 M Na_2CO_3 (aq), CH_2Cl_2; (viii) palmitoyl chloride, Et_3N, CH_2Cl_2.

Scheme 4.12: Different synthetic pathways for sugar amide **67**.

To introduce the aglycone moiety, ester glycosylation was attempted as shown in **Scheme 4.13**. However, it resulted in a complex mixture of compounds, which rendered the identification of the target compound on TLC impossible. Instead the glycosyl acetate was converted into a more reactive bromide and reaction with 2-chloroethanol in the presence of tertra-n-butylammonium bromide catalyst was attempted (Jia *et al.*, 2006). However, the resulting compound was a stable oxazoline **71**, instead of the targeted amide

69. Opening of the oxazoline under acidic condition was attempted (Szabo, 1989), but a complex mixture of highly polar products was obtained which rendered the identification of the target compound impossible.

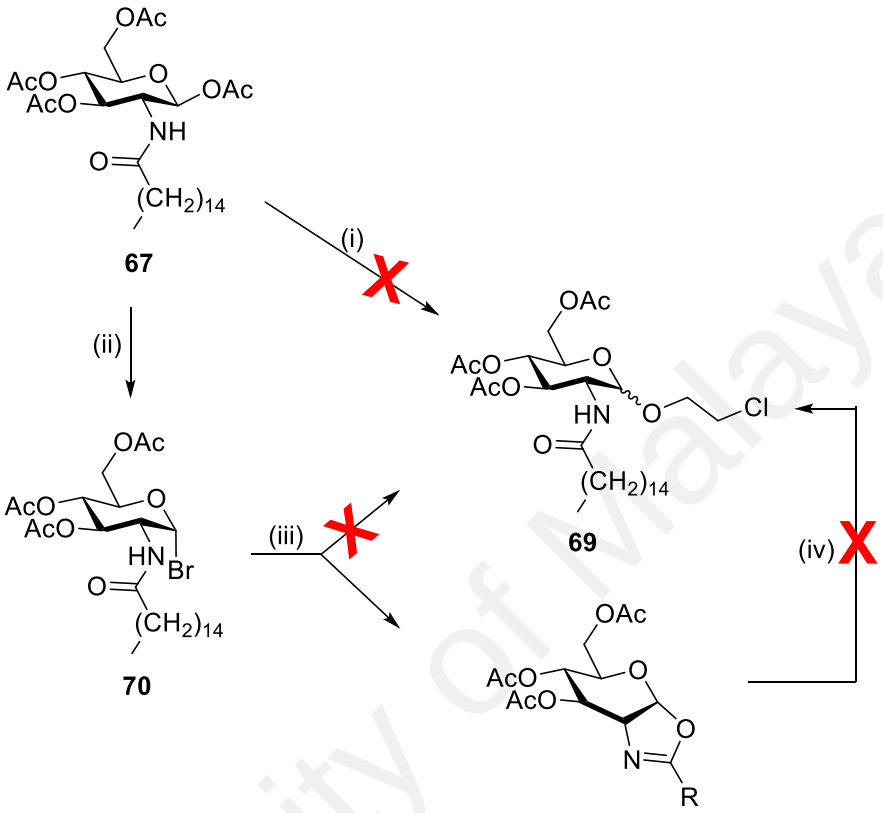

(i) 2-Chloroethanol, $BF_3.Et_2O$, CH_2Cl_2; (ii) 33 % HBr in AcOH, AcOH; (iii) 10 % Na_2CO_3 (aq), TBAB, 2-chloroethanol, CH_2Cl_2;
(iv) *p*-TsOH, 2-chloroethanol, $Cl(CH_2)_2Cl$, 50 ^oC.

Scheme 4.13: Attempts to introduce the aglycone.

4.4 Physical Properties Studies

4.4.1 Studies of Bis-(alkylimidazolium)-glycosides

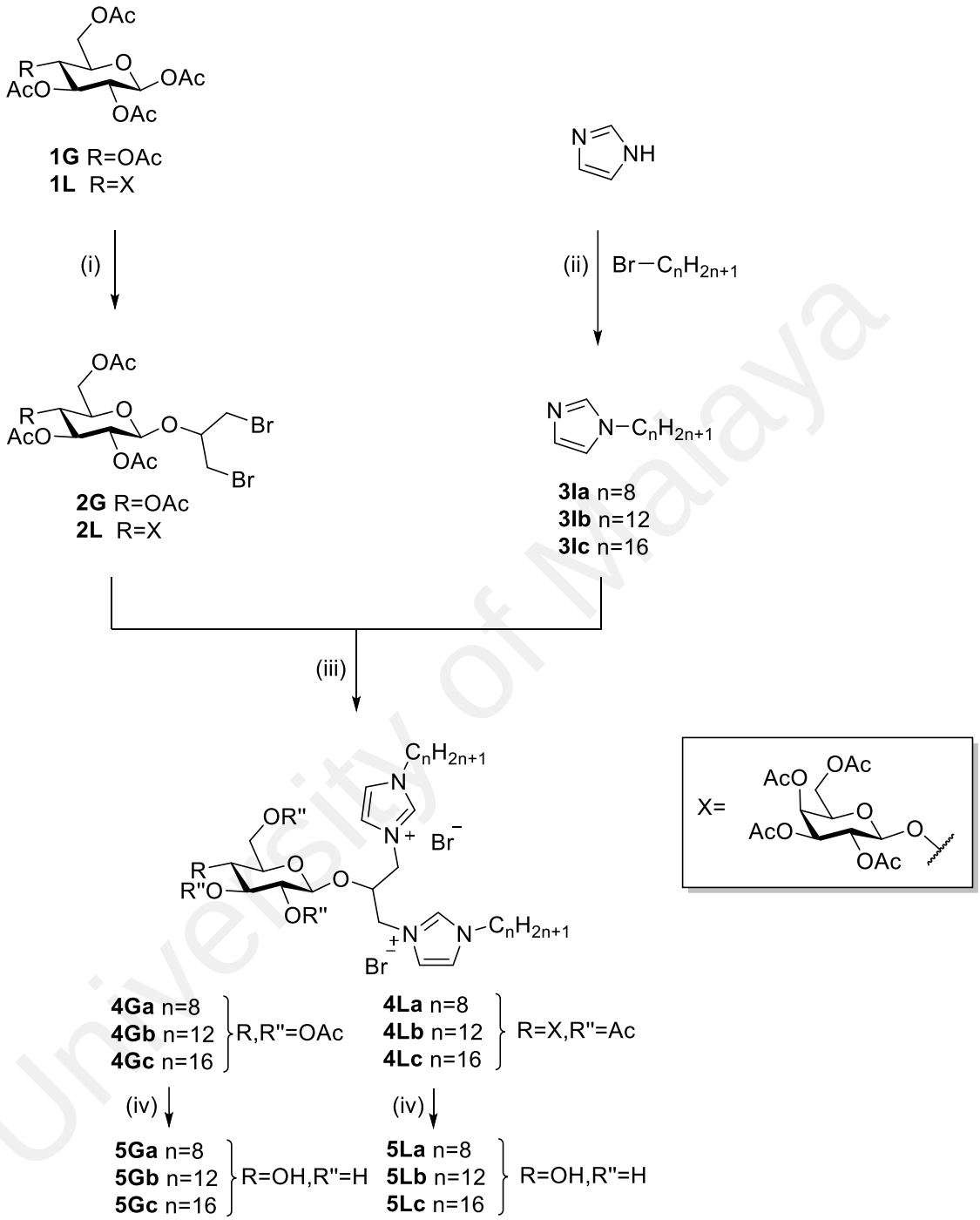

(i) 1,3-Dibromo-2-propanol, $BF_3.Et_2O$, CH_2Cl_2;
(ii) NaH, THF; (iii) xylene, 130 ^oC; (iv) $NaOCH_3$, CH_3OH

Scheme 4.14: Synthesis of bis-(alkylimidazolium)-glycosides.

The physical properties of two series of bi-antennary di-cationic glycosides, as shown in **Scheme 4.14** were studied to examine the effect of imidazolium component on the surfactant properties. The structures share the imidazolium linkage with the targeted functionalized glycolipids and were investigated as model compounds. The surfactants exhibited interesting assembly behaviour, particularly in the presence of anionic co-surfactants owing to strong ionic interactions.

4.4.1.1 Lyotropic Behaviour of Bis-(alkylimidazolium)-glycosides

The lyotropic assembly behaviour of the glycosides was studied using the solvent penetration method. The observations are summarized in **Table 4.1**. All glucosides exhibited low affinity for hydrophobic medium, while the lactosides displayed inverted hexagonal (H_{II}) phase when in contact with oil.

The penetration experiments with water revealed that both series were well soluble in water. As shown in **Figure 4.3** a non-birefringent dark band was observed in most of the glycosides within the water penetration zone indicated the formation of discontinuous cubic phase, reflecting a micellar assembly. Only lactoside **5Lc** displayed a less curved hexagonal phase (H_I), owing its larger hydrophobic volume resulting from the longer hydrophobic chain length. Since catanionic surfactants, *i.e.* mixtures containing both cationic and anionic surfactants at a desired molar ratio, have shown novel synergistic and enhanced surface properties (Khan & Marques, 1997), both **5Gb** and **5Lb** were subjected for a mixed surfactant study using commercially available anionic surfactants to provide insights into the effect on the assembly behaviour based on their electrostatic interaction. Their lyotropic assembly behaviour was evaluated based on observed textures, as shown in **Figure 4.4** and summarized in **Table 4.2**.

Figure 4.5 depicts the assembly of catanionic surfactants, reflecting their interaction with each other in the mixture. The incorporation of straight chain-based

anionic surfactant (SDS or sodium laurate) into the bis-imidazolium based surfactant by means of electrostatic interaction increased the hydrophobic volume to an extent where a balance between hydrophilic and hydrophobic domains was achieved, thus leading to a planar assembly. It explains the observation of lamellar phases, which was indicated by formation of Myelin (Al-Mohammed, Duali Hussen, Alias*, et al.*, 2015; Mak *et al.*, 2015), Maltese cross (Caboi & Monduzzi, 1996; Bibi *et al.*, 2011) and fan-shaped textures (Hashim *et al.*, 2006; Ali *et al.*, 2015) as shown in **Figure 4.4**. However, branched chain surfactant sodium 2-hexyl decanoate overcompensated the hydrophilic surface area, thus resulting in the formation of an inverted phase, due to the hydrophobic dominance.

Myelin textures were also observed when the glycolipids **5Gb** and **5Lb** were in contact with a phosphate-buffered solution. This indicated the ability of the phosphate anion to reduce the relative hydrophilic surface area due to ionic interaction with the imidazolium ion. The existence of such strong ionic interaction was also substantiated by presence of unusual peaks in the ESI-mass spectra, reflecting ionic aggregates of the doubly charged glycolipid with a bromide ion (Salman *et al.*, 2016).

Table 4.1: Lyotropic behaviour of **5G** and **5L**.

Glycosides	1-Nonanol	Water
5Ga	Insoluble	Cubic, H_I
5Gb	Insoluble	Cubic
5Gc	Insoluble	Cubic
5La	H_{II}	Cubic
5Lb	H_{II}	Cubic
5Lc	H_{II}	H_I

H_I - hexagonal phase; H_{II} - inverted hexagonal phase; Cubic – discontinuous or bi-continuous cubic phase.

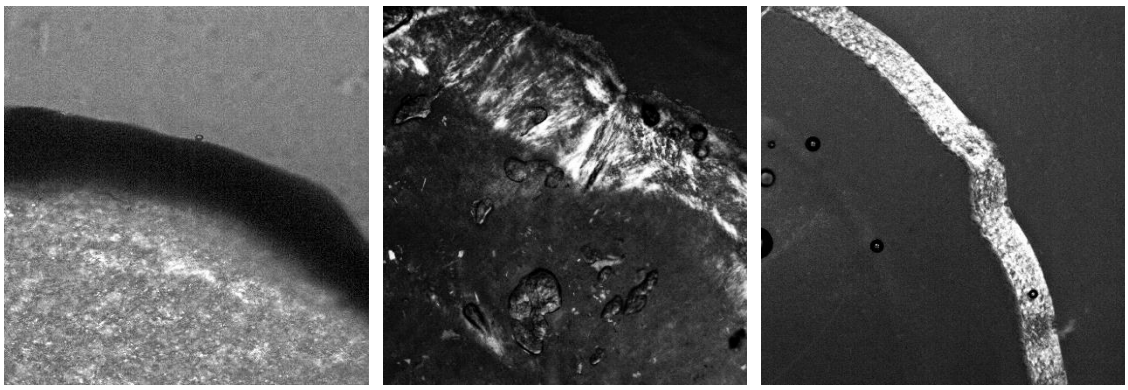

5Gb with H_2O **5Lc** with H_2O **5La** with 1-nonanol

Figure 4.3: Penetration experiments of bis-(alkylimidazolium)-gycosides.

Table 4.2: Lyotropic behaviour of surfactant mixture.

Cationic surfactant	Anionic surfactant	Ratio	Water	PO_4^{3-} buffer solution of pH 11
5Gb	-		C	L_α
	$C_{11}CO_2Na$	1:1	C	L_α
5Lb	-		C	L_I
	$C_{11}CO_2Na$	1:1	L_α	L_α
	$C_{11}CO_2Na$	1:2	L_α	H_I, L_α
	$C_9C_6CO_2Na$	1:1	C, L_α, H_{II}	C, L_α, H_{II}
	$C_9C_6CO_2Na$	1:2	I_{II}	I_{II}
	SDS	1:1	I_I, H_I, L_α	L_α
	SDS	1:2	L_α	L_α

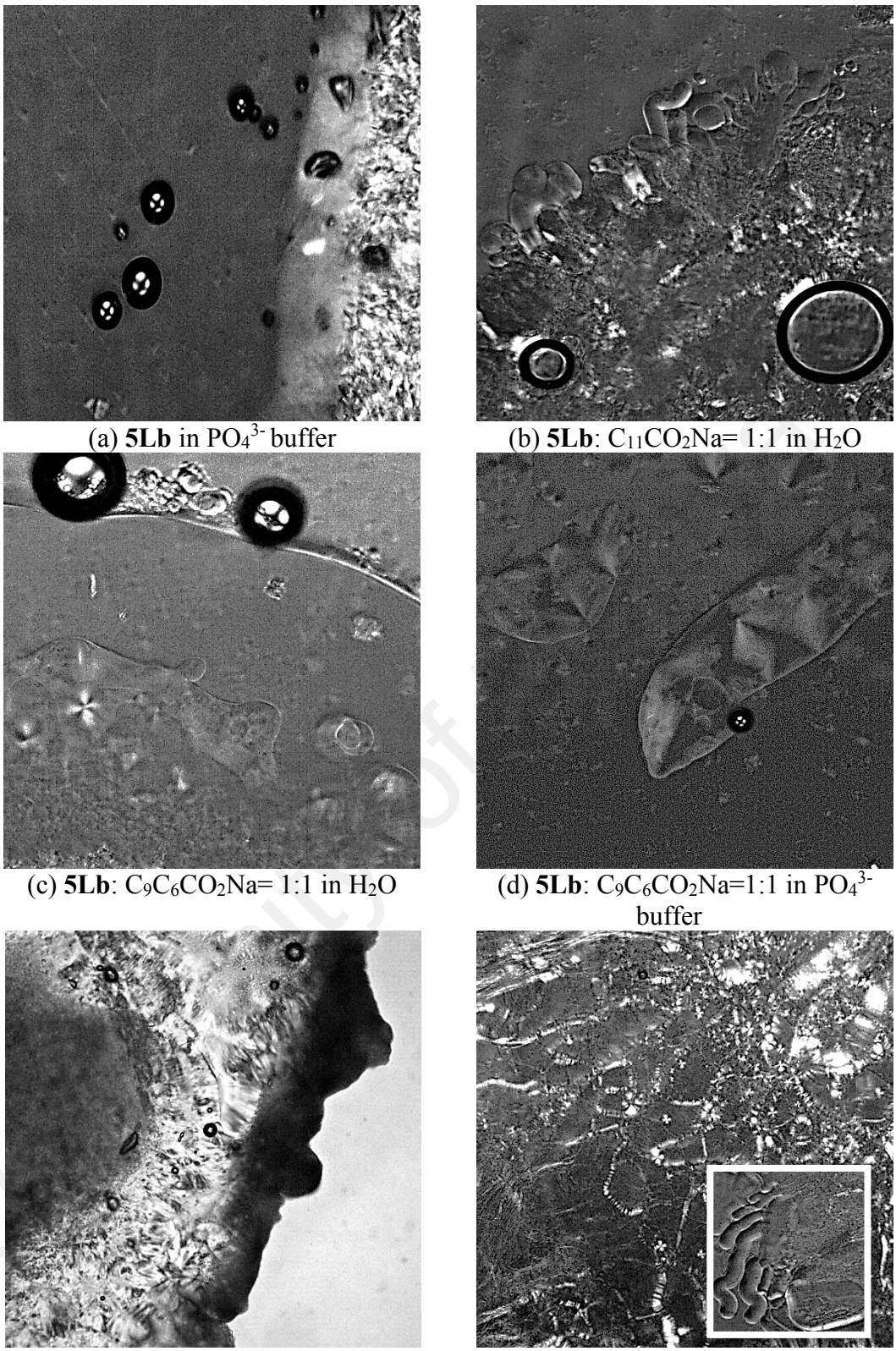

(a) **5Lb** in PO_4^{3-} buffer

(b) **5Lb**: $C_{11}CO_2Na$= 1:1 in H_2O

(c) **5Lb**: $C_9C_6CO_2Na$= 1:1 in H_2O

(d) **5Lb**: $C_9C_6CO_2Na$=1:1 in PO_4^{3-} buffer

(e) **5Lb**: SDS= 1:1 in H_2O

(f) **5Lb**: SDS= 1:1 in H_2O after 10 min

Figure 4.4: Lytropic LC textures: (a) Maltese cross; (b) Myelin; (c) focal conic fan; (d) H_{II}; (e) H_I and C; (f) lamellar phase.

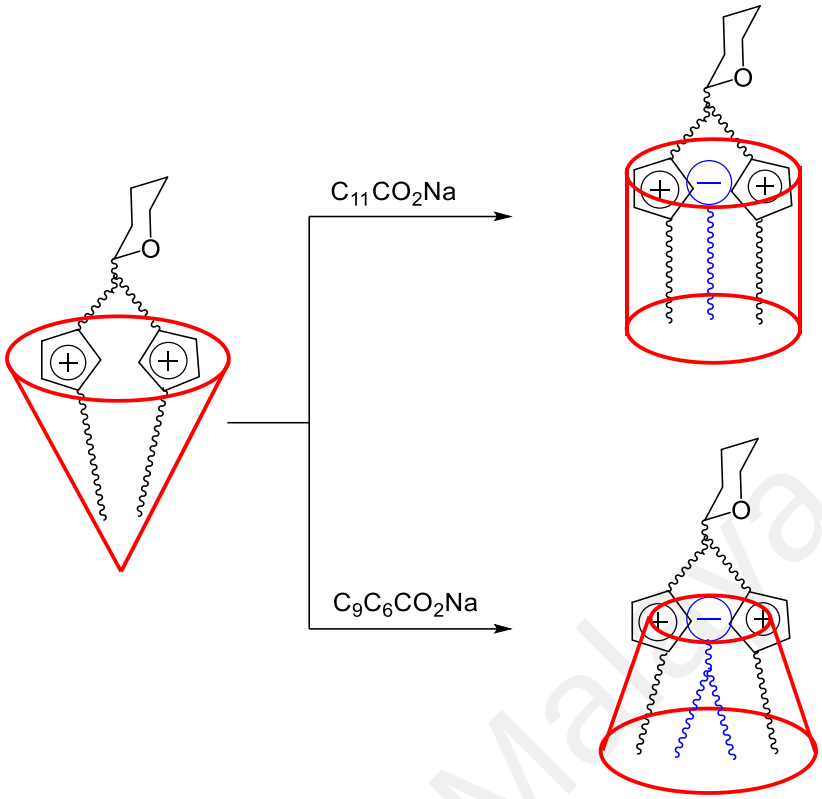

Figure 4.5: The effect of anionic surfactants on the overall surfactant's hydrophobic volume.

4.4.1.2 Surface Properties of Bis-(alkylimidazolium)-glycosides

The critical aggregation concentrations (CACs) of surfactants were determined based on surface tension measurements using Du Nouy ring method to evaluate their assembly stability. Both glycosides **5Ga** and **5La** were exempted for this material-consuming study, owing to their limited amounts.

The CACs of the glycosides, presented in **Table 4.3**, are all in good agreement with the glycolipids of similar chain lengths (Coppola *et al.*, 2002; Hussen, 2012; Sani *et al.*, 2012; Salman *et al.*, 2014; Al-Mohammed, Duali Hussen, Ali, *et al.*, 2015; Al-Mohammed, Duali Hussen, Alias, *et al.*, 2015). The hydrocarbon chain length appeared to be the major factor governing the CAC, as compared to the hydrophilic carbohydrate domain (Nilsson *et al.*, 1998; Hussen, 2010). The minima at the region of high surfactant

concentration as shown in **Figure 4.6**, indicated the presence of surface active impurities (Frese *et al*, 2003), which might be the unreacted alkyl imidazole **3lb**.

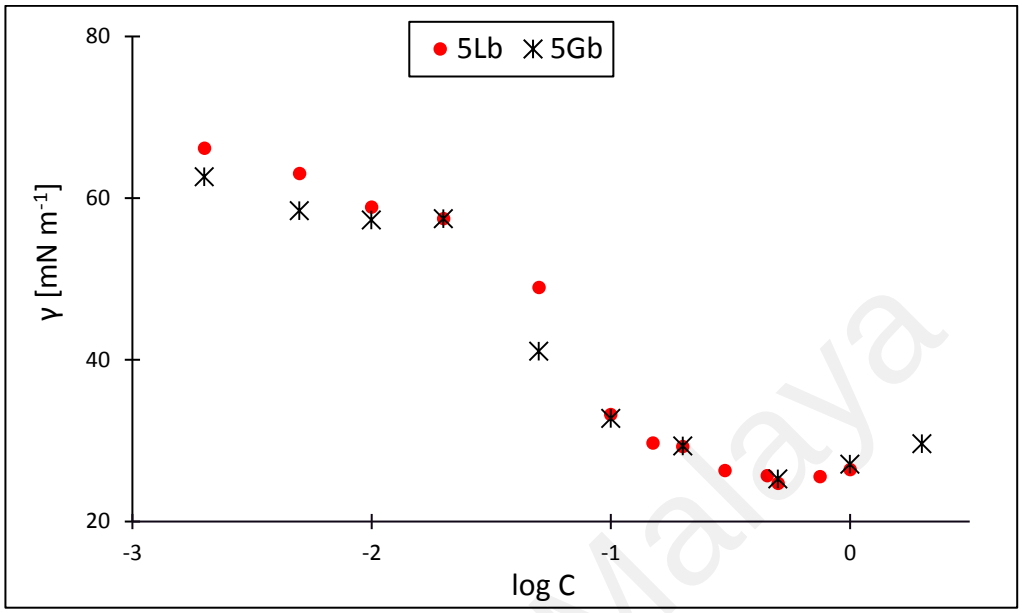

Figure 4.6: CACs determination for **5Gb** and **5Lb**.

Table 4.3: Surface properties.

Surfactant	CAC, mM	γ_{CAC}, mN m^{-1}	$A_{interface}$, Å^2	A/chain, Å^2
5Gb	0.18	29	114*	57
5Gc	0.03	41	120*	60
5Lb	0.21	26	126*	63
5Lc	0.02	40	120*	60
5Lb : SDS (1:1)	0.19	23	156#	52

Equation (3.1): * $n = 3$; # $n = 2$

In view of the interesting observation obtained from the catanionic surfactants during lyotropic phase studies, their mixing behaviour in water was then evaluated based on their interaction parameter, β which was determined from surface tension measurements (Hoffmann & Poessnecker, 1994). A surfactant mixture containing **5Lb** and SDS was chosen for this study, in view of the available amount of **5Lb**.

Figure 4.7 indicates synergistic effect, reflecting the lowered CAC of catanionic surfactants compared to that of the pure component **5Lb** (Sarmoria *et al.*, 1992). This suggested the formation of more stable aggregate in water according to the thermodynamics of aggregation, as demonstrated in equation 4.1 (Butt *et al.*, 2003; Nagarajan, 2003). The reduction in free energy of aggregation, ΔG_{agg} was caused by the cutback of electrostatic repulsion between the imidazolium cations, due to the presence of oppositely charged SDS as counterions (Tondre & Caillet, 2001; Sohrabi *et al.*, 2008).

$$\Delta G_{agg} = RT\ ln\ CAC \qquad (4.1)$$

Where,

R = gas constant and

T = temperature.

Besides, enhanced surface activity of the catanionic mixture was indicated by its lowered minimum surface tension, γ_{CAC}. Oppositely charged surfactants were packed more closely, due to their strong electrostatic attraction, and it allowed more surfactant molecules to be adsorbed at water/ air interface, thus reducing the surface tension more effectively (Wong *et al.*, 2011).

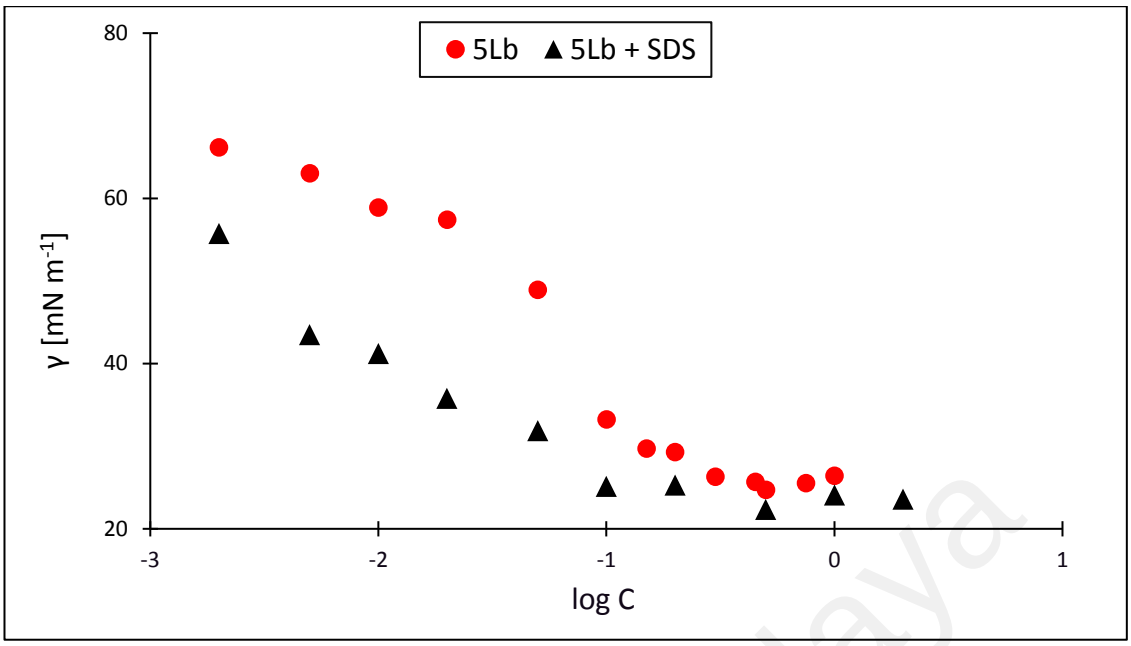

Figure 4.7: Surface properties of **5Lb** and the surfactant mixture.

The interaction parameter, β, of the catanionic mixture was determined based on the following equations (Zhang *et al*, 2004; Negm & Sabagh, 2011).

$$\frac{X_1^2 ln(\frac{\propto_1 C_{12}}{X_1 C_1^0})}{(1-X_1)^2 ln\frac{(1-\propto_1)C_{12}}{(1-X_1)C_2^0}} = 1 \qquad (4.2)$$

$$\frac{\ln(\frac{\propto_1 C_{12}}{X_1 C_1^0})}{(1-X_1)^2} = \beta \qquad (4.3)$$

Where,

X_1 = mole fraction of surfactant 1 (**5Lb**) in mixed micelles;

$\propto_1$ = mole fraction of surfactant 1 in total concentration;

C_1^0 = CAC of surfactant 1;

C_2^0 = CAC of surfactant 2 (SDS) and

C_{12}^0 = CAC of the catanionic mixture.

Table 4.4: Surface tension data analysis for 5Lb and SDS.

5Lb:SDS	1:0	1:1	0:1
CAC (mM)	0.21	0.19	8.0*
5Lb micellar mole fraction, X_{5Lb}		0.72	
Interaction parameter, β		-6.0	
*Literature reported value (Zhang et al, 2004)			

As shown in **Table 4.4**, the negative value of β implies strong ionic attraction between the oppositely charged surfactants, which in line with the observation of their lyotropic behaviour.

Both surface excess concentration, Γ_{max} and surface area per molecule, A_{min} were determined based on equations 3.1 and 3.2. There was no significant difference found among the glycolipids' A_{min}, therefore implying neither carbohydrate head group nor hydrocarbon chain lengths gave notable influence on A_{min}. However, A_{min} of the surfactant mixture was found to increase significantly, which is reflected in its reduced slope at the concentration depending region, as presented in **Figure 4.7**. This result contradicted the previous observation of the phase behaviour that suggested hydrophobic dominance in the surfactant mixture. In order to rationalize it, the value of factor n in equation 3.1 was taken into consideration and assigned according to the types of the surfactant system. For surfactant solutions containing only the pure glycolipid is assumed to have n= 3, owing to the presence of a divalent ionic gemini glycolipid and a monovalent counter ion. Considering the strong electrostatic interaction between **5Lb** and SDS, the surfactants were assumed to appear as a cluster instead of individual species, in which one of the imidazolium ions was neutralized by an anionic head group of SDS (Zana, 2005). This gave n= 2 instead of n= 3. Taking into account the number of hydrophobic chains, the surfactant mixture (**5Lb** and SDS) demonstrated a decrease in the A_{min}, as shown in **Table 4.3**, which tallies with the results of their lyotropic phase behaviour.

4.4.1.3 Vesicle Preparation and Size Determination

The catanionic mixture of **5Lb** and SDS was used for vesicle preparation based on the expected potential for micelles-to-vesicles transition upon mixing the two surfactants (Yaacob & Bose, 1996; Söderman *et al.*, 1997; Marques *et al.*, 1998). Surfactant solutions of **5Lb** and SDS at concentrations above their respective CACs were physically mixed following a molar ratio of 1: 2 to furnish a clear vesicle dispersion. The vesicle size was determined based on dynamic light scattering. The result was a uniform average diameter of 65 nm, as shown in **Figure 4.8**.

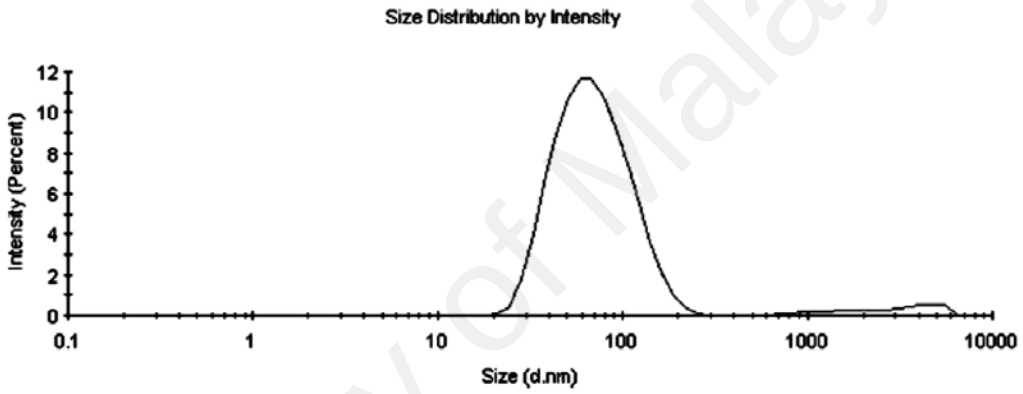

Figure 4.8: Vesicle size distribution of surfactant mixture **(5Lb** and **SDS**).

The appearance of the freshly prepared vesicles dispersion was translucent, owing to the formation of small-sized vesicles. However, the dispersion was found cloudy and turned opaque after 2 weeks of storage, due to the aging process whereby the small vesicles aggregated to form larger vesicles over time as shown in **Figure 4.9**. The transition of micelles-to-vesicles was depending on the overall packing parameter after mixing **5Lb** with SDS. Therefore it was assumed that the hydrolysis of SDS into dodecyl alcohol did not affect the stability of vesicles (Marques, 2000; Stuart & Boekema, 2007). The vesicle stability might be improved by inclusion of cholesterol, which could create

spacing effects that reduce the tendency of counter ion binding onto the vesicular surface (Kuo *et al.*, 2018).

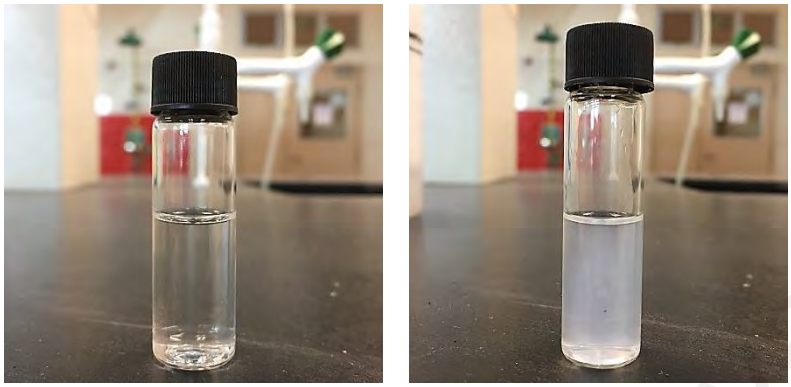

Figure 4.9: Freshly prepared vesicle dispersion (left) and after 2 weeks (right).

4.4.2 Studies of Functionalized Glycolipids

4.4.2.1 Lyotropic Behaviour of Functionalized Glycolipids

The lyotropic assembly behaviour of the functionalized glycolipids were evaluated based on the water penetration technique. The observations are summarized in **Table 4.5**.

Table 4.5: Lyotropic behaviour of functionalized glycolipids.

Surfactant	Lyotropic phases
18	L_I #
14a	soluble
14b	soluble
14c	soluble
16a	soluble
16b	soluble
37	C
48a	H_I, V_I, $L\alpha$
60	H_I

C- cubic (bicontinuous or discontinuous cubic phase); H_I - hexagonal phase; H_{II} – inverted hexagonal phase; V_I – bicontinuous cubic phase; L_α - lamellar; L_I – micellar solution. # (Boyd *et al.*, 2000)

All C-6 functionalized glycolipids exhibited excellent water solubility with no clear phase boundary between water and the surfactant, thus suggesting formation of a micellar solution (Ali *et al.*, 2014). Their strong affinity for water was due to the charge effects of the imidazolium ion and hydrogen bonding interactions of the glucose head group. The functionalized glycolipids, mostly formed curved assemblies, which reflected the ionic repulsion between the imidazolium cations thereby leading to an increased hydrophilic surface.

Similar to glucoside **18** (Boyd *et al.*, 2000), hydrophilic dominance in glycolipid **37** was indicated by the observation of a viscous isotropic cubic phase at high water concentration (Brooks *et al.*, 2011). However, replacing the straight chain domain with a longer and branched chain compensated the hydrophilic dominance and led to a balance between hydrophilic and hydrophobic regions, as indicated by the expression of the lamellar phase (Maltese cross texture) in glycolipid **48a** as shown in **Figure 4.10**.

On the other hand, the expression of a hexagonal phase by glycolipid **60**, suggested dominance of the hydrophilic cross sectional area. The observation is in line with previous observation for the corresponding methyl glucoside (Salman *et al.*, 2014). The incorporation of the imidazolium and the EO based linker did not alter the CPP to an extent where a more curved cubic assembly was formed.

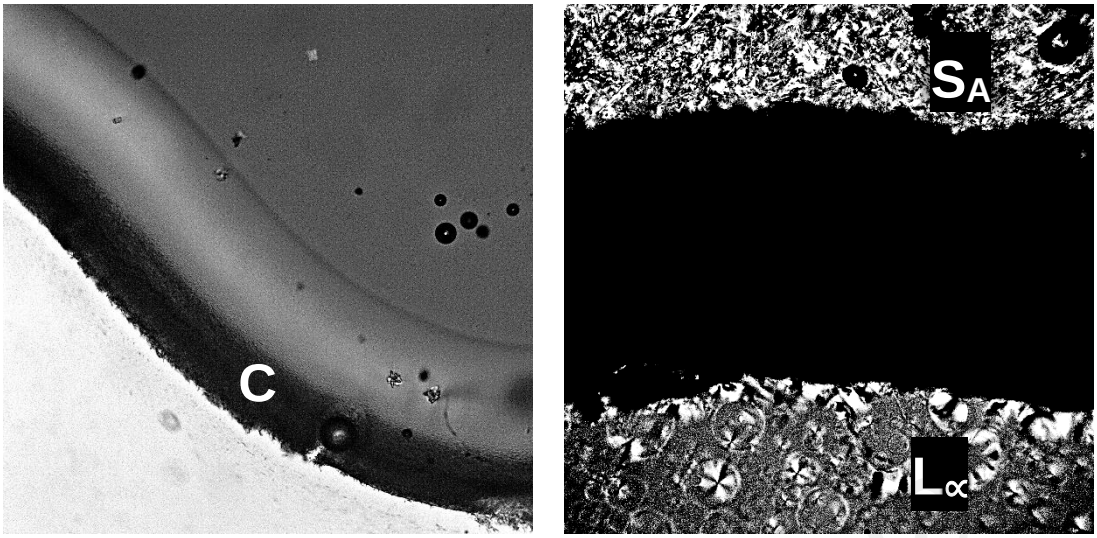

Figure 4.10: OPM images of **37** (left) and **48a** (right).

The functionalized glycolipids were aimed to be employed as co-surfactant, while an anomeric mixture of 2-hexyl-1-decyl-D-lactoside (**LacC$_{10}$C$_6$**) ($\propto$: β= 3:1) formed the base surfactant for the vesicle formulation. The latter was chosen owing to its high potential to form vesicles (Hussen, 2010). Similar to the phase behaviour of **LacC$_{10}$C$_6$**, the surfactant mixtures expressed lamellar phases (Myelin textures) in contact with water as presented in **Figure 4.11**. The inclusion of functionalized glycolipids did not induce a significant change in the CPP, thus suggesting their applicability as co-surfactants for vesicle preparations.

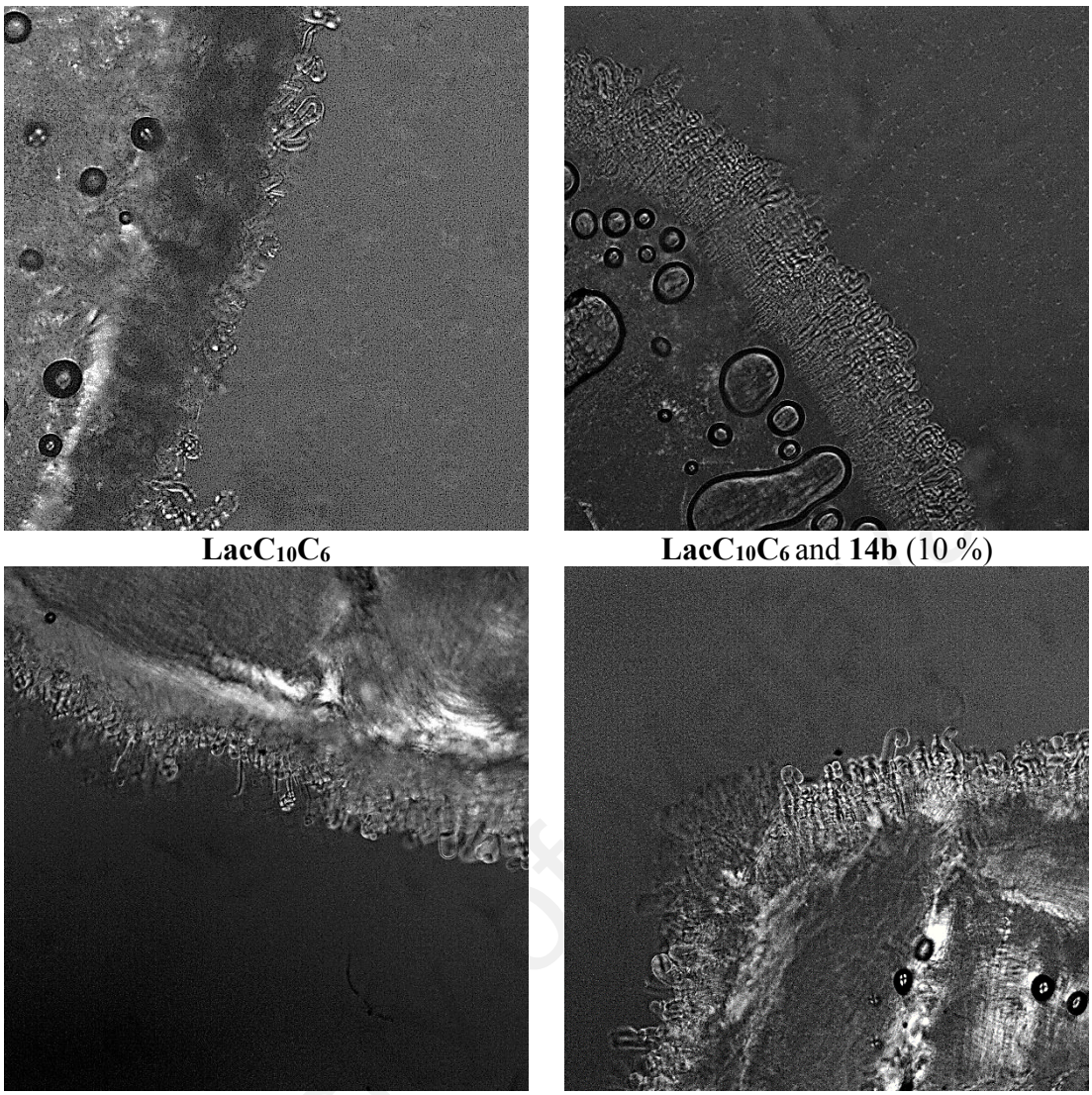

LacC$_{10}$C$_6$ | **LacC$_{10}$C$_6$** and **14b** (10 %)

LacC$_{10}$C$_6$ and **60** (5 %) | **LacC$_{10}$C$_6$** and **48a** (5 %)

Figure 4.11: Myelin textures observed in LacC$_{10}$C$_6$ and other surfactant mixtures.

4.4.2.2 Surface Properties of Functionalized Glycolipids

In view of the material availability and the expected CAC, the surface properties study was limited only to the C_{16} –based glycolipids. The CACs of glycolipids **14b**, **14c**, **48a** and **60** were determined from the intersection of two regression lines for concentration dependent and independent regions in the respective graphs of the surface tension versus the logarithmic surfactant concentration. As summarized in **Table 4.6**, the CACs of the three branched chain glycolipids, **48a**, **14b** and **14c**, are in good agreement with the previously reported glycolipids of similar chain length (Drummond & Wells, 1998; Hussen, 2010; Salman *et al.*, 2016; Tabandeh *et al.*, 2018).

Table 4.6: Surface properties of functionalized glycolipids.

Surfactant	CAC, μM	γ_{CAC}, mN m^{-1}	$A_{interface}$, $Å^2$
14b	18	31	49
14c	24	31	47
48a	16	30	46
60	48	38	55

The effect of additional hydrophilic groups, like an EO chain, on the CAC is found significant in common non-ionic surfactants (Chen *et al.*, 1998; Attwood & Florence, 2008; Sohrabi *et al.*, 2010). The effect appeared notable for the C-6 functionalized glycolipids, reflecting the slight increase of the CAC of **14c** with respect to **14b**, which differs in one additional ethylene oxide unit. On the other hand, surfactant **60** exhibited a substantially higher CAC than the other glycolipids, which was attributed to its relatively better water solubility because of the amide linkage, as well as its shorter hydrophobic chain, considering that the carbonyl carbon is part of the hydrophilic domain.

Despite the ionic character due to the imidazolium group, the functionalized glycolipids still exhibited good interfacial activity as indicated by the surface tensions at their respective CACs. They are not significantly different from the previously reported glycolipids of similar chain length (Hussen, 2012; Tabandeh *et al.*, 2018). In comparison to the previously reported C_{12}-analogue (Salman *et al.*, 2014), glycolipid **60** exhibited significantly lower interfacial activity. This was attributed to its longer hydrophobic chain that gave rise to steric hindrance at the liquid/ air interface, thereby the surfactant molecules were less tightly packed at the interface (Rosen, 2004).

The slightly bigger A_{min} of amide-based glycolipid **60** compared to the others was due to the formation of an 8-membered ring hydrogen bonding between the $\underline{H}$-OC_4 and the carbonyl oxygen, leading to a tilted hydrophobic chain (Salman *et al.*, 2014). Besides,

the highly acidic hydrogen at imidazolium carbon-2 can also be involved in hydrogen bonding (Thar *et al.*, 2009). Thus, a molecular modelling study was performed on the structures, involving 6-membered ring intramolecular hydrogen bonding (a), (b) and a reference structure exhibiting no hydrogen bonding, while the hydrogen bonding between the C=O and H-OC_4 was still taken into account in all the aforementioned structures as illustrated in **Figure 4.12**. To avoid lengthy calculation time, the computational study was done based on a model structure, which had the long hydrocarbon chain replaced by a simple methyl group.

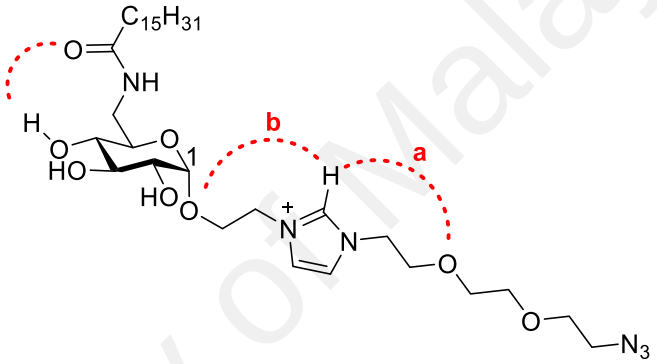

Figure 4.12: Potential intramolecular H-bonding of **60**.

As summarized in **Table 4.7**, the hydrogen bonding between the C=O and H-OC_4 remained intact in all the structures after structural optimization. Comparing their respective energies, the structure with hydrogen bonding (a) appears to be the most stable among all. The effect of the hydrogen bonding is a bending of the linker towards the sugar unit, which results in a bigger hydrophilic surface area. This explains the relatively higher molecular surface area of **60**, as depicted in **Figure 4.13**.

Table 4.7: Relative stability of different conformations.

H-bonding	Structure	Energy, E/ a. u.	ΔE/ kJ mol^{-1}
none	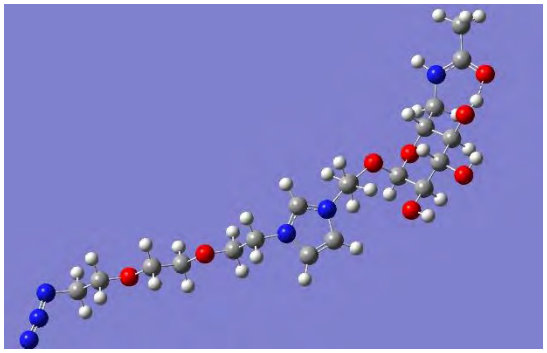	-1673.9851	reference
a	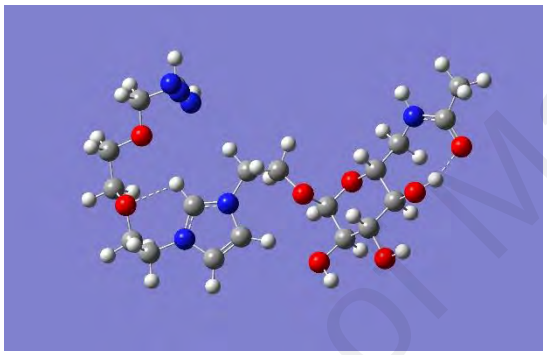	-1674.0118	-70
b	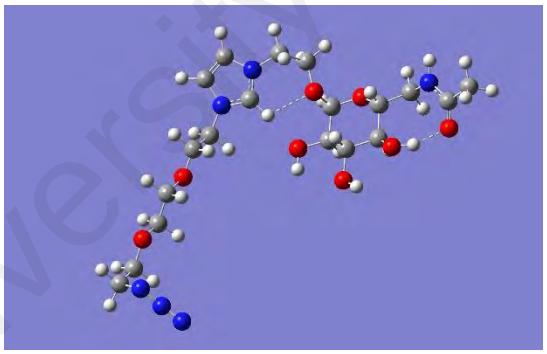	-1673.9991	-37

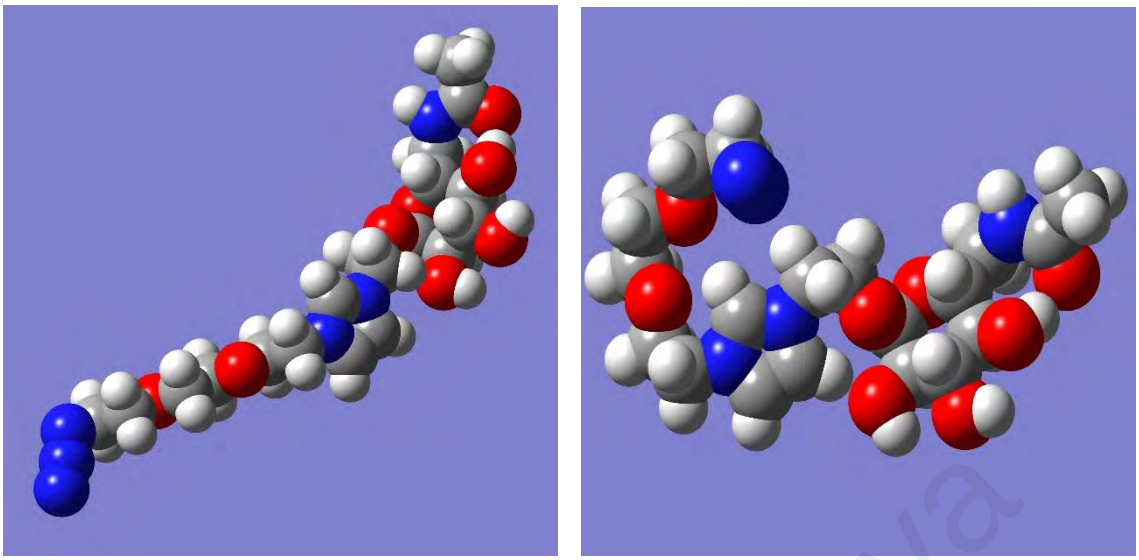

Figure 4.13: Structures with H-bonding type (a) (right) and without H-bonding (left).

4.4.2.3 Vesicle Formulation and Characterization

Functionalized glycolipids were employed as co-surfactant, together with the **LacC$_{10}$C$_6$** as base surfactant, based on the ethanol injection method following the procedure as stated in section **3.2.3** to prepare the functionalized vesicles. Their respective vesicle sizes and zeta potentials were measured on the same day they were prepared. The results are tabulated in **Table 4.8**.

Table 4.8: Vesicular sizes and zeta potentials.

Sample	Content (%)				Diameter (nm)	ζ (mV)
	LacC$_{10}$C$_6$	**60**	**48a**	**14b**		
1	100				71	-25
2	95	5			18	+55
3	99		1		38	+8
4	95		5		13	+53
5	95			5	27	+37
5*	95			5	33	+41
6[a]	95			5	89	+13
7[b]	95			5	113	+16
8	90			10	20	+55

* After one week of storage; a: CLICK reaction with **IMI** and b: CLICK reaction with **ACID**.

The successful incorporation of functionalized glycolipids into the vesicles was proven by their positive zeta-potentials (ZPs), which resulted from the imidazolium cations. Similar to other ionic co-surfactants, the functionalized glycolipids improved the distribution of non-ionic **LacC$_{10}$C$_6$** in water (Mak *et al.*, 2015), thus resulting in smaller sized vesicles (Bnyan *et al.*, 2018), as observed in **Table 4.8**. This effect was more significant when a higher percentage of the cosurfactant was used. Besides, the vesicles were relatively stable as implied by their ZPs of higher than +30 mV (Sun *et al.*, 2016), which created reasonably strong electrostatic repulsion between the vesicles, thus avoiding the aggregation processes (Singh *et al.*, 2016). The effect was also supported by the insignificant change observed in vesicle size and ZP of sample 5 after one week of storage.

A comparison was made between two vesicle dispersions that applied **LacC$_{10}$C$_6$** with a commercial cationic cosurfactant (DTAB) and a functionalized glycolipid (**14b**) as co-surfactants, respectively. As shown in **Figure 4.14**, the dispersion containing the functionalized glycolipid appears relatively clearer, indicating the presence of smaller sized particles. This suggested better effectiveness of the functionalized glycolipids in forming smaller sized vesicles compared to the commercial DTAB.

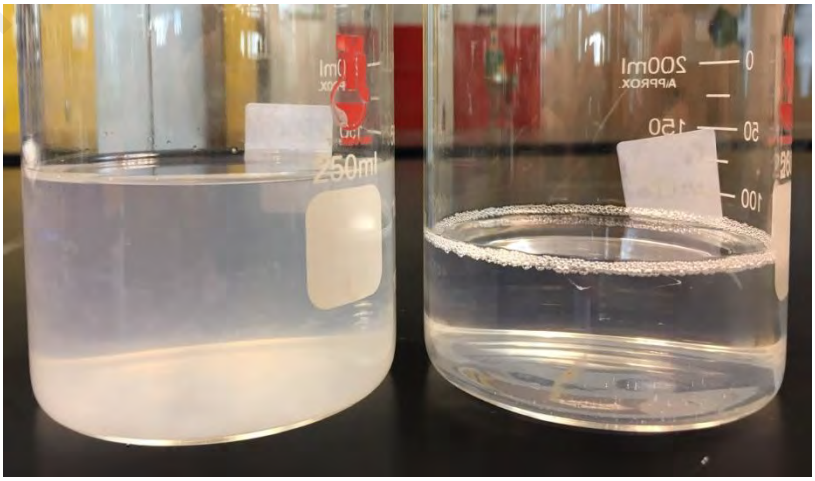

Figure 4.14: Vesicle dispersions containing 2 % DTAB (left) and 2 % **14b** (right).

PBS, or phosphate-buffered saline, is commonly preferred as a medium for vesicle preparation (Cheng & London, 2011; Sankhyan & Pawar, 2013), owing to its similar osmolarity and ion concentration to that of human body fluids, like blood (Obeid *et al.*, 2017). Therefore, an attempt to prepare vesicles through injection of ethanolic surfactant solution into PBS of pH 7.4 at 25 °C was made. However, the resulting dispersion appeared opaque and the measurement of its vesicle size and ZP were inconsistent. This could be due to the strong ionic interaction between the cationic glycolipid and multivalent phosphate ion, which affected the formulation of vesicles. Therefore, PBS is considered as an unsuitable medium for the vesicle preparation.

4.4.2.4 Assessment of CLICK Functionality

To assess the CLICK functionality in water, a CLICK reaction was performed on aggregates formed by functionalized glycolipid **14a**, as illustrated in **Scheme 4.15**. A micellar dispersion of the surfactant above the CAC was used. As for the complementary part, a well water soluble alkyne-terminated tryptophan ester, **TrypEster**, was applied. The procedure is described in section **5.3**.

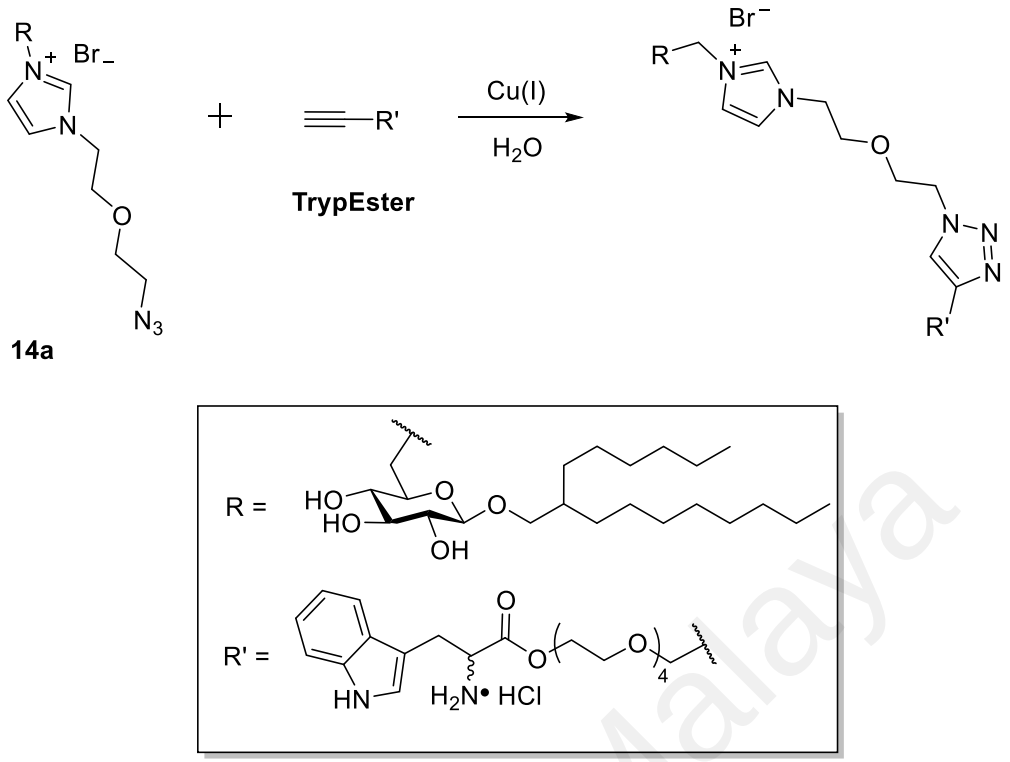

Scheme 4.15: CLICK reaction with **TrypEster** in water.

Water was removed by freeze-drying to avoid high temperature condition that could lead to the hydrolysis of the **TrypEster**. A comparison between the IR-spectra of the reaction mixtures before and after the reaction (as shown in the **Figure 4.15**) suggested a successful CLICK reaction in water, as indicated by the disappearance of azido peak at 2100 cm^{-1} after the reaction. The highly polar triazole product rendered a chromatographic purification impossible, while the complicated ^{1}H NMR spectrum made a structural elucidation impractical. Moreover, the indistinctive UV absorption of **TrypEster** limited its applicability for a quantitative study based on UV or fluorescence spectroscopy.

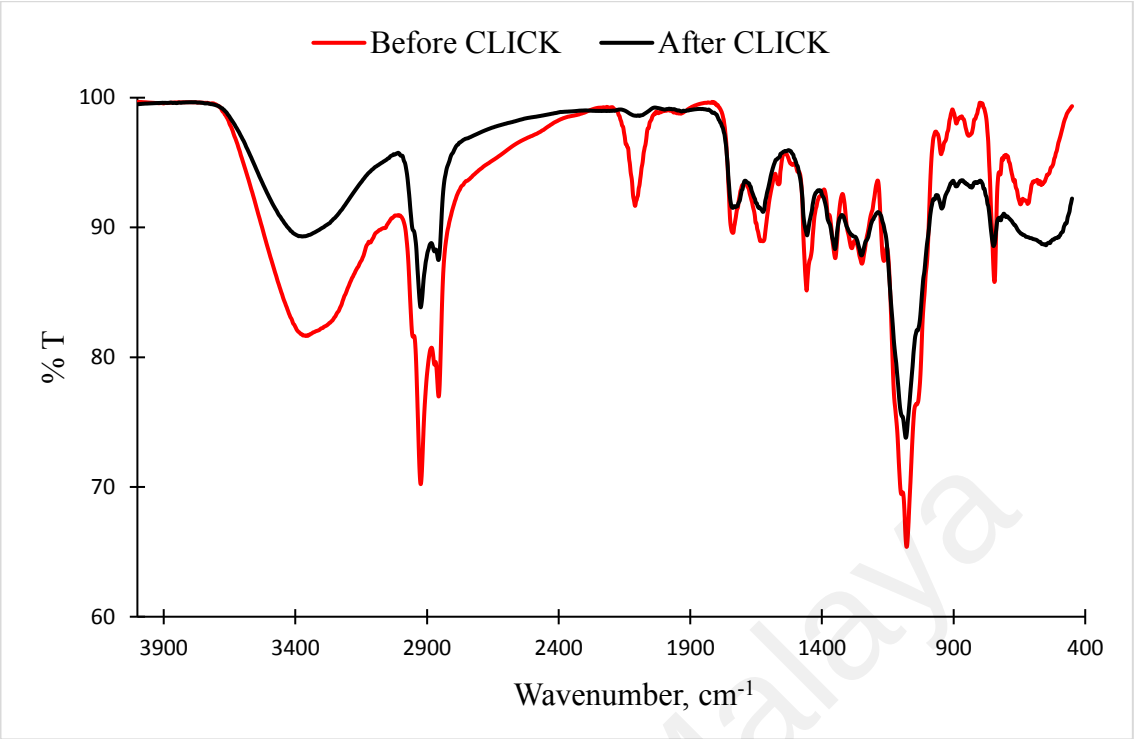

Figure 4.15: IR-spectra before and after CLICK reaction with **TrypEster**.

In order to ease the identification of the triazole proton signal, which would further substantiate the success of the CLICK reaction in water, propargyl alcohol with a simple molecular structure was used, as depicted in **Scheme 4.16**. The reaction procedures are described in section **5.3**.

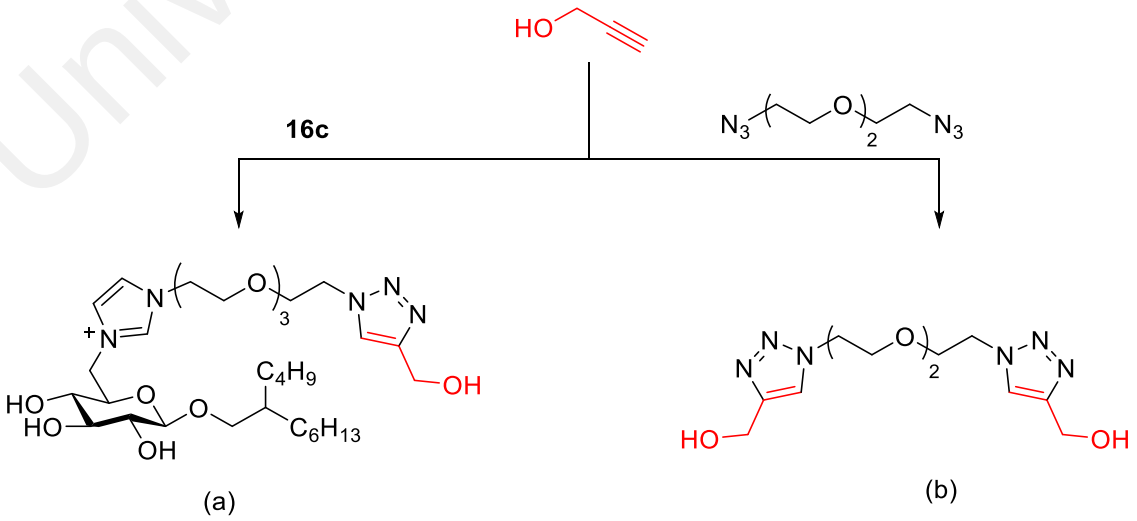

Scheme 4.16: (a) Glycolipid **16c**-based and (b) analogue CLICK products.

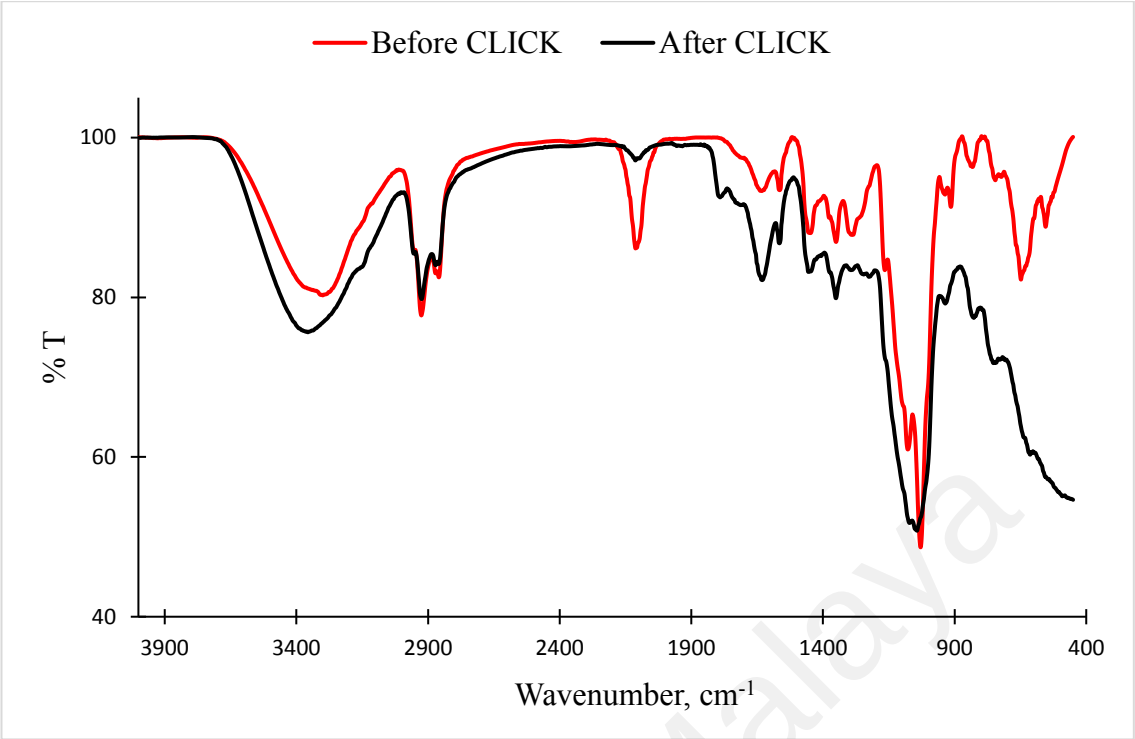

Figure 4.16: IR-spectra before and after CLICK reaction with propargyl alcohol.

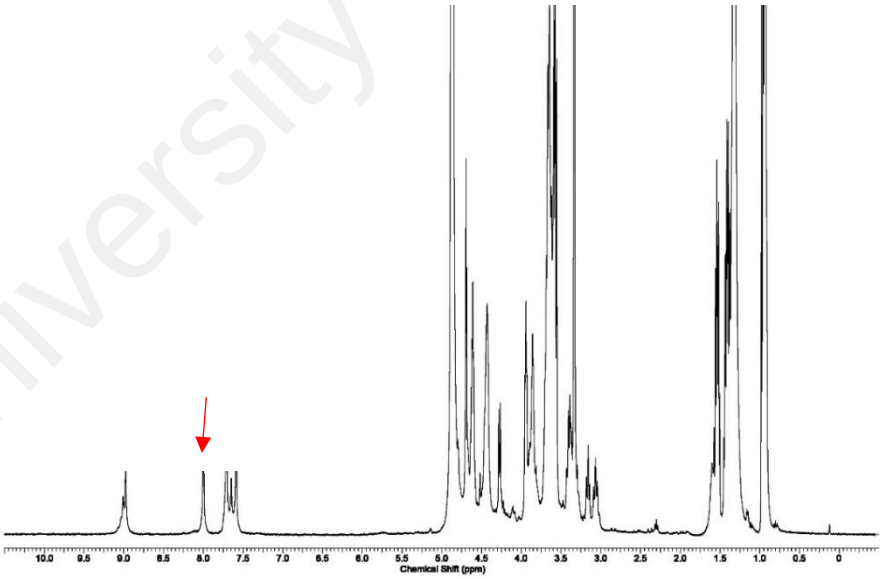

Figure 4.17: ^{1}H NMR of the crude material after CLICK reaction.

Both IR and NMR spectra of the resulting crude material were recorded. **Figure 4.16** shows that the CLICK reaction proceeded as indicated based on the reduced

intensity of the azide peak (~2100 cm^{-1}). Compared to the ^1H NMR of functionalized glycolipid **16c**, **Figure 4.17** (red arrow) shows an additional ^1H signal at the aromatic region reflecting the triazole from the CLICK coupling. An analogue model compound, as shown in **Scheme 4.16**, was synthesized and used as a reference for the triazole signal of the CLICK product as indicated by the red arrows in **Figure 4.18**.

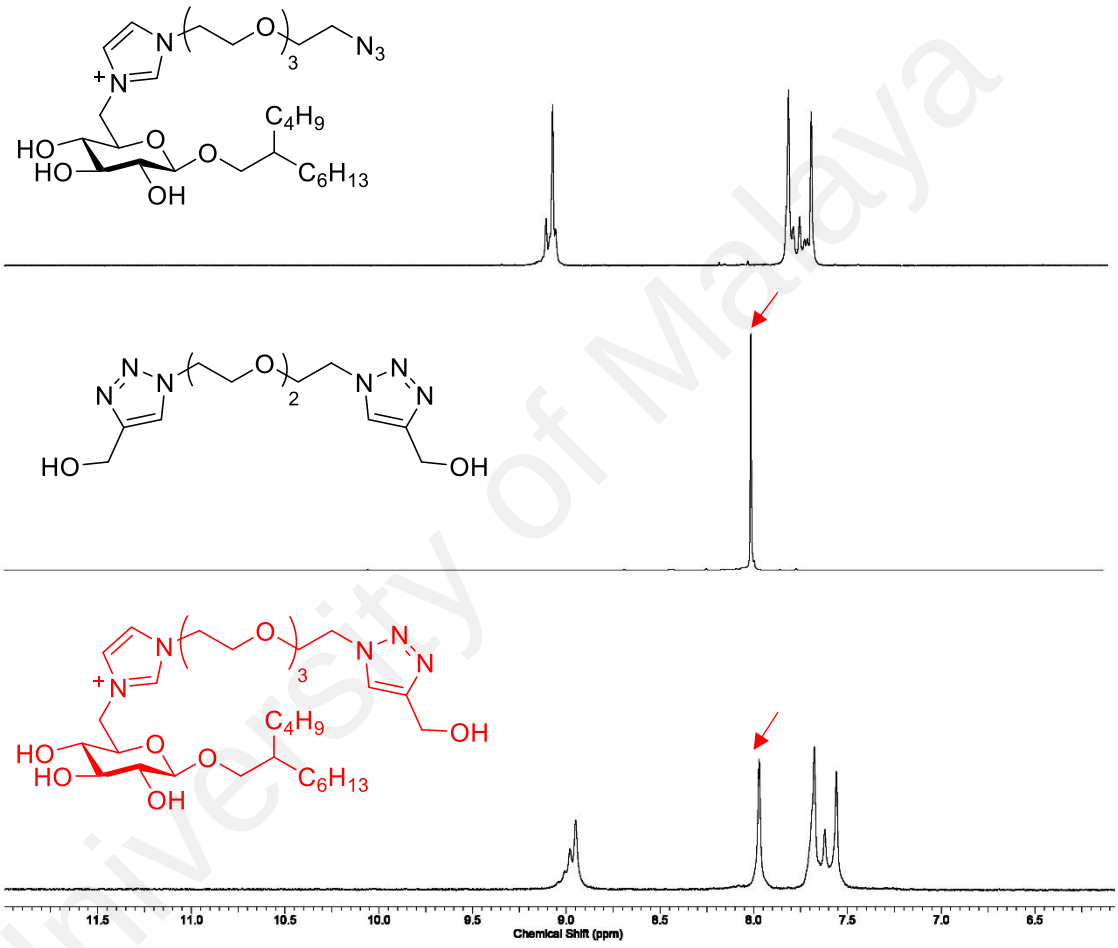

Figure 4.18: Aromatic ^1H signals of both triazole compounds and **16c**.

CLICK coupling of the functionalized vesicles with either a carboxylic acid or an imidazolium terminated compounds was expected to cause changes in the zeta potential. This approach was employed in the attempt to evaluate the accessibility of the CLICK functionality on the vesicular surface by using two simple alkyne terminated compounds

(**IMI** and **ACID**) as depicted in **Figure 4.19**, which were prepared following the procedures reported in the literature (Kuang *et al.*, 2012; Morimoto *et al.*, 2013).

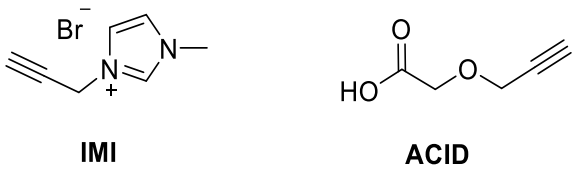

IMI **ACID**

Figure 4.19: Alkyne-terminated compounds for CLICK coupling.

A vesicle dispersion containing both **LacC$_{10}$C$_6$** and **14b** (5 %) was prepared according to general procedure **3.2.3** and subjected to CLICK reactions with **IMI** and **ACID**, respectively, following general procedure **3.4.16**. Unexpectedly, the resulting vesicles were found exhibiting bigger sizes and lower absolute ZP values as presented in **Table 4.8**. The increased vesicle sizes probably reflected high ionic strength, owing to the presence of other counter ions that originated from the catalysts used. These counter ions may have been adsorbed onto the vesicle surface, thus neutralizing the positively charged surface and rendering the aggregation of small vesicles more feasible (Claessens *et al.*, 2004). The unexpected ZPs obtained after CLICK reaction raised doubts on the range of distance from the vesicle surface that the ZP measurement covered. As illustrated in **Figure 4.20,** the EO spacer provided a significant distance between the vesicle surface and the carboxylate anion or the imidazolium cation, to an extent where the ionic charges of these two components may be outside the measurement range, thus preventing the effect on the overall zeta potential.

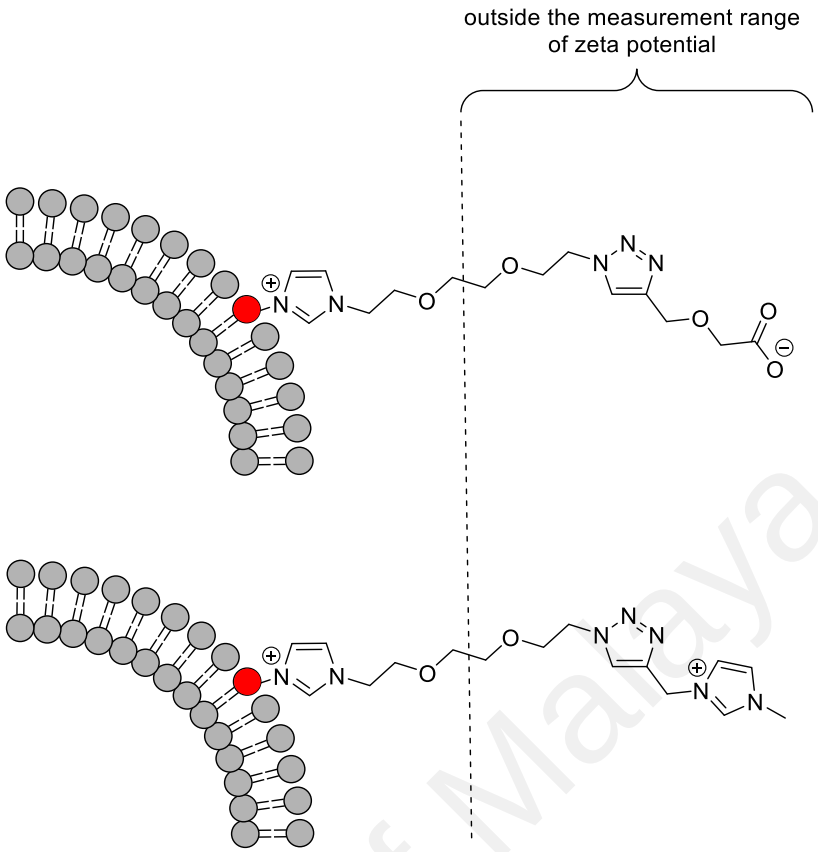

Figure 4.20: Illustration of the measurement range for ZP.

4.4.2.5 Rhodamine-based Fluorescent Probe

Fluorescent probing has been commonly used as a quantifying method for compounds of interest, like DNA. In view of the interest to quantify the CLICK functionality of the functionalized vesicles, an alkyne-bearing fluorescent probe was targeted for the study.

Rhodamine belongs to the xanthenes family and its excellent photophysical properties make it a good fluorescent probe, especially for labelling and characterization of nanoparticle surfaces (Farinha *et al.*, 2001; Krasnici *et al.*, 2003; Biswas *et al.*, 2011). Rhodamine B and Rhodamine 6G are less expensive among the other rhodamine

derivatives (Magde *et al.*, 2002), and Rhodamine B was employed for the study, seeing that its reasonably good water solubility results from its ionic character.

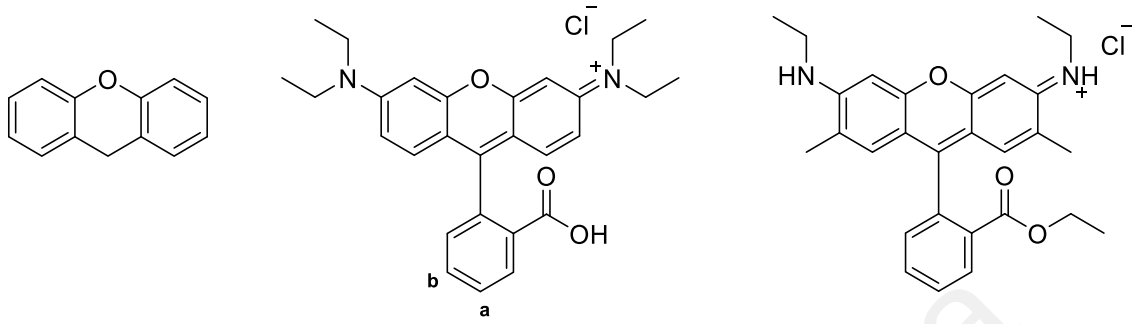

Figure 4.21: Xanthene (right), Rhodamine B (middle) and Rhodamine 6G (left).

Functionalization or modification of rhodamine derivatives are usually performed on the amino groups of the xanthene moiety (Tang *et al.*, 2007), the carboxyphenyl ring (Jackson *et al.*, 2005) and the carboxylic acid group (Afonso *et al.*, 2003). Modification of both amino groups may result in the formation of a lactone, which renders the conjugation system disrupted, thus causing the loss of fluorescence (Drexhage, 1976; Leytus *et al.*, 1983). As indicated in **Figure 4.21**, both positions a and b of carboxyphenyl ring are more preferable for functionalization since the others are sterically hindered. Nevertheless, this kind of modification is usually carried out before the xanthene ring is formed and the reaction involved is weakly regioselective, thus always giving rise to non-isomerically pure rhodamine derivatives (Menchen & Fung, 1988) that can affect the reproducibility of results during a fluorescence study (Corrie & Craik, 1994). Therefore, the carboxylic acid group was considered as the easiest functionalization site.

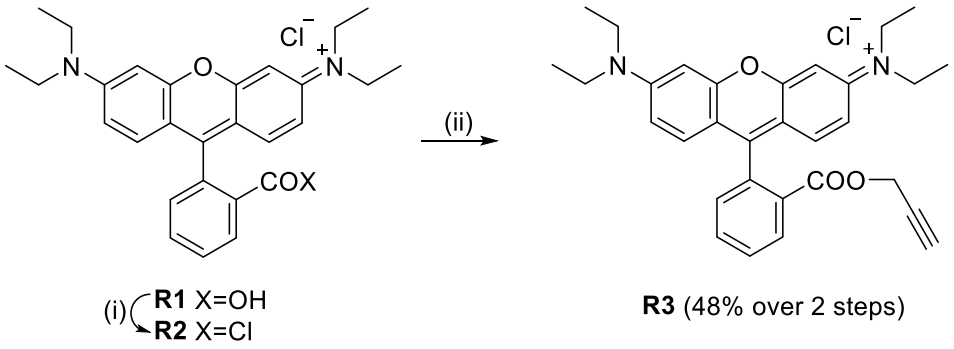

(i) $(COCl)_2$, $CHCl_3$, reflux; (ii) propagyl alcohol, TEA, CH_3CN, reflux.

Scheme 4.17: Synthesis of alkyne-bearing **R3**.

As shown in **Scheme 4.17**, the carboxylic group of rhodamine B was first activated as an acid chloride, followed by esterification with propyn-1-ol to furnish a new fluorescent probe **R3**, whose photophysical properties are summarized in **Table 4.9**. The compound was found only sparingly water soluble despite its cationic character. This resulted in a calibration curve of poor linearity for the **R3** fluorescent emission in water. Consequently, a fluorescence calibration curve of **R3** was obtained in methanol, in which the probe exhibited better solubility.

Table 4.9: Absorption and emission maxima of **R3**.

Solvent	λ_{abs}^{max} (nm)	λ_{em}^{max} (nm)
H_2O	560	584
CH_3OH	555	578

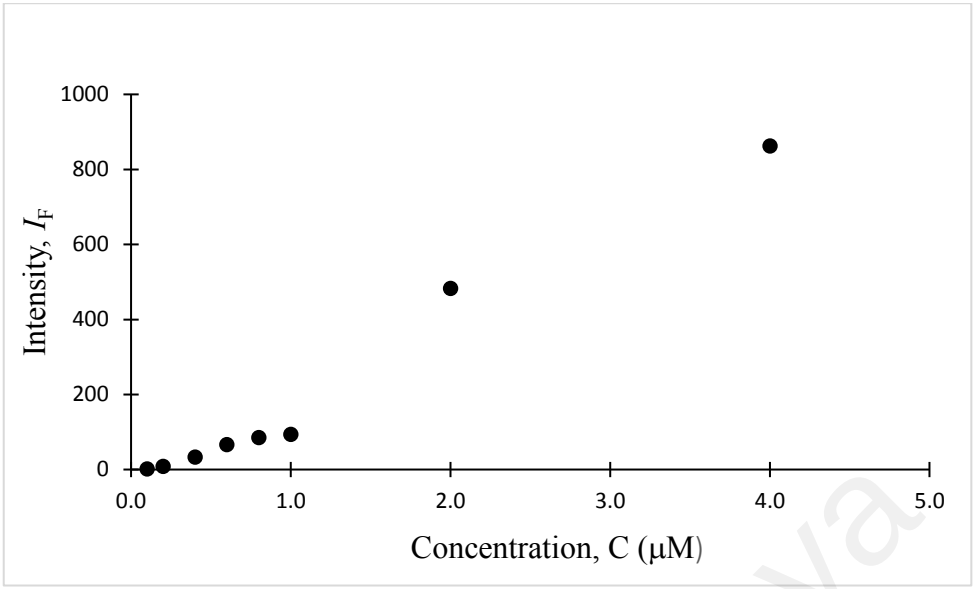

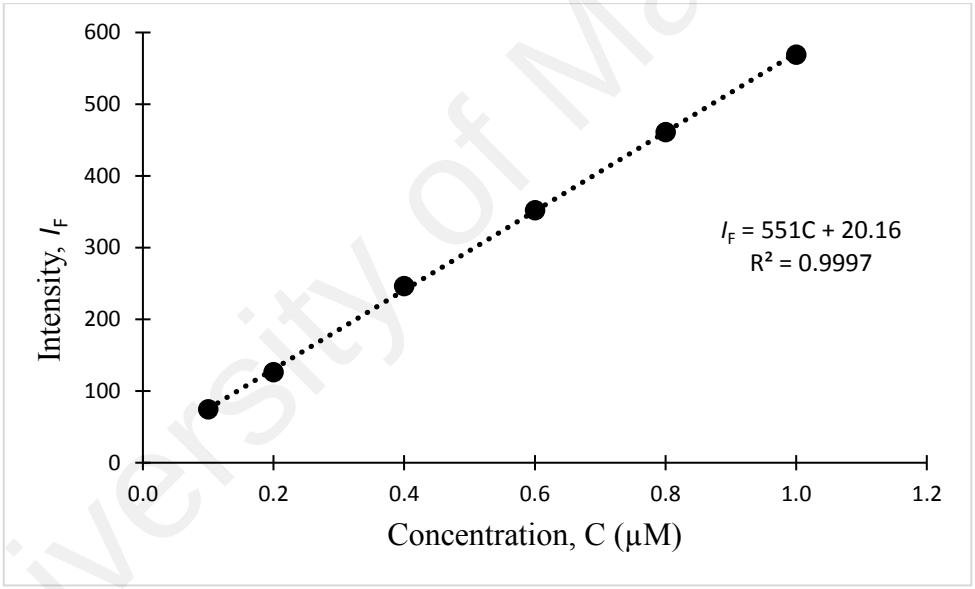

Figure 4.22: Fluorescence studies of **R3** in H_2O (above) and CH_3OH (below).

As described in section **3.2.3**, a vesicle dispersion (2 mM) based on **LactoC$_{10}$C$_6$** containing 2 % cosurfactant **14b** (1 equiv) was prepared. Subsequently, the resulting vesicle solution was subjected to CLICK reaction with probe **R3** (5 equiv), in the presence of copper (II) acetate (0.15 equiv) and sodium ascorbate (0.45 equiv) as catalysts, as illustrated in **Figure 4.23**. The mixture was left with stirring at room temperature for 24 hours.

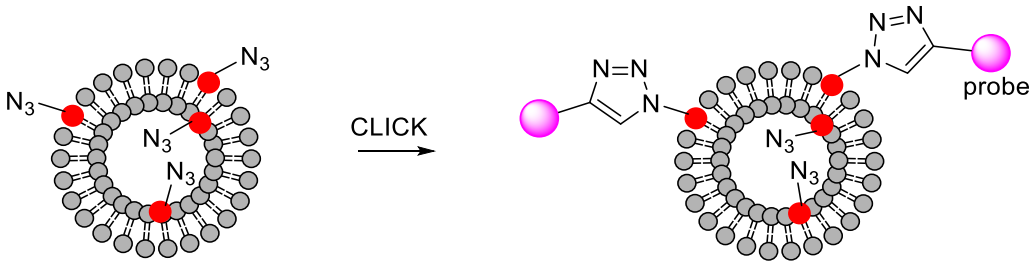

Figure 4.23: Functionalized vesicles coupled with probe **R3**.

Separation of the probe-coupled vesicles by dialysis was attempted, while a control of the same composition except for absence of copper (II) acetate, and a blank containing only the catalysts and probes were treated the same way. The release of probe was assessed by monitoring the external bulk water over time by UV-vis absorption spectroscopy. The bulk medium was replaced daily to ensure optimum removal of the unreacted probe. After 10 days, the dialysis process was considered complete as indicated by the absence of an absorption peak (560 nm) corresponding to probe **R3** in the external medium. The experiment is illustrated in **Figure 4.24**.

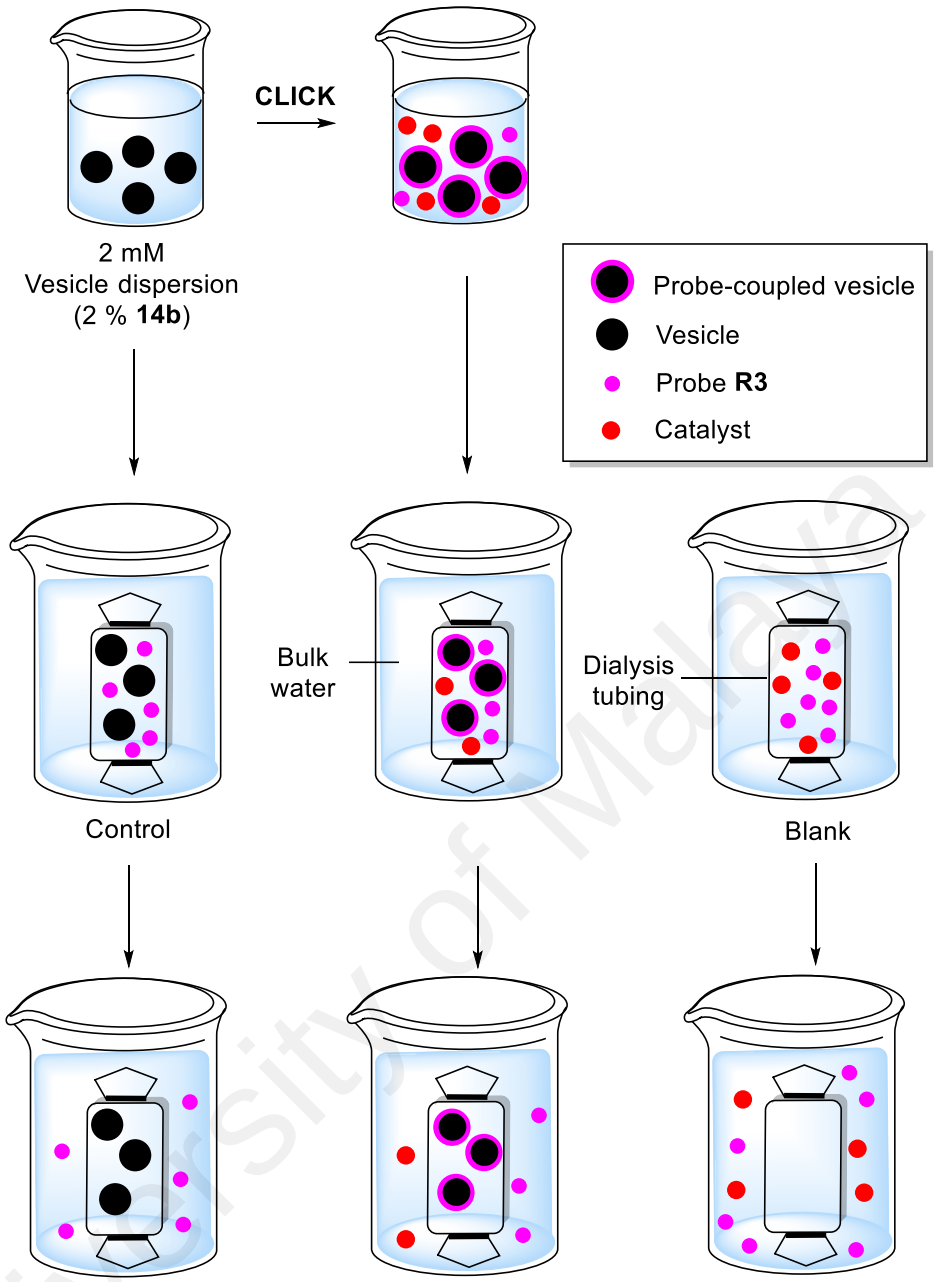

Figure 4.24: Schematic diagram of dialysis experiment.

However, pink precipitates (as shown in **Figure 4.25**) were observed in both, the probe-coupled vesicle dispersion and the control, which may be explained by attachment of **R3** onto the vesicular surface by physical adsorption. Water was evaporated from the vesicle solutions and the residues were dissolved in 20 mL methanol for their fluorescence measurement. All three resulting methanolic solutions were found exhibiting fluorescent emission at 578 nm, indicating the presence of probe **R3**. Neither blank nor control were

expected to exhibit fluorescent emission, since this was considered as evidence for a successful CLICK coupling on the vesicles. The unexpected findings could be due to insufficient water solubility of **R3**, as indicated by its calibration curve in water, which caused a strong retention of **R3** on the vesicular surface, as well as the dialysis tubing by adsorption and deterred an effective osmosis process.

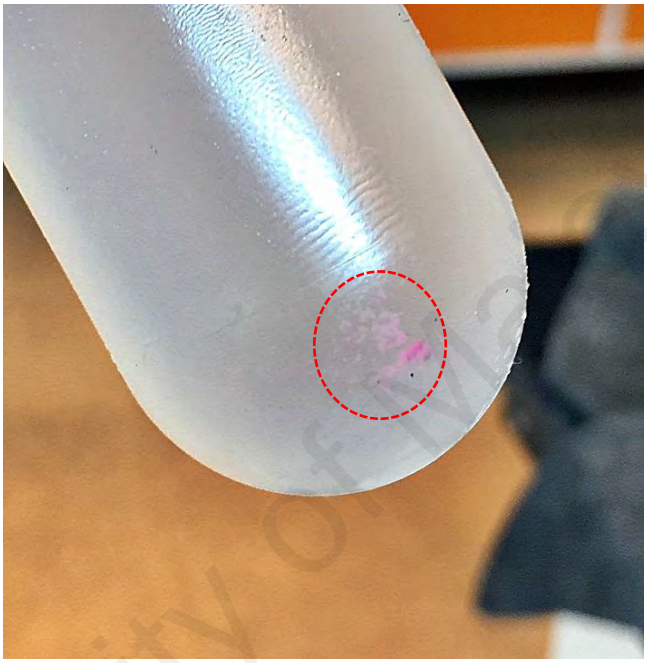

Figure 4.25: Pink precipitates observed.

4.4.2.6 Attempted Synthesis of Pyrene-labelling Glycolipid

Pyrene has been widely used for fluorescence probing to characterize macromolecules or supramolecular structures, such as vesicles based on its excimer formation (L'Heureux & Fragata, 1989; Lianos & Duportail, 1992; Siu & Duhamel, 2004; Duhamel, 2012). As illustrated in **Figure 4.26**, an eximer, **(Py-Py)*** is formed when an excited pyrene, **Py***, approaches a ground-state pyrene, **Py**, or a ground state pyrene dimer, **(Py-Py)** is excited upon absorption of a photon. Since the fluorescence of pyrene monomers and eximers differ in both spectrum and lifetime, fluorescence studies can differentiate between these two states (Birks, 1970; Duhamel, 2012).

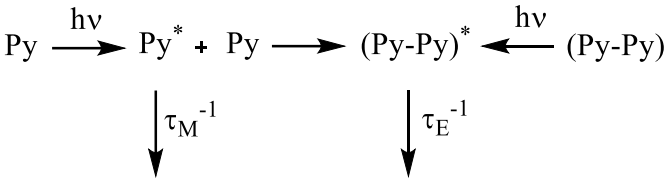

Figure 4.26: Modified scheme of excimer formation.

In a vesicle aggregate, a close proximity of functionalized glycolipids to each other may result in steric hindrance that can preclude an efficient bio-functionalization of the vesicular surface, as well as the interaction between the vesicle and the target cell. Therefore, in order to evaluate the distribution of functionalized glycolipids in vesicles, a pyrene-labelled glycolipid (PLG) of the structure as shown in **Figure 4.28** was targeted for vesicle formulation. Conceptually, a close distance between PLGs will give rise to the formation of excimers, while this does not occur for discretely distributed PLGs, as illustrated in **Figure 4.27**. And, the key feature for identifying the type of distribution will be based on the exceptionally distinctive fluorescence emissions for the excimer (~480 nm) and monomer, **Py*** (370-430 nm) (Winnik, 1993).

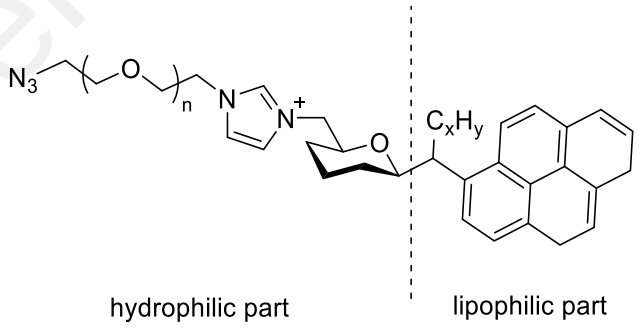

Figure 4.27: Targeted PLG structure.

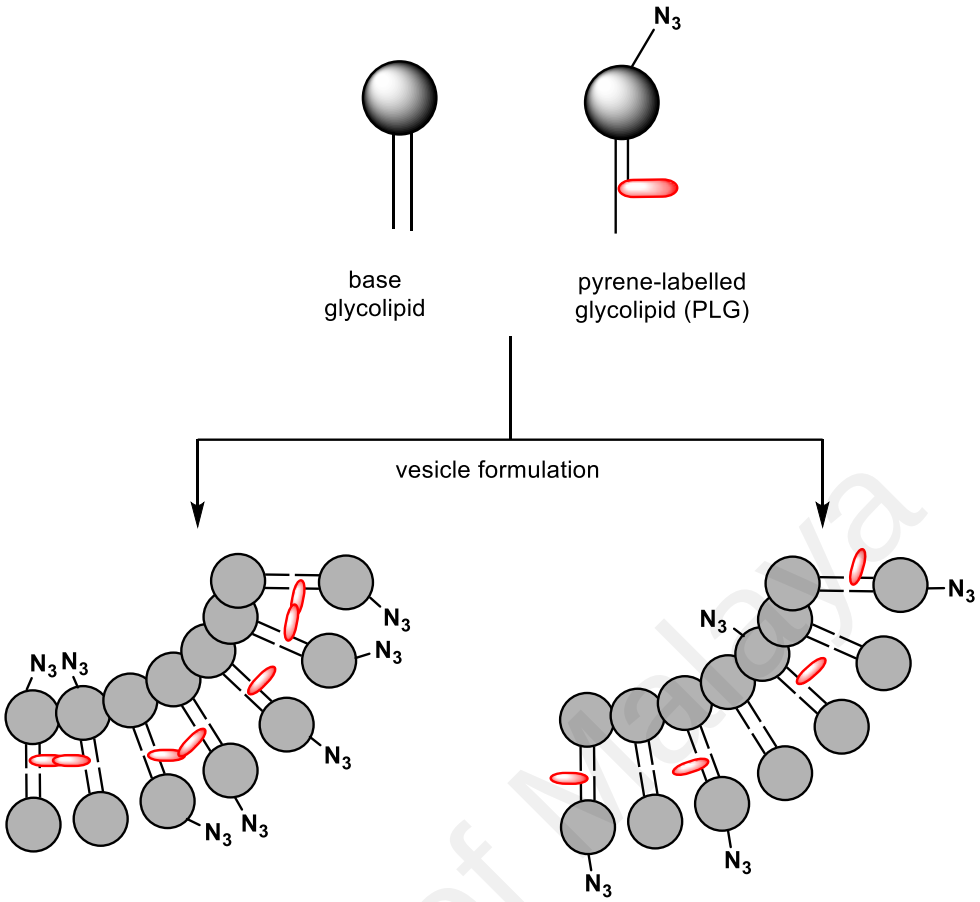

Figure 4.28: Possible PLG distributions in a vesicular assembly.

Scheme 4.18 shows the attempted synthesis of PLG, which involved an aldol-condensation between sugar ketone **P6** and 1-pyrenecarboxaldehyde to furnish a trans-product **P7** as indicated by its vicinal protons coupling constant. In view of the instability of acetate groups towards base, which was necessary for a targeted substitution reaction with 1-bromohexadecane, a more stable benzyl protecting group was employed. Compound **P6** was synthesized based on a six-step sequence from glucose, which involved the initial protection of the ketone as a ketal, instead of direct introduction of benzyl groups after formation of *C*-glycosylketone **P1**, which had been reported unsuccessful in the literature (Norsikian *et al.*, 2007). Reduction of ketone **P7** furnished a secondary hydroxyl group, which was then treated with sodium hydride to generate an alkoxide for subsequent substitution with 1-bromohexadecane. However, the

amphiphilicity of the glycolipid could not be restored, as the hydrogenolysis of the benzyl protecting groups was unsuccessful as indicated by TLC, thus restricting the applicability of the compound for the targeted study.

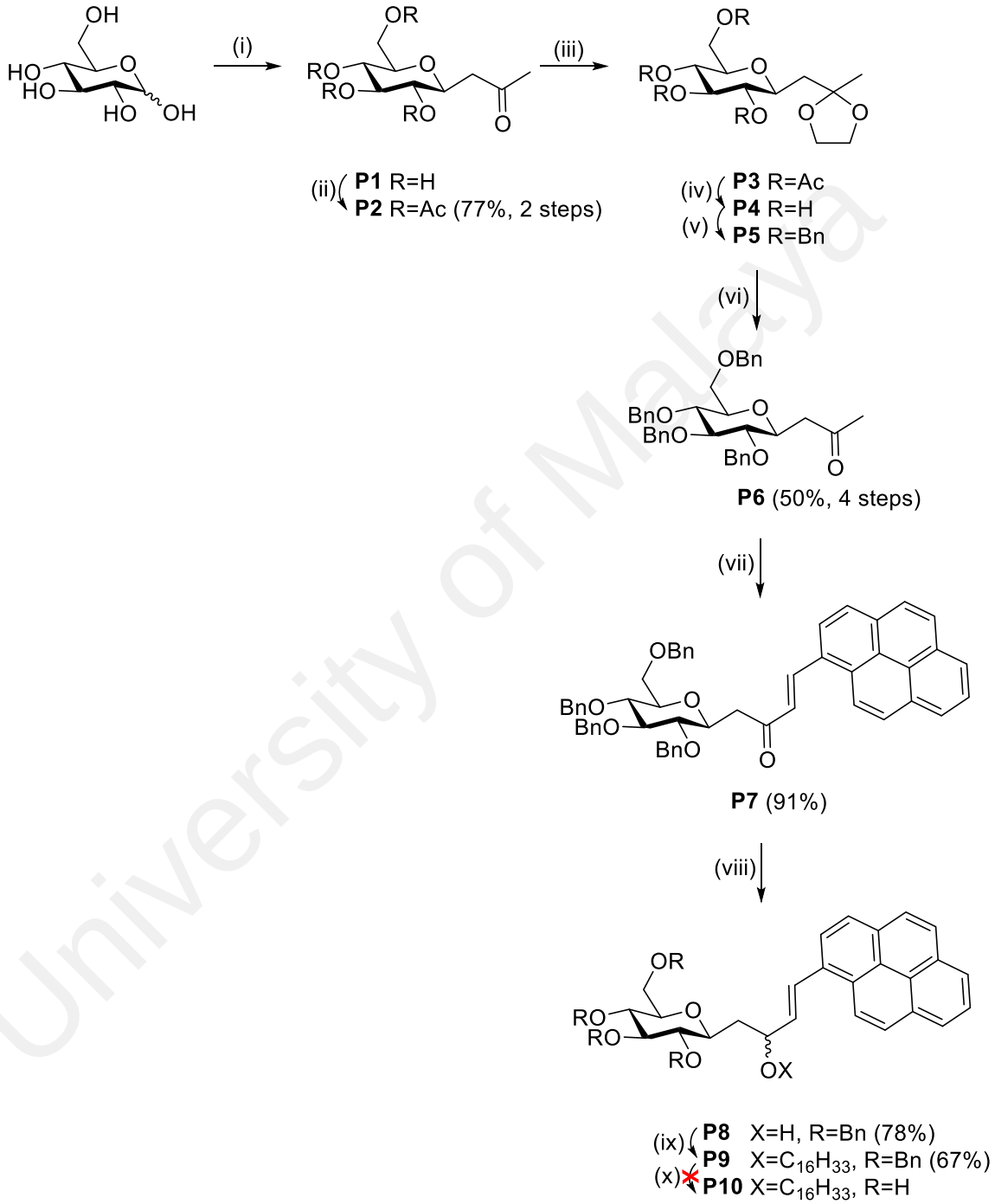

(i) Acetylacetone, $NaHCO_3$, H_2O, 80 ^oC; (ii) Ac_2O, pyridine;
(iii) $(HOCH_2)_2$, PPTS, toluene, reflux; (iv) $NaOCH_3$, CH_3OH;
(v) NaH, BnBr, DMF; (vi) TFA, H_2O; (vii) 1-pyrenecarboxaldehyde, $(CH_2)_4NH$, CH_2Cl_2;
(viii) $NaBH_4$, THF: CH_3OH (1:1); (ix) NaH, $CH_3(CH_2)_{15}Br$, DMF; (x) H_2, Pd/C, CH_3OH

Scheme 4.18: Attempted synthesis of PLG.

CHAPTER 5: EXPERIMENTAL DETAILS

5.1 Chemicals and General Techniques

Reagents and solvents (AR grade) were used as purchased from various commercial sources without prior purification. Reactions were monitored by thin layer chromatography (TLC), which was performed using pre-coated silica gel 60 F_{254} aluminium sheets. Sugar compounds were detected by treating the developed TLCs with 15 % ethanolic sulphuric acid followed by heating, while TLCs with alkyl imidazoles were developed with basic $KMnO_4$ solution and subsequent heating instead. Flash column chromatograph applied silica gel 60 (35-60 mesh).

5.2 Instrumentation

NMR spectra were recorded on 400 MHz spectrometers, a BrukerAvance III and a JEOL JNM, while IR spectra were recorded on a Perkin Elmer ATR FTIR using 4 scans at a resolution of 4 cm^{-1}, covering range from 4000 cm^{-1} to 450 cm^{-1}. An Agilent 6550 Q-TOF and a JEOL Accu TOFDART mass spectrometers were used to record high resolution mass spectra. Surface tensions of glycolipid solutions were measured on a SKV Sigma 702 tensiometer at 25 °C based on the Du Nouy ring method (Macy, 1935). Particle sizes and zeta potentials were measured on a Malvern Zetasizer Nano ZS, which uses a 633 nm 4 mW HeNe laser and records the backscattering at an angle of 173°. Specific optical rotations were determined at room temperature on a JASCO P-1020 automatic digital polarimeter using the sodium D-line. UV-vis spectra were obtained on a Shimadzu UV-3101PC spectrophotometer, while fluorescence spectra were recorded on an Agilent Cary Eclipse spectrometer in 1 cm quartz cuvettes at room temperature.

5.3 Experimental Data

1-(2-(2-Chloroethoxy)ethyl)-1*H*-imidazole (2a) (Yan *et al.*, 1998)

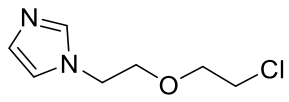

A solution of imidazole (0.30 g, 4.4 mmol) and NaH (60% suspension in paraffin oil) (0.31 g, 7.8 mmol) in THF (40 mL) was treated with bis(chloroethyl) ether **1a** (2.1 mL, 18 mmol) according to general procedure **3.6.1** and furnished **2a** as a yellow liquid (0.48 g, 62 %). ^{1}H NMR (400 MHz, $CDCl_3$): δ 7.49 (1H, s, N=C*H*-N), 6.99-6.96 (2H, m, N-CH=CH), 4.09-4.06 (2H, m, -NCH_2-), 3.72-3.69 (2H, m, -NCH_2CH_2O-), 3.65-3.61 (2H, m, -CH_2Cl), 3.56-3.52 (2H, m, -OCH_2CH_2Cl); ^{13}C NMR (100 MHz, $CDCl_3$): δ 137.3 (N=*C*H-N), 129.0 (N-CH=*C*H), 119.3 (N-*C*H=CH), 71.1 (-*C*$H_2OCH_2CH_2Cl$), 70.3 (-$CH_2OCH_2CH_2Cl$), 46.8 (-NCH_2-), 42.5 (-CH_2Cl).

1-(2-(2-(2-Chloroethoxy)ethoxy)ethyl)-1*H*-imidazole (2b) (Akiyama *et al.*, 2010)

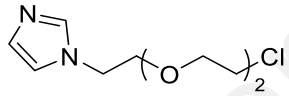

A solution of imidazole (0.30 g, 4.4 mmol) and NaH (60% suspension in paraffin oil) (0.32 g, 8.0 mmol) in THF (40 mL) was treated with 1, 2-bis-(2-chloroethoxy) ethane **1b** (2.8 mL, 18 mmol) according to general procedure **3.6.1** furnishing **2b** as a yellow liquid (0.58 g, 60 %). ^{1}H NMR (400 MHz, $CDCl_3$): δ 7.49 (1H, s, N=C*H*-N), 6.99 (1H, m, N-CH=C*H*), 6.95 (1H, m, N-C*H*=CH), 4.08-4.05 (2H, m, -NCH_2-), 3.72-3.55 (10H, m, -$CH_2OCH_2CH_2$ OCH_2CH_2Cl); ^{13}C NMR (100 MHz, $CDCl_3$): δ 137.4 (N=*C*H-N), 129.0 (N-CH=*C*H), 119.3 (N-*C*H=CH), 71.2 (-NCH_2CH_2O-), 70.5, 70.4 (-OCH_2CH_2 OCH_2CH_2Cl), 46.9 (-NCH_2-), 42.7 (-CH_2Cl).

1-(2-(2-(2-(2-Chloroethoxy)ethoxy)ethoxy)ethyl)-1*H*-imidazole (2c) (Ishida *et al.*, 2004)

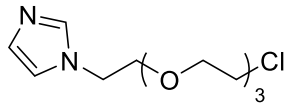

In a two necked round bottom flask, a solution of tetraethylene glycol (10 mL) and pyridine (10 mL) in toluene (50 mL) was heated to reflux. $SOCl_2$ (9 mL) was added dropwise within 3 hours. The mixture was left refluxed overnight and cooled to room temperature before 2 N HCl (aq) was added slowly. The organic layer was dried over $MgSO_4$ and concentrated to furnish crude **1c** (11 g, 68 %) as a yellow liquid (Yakuphanoglu *et al.*, 2005). The material was used for the subsequent reaction without prior purification.

A solution of imidazole (1.6 g, 24 mmol) and NaH (60% suspension in paraffin oil) (1.1 g, 28 mmol) in THF (50 mL) was treated with crude **1c** (11 g, 48 mmol) according to general procedure **3.6.1** to furnish **2c** as a yellow liquid (2.6 g, 42 %). ^{1}H NMR (400 MHz, $CDCl_3$): δ 7.44 (1H, s, N=C*H*-N), 6.91 (2H, m, N-C*H*=C*H*), 4.01-3.99 (2H, m, -NCH_2-), 3.64-3.52 (14H, m, -CH_2OCH_2CH_2 OCH_2CH_2 OCH_2CH_2Cl); ^{13}C NMR (100 MHz, $CDCl_3$): δ 137.2 (N=*C*H-N), 128.6 (N-CH=*C*H), 119.1 (N-*C*H=CH), 70.9 (-NCH_2*C*H_2O-), 70.3, 70.23, 70.18, 70.1 (O*C*H_2*C*H_2O*C*H_2*C*H_2O*C*$H_2$$CH_2$Cl), 46.7 (-$NCH_2$), 42.5 (-$CH_2$Cl).

1-(2-(2-Azidoethoxy)ethyl)-1*H*-imidazole (3a)

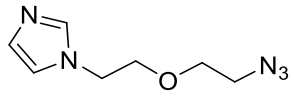

A solution of **2a** (0.42 g, 2.4 mmol) in DMF (10 mL) was treated with NaN_3 (0.31 g, 4.8 mmol) and subsequently heated up according to general procedure **3.6.2** to provide **3a** as a yellow liquid (0.40 g, 92 %). IR [neat] ν/cm^{-1} 2931, 2873 (CH), 2102 (N_3). ^{1}H NMR (400 MHz, $CDCl_3$): δ 7.53 (1H, s, N=C*H*-N), 7.04-6.98 (2H, 2 s, N-C*H*=C*H*), 4.14-4.12 (2H, m, -NCH_2-), 3.74-3.72 (2H, m, -NCH_2CH_2O-), 3.60-3.58 (2H, m, -$OCH_2CH_2N_3$), 3.35 (2H, m, -CH_2N_3); ^{13}C NMR (100 MHz, $CDCl_3$): δ 137.4 (N=*C*H-N), 129.2 (CH=N-*C*H), 119.4 (CH=*C*H-N), 70.5 (-$CH_2OCH_2CH_2N_3$), 70.1 (-$CH_2OCH_2CH_2N_3$), 50.6 (-CH_2N_3), 47.1 (-NCH_2-). HRESIMS: Calcd. for $[M+H]^+$ $[C_7H_{11}N_5O+H]^+$ 182.1042; found 182.1032.

1-(2-(2-(2-Azidoethoxy)ethoxy)ethyl)-1*H*-imidazole (3b)

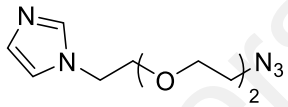

A solution of **2b** (0.54 g, 2.5 mmol) in DMF (10 mL) was treated with NaN_3 (0.40 g, 6.2 mmol) and heated according to general procedure **3.6.2** to provide **3b** as a yellow liquid (0.51 g, 92%). IR [neat] ν/cm^{-1} 2872 (CH), 2102 (N_3). ^{1}H NMR (400 MHz, $CDCl_3$): δ 7.46 (1H, s, N=C*H*-N), 6.95-6.92 (2H, m, N-C*H*=C*H*), 4.06-4.02 (2H, m, -NCH_2-), 3.70-3.66 (2H, m, –NCH_2CH_2-), 3.56-3.53 (6H, m, -$OCH_2CH_2OCH_2CH_2N_3$), 3.30-3.28 (2H, m, -CH_2N_3); ^{13}C NMR (100 MHz, $CDCl_3$): δ 137.4 (N=*C*H-N), 129.0 (CH=N-*C*H), 119.3 (CH=*C*H-N), 70.6, 70.54, 70.50, 70.0 (-$CH_2OCH_2CH_2OCH_2CH_2N_3$), 50.6 (-$CH_2N_3$), 47.0 (-$NCH_2$). HRESIMS: Calcd. for $[M+H]^+$ $[C_9H_{15}N_5O_2+H]^+$ 226.1304; found 226.1304.

1-(2-(2-(2-(2-Azidoethoxy)ethoxy)ethoxy)ethyl)-1*H*-imidazole (3c)

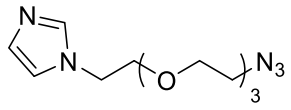

A solution of **2c** (0.30 g, 1.1 mmol) in DMF (20 mL) was treated with NaN_3 (0.15 g, 2.3 mmol) and heated up according to general procedure **3.6.2** to provide **3c** as a yellow liquid (0.27 g, 91%). IR [neat] ν/cm^{-1} 2873 (CH), 2102 (N_3). ^{1}H NMR (400 MHz, $CDCl_3$): δ 7.52 (1H, s, N=C*H*-N), 7.01 (1H, s, CH=N-C*H*), 6.97 (1H, S, CH=C*H*-N), 4.10-4.07 (2H, t, -NCH_2-), 3.73-3.71 (2H, t, –NCH_2CH_2-), 3.66-3.56 (12H, m, $CH_2(OCH_2CH_2)_2CH_2$), 3.37-3.35 (2H, t, -CH_2N_3); ^{13}C NMR (100 MHz, $CDCl_3$): δ 137.4 (N=*C*H-N), 129.0 (CH=N-*C*H), 119.3 (CH=*C*H-N), 70.6, 70.51, 70.50, 70.4, 69.9 ($CH_2(OCH_2CH_2)_2CH_2$), 50.6 (-CH_2N_3), 47.0 (-NCH_2). HRESIMS: Calcd. for $[M+H]^+$ $[C_{11}H_{19}N_5O_3+H]^+$ 270.1566; found 270.1563.

2-(2-(prop-2-yn-1-yloxy)ethoxy)ethan-1-ol (4) (Diot *et al.*, 2009; Salman & Heidelberg, 2014)

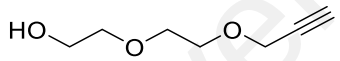

Diethylene glycol (15 mL) was dissolved in THF (60 mL) and treated with NaH (60% suspension in paraffin oil) (1.6 g, 40 mmol). The mixture was stirred at room temperature for an hour. Propargyl bromide (3.3 mL, 37 mmol) was added slowly at 0 °C and the reaction was subsequently stirred at room temperature overnight. The reaction was quenched by addition of CH_3OH (10 mL). The solvent was evaporated and the residue was dissolved in CH_2Cl_2 and washed twice with water. The organic layer was dried over $MgSO_4$ and concentrated. A light yellow liquid **4** (3.8 g, 70 %) was obtained by column chromatography (EtOAc: hexane = 1:3). ^{1}H NMR (400 MHz, $CDCl_3$): δ 4.17-

4.15 (2H, d, -OC*H*$_2$CCH), 3.68-3.53 (8H, m, HO(CH$_2$CH$_2$O)$_2$), 2.96 (1H, bs, -OH), 2.44-2.43 (1H, t, C≡CH); $^4J_{propargyl}$= 2.5 Hz; ^{13}C NMR (100 MHz, CDCl$_3$): δ 79.2 (*C*≡CH), 74.7 (C≡*C*H), 72.4, 69.9, 68.9 (HO(CH$_2$CH$_2$O)$_2$), 61.4 (CH$_2$OH), 58.2 (O*C*H$_2$CCH).

2-(2-(Prop-2-yn-1-yloxy)ethoxy)ethyl-4-methylbenzensulfonate (5) (Diot *et al.*, 2009)

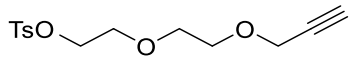

A solution of **4** (1.9 g, 13 mmol) in THF (30 mL) was cooled in an ice bath before NaOH pellets (0.68 g, 17 mmol) was added. TsCl (2.7 g, 14 mmol) was added at 0 °C. The mixture was left with stirring at room temperature overnight. THF was evaporated and the residue was dissolved in CH$_2$Cl$_2$ and washed twice with water. The organic layer was dried over MgSO$_4$ and the solvent was evaporated. Compound **5** (3.4 g, 87 %) was obtained as a yellow liquid by chromatography over silica gel (EtOAc: hexane= 1:7). ^{1}H NMR (400 MHz, CDCl$_3$): δ 7.76-7.74 (2H, d, aromatic –CH), 7.32 (2H, bs, aromatic -CH), 4.11 (4H, bs, -SOCH$_2$, C*H*$_2$CCH), 3.64-3.56 (7H, m, CH$_2$OCH$_2$CH$_2$O, C≡CH), 2.4 (3H, bs, CH$_3$); ^{13}C NMR (100 MHz, CDCl$_3$): δ 144.8, 132.8 (aromatic C), 129.8, 127.9 (aromatic -CH), 79.4 (*C*≡CH), 74.6 (C≡*C*H), 70.4, 69.1, 68.9, 68.6 ((CH$_2$CH$_2$O)$_2$), 58.3 (*C*H$_2$CCH), 21.5 (CH$_3$).

3-(2-(2-Iodoethoxy)ethoxy)prop-1-yne (6) (Piron *et al.*, 2010)

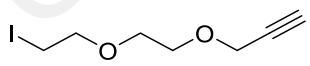

A solution of **5** (3.0 g, 10 mmol) in acetone (40 mL) was treated with NaI (3.0 g, 20 mmol). The reaction was stirred at room temperature overnight. The reaction was concentrated and the residue was distributed between CH$_2$Cl$_2$ and water. The organic layer was washed successively with 10 % Na$_2$S$_2$O$_3$ (aq) and water. The organic layer was dried over MgSO$_4$ and concentrated. A colourless liquid **6** (2.2 g, 88 %) was obtained and

used for the subsequent reaction without further purification. ^{1}H NMR (400 MHz, $CDCl_3$): δ 4.23 (2H, s, OC*H*$_2$C≡CH), 3.79-3.75 (2H, t, OC*H*$_2$CH$_2$I), 3.71 (4H, bs, OCH_2CH_2O), 3.29-3.26 (2H, t, CH_2I), 2.45-2.44 (1H, bs, C≡CH); ^{13}C NMR (100 MHz, $CDCl_3$): δ 79.5 (*C*≡CH), 74.6 (C≡*C*H), 72.0, 70.0, 69.1 (-$CH_2OCH_2CH_2O$-), 58.5 (*C*H_2C≡CH), 2.7 (CH_2I).

2-Hexyl-decyl 2,3,4,6-tetra-*O*-acetyl-β-D-glucopyranoside (7) (Hashim *et al.*, 2006)

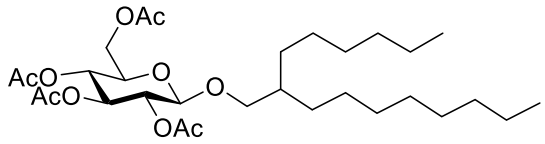

β-D-glucose pentaacetate (13 g, 33 mmol) and 2-hexyl-1-decanol (12 mL, 40 mmol) were dissolved in CH_2Cl_2 (70 mL), followed by addition of $BF_3{\cdot}OEt_2$ (5.8 mL, 46 mmol) according to general procedure **3.6.4**. Compound **7** was obtained as a yellow syrup (7.5 g, 40 %) by chromatography over silica gel (EtOAc: hexane= 1:7). $[\propto]_D^{25}$ = -14 (c 0.89, $CHCl_3$). ^{1}H NMR (400 MHz, $CDCl_3$): δ 5.21-5.16 (1H, dd~t, H-3), 5.10-5.05 (1H, dd~t, H-4), 5.00-4.96 (1H, dd, H-2), 4.45-4.43 (1H, d, H-1), 4.28-4.24 (1H, dd, H-6a), 4.14-4.10 (1H, dd, H-6b), 3.81-3.78 (1H, dd, -OCH_2a), 3.69-3.65 (1H, ddd, H-5), 3.30-3.26 (1H-, dd, -OCH_2b), 2.07, 2.01(2), 1.99 (12H, 4 s, Ac), 1.53 (1H, bs, -OCH_2C*H*), 1.30-1.23 (24H, m, bulk –CH_2), 0.88-0.85 (6H, t, -CH_3); $^{3}J_{1,2}$= 8.0, $^{3}J_{2,3}$=10.0, $^{3}J_{3,4}$= 10.0, $^{3}J_{4,5}$= 10.0, $^{3}J_{5,6a}$= 5.0, $^{3}J_{5,6b}$= 2.5, $^{2}J_{6a,6b}$= 12.0 Hz; ^{13}C NMR (100 MHz, $CDCl_3$): δ 170.7, 170.3, 169.4, 169.1 (C=O), 101.1 (C-1), 73.0 (-OCH_2), 72.8 (C-3), 71.6 (C-2), 71.3 (C-5), 68.5 (C-4), 61.9 (C-6), 37.9 (-OCH_2*C*H), 31.82/ 31.80, 31.0, 30.8, 30.00/ 29.96, 29.65/ 29.62, 29.5, 29.3, 26.73/ 26.68, 26.53/ 26.48 (bulk –CH_2), 22.6 (ω-1), 20.7, 20.6, 20.5 (Ac), 14.0 (ω).

2-butyl-octyl 2,3,4,6-tetra-*O*-acetyl-β-D-glucopyranoside (8) (Hashim *et al.*, 2006)

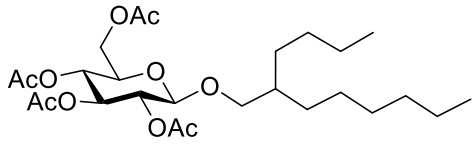

β-D-glucose pentaacetate (3.6 g, 9.2 mmol) and 2-butyl-1-octanol (2.5 mL, 11 mmol) were dissolved in CH_2Cl_2 (40 mL). $BF_3 \cdot OEt_2$ (1.5 mL, 12 mmol) was added according to general procedure **3.6.4**. Compound **8** was obtained as a yellow syrup (1.9 g, 40 %) by chromatography over silica gel (EtOAc: hexane= 1:7). $[\propto]_D^{25}$ = -14 (c 1.00, $CHCl_3$). ^{1}H NMR (400 MHz, $CDCl_3$): δ 5.18-5.13 (1H, dd~t, H-3), 5.06-5.01 (1H, dd~t, H-4), 4.96-4.92 (1H, dd, H-2), 4.42-4.40 (1H, d, H-1), 4.24-4.20 (1H, dd, H-6a), 4.10-4.06 (1H, dd, H-6b), 3.78-3.74 (1H, dd, -OCH_2a), 3.66-3.62 (1H, ddd, H-5), 3.27-3.23 (1H, dd, -OCH_2b), 2.03, 1.97 (2), 1.95 (12H, 4 s, Ac), 1.50 (1H, bs, OCH_2CH), 1.19 (16H, bs, bulk -CH_2), 0.84-0.81 (6H, t~m, -CH_3); $^3J_{1,2}$=8.0, $^3J_{2,3}$=10.0, $^3J_{3,4}$=10.0, $^3J_{4,5}$=10.0, $^3J_{5,6a}$=5.0, $^3J_{5,6b}$=3.0, $^2J_{6a,6b}$=12.0 Hz; ^{13}C NMR (100 MHz, $CDCl_3$): δ 170.5, 170.2, 169.3, 169.0 (C=O), 101.0 (C-1), 72.9 (OCH_2), 72.7 (C-3), 71.5 (C-5), 71.2 (C-2), 68.4 (C-4), 61.9 (C-6), 37.8 (OCH_2CH), 31.7, 30.9, 30.7, 30.6, 30.4, 29.53/ 29.51, 28.8, 28.6, 26.6, 26.4, 22.89/ 22.86 (bulk -CH_2), 22.5 (ω-1), 20.5, 20.43, 20.41 (Ac), 13.9 (ω).

2-Hexyl-decyl β-D-glucopyranoside (9) (Hashim *et al.*, 2006)

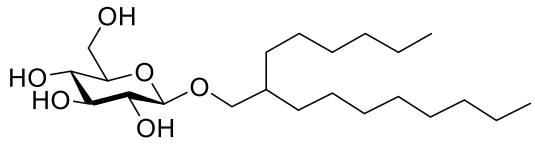

A solution of **7** (5.0 g, 8.7 mmol) in CH_3OH (70 mL) was treated with a catalytic amount of $NaOCH_3$ according to general procedure **3.6.5** to provide **9** (3.3 g, 98%) as a

light yellow syrup. The material was used for subsequent reaction without further purification.

2-Butyl-octyl β-D-glucopyranoside (10) (Hashim *et al.*, 2006)

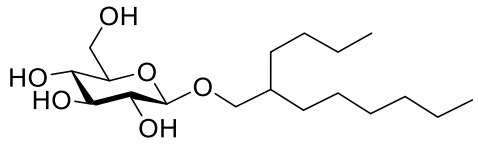

A solution of **8** (3.1 g, 6.0 mmol) in CH_3OH (70 mL) was treated with a catalytic amount of $NaOCH_3$ according to general procedure **3.6.5** to provide **10** (2.0 g, 95%) as a light yellow syrup. The material was used for subsequent reaction without prior purification.

2-Hexyl-decyl 6-bromo-6-deoxy-2,3,4-tri-*O*-acetyl-β-D-glucopyranoside (11)

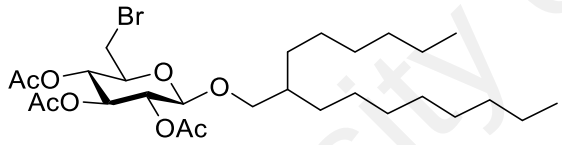

Following general procedure **3.6.6**, a solution of **9** (1.7 g, 4.2 mmol) in DMF (12 mL) was treated with PPh_3 (2.2 g, 8.4 mmol) and NBS (1.5 g, 8.4 mmol). The crude obtained was then treated with Ac_2O (4.0 mL, 42 mmol) in pyridine (12 mL), according to general procedure **3.6.7**. A yellow syrup **11** (1.3 g, 52%) was obtained by chromatography over silica gel (EtOAc: hexane=1:9). $[\propto]_D^{25}$ = -4 (c 0.20, $CHCl_3$). ^{1}H NMR (400 MHz, $CDCl_3$): δ 5.23-5.18 (1H, dd~t, H-3), 5.01-4.94 (2H, m, H-4, H-2), 4.49-4.48 (1H, d, H-1), 3.86-3.82 (1H, dd, -OCH_2a), 3.71-3.66 (1H, m, H-5), 3.47-3.44 (1H, dd, H-6a), 3.41-3.33 (2H, m, H-6b, -OCH_2b), 2.06, 2.03, 2.01 (9H, 3 s, Ac), 1.56 (1H, bs, -OCH_2CH), 1.26 (24H, bs, bulk -CH_2), 0.90-0.87 (6H, t, -CH_3); $^3J_{1,2}$=8.0, $^3J_{2,3}$=10.0, $^3J_{3,4}$=10.0, $^3J_{4,5}$=10.0, $^3J_{5,6a}$=3.0, $^3J_{5,6b}$=6.0, $^2J_{6a,6b}$=11.0 Hz; ^{13}C NMR (100

MHz, $CDCl_3$): δ 170.3, 169.5, 169.1 (C=O), 100.8 (C-1), 73.3 (C-5), 72.9 (-O*C*H_2CH), 72.7 (C-3), 71.4 (C-4), 71.2 (C-2), 37.9 (-OCH_2*C*H), 31.87/ 31.84, 31.1 (bulk -CH_2), 30.9 (C-6), 30.7, 30.04/ 30.02, 29.69/ 29.67, 29.6, 29.3, 26.76/ 26.71, 26.61/ 26.56 (bulk –CH_2), 22.7 (ω-1), 20.7, 20.60, 20.57 (Ac), 14.1 (ω).

2-Butyl-octyl 6-bromo-6-deoxy-2,3,4-tri-*O*-acetyl-β-D-glucopyranoside (12)

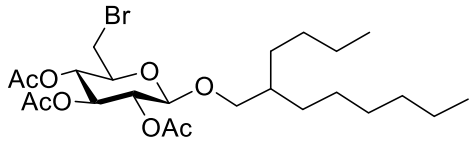

Following general procedure **3.6.6**, a solution of **10** (2.0 g, 5.7 mmol) in DMF (20 mL) was treated with PPh_3 (3.0 g, 11 mmol) and NBS (2.0 g, 11 mmol). The crude obtained was treated with Ac_2O (4.0 mL, 42 mmol) in pyridine (20 mL), according to general procedure **3.6.7**. Compound **12** (1.6 g, 52%) was obtained as a yellow syrup by chromatography over silica gel (EtOAc: hexane= 1:7). $[\propto]_D^{25}$ = -5 (c 0.30, $CHCl_3$). ^{1}H NMR (400 MHz, $CDCl_3$): δ 5.22-5.17 (1H, dd~t, H-3), 5.00-4.93 (2H, m, H-4, H-2), 4.48-4.46 (1H, d, H-1), 3.85-3.81 (1H, dd, -OCH_2a), 3.70-3.65 (1H, m, H-5), 3.46-3.43 (1H, dd, H-6a), 3.40-3.32 (2H, m, H-6b, -OCH_2b), 2.04, 2.01, 1.99 (Ac), 1.55 (1H, bs, -OCH_2C*H*), 1.29-1.24 (16H, bs, bulk -CH_2), 0.88-0.85 (6H, t~m, -CH_3); $^3J_{1,2}$=8.0, $^3J_{2,3}$=10.0, $^3J_{3,4}$=10.0, $^3J_{4,5}$=10.0, $^3J_{5,6a}$=5.0, $^3J_{5,6b}$=3.0, $^2J_{6a,6b}$=11.0 Hz; ^{13}C NMR (100 MHz, $CDCl_3$): δ 170.2, 169.5, 169.1 (C=O), 100.8 (C-1), 73.3 (C-5), 72.89/ 72.84 (OCH_2), 72.6 (C-3), 71.4 (C-4), 71.2 (C-2), 37.9 (-OCH_2*C*H), 31.8, 31.1, 30.9, 30.8, 30.7 (bulk –CH_2), 30.6 (C-6), 29.64/ 29.63, 28.9, 28.8, 26.7, 26.5, 23.00/ 22.98 (bulk –CH_2), 22.6 (ω-1), 20.61, 20.55, 20.5 (Ac), 14.0 (ω).

2-Hexyl-decyl 6-deoxy-6-[3-(5-azido-3-oxa-pentyl)-imidazolium]-2,3,4-tri-*O*-acetyl-β-D-glucopyranoside bromide (13a)

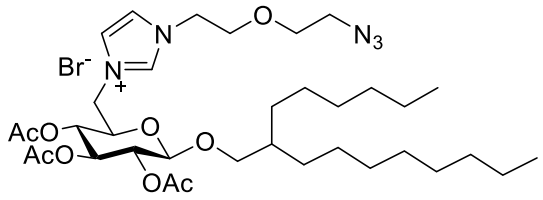

A solution containing **3a** (37 mg, 0.20 mmol) and **11** (0.12 g, 0.20 mmol) in xylene (2 mL) was heated to 130 °C according to general procedure **3.6.15** to provide **13a** (0.14 g, 89 %) as a yellow syrup. $[\propto]_D^{25}$ = -20 (c 0.1, $CHCl_3$). ^{1}H NMR (400 MHz, $CDCl_3$): δ 10.46 (1 H, s, N=C*H*-N), 7.38 (2H, s, N-C*H*=C*H*), 5.25-5.21 (1H, dd~t, H-3), 4.92-4.88 (1H, dd, H-2), 4.73-4.68 (3H, m, H-6a, H-4), 4.60-4.50 (4H, m, H-6b, -NCH_2CH$_2$, H-1), 4.08-4.03 (1H, ddd~dt, H-5), 3.97-3.94 (2H, m, -CH_2OCH$_2$CH$_2$N$_3$), 3.75-3.71 (3H, -OCH_2*a*-CH, -OCH_2CH$_2$N$_3$), 3.42-3.39 (2H, m, -CH$_2$N$_3$), 3.34-3.30 (1H, dd, -OCH_2*b*-CH), 2.27, 2.01, 1.97 (9H, 3 s, Ac), 1.52 (1H, bs, -OCH$_2$C*H*), 1.24 (24H, bs, bulk -CH$_2$), 0.89-0.85 (6H, t, -CH$_3$); $^3J_{1,2}$=8.0, $^3J_{2,3}$=9.5, $^3J_{3,4}$=9.5, $^3J_{4,5}$=10.0, $^3J_{5,6a}$=4.0, $^3J_{5,6b}$=4.5, $^2J_{6a,6b}$=14.0 Hz; ^{13}C NMR (100 MHz, $CDCl_3$): δ 170.5, 169.7, 169.1 (C=O), 138.4 (N=CH-N), 122.8 (CH=N-*C*H), 122.5 (CH=*C*H-N), 101.0 (C-1), 73.4 (-O*C*H$_2$CH), 72.1 (C-3), 71.3 (C-5), 70.9 (C-2), 70.1 (-O*C*H$_2$CH$_2$N$_3$), 68.8 (-*C*H$_2$OCH$_2$CH$_2$N$_3$), 68.3 (C-4), 50.5 (-CH$_2$N$_3$), 50.1 (-N*C*H$_2$CH$_2$), 49.5 (C-6), 37.9 (-OCH$_2$*C*H-), 31.8, 30.9, 30.7, 29.93/ 29.90, 29.57/ 29.50, 29.2, 26.74, 26.68, 26.6 (bulk -CH$_2$), 22.5 (ω-1), 21.3, 20.42, 20.38 (Ac), 14.0 (ω).

2-Hexyl-decyl 6-deoxy-6-[3-(8-azido-3,6-dioxa-octyl)-imidazolium]-2,3,4-tri-*O*-acetyl-β-D-glucopyranoside bromide (13b)

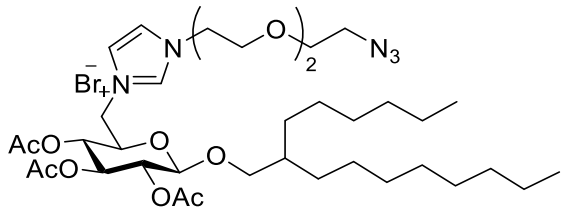

A mixture of **3b** (83 mg, 0.37 mmol) and **11** (0.22 g, 0.37 mmol) in xylene (1 mL) was heated to 130 °C according to the procedure **3.6.15** and provided **13b** (0.27 g, 89 %) as a yellow syrup. $[\propto]_D^{25}$ = -16 (c 0.56, $CHCl_3$). ^{1}H NMR (400 MHz, $CDCl_3$): δ 10.15 1 H, s, N=C*H*-N), 7.47 (1 H, s, CH=N-C*H*), 7.36 (1H, s, CH=C*H*-N), 5.21-5.16 (1 H, dd~t, H-3), 4.87-4.83 (1H, dd, H-2), 4.75- 4.62 (3H, m, H-6, H-4), 4.54-4.39 (3H, m, H-1, -NCH_2CH$_2$), 4.08-4.03 (1H, m, H-5), 3.89-3.86 (2H, m, -NCH$_2$CH_2), 3.66-3.58 (7H, m, -OCH_2a-CH, -OCH_2CH_2OCH_2CH$_2$N$_3$), 3.36-3.33 (2H, t, -CH_2N$_3$), 3.29-3.25 (1H,dd, -OCH_2b-CH), 2.21, 1.96, 1.92 (9H, 3 s, Ac), 1.46 (1H, bs, -OCH$_2$C*H*), 1.26-1.18 (24H, m, bulk -CH$_2$), 0.84-0.80 (6H, t, -CH$_3$); $^3J_{1,2}$=8.0, $^3J_{2,3}$=9.5, $^3J_{3,4}$=9.5, $^3J_{4,5}$=9.5, $^3J_{5,6a}$=2.5, $^3J_{5,6b}$=6.0, $^2J_{6a,6b}$=14.5, $^3J_{imidazole}$=1.5 Hz. ^{13}C NMR (100 MHz, $CDCl_3$): δ 170.5, 169.6, 169.1 (C=O), 138.3 (N=*C*H-N), 122.7 (CH=N-*CH*), 122.6 (CH=*C*H-N), 101.0 (C-1), 73.28/ 73.25 (-O*C*H$_2$CH), 72.0 (C-3), 71.2 (C-5), 70.9 (C-2), 70.2, 70.1 69.8 (-O*C*H$_2$*C*H$_2$O*C*H$_2$CH$_2$N$_3$), 68.7 (-NCH$_2$*C*H$_2$), 68.2 (C-4), 50.5 (-CH_2N$_3$), 49.9 (-NCH$_2$CH$_2$), 49.4 (C-6), 37.9 (-OCH$_2$*C*H), 31.68/ 31.66, 30.9, 30.62/ 30.61, 29.87/ 29.84 29.50/ 29.48, 29.4 29.2, 26.7, 26.6, 26.5 (bulk CH$_2$), 26.5 (γ), 22.5 (ω-1), 21.3, 20.4, 20.3 (Ac), 13.9 (ω).

2-Hexyl-decyl 6-deoxy-6-[3-(11-azido-3,6,9-trioxa-undecyl)-imidazolium]-2,3,4-tri-*O*-acetyl-β-D-glucopyranoside bromide (13c)

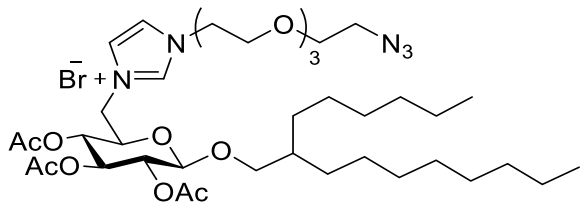

A solution containing **11** (0.14 g, 0.24 mmol) and **3c** (64 mg, 0.24 mmol) were in xylene (2 mL) was heated to 130 °C, following general procedure **3.6.15**. A yellow syrup **13c** (0.18 g, 88 %) was obtained. $[\propto]_D^{25}$ = -17 (c 0.20, $CHCl_3$). ^{1}H NMR (400 MHz, $CDCl_3$): δ 10.44 (1 H, N=C*H*-N), 7.51-7.50 (1H, t, CH=N-C*H*), 7.39-7.38 (1H, t, CH=C*H*-N), 5.25-5.20 (1H, dd~t, H-3), 4.92-4.87 (1H, dd, H-2), 4.82-4.77 (1H, dd, H-6a), 4.72-4.65 (2H, m, H-6b, H-4), 4.57-4.40 (3H, m, H-1, -NCH_2CH$_2$), 4.08-4.04 (1H, ddd, H-5), 3.92-3.89 (2H, m, -NCH$_2$CH_2), 3.76-3.72 (1H, m, -OCH_2*a*-CH), 3.68-3.63 (10H, m, -OCH_2CH_2OCH_2CH_2OCH_2CH$_2$N$_3$), 3.40-3.37 (2H, t, -CH_2N$_3$), 3.34-3.30 (1H, dd, -OCH_2*b*-CH), 2.27, 2.01, 1.96 (9H, 3 s, Ac), 1.51 (1H, bs, -OCH$_2$C*H*), 1.29-1.24 (24H, m, bulk -CH$_2$), 0.89-0.85 (6H, t, CH$_3$); $^3J_{1,2}$=8.0, $^3J_{2,3}$=9.5, $^3J_{3,4}$=9.5, $^3J_{4,5}$=10.0, $^3J_{5,6a}$=5.5, $^3J_{5,6b}$=2.5, $^2J_{6a,6b}$=15.0, $^3J_{\text{imidazole}}$=1.5 Hz; ^{13}C NMR (100 MHz, $CDCl_3$): δ 170.6, 169.7, 169.2 (C=O), 138.8 (N=*C*H-N), 122.8 (CH=N-*C*H), 122.7 (CH=*C*H-N), 101.2 (C-1), 73.49/ 73.46 (-O*C*H$_2$CH), 72.1 (C-3) 71.4 (C-5), 71.0 (C-2), 70.6, 70.40, 70.39, 70.3, 70.0 (-O*C*H$_2$*C*H$_2$O*C*H$_2$*C*H$_2$O*C*H$_2$CH$_2$N$_3$), 68.9 (-NCH$_2$*C*H$_2$), 68.1 (C-4), 50.6 (-CH$_2$N$_3$), 49.9 (-N*C*H$_2$CH$_2$), 49.4 (C-6), 38.0 (-OCH$_2$*C*H), 31.82/ 31.79, 31.0, 30.8, 30.00, 29.98, 29.64/ 29.61, 29.57/ 29.56, 29.3, 26.8, 26.7, 26.63 (bulk-CH$_2$), 26.59 (γ), 22.6 (ω-1), 21.4, 20.5, 20.4 (Ac), 14.0 (ω).

2-Hexyl-decyl 6-deoxy-6-[3-(5-azido-3-oxa-pentyl)-imidazolium]-β-D-glucopyranoside bromide (14a)

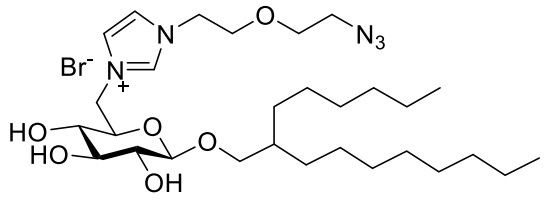

Compound **13a** (0.12 g, 0.15 mmol) was subjected to a deacetylation reaction in CH_3OH (5 mL) based on procedure **3.6.5** to yield **14a** (90 mg, 92 %) as a yellow syrup. IR [neat] ν/cm^{-1} 3365 (OH), 2955, 2924, 2855 (CH), 2108 (N_3). $[\propto]_D^{25}$ = -13(c 0.12, CH_3OH). ^{1}H NMR (400 MHz, CD_3OD): δ 8.55 (<1H, bs, N=C*H*-N) 7.70-7.69 (1H, d, CH=N-C*H*), 7.60-7.59 (1H, d, CH=C*H*-N), 4.66-4.62 (1H, dd, H-6a), 4.47-4.45 (2H, t, -NC*H*$_2$CH$_2$), 4.44-4.38 (1H, dd, H-6b), 4.25-4.23 (1H, d, H-1), 3.90-3.88 (2H, t, -NCH$_2$C*H*$_2$), 3.71-3.65 (3H, m, -OCH$_2$C*H*$_2$N$_3$, -OC*H*$_2$*a*-CH), 3.63-3.58 (1H, m, H-5), 3.40-3.33 (2H, m, H-3, -OC*H*$_2$*b*-CH), 3.17-3.13 (1H, dd, H-2), 3.08-3.03 (1H, dd~t, H-4), 1.59 (1H, bs, -OCH$_2$C*H*), 1.34-1.27 (24H, bulk –CH$_2$), 0.92-0.89 (6H, t, -CH$_3$); $^3J_{imidazole}$=2.0, $^3J_{1,2}$=8.0, $^3J_{2,3}$=9.0, $^3J_{3,4}$=9.0 $^3J_{4,5}$=9.5, $^3J_{5,6a}$=2.5, $^3J_{5,6b}$=7.0, $^2J_{6a,6b}$=14.5 Hz; ^{13}C NMR (100 MHz, CD_3OD): δ 138.8 (N=CH-N), 124.9 (CH=N-*C*H), 123.9 (CH=*C*H-N), 105.0 (C-1), 77.5 (C-3), 75.1 (C-2), 74.9 (C-5), 74.3 (-O*C*H$_2$CH), 72.5 (C-4), 71.4 (-O*C*H$_2$CH$_2$N$_3$), 69.8 (-NCH$_2$*C*H$_2$), 51.9 (C-6), 51.8 (-*C*H$_2$N$_3$), 51.1 (-N*C*H$_2$CH$_2$), 39.7 (-OCH$_2$*C*H), 33.9, 33.2, 32.4, 32.3, 31.3, 31.0, 30.9, 30.6, 28.0, 28.0, 28.0 (bulk –CH$_2$), 23.9 (ω-1) 14.6 (ω). HRDARTMS: Calcd. for M^+ $[C_{29}H_{54}N_5O_6]^+$ 568.4074; found 568.4056.

2-Hexyl-decyl 6-deoxy-6-[3-(8-azido-3,6-dioxa-octyl)-imidazolium]-β-D-glucopyranoside bromide (14b)

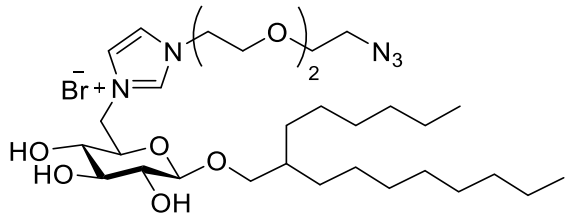

Compound **13b** (0.27 g, 0.33 mmol) underwent a deacetylation reaction in CH_3OH (3 mL) according to the procedure **3.6.5** to furnish **14b** (0.22 g, 97 %) as a yellow syrup. IR [neat] ν/cm^{-1} 3354 (OH), 2824, 2856 (CH), 2104 (N_3). $[\propto]_D^{25}$ = -13 (c 0.14, CH_3OH). ^{1}H NMR (400 MHz, CD_3OD): δ 8.52 (<1H, bs, N=CH-N), 7.70 (1H, s, CH=N-C*H*), 7.59 (1H, s, CH=C*H*-N), 4.67-4.63 (1H, dd~d, H-6a), 4.46-4.41 (3H, m, -NC*H*$_2$CH$_2$, H-6b), 4.26-4.24 (1H, d, H-1), 3.89-3.87 (2H, t, -NCH$_2$C*H*$_2$), 3.67-3.61 (8H, m, -OC*H*$_2$C*H*$_2$OC*H*$_2$CH$_2$N$_3$, -OC*H*$_2$*a*-CH, H-5), 3.41-3.35 (4H, m, -CH$_2$N$_3$, -OC*H*$_2$*b*-CH, H-3), 3.17-3.12 (1H, dd~t, H-2), 3.08-3.03 (1H, dd~t, H-4), 1.59 (1H, bs, -OCH$_2$C*H*), 1.42-1.30 (24H, m, bulk -CH$_2$), 0.92-0.89 (6H, t, -CH$_3$); $^3J_{1,2}$=8.0, $^3J_{2,3}$=9.0, $^3J_{3,4}$=9.0, $^2J_{6a,6b}$=14.5 Hz; ^{13}C NMR (100 MHz, CD_3OD): δ 138.7 (N=CH-N), 124.7 (CH=N-*C*H), 124.1 (CH=*C*H-N), 105.0 (C-1), 77.7 (C-3), 75.1 (C-2), 74.9 (C-5), 74.3 (-O*C*H$_2$CH), 72.5 (C-4), 71.59, 71.58, 71.2 (-O*C*H$_2$*C*H$_2$O*C*H$_2$CH$_2$N$_3$), 70.0 (-NCH$_2$*C*H$_2$), 51.9 (CH$_2$N$_3$), 51.9 (-C6), 51.1 (-N*C*H$_2$CH$_2$), 39.6 (-OCH$_2$*C*H), 33.2, 32.34/ 32.33, 32.28/ 32.26, 31.30/ 31.29, 31.0, 30.88/ 30.86, 30.6, 28.02, 28.01, 27.96, 27.95 (bulk -CH$_2$), 23.9 (ω-1), 14.6 (ω). HRDARTMS: Calcd. for M^+ $[C_{31}H_{58}N_5O_7]^+$ 612.4337 (100 %), 613.4370 (34 %), 614.4404 (5 %); found 612.4337 (100 %), 613.4354 (40 %), 614.4410 (12 %).

2-Hexyl-decyl 6-deoxy-6-[3-(11-azido-3,6,9-trioxa-undecyl)-imidazolium]-β-D-glucopyranoside bromide (14c)

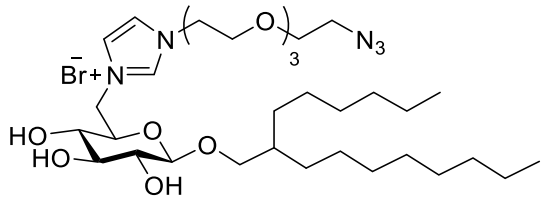

Compound **13c** (0.18 g, 0.21 mmol) was deacetylated in CH_3OH (3 mL), following general procedure **3.6.5** to provide **14c** (0.14 g, 90 %) as a yellow syrup. IR [neat] ν/cm^{-1} 3355 (OH), 2923, 2855 (CH), 2104 (N_3). $[\propto]_D^{25}$ = -12 (c 0.49, CH_3OH). ^{1}H NMR (400 MHz, CD_3OD): δ 9.02 (<1H, bs, N=CH-N), 7.72 (1H, d, CH=N-C*H*), 7.59 (1 H, d, CH=C*H*-N), 4.68-4.64 (1H, dd, H-6a), 4.47-4.43 (3H, m, -NCH_2CH_2, H-6b), 4.27-4.25 (1H, d, H-1), 3.89-3.87 (2H, t, -NCH$_2$CH_2), 3.69-3.61 (12H, m$_c$, -(OCH_2CH_2)$_2$ CH_2CH$_2$N$_3$, -OCH_2*a*-CH, H-5), 3.40-3.35 (4H, m, -CH$_2$N$_3$, -OCH_2*b*-CH, H-3), 3.17-3.13 (1H, dd, H-2), 3.09-3.04 (1H, dd~t, H-4), 1.59 (1H, bs, -OCH$_2$C*H*), 1.34-1.27 (24H, m, bulk -CH$_2$), 0.92-0.89 (6H, t, -CH$_3$); $^3J_{1,2}$=8.0, $^3J_{2,3}$=9.0, $^3J_{3,4}$=9.5, $^3J_{5,6a}$=2.5, $^3J_{5,6a}$=7.5, $^2J_{6a,\ 6b}$= 14.5 Hz, $^3J_{imidazole}$=2.0 Hz; ^{13}C NMR (100 MHz, CD_3OD): 139.0 (N=CH-N), 124.6 (CH=N-*C*H), 124.1 (CH=*C*H-N), 105.0 (C-1), 77.7 (C-3), 75.1 (C-2), 74.9 (C-5), 74.3 (-O*C*H$_2$CH), 72.4 (C-4), 71.7, 71.64, 71.58, 71.5, 71.1 (-(O*C*H$_2$*C*H$_2$)$_2$O*C*H$_2$CH$_2$N$_3$), 69.9 (-NCH$_2$*C*H), 51.92 (-CH2N3), 51.86 (C-6), 51.1 (-N*C*H$_2$CH$_2$), 39.60 (-OCH$_2$*C*H), 33.18, 33.17, 32.30, 32.24, 31.28, 30.96, 30.86/ 30.84, 30.6, 28.00/ 27.98, 27.93/ 27.92, (bulk -CH$_2$), 23.9 (ω-1) 14.6 (ω). HRDARTMS: Calcd. for M$^+$ [$C_{33}H_{62}N_5O_8$]$^+$ 656.4599 (100 %), 657.4632 (36 %), 658.4666 (6 %); found 656.4587 (100 %), 657.4616 (41 %), 658.4697 (11 %).

2-Butyl-octyl 6-deoxy-6-[3-(5-azido-3-oxa-pentyl)-imidazolium]-2,3,4-tri-*O*-acetyl-β-D-glucopyranoside bromide (15a)

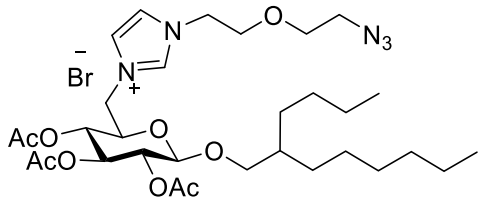

A solution containing **12** (0.18 g, 0.33 mmol) and **3a** (60 mg, 0.33 mmol) in xylene (4 mL) was heated to 130 °C, following to general procedure **3.6.15** to furnish a yellow syrup **15a** (0.23 g, 97 %). $[\propto]_D^{25}$ = -18 (c 0.28, $CHCl_3$). ^{1}H NMR (400 MHz, $CDCl_3$): δ 10.04 (1H, s, N=C*H*-N), 7.42 (1H, s, CH=N-C*H*), 7.36 (1H, s, CH=C*H*-N), 5.20-5.16 (1H, dd~t, H-3), 4.87-4.83 (1H, dd~t, H-2), 4.75-4.65 (2H, m, H-6a, H-4), 4.58-4.51 (4H, m, H-6b, -NC*H*$_2$CH$_2$, H-1), 4.06-4.02 (1H, m, H-5), 3.91 (2H, bs, -NCH$_2$C*H*$_2$), 3.72-3.67 (3H, m, -OC*H*$_2$CH$_2$N$_3$, -OC*H*$_2$*a*-CH), 3.35-3.25 (3H, m, -CH$_2$N$_3$, -OC*H*$_2$*b*-CH), 2.19, 1.96, 1.92 (9H, 3 s, Ac), 1.46 (1H, bs, -OCH$_2$C*H*), 1.18 (16H, bs, bulk -CH$_2$), 0.83-0.82 (6H, bs, -CH$_3$); $^3J_{1,2}$=8.0, $^3J_{2,3}$=9.0, $^3J_{3,4}$=9.0, $^3J_{4,5}$=9.0, $^2J_{6a,6b}$=11.5 Hz; ^{13}C NMR (100 MHz, $CDCl_3$): δ 170.5, 169.7, 169.8 (C=O), 138.1 (N-CH=N), 122.8 (CH=N-*C*H), 122.4 (CH=*C*H-N), 100.8 (C-1), 73.20/ 73.18 (-O*C*H$_2$CH), 72.0 (C-3), 71.2 (C-5), 70.9 (C-2), 70.0 (-*C*H$_2$CH$_2$N$_3$), 68.7 (-NCH$_2$*C*H$_2$), 68.3 (C-4), 50.4 (-CH$_2$N$_3$), 50.0 (-N*C*H$_2$CH$_2$), 49.4 (C-6), 37.8 (-OCH$_2$*C*H), 31.7, 30.88/ 30.63, 30.54/ 30.28, 29.49/ 29.46, 28.81/ 28.66, 26.61/ 26.45, 22.83/ 22.82 (bulk -CH$_2$), 22.5 (ω-1), 21.3, 20.4, 20.3 (Ac), 13.9 (ω).

2-Butyl-octyl 6-deoxy-6-[3-(8-azido-3,6-dioxa-octyl)-imidazolium]-2,3,4-tri-*O*-acetyl-β-D-glucopyranoside bromide (15b)

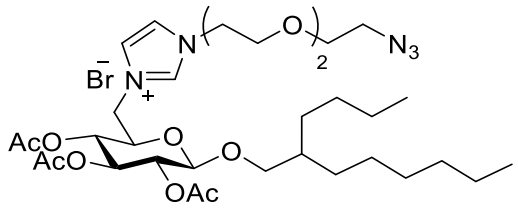

A solution containing **12** (0.21 g, 0.39 mmol) and **3b** (88 mg, 0.39 mmol) in xylene (3 mL) was heated to 130 °C based on general procedure **3.6.15** to provide **15b** (0.27 g, 91 %) as a yellow syrup. $[\propto]_D^{25}$ = -20 (c 0.38, $CHCl_3$). ^{1}H NMR (400 MHz, $CDCl_3$): δ 10.07 (1H, s, N=C*H*-N), 7.48 (1H, s, CH=N-C*H*), 7.35 (1H, s, CH=C*H*-N), 5.20-5.15 (1H, dd~t, H-3), 4.86-4.82 (1H, dd, H-2), 4.75-4.60 (3H, m, H-6, H-4), 4.53-4.39 (3H, m, -NC$H_2$$CH_2$, H-1), 4.07-4.03 (1H, m, H-5), 3.88-3.85 (2H, m, -$NCH_2C$$H_2$), 3.69-3.55 (7H, m, -O$CH_2CH_2OCH_2CH_2N_3$, -O$CH_2a$-CH), 3.35-3.32 (2H, m, -CH_2N_3), 3.28-3.24 (1H, dd, -OCH_2b-CH), 2.19, 1.95, 1.90 (9H, 3 s, Ac), 1.45 (1H, bs, -OCH_2CH), 1.17 (16H, bs, bulk -CH_2), 0.82-0.79 (6H, m, -CH_3); $^3J_{1,2}$= 8.0, $^3J_{2,3}$= 9.5, $^3J_{3,4}$= 9.5, $^3J_{4,5}$= 9.5, $^3J_{5,6a}$= 3.0, $^3J_{5,6b}$= 6.0, $^2J_{6a,6b}$= 14.5 Hz; ^{13}C NMR (100 MHz, $CDCl_3$): δ 170.4, 169.6, 169.1 (C=O), 138.2 (N=*C*H-N), 122.7 (CH=N-*C*H), 122.5 (CH=*C*H-N), 100.8 (C-1), 73.19/ 73.15 (-O*C*H_2CH), 72.0 (C-3), 71.2 (C-5), 70.9 (C-2), 70.14, 70.09, 69.8 (-$OCH_2CH_2OCH_2CH_2N_3$), 68.7 (-NCH_2CH_2), 68.2 (C-4), 50.5 (-CH_2N_3), 49.8 (-NCH_2CH_2), 49.1 (C-6), 37.77/ 37.75 (-OCH_2CH), 31.6, 30.85/ 30.60, 30.50/ 30.25, 29.46/ 29.44, 28.79/ 28.63, 26.59/ 26.42, 22.81/ 22.79 (bulk -CH_2), 22.4 (ω-1), 21.3, 20.33, 20.29 (Ac), 13.9 (ω).

2-Butyl-octyl 6-deoxy-6-[3-(11-azido-3,6,9-trioxa-undecyl)-imidazolium]-2,3,4-tri-*O*-acetyl-β-D-glucopyranoside bromide (15c)

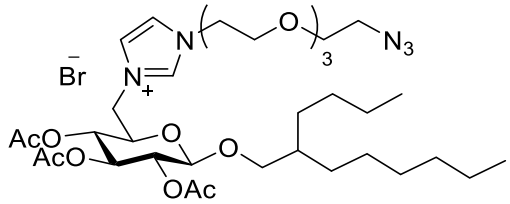

Following general procedure **3.6.15**, a solution containing **12** (0.19 g, 0.35 mmol) and **3c** (96 mg, 0.35 mmol) in xylene (3 mL) was heated to 130 °C to furnish **15c** (0.25 g, 85 %) as a yellow syrup. $[\propto]_D^{25}$ = -24 (c 0.30, $CHCl_3$). ^{1}H NMR (400 MHz, $CDCl_3$): δ 10.15 (1H, bs, N=C*H*-N), 7.52 (1H, s, CH=N-C*H*), 7.37 (1H, s, CH=C*H*-N), 5.19-5.14 (1H, dd~t, H-3), 4.85-4.81 (1H, dd~t, H-2), 4.73-4.56 (3H, m, H-6, H-4), 4.52-4.39 (3H, m, H-1, -NCH_2CH$_2$), 4.07-4.03 (1H, m, H-5), 3.87-3.81 (2H, m, -NCH$_2$CH_2), 3.67-3.59 (11H, m, -(OCH_2CH_2)$_2$OCH_2CH$_2$N$_3$, -OCH_2*a*-CH), 3.33 (2H, m, -CH$_2$N$_3$), 3.26-3.23 (1H, dd~t, -OCH_2*b*-CH), 2.17, 1.94, 1.90 (9H, 3 s, Ac), 1.44 (1H, bs, -OCH$_2$C*H*), 1.16 (16H, bs, bulk -CH$_2$), 0.80 (6H, bs, -CH$_3$); $^3J_{1,2}$= 8.0, $^3J_{2,3}$= 9.5, $^3J_{3,4}$= 9.5, $^3J_{4,5}$= 10.0, $^3J_{5,6b}$= 3.5, $^3J_{5,6b}$= 5.0, $^2J_{6a,6b}$=14.0 Hz; ^{13}C NMR (100 MHz, $CDCl_3$): δ 170.4, 169.6, 169.1 (C=O), 138.1 (N=*C*H-N), 128.6 (CH=N-*C*H), 122.7 (CH=CH-N), 100.8 (C-1), 73.19/ 73.15 (-O*C*H$_2$CH), 72.0 (C-3), 71.1 (C-5), 70.8 (C-2), 70.3, 70.1 (2), 69.7 (-(O*C*H$_2$*C*H$_2$)$_2$O*C*H$_2$CH$_2$N$_3$), 68.7 (-NCH$_2$*C*H$_2$), 68.2 (C-4), 50.4 (-CH$_2$N$_3$), 49.7 (-NCH$_2$CH$_2$), 49.3 (C-6), 37.7 (-OCH$_2$*C*H), 31.6, 30.82/ 30.57, 30.47/ 30.22, 29.44/ 29.42, 28.76/ 28.60, 26.56/ 26.38, 22.79 (bulk CH$_2$), 22.4 (ω-1), 21.2, 20.30, 20.27 (Ac), 13.9 (ω).

2-Butyl-octyl 6-deoxy-6-[3-(5-azido-3-oxa-pentyl)-imidazolium]-β-D-glucopyranoside bromide (16a)

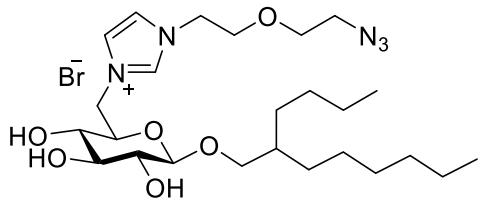

A deacetylation reaction based on general procedure **3.6.5** was applied on compound **15a** (0.11 g, 0.15 mmol) in CH_3OH (5 mL) to produce compound **16a** (85 mg, 93 %) as a yellow syrup. IR [neat] ν/cm^{-1} 3376 (OH), 2955, 2925, 2858 (CH), 2107 (N_3). $[\propto]_D^{25}$ = -14(c 0.23, CH_3OH). ^{1}H NMR (400 MHz, CD_3OD): δ 8.55 (<1H, bs, N=CH-N), 7.72 (1H, s, CH=N-C*H*), 7.62 (1H, s, CH=CH-N), 4.68-4.64 (1H, d, H-6a), 4.48-4.41 (3H, m, -NC*H*$_2$CH$_2$, H-6b), 4.27-4.25 (1H, d, H-1), 3.92-3.90 (2H, t, -NCH$_2$C*H*$_2$), 3.73-3.61 (4H, m, -OC*H*$_2$CH$_2$N$_3$, -OC*H*$_2$*a*-CH, H-5), 3.42-3.36 (4H, m, -CH$_2$N$_3$, H-3, -OC*H*$_2$*b*-CH), 3.19-3.14 (1H, dd~t, H-2), 3.10-3.05 (1H, dd~t, H-4), 1.62-1.60 (1H, m, -OCH$_2$C*H*), 1.40-1.32 (16H, m, bulk -CH$_2$), 0.95-0.91 (6H, m, -CH$_3$); $^3J_{1,2}$= 8.0, $^3J_{2,3}$= 9.5, $^3J_{3,4}$= 9.5 $^3J_{4,5}$= 9.5, $^3J_{5,6a}$<2.0, $^3J_{5,6b}$= 7.0, $^2J_{6a,6b}$= 14.0 Hz; ^{13}C NMR (100 MHz, CD_3OD): δ 138.7 (N=CH-N), 125.0 (CH=N-*C*H), 123.9 (CH=*C*H-N), 105.0 (C-1), 77.8 (C-3), 75.1 (C-2), 74.9 (C-5), 74.32/ 74.30 (-O*C*H$_2$CH), 72.5 (C-4), 71.4 (-O*C*H$_2$CH$_2$N$_3$), 69.8 (-NCH$_2$*C*H$_2$), 51.9 (C-6), 51.8 (-CH$_2$N$_3$), 51.1 (-N*C*H$_2$CH$_2$), 39.7 (-OCH$_2$*C*H), 33.2, 32.41/ 32.35, 32.08/ 32.02, 31.0, 30.33/ 30.28, 28.04/ 27.98, 24.3 (bulk –CH$_2$), 23.9 (ω-1), 14.6 (ω). HRDARTMS: Calcd. for $[M]^+$ $[C_{25}H_{46}N_5O_6]^+$ 512.3448 (100 %), 513.3482 (27 %); found 512.3437 (100 %), 513.3470 (32 %).

2-Butyl-octyl 6-deoxy-6-[3-(8-azido-3,6-dioxa-octyl)-imidazolium]-β-D-glucopyranoside bromide (16b)

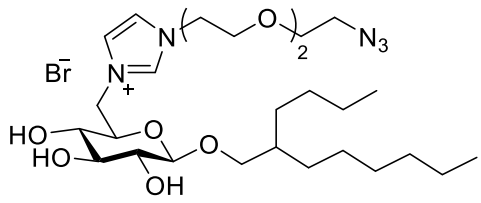

In CH_3OH (5 mL), **15b** (72 mg, 0.09 mmol) was deacetylated according to general procedure **3.6.5** to furnish **16b** (54 mg, 89 %) as a yellow syrup. IR [neat] ν/cm^{-1} 3370 (OH), 2925, 2858 (CH), 2106 (N_3). $[\propto]_D^{25}$ = -12 (c 0.24, CH_3OH). ^{1}H NMR (400 MHz, CD_3OD): δ 9.00 (1H, bs, N=CH-N), 7.73 (1H, s, CH=N-C*H*), 7.61 (1H, s, CH=C*H*-N), 4.70-4.65 (1H, dd, H-6a), 4.48-4.43 (3H, m, H-6b, -NC*H*$_2$CH$_2$), 4.29-4.27 (1H, d, H-1), 3.91-3.89 (2H, m, -NCH$_2$C*H*$_2$), 3.71-3.64 (8H, m, -OC*H*$_2$C*H*$_2$OC*H*$_2$CH$_2$N$_3$, -OC*H*$_2$*a*-CH, H-5), 3.43-3.36 (4H, m, -CH$_2$N$_3$, -OC*H*$_2$*b*-CH, H-3), 3.19-3.14 (1H, dd~t, H-2), 3.10-3.06 (1H, dd~t, H-4), 1.60 (1H, bs, -OCH$_2$C*H*), 1.32 (16H, bs, bulk -CH$_2$), 0.95-0.91 (6H, m, -CH$_3$); $^3J_{1,2}$= 8.0, $^3J_{2,3}$= 9.5, $^3J_{3,4}$= 9.5, $^3J_{4,5}$= 9.5, $^3J_{5,6a}$= 2.0, $^3J_{6a,6b}$= 14.5 Hz; ^{13}C NMR (100 MHz, CD_3OD): δ 138.7 (N=*C*H-N), 124.7 (CH=N-*C*H), 124.1 (CH=*C*H-N), 105.00 (C-1), 77.7 (C-3), 75.1 (C-2), 74.9 (C-5), 74.29/ 74.26 (-O*C*H$_2$CH), 72.5 (C-4), 71.6 (2), 71.2 (-O*C*H$_2$*C*H$_2$O*C*H$_2$CH$_2$N$_3$), 70.0 (-NCH$_2$*C*H$_2$), 51.93 (C-6), 51.90 (-CH$_2$N$_3$), 51.1 (-N*C*H$_2$CH$_2$), 39.6 (-OCH$_2$*C*H), 33.2, 32.39/ 32.33, 32.05/ 31.99, 31.0, 30.31/ 30.25, 28.03/ 27.96, 24.3 (bulk CH$_2$), 23.9 (ω-1), 14.6 (ω). HRDARTMS: Calcd. for $[M]^+$ $[C_{27}H_{50}N_5O_7]^+$ 556.3710 (100 %), 557.3744 (29 %); found 556.3727 (100 %),557.3757 (33 %).

2-Butyl-octyl 6-deoxy-6-[3-(11-azido-3,6,9-trioxa-undecyl)-imidazolium]-β-D-glucopyranoside bromide (16c)

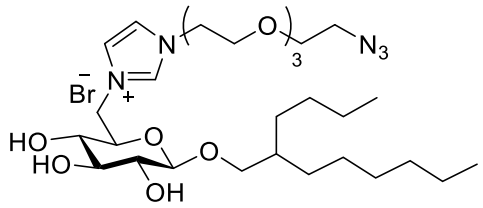

15c (92 mg, 0.11 mmol) in CH_3OH (5 mL) was deactylated according to general procedure **3.6.5** and produced compound **16c** (70 mg, 90 %) as a yellow syrup. IR [neat] ν/cm^{-1} 3372 (OH), 2925, 2859 (CH), 2105 (N_3). $[\propto]_D^{25}$ = -9 (c 0.10, CH_3OH). ^{1}H NMR (400 MHz, CD_3OD): δ 9.02 (<1H, s, N=CH-N), 7.73 (1H, s, CH=N-C*H*), 7.61 (1H, s, CH=C*H*-N), 4.69-4.65 (1H, dd, H-6a), 4.49-4.44 (3H, m, -NC*H*$_2$CH$_2$, H-6b), 4.28-4.26 (1H, d, H-1), 3.90 -3.88 (2H, t, -NCH$_2$C*H*$_2$), 3.71-3.68 (12H, m, -(OC*H*$_2$C*H*$_2$)$_2$OC*H*$_2$CH$_2$N$_3$, -OC*H*$_2$*a*-CH, H-5), 3.43-3.35 (4H, m, -CH$_2$N$_3$, H-3, -OC*H*$_2$*b*-CH), 3.18-3.14 (1H, dd~t, H-2), 3.10-3.05 (1H, dd~t, H-4), 1.60 (1H, bs, -OCH$_2$C*H*), 1.32 (16H, bs, bulk -CH$_2$), 0.95-0.91 (6H, m, -CH$_3$); $^3J_{1,2}$= 8.0, $^3J_{2,3}$= 10.0, $^3J_{3,4}$= 10.0, $^3J_{4,5}$= 10.0, $^3J_{5,6a}$= 2.5; $^2J_{6a,6b}$= 14.5 Hz; ^{13}C NMR (100 MHz, CD_3OD): δ 138.8 (N=CH-N), 124.7 (CH=N-*C*H), 124.1 (CH=*C*H-N), 105.0 (C-1), 77.8 (C-3), 75.1 (C-2), 74.9 (C-5), 74.30/ 74.28 (-O*C*H$_2$CH), 72.5 (C-4), 71.68, 71.65, 71.50, 71.51, 71.2 (-(O*C*H$_2$*C*H$_2$)$_2$ O*C*H$_2$CH$_2$N$_3$), 69.9 (-NCH$_2$*C*H$_2$), 51.9 (C-6), 51.1 (-CH$_2$N$_3$), 51.0 (-N*C*H$_2$CH$_2$), 39.6 (-OCH$_2$*C*H), 33.2, 32.38/ 32.32, 32.05/ 31.99, 31.0, 30.31/ 30.25, 28.02/ 27.95, 24.3 (bulk -CH$_2$), 23.9 (ω-1), 14.6 (ω). HRDARTMAS: Calcd. for $[M]^+$ $[C_{29}H_{54}N_5O_8]^+$ 600.3973 (100 %), 601.4006 (31 %); found 600.3958 (100 %), 601.3986 (38 %).

Dodecyl 2,3,4,6-tetra-*O*-acetyl-β-D-glucopyranoside (17) (Sabah *et al.*, 2011)

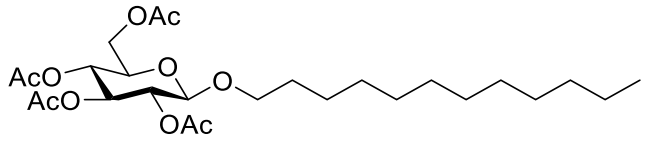

A solution containing β-D-glucose pentaacetate (14 g, 36 mmol) and 1-dodecanol (8.9 mL, 40 mmol) in CH_2Cl_2 (70 mL) was treated with $BF_3{\cdot}OEt_2$ (5.8 mL, 47 mmol) following general procedure **3.6.4**. A yellow syrup **17** was obtained (7.7 g, 41 %) by chromatography over silica gel (EtOAc: hexane= 1:7). ^{1}H NMR (400 MHz, $CDCl_3$): δ 5.22-5.18 (1H, dd~t, H-3), 5.10-5.06 (1H, dd~t, H-4), 5.00-4.96 (1H, dd, H-2), 4.50-4.48 (1H, d, H-1),4.28-4.24 (1H, dd, H-6a), 4.15-4.11 (1H, dd, H-6b), 3.89-3.83 (1H, m, ∝CH_2a), 3.70-3.66 (1H, ddd, H-5), 3.49-3.43 (1H, m, ∝CH_2b), 2.08, 2.03, 2.02, 2.00 (9H, 4s, OAc), 1.59-1.50 (2H, m, βCH_2), 1.25 (18H, bs, bulk –CH_2), 0.89-0.86 (3H, t, -CH_3); $^3J_{1,2}$=8.0, $^3J_{2,3}$=10.0, $^3J_{3,4}$=10.0, $^3J_{4,5}$=10.0, $^3J_{5,6a}$=5.0, $^3J_{5,6b}$=2.5, $^2J_{6a,6b}$=12.0 Hz; ^{13}C NMR (100 MHz, $CDCl_3$): δ 170.7, 170.3, 169.4, 169.2 (C=O), 100.8 (C-1), 72.9 (C-3), 71.7 (C-5), 71.4 (C-2), 70.2 (∝CH_2), 68.5 (C-4), 62.0 (C-6), 31.9, 29.61, 29.58 29.56, 29.4, 29.3, 25.8 (βCH_2, bulk –CH_2), 22.6 (ω-1), 20.7, 20.59, 20.58, 20.56 (Ac), 14.1 (ω).

Dodecyl β-D-glucopyranoside (18) (Sabah *et al.*, 2011)

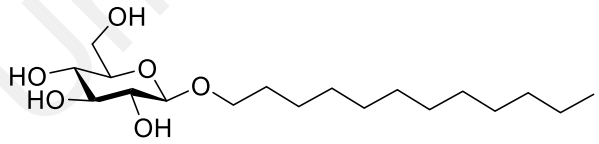

A solution of **17** (7.2 g, 14 mmol) in CH_3OH (50 mL) was treated with $NaOCH_3$ according to general procedure **3.6.5** to furnish glucoside **18** (4.4 g, 90 %) as a yellow syrup which was used for subsequent reaction without further purification.

Dodecyl 4,6-*O*-benzylidene-β-D-glucopyranoside (19) (Sabah *et al.*, 2011)

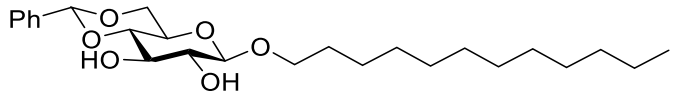

A solution of **18** (4.2 g, 12 mmol) in CH_2Cl_2 (70 mL) was treated with $PhCH(OCH_3)_2$ (4.3 mL, 29 mmol) and *p*-TsOH·H_2O (0.10 g) according to general procedure **3.6.8**. Precipitate was formed after 30 minutes stirring the residue in hexane (30 mL). The precipitate was collected and washed with hexane to obtain β-anomer **19** (4.8 g, 92 %) as a white solid. $[\propto]_D^{25}$ = -39 (c 0.20, $CHCl_3$).

Dodecyl 2,3-di-*O*-benzyl-4,6-*O*-benzylidene-β-D-glucopyranoside (20) (Sabah *et al.*, 2011)

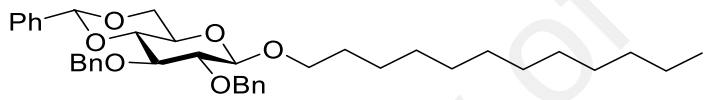

A solution **19** (4.8 g, 11 mmol) in DMF (60 mL) was treated with NaH (60 % suspension in paraffin oil) (1.8 g, 45 mmol), followed by addition of BnBr (3.9 mL, 33 mmol) at 0 °C according to general procedure **3.6.9**. The reaction was quenched by addition of CH_3OH (20 mL) and H_2O (20 mL). The white precipitate was collected and washed with CH_3OH to provide **20** (5.5 g, 81 %) as a white solid**.** ^{1}H NMR (400 MHz, $CDCl_3$): δ 7.51-7.48, 7.39-7.27 (15H, m, aromatic -CH), 5.58 (1H, s, Ph-CH), 4.93-4.76 (4H, m, $-CH_2Ph$), 4.52-4.50 (1H, d, H-1), 4.38-4.34 (1H, dd, H-6eq), 3.96-3.90 (1H, dt, $\propto CH_2$a), 3.83-3.67 (3H, m, H-6ax, H-2, H-3), 3.60-3.54 (1H, dt, $\propto CH_2$b), 3.50-3.38 (2H, m, H-4, H-5), 1.69-1.64 (2H, m, βCH_2), 1.33-1.26 (18H, m, bulk $-CH_2$), 0.91-0.87 (3H, t, CH_3); $^3J_{1,2}$= 8.0, $^3J_{2,3}$= 10.0, $^3J_{3,4}$= 10.0, $^3J_{5,6eq}$= 5.5, $^3J_{5,6ax}$= 10.0, $^2J_6$=11.0 Hz; ^{13}C NMR (100 MHz, $CDCl_3$): δ 139.8, 138.4, 137.4 (aromatic -C), 128.9, 128.32, 128.28, 128.2, 128.1, 128.0, 127.7, 127.6, 126.0 (aromatic -CH), 104.2 (C-1), 101.1 (Ph-CH),

82.2 (C-2), 81.5 (C-4), 80.9 (C-3), 75.3, 75.1 (-CH_2Ph), 70.7 (∝CH_2), 68.8 (C-6), 66.0 (C-5), 31.9, 29.8, 29.7, 29.63, 29.58, 29.5, 29.4, 26.1 (bulk –CH_2, βCH_2), 22.7 (ω-1), 14.1 (ω).

Dodecyl 2,3,6-tri-*O*-benzyl -β-D-glucopyranoside (21)

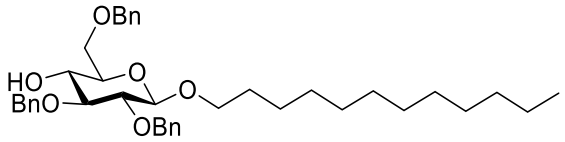

Procedure I (Rao *et al.*, 2010)**:** Into a solution of **20** (1.1 g, 1.8 mmol) in CH_3CN (20 mL) with activated 4 Å molecular sieves (0.5 g), $NaCNBH_3$ (0.55 g, 8.8 mmol) was added and the mixture was stirred for 5 minutes. I_2 (1.6 g, 6.3 mmol) was added portion-wise over 15 minutes. The mixture was diluted with CH_2Cl_2 and filtered through a Celite pad. The filtrate was washed successively with saturated $NaHCO_3$ (aq) and water. The organic layer was dried over $MgSO_4$ and concentrated under reduced pressure. Compound **21** (0.15 g, 13 %) was obtained as a colourless syrup.

Procedure II (Yoneda *et al.*, 2005; Kasuya *et al.*, 2007)**:** A solution containing **20** (5.5 g, 8.9 mmol) in CH_2Cl_2 (70 mL) was treated with activated 4 Å molecular sieves, followed by addition of Et_3SiH (8.7 mL, 54 mmol) and TFA (4.2 ml, 55 mmol) at 0 °C according to general procedure **3.6.10**. The residue was subjected to column chromatography (EtOAc: hexane= 1:9) to provide **21** (3.0 g, 55 %) as a colourless syrup. $[\propto]_D^{25}$ = -17 (c 0.11, $CHCl_3$); ^{1}H NMR (400 MHz, $CDCl_3$): δ 7.34-7.29 (15H, m, aromatic -CH), 4.96-4.91, 4.73-4.69, 4.61-4.55, (6H, 3 dd, -CH_2Ph), 4.41-4.39 (1H, d, H-1), 3.96-3.91 (1H, dt, αCH_2a), 3.78-3.75 (1H, dd, H-6a), 3.71-3.67 (1H, dd, H-6b), 3.59-3.49 (2H, m, H-3, αCH_2b), 3.47-3.38 (3H, m, H-4, H-5, H-2), 2.54 (1H, m, -OH), 1.66-1.62 (2H, m, βCH_2), 1.35-1.24 (18H, m, bulk -CH_2), 0.89-0.85 (3H, t, -CH_3);$^3J_{1,2}$=7.5, $^3J_{3,4}$=9.0, $^3J_{4,5}$=9.0 $^3J_{5,6a}$=4.0, $^3J_{5,6b}$=5.5, $^2J_{6a,6b}$=10.5 Hz; ^{13}C NMR (100 MHz, $CDCl_3$): δ 138.6,

138.4, 137.9 (aromatic -C), 128.5, 128.39, 128.35, 128.1, 128.0, 127.8, 127.7 (aromatic -CH), 103.7 (C-1), 84.0 (C-4), 81.7 (C-2), 75.3, 74.7 (CH_2Ph), 74.0 (C-5), 73.6 (CH_2Ph), 71.6 (C-3), 70.3 (C-6), 70.2 (αCH_2), 31.9, 29.9, 29.8, 29.7, 29.61, 29.58, 29.4, 29.3, 26.2 (βCH_2, bulk- CH_2), 22.7 (ω-1), 14.2 (ω).

Oxybis(ethane-2,1-diyl) bis(4-methylbenzenesulfonate) (22) (Ouchi *et al.*, 1990)

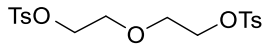

A solution of diethylene glycol (1.0 mL, 11 mmol) in THF (20 mL) was stirred with NaOH pellets (1.0 g, 25 mmol) at 0 °C for about 5 minutes, followed by addition of TsCl (4.4 g, 23 mmol) portionwise. Stirring was continued overnight at room temperature. THF was evaporated, the resulting residue was diluted with CH_2Cl_2 and washed twice with H_2O. The organic layer was dried over $MgSO_4$ and concentrated under reduced pressure. A white solid **22** (2.1 g, 46 %) was obtained by crystallization from EtOH. ^{1}H NMR (400 MHz, $CDCl_3$): δ 7.80-7.78, 7.37-7.35 (8H, 2 d, aromatic -CH), 4.11-4.09 (4H, t, TsOC*H*$_2$), 3.63-3.60 (4H, t, -OCH_2), 2.46 (6H, s, Ph-CH_3); ^{13}C NMR (100 MHz, $CDCl_3$): δ 144.9 (aromatic C-S), 132.8 (aromatic *C*-CH_3), 129.9, 127.9 (aromatic -CH), 69.0 (-OCH_2), 68.7 (-COTs), 21.6 (CH_3).

1-Bromo-2-(2-bromoethoxy)ethane (23) (Guo *et al.*, 2015)

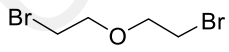

Diethylene glycol (10 mL, 0.11 mol) was cooled in an ice bath and PBr_3 (8.0 ml, 84 mmol) was then added slowly. The mixture was heated to 80 °C for another 4 hours with stirring. The mixture was poured into a saturated solution of $NaHCO_3$ after being cooled to room temperature. The organic layer was washed thrice with H_2O, dried over $MgSO_4$ and concentrated to provide **23** (11 g, 56 %) as a brown liquid. ^{1}H NMR

(400 MHz, $CDCl_3$): δ 3.80-3.75 (4H, m, -CH_2Br), 3.44-3.41 (4H, m, -OCH_2); ^{13}C NMR (100 MHz, $CDCl_3$): δ 75.7 (CH_2O), 35.2 (CH_2Br).

Dodecyl 2,3,6-*O*-tri-acetyl-4-*O*-(2-bromoethoxy)ethyl-β-D-glucopyranoside (26)

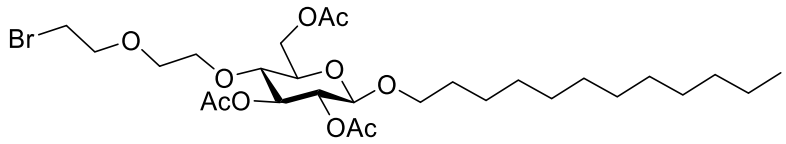

A solution of **21** (0.48 g, 0.78 mmol) in DMF (10 mL) was treated with NaH (60 % suspension in paraffin oil) (0.10 g, 2.5 mmol) and stirred at room temperature for an hour. Compound **23** (0.93 g, 4.0 mmol) was added at 0 °C and the mixture was stirred overnight at room temperature. CH_3OH (3 mL) was added and the solvents were evaporated. The residue was diluted with CH_2Cl_2 and washed twice with water. The organic layer was dried over $MgSO_4$ and concentrated to provide crude **24**, which underwent a hydrogenation according to general procedure **3.6.11**, except glacial AcOH (1 ml) was added instead of conc. HCl to furnish crude glucoside **25**. The resulting compound was dissolved in pyridine (3 mL), followed by addition of Ac_2O (0.05 mL) according to general procedure **3.6.7**. Compound **26** (40 mg, 8.0 % over 3 steps) was obtained as a yellow syrup by column chromatography (EtOAc: hexane= 1:10). $[\propto]_D^{25}$ = -87 (c 0.04, $CHCl_3$); ^{1}H NMR (400 MHz, $CDCl_3$): δ 5.21-5.16 (1H, dd~t, H-3), 4.89-4.84 (1H, dd, H-2), 4.46-4.42 (2H, m, H-1, H-6a), 4.27-4.23 (1H, dd, H-6b), 3.87-3.81 (1H, dt, αCH_2a), 3.76-3.74, 3.70-3.67 (2H, m, -OC*H*$_2$C*H*$_2$O), 3.57-3.51 (4H, m, -C*H*$_2$$CH_2$Br, H-5, H-4), 3.48-3.43 (3H, m$_c$, αCH_2b, CH_2Br), 2.10, 2.07, 2.03 (9H, 3 s, OAc), 1.59-1.52 (2H, m, βCH_2), 1.30-1.25 (18H, m$_c$, bulk CH_2), 0.90-0.86 (3H, t, CH_3); $^3J_{1,2}$= 8.0, $^3J_{2,3}$= 10.0, $^3J_{3,4}$= 10.0, $^3J_{5,6a}$= 2.0, $^3J_{5,6b}$= 5.0, $^2J_{6a,6b}$= 11.0 Hz; ^{13}C NMR (100 MHz, $CDCl_3$): δ 170.7, 170.1, 169.7 (C=O), 100.7 (C-1), 76.8 (C-4), 75.0 (C-3), 72.8 (C-5), 72.1 (-O*C*$H_2$$CH_2$O), 71.9 (C-2), 71.2 (-OCH_2*C*H_2O), 70.3 (*C*$H_2$$CH_2$Br), 70.2 (α$CH_2$),

62.9 (C-6), 31.9 (bulk -CH_2), 30.2 (CH_2Br), 29.7, 29.64, 29.61, 29.59, 29.4, 29.3, 25.8 (β-CH_2, bulk CH_2), 22.7 (ω-1), 20.95, 20.86, 20.7 (Ac), 14.1 (ω).

Dodecyl 2,3,6-tri-*O*-benzyl-4-*O*-(2-hydroxyethyl)-β-D-glucopyranoside (28)

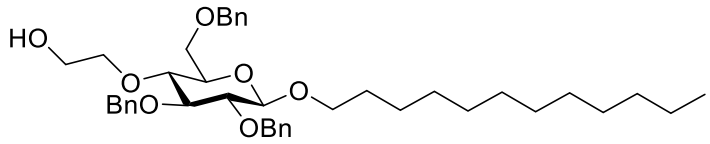

Compound **21** (2.6 g, 4.2 mmol) was dissolved in toluene (30 mL) and 50 % NaOH (aq) (15 mL) was added, followed by TBAB (1.3 g, 4.0 mmol). $BrCH_2COOtBu$ (0.92 ml, 6.3 mmol) was then added following general procedure **3.6.12** to provide crude compound **27**. The resulting compound was dissolved in THF (50 mL) and cooled to 0 °C, followed by the addition of $LiAlH_4$ (1.0 g, 27 mmol) according to ester reduction procedure **3.6.13**. Compound **28** (1.9 g, 68 % over 2 steps) was obtained as a yellow syrup by column chromatography over silica gel (EtOAc: hexane= 1:5). $[\propto]_D^{25}$ = +6 (c 0.29, $CHCl_3$); ^{1}H NMR (400 MHz, $CDCl_3$): δ 7.39-7.29 (15H, m, aromatic -CH), 5.01-4.96, 4.80-4.71, 4.71-4.59 (6H, 3 dd, -CH_2Ph), 4.42-4.40 (1H, d, H-1), 4.00-3.95 (1H, dt, ∝CH_2a), 3.83-3.76 (3H, m, H-6a, -C*H*$_2$OH), 3.70-3.65 (1H, m, H-6b), 3.61- 3.52 (5H, m, H-4, H-2, -OC*H*$_2$$CH_2$OH, ∝$CH_2$b), 3.48-3.44 (1H, dd~t, H-3), 3.42-3.38 (1H, m, H-5), 1.72-1.65 (2H, m, βCH_2), 1.45-1.29 (18H, m, bulk –CH_2), 0.93-0.90 (3H, t, -CH_3); $^3J_{1,2}$= 8.0, $^3J_{2,3}$= 9.0, $^3J_{4,5}$= 9.0, $^3J_{5,6a}$= 5.0, $^3J_{5,6b}$= 3.0, $^2J_{6a,6b}$= 11.0 Hz; ^{13}C NMR (100 MHz, $CDCl_3$): δ 138.4, 138.2, 138.0 (aromatic-C), 128.42, 128.38, 128.37, 128.2, 128.1, 127.9, 127.8, 127.7 (aromatic -CH), 103.7 (C-1), 84.2 (C-4), 82.4 (C-3), 78.4 (C-2), 75.7 (-CH_2Ph), 74.9 (C-5), 74.7 (-CH_2Ph), 74.1 (C-6), 73.6 (-CH_2Ph), 70.2 (∝CH_2), 69.0 (-CH_2OH), 62.6 (-O*C*$H_2$$CH_2$OH), 31.9, 29.8, 29.70, 29.65, 29.6, 29.5, 29.4, 26.2 (βCH_2, bulk –CH_2), 22.7 (ω-1), 14.1 (ω).

Dodecyl 2,3,6-tri-*O*-benzyl-4-*O*-(2-tosyloxyethyl)-β-D-glucopyranoside (29)

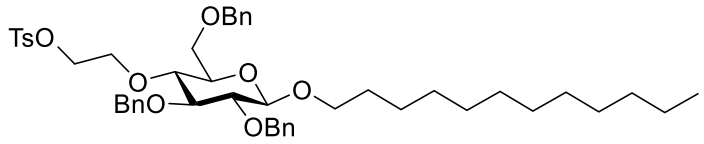

To a solution of compound **28** (0.40 g, 0.60 mmol) in THF (30 mL) NaH (60 % suspension in paraffin oil) (50 mg, 1.3 mmol) was added. After 15 minutes of stirring, TsCl (0.20 g, 1.0 mmol) was added at 0 °C and the mixture was left for overnight stirring at room temperature. THF was evaporated after quenching the reaction with CH_3OH (3 mL), followed by extraction with CH_2Cl_2 versus H_2O. The organic layer was dried over $MgSO_4$ and the solvent was evaporated. Compound **29** (0.20 g, 41 %) was obtained as a light yellow syrup by column chromatography (EtOAc: hexane= 1:9). $[\propto]_D^{25}$ = +11 (c 0.07, $CHCl_3$); ^{1}H NMR (400 MHz, CDCl3): δ 7.75-7.73 (2H, d, tosyl-), 7.35-7.26 (17H, m, tosyl-, aromatic –CH), 4.97-4.53 (6H, 3 dd, -CH_2Ph), 4.36-4.34 (1H, d, H-1), 4.01-3.89 (4H, m_c, -CH_2OTs, ∝CH_2a, H-6a), 3.73-3.63 (3H, m, -C*H*$_2$$CH_2$OTs, H-6b), 3.56-3.48 (2H, m, ∝CH_2b, H-4), 3.41-3.36 (2H, m, H-3, H-2), 3.33-3.29 (1H, m, H-5), 2.44 (3H, s, CH_3 of tosyl), 1.67-1.64 (2H, m, βCH_2), 1.41-1.27 (18H, m, bulk-CH_2), 0.92-0.89 (3H, t, -CH_3); $^3J_{1,2}$= 8.0, $^3J_{3,4}$= 9.0, $^3J_{4,5}$= 9.0 Hz; ^{13}C NMR (100 MHz, $CDCl_3$): δ 144.7, 138.54, 138.46, 138.3, 133.1 (aromatic -C), 129.8, 128.34, 128.31, 128.1, 127.95, 127.85, 127.8, 127.7, 127.59, 127.55 (aromatic -CH), 103.7 (C-1), 84.3 (C-4), 82.2 (C-3), 78.2 (C-2), 75.5, 74.7 (-CH_2Ph), 74.6 (C-5), 73.4 (-CH_2Ph), 70.2 (C-6), 70.1 (∝CH_2), 69.3 (-CH_2OTs), 68.8 (-*C*$H_2$$CH_2$OTs), 31.9, 29.8, 29.7, 29.64, 29.61, 29.5, 29.4, 26.2 (bulk-CH_2, βCH_2), 22.7 (ω-1), 21.6 (-CH_3 of tosyl group), 14.1 (ω).

Dodecyl 2,3,6-tri-*O*-benzyl-4-*O*-(2-iodoethyl)-β-D-glucopyranoside (32)

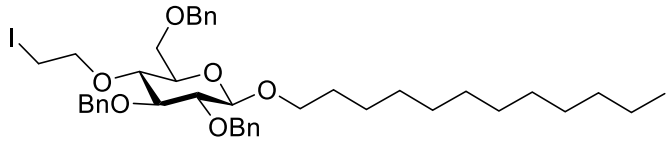

To a solution of compound **28** (1.9 g, 2.9 mmol) in toluene (60 mL), I_2 (1.1 g, 4.3 mmol), PPh_3 (1.1 g, 4.2 mmol) and imidazole (0.60 g, 8.8 mmol) were added in, following general procedure **3.6.14**. Compound **32** (1.7 g, 77 %) was obtained as a yellow syrup by column chromatography over silica gel (EtOAc: hexane= 1:16). $[\propto]_D^{25}$ = +9 (c 0.27, $CHCl_3$); ^{1}H NMR (400 MHz, $CDCl_3$): δ 7.27-7.18 (15H, m, aromatic-CH), 4.89-4.48 (6H, m, -CH_2Ph), 4.30-4.28 (1H, d, H-1), 3.94-3.85 (2H, m, H-6a, αCH_2a), 3.69-3.61 (3H, m, -OC*H*$_2$$CH_2$I, ∝$CH_2$b), 3.51-3.41 (2H, m, H-4, H-6b), 3.39-3.30 (3H, m, H-3, H-2, H-5), 3.02-2.92 (2H, m, -CH_2I), 1.60-1.55 (2H, m, βCH_2), 1.26-1.18 (18H, m, bulk -CH_2), 0.82-0.79 (3H, t, -CH_3). $^3J_{1,2}$=8.0, $^3J_{3,4}$=9.0, $^3J_{4,5}$=9.0, $^3J_{5,6a}$=6.0, $^3J_{5,6b}$=4.0, $^2J_{6a,6b}$=12.0 Hz; ^{13}C NMR (100 MHz, $CDCl_3$): δ 138.52, 138.47, 138.2 (aromatic -C), 128.42, 128.38, 128.2, 128.0, 127.9, 127.69, 127.65 (aromatic -CH), 103.7 (C-1), 84.5 (C-4), 82.2 (C-3), 77.8 (C-2), 75.6, 74.8 (-CH_2Ph), 74.6 (C-5), 73.5 (-CH_2Ph), 73.0 (αCH_2), 70.2 (C-6), 68.7 (-O*C*$H_2$$CH_2$I), 32.0 (bulk CH_2), 29.8, 29.71, 29.67, 29.6, 29.5, 29.4, 22.6 (β-CH_2, bulk CH_2), 22.7 (ω-1), 14.2 (ω), 3.6 (-CH_2I).

Dodecyl 2,3,6-tri-*O*-benzyl-4-*O*-(2-(1*H*-imidazol-1-yl)ethyl)-β-D-glucopyranoside (33)

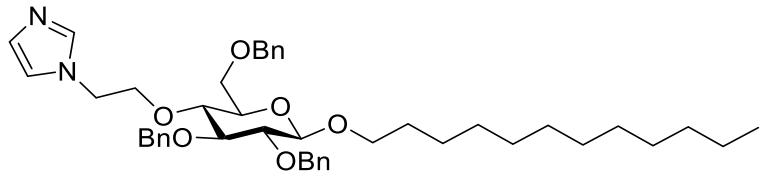

A solution of imidazole (0.30 g, 4.4 mmol) in THF (30 mL) was treated with NaH (60 % suspension in paraffin oil) (0.18 g, 4.5 mmol) for an hour stirring at room temperature. Compound **32** (1.7 g, 2.2 mmol) was then added into the reaction mixture, following general procedure **3.6.1**. Compound **33** (1.1 g, 69 %) was obtained as a yellow syrup by column chromatography (EtOAc: hexane= 1:1). $[\propto]_D^{25}$ = -15 (c 0.06, $CHCl_3$); ^{1}H NMR (400 MHz, $CDCl_3$): δ 7.48 (1H, s, C*H*=N-CH), 7.25-7.14 (15H, m, aromatic -CH), 6.96 (1H, s, CH=N-C*H*), 6.72 (1H, s, CH=C*H*-N), 4.90-4.32 (6H, 3 dd, -CH_2Ph), 4.30-4.28 (1H, d, H-1), 3.91-3.84 (2H, m, -OC*H*$_2$aCH_2, αCH_2a,), 3.79-3.76 (2H, t, -CH_2N), 3.57-3.52 (1H, m, -OC*H*$_2$bCH_2), 3.47-3.42 (3H, m, αCH_2b, H-6a, H-4), 3.38-3.32 (3H, m, H-6b, H-3, H-2), 3.24-3.20 (1H, m, H-5), 1.60-1.55 (2H, m, βCH_2), 1.21-1.17 (18H, m, bulk -CH_2), 0.84-0.80 (3H, t, CH_3); $^3J_{1,2}$=8.0 Hz; ^{13}C NMR (100 MHz, $CDCl_3$): δ 138.6, 138.4, 138.2 (aromatic -C), 137.2 (*C*H=N-CH), 128.6, 128.5, 128.39, 128.35, 128.1, 127.8, 127.73, 127.66, 127.6 (aromatic-CH, CH=N-*C*H), 119.4 (CH=*C*H-N), 103.7 (C-1), 84.4 (C-4), 82.2 (C-3), 77.8 (C-2), 75.4, 74.7 (-CH_2Ph), 74.4 (C-5), 73.4 (-CH_2Ph), 71.4 (∝CH_2), 70.2 (-O*C*$H_2$$CH_2$N), 68.4 (C-6), 47.6 (-$CH_2$N), 31.9, 29.8, 29.70, 29.69, 29.64, 29.61, 29.5, 29.4, 26.2 (bulk-CH_2, βCH_2), 22.7 (ω-1), 14.1 (ω).

Dodecyl 2,3,6-tri-*O*-acetyl-4-*O*-(2-(1*H*-imidazol-1-yl)ethyl)-β-D-glucopyranoside (35)

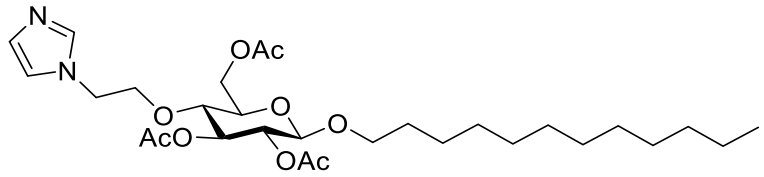

Benzylated compound **33** (1.0 g, 1.4 mmol) was dissolved in CH_3OH (100 mL). Conc. HCl (0.5 mL) and catalyst Pd/C (10 %, 30 mg) and the reaction was under H_2 atmosphere according to general procedure **3.6.11** to yield the crude compound **34**.

Following general procedure **3.6.7**, crude compound **34** was dissolved in pyridine (20 mL) in the presence of Ac_2O (0.80 mL, 8.5 mmol). By column chromatography (EtOAc: acetone= 1:8) over silica gel, acetylated compound **35** (0.40 g, 50 %) was obtained as a yellow syrup. $[\propto]_D^{25}$ = -25 (c 0.49, $CHCl_3$); ^{1}H NMR (400 MHz, $CDCl_3$): δ 8.04 (1H, s, C*H*=N-CH), 7.08 (1H, s, CH=N-C*H*), 6.97 (1H, s, CH=C*H*-N), 5.14-5.09 (1H, dd~t, H-3), 4.80-4.76 (1H, dd, H-2), 4.42-4.40 (1H, d, H-1), 4.24-4.20 (1H, dd, H-6a), 4.17-4.14 (2H, t, -CH_2N), 4.01-3.97 (1H, dd, H-6b), 3.85-3.75 (3H, m, -OC*H*$_2$$CH_2$, α$CH_2$a), 3.50-3.37 (3H, m, H-4,H-5, αCH_2b), 2.05, 1.98, 1.92 (9H, 3s, Ac), 1.55-1.44 (2H, m, βCH_2), 1.21 (18H, m, bulk -CH_2), 0.85-0.82 (3H, t, -CH_3); $^3J_{1,2}$=8.0, $^3J_{2,3}$=9.5, $^3J_{3,4}$=9.5, $^3J_{4,5}$=10.0, $^3J_{5,6a}$=1.5, $^3J_{5,6b}$=4.0, $^2J_{6a,6b}$=12.0 Hz; ^{13}C NMR (100 MHz, $CDCl_3$): δ 170.4, 169.9, 169.5 (C=O), 136.9 (*C*H=N-CH), 126.5 (CH=N-*C*H), 119.8 (CH=*C*H-N), 100.4 (C-1), 76.3 (C-4), 74.4 (C-3), 72.4 (C-5), 71.7 (C-2), 71.3 (-O*C*H$_2$$CH_2$), 70.1 (α$CH_2$), 62.2 (C-6), 47.7 (-$CH_2$N), 31.8, 29.51, 29.47, 29.45, 29.24, 29.19, 29.17, 25.7 (bulk -CH_2, βCH_2), 22.5 (ω-1), 20.73, 20.66, 20.5 (Ac), 14.0 (ω).

Dodecyl 4-*O*-[[1-(1-propyn-4,7-dioxa-nonyl)-3-ethyl]-imidazolium]-2,3,6-tri-*O*-acetyl-β-D-glucopyranoside iodide (36)

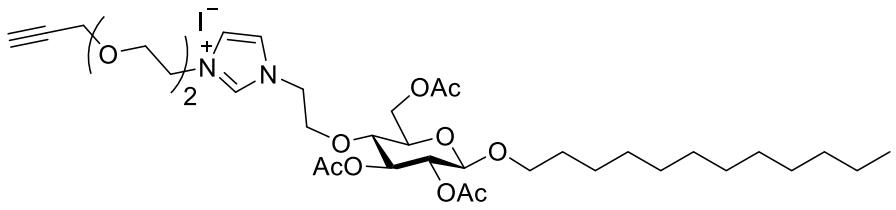

Compound **35** (0.20 g, 0.35 mmol) and linker **6** (89 mg, 0.35 mmol) were both dissolved in toluene (4 mL) and heated to 90 °C with TLC monitoring according to general procedure **3.6.15** to yield compound **36** (0.26 g, 91 %) as a brown syrup. $[\propto]_D^{25}$ = -19 (c 0.60, $CHCl_3$); ^{1}H NMR (400 MHz, $CDCl_3$): δ 9.96 (1H, s, C*H*=N-CH), 7.51 (1H, s, CH=N-C*H*), 7.34 (1H, s, N-CH=C*H*-N), 5.20-5.15 (1H, dd~t, H-3), 4.87-4.83 (1H, dd~t, H-2), 4.57-4.54 (2H, m, -CH_2N^+), 4.49-4.47 (1H, d, H-1), 4.28-4.19 (3H, m, H-6a, -CH_2N), 4.12-4.08 (1H, dd, H-6b), 4.02-3.89 (4H, m, $N^+CH_2CH_2$, NCH_2CH_2O), 3.87-3.81 (1H, m, ∝CH_2a), 3.79-3.62 (7H, m_c, $OCH_2CH_2OCH_2C{\equiv}C$, H-5),3.56-3.51 (1H, dd~t, H-4), 3.48-3.42 (1H, m, ∝CH_2b), 2.52 (1H, s, C≡CH), 2.13, 2.04, 2.02 (9H, 3s, Ac), 1.55 (2H, bs, βCH_2), 1.26 (18H, bs, bulk -CH_2), 0.90-0.87 (3H, t, CH_3); $^3J_{1,2}$=8.5, $^3J_{2,3}$=9.0, $^3J_{3,4}$=9.0, $^3J_{4,5}$=9.0, $^3J_{5,6a}$=2.0, $^3J_{5,6b}$=5.0, $^2J_{6a,6b}$=11.0 Hz; ^{13}C NMR (100 MHz, $CDCl_3$): δ 170.7, 170.1, 169.3 (C=O), 136.7 (C*H*=N-CH), 122.9 (CH=N-*C*H), 122.4 (CH=*C*H-N), 100.3 (C-1), 79.3 (*C*≡CH), 76.0 (C-4), 75.0 (C≡*C*H), 74.5 (C-3), 72.2 (C-5), 71.6 (C-2), 70.1, 70.03, 69.95, 68.8, 68.4 (-*C*$H_2CH_2N^+$, -*C*H_2CH_2O, ∝CH_2, -$OCH_2CH_2OCH_2C{\equiv}C$), 62.2 (C-6), 58.3 (-*C*H_2N), 49.8 (-CH_2N^+), 31.78/ 31.74, 31.0, 30.7, 29.97/ 29.93, 29.61/ 29.58, 29.5, 29.24/ 29.22, 26.7, 26.6, 26.5, 26.4 (bulk -CH_2), 22.6 (ω-1), 21.0, 20.9, 20.5 (Ac), 13.9 (ω).

Dodecyl 4-*O*-[[1-(1-propyn-4,7-dioxa-nonyl)-3-ethyl]-imidazolium]β-D-glucopyranoside iodide (37)

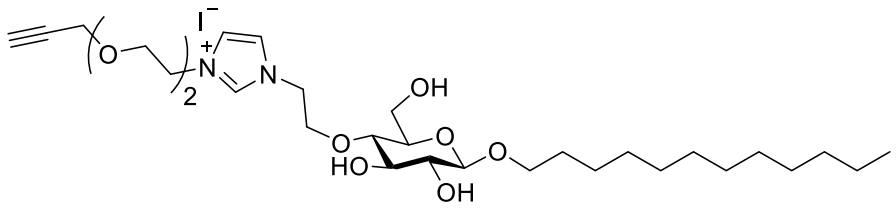

Following general procedure **3.6.5**, compound **36** (0.20 g, 0.24 mmol) was deacetylated in CH_3OH (5 mL) to provide compound **37** (0.16 g, 96 %) as a brown syrup. IR [neat] ν/cm^{-1} 3391 (OH), 2923, 2854 (CH), 2107 (C≡C). $[\propto]_D^{25}$ = -8 (c 0.15, CH_3OH); ^{1}H NMR (400 MHz, CD_3OD): δ 9.13 (1H, s, C*H*=N-CH), 7.75 (2H, s, CH=CH-N), 4.53-4.51 (4H, m, -CH_2N^+, -CH_2N), 4.31-4.29 (1H, d, H-1), 4.26 (3H, bs, $CH_2C{\equiv}C$, -C*H*$_2CH_2N^+$), 4.12-4.08 (1H, m, -C*H*$_2CH_2N^+$), 3.96-3.90 (3H, m, -C*H*$_2CH_2N$, ∝CH_2a), 3.76-3.73 (5H, H-6a, -OCH_2CH_2O), 3.62-3.52 (3H, m, H-6b, ∝CH_2b, H-3) 3.40-3.33 (2H, m, H-4, H-5), 3.25-3.21 (1H, dd~t, H-2), 2.98 (1H, bs, C≡CH), 1.69-1.64 (2H, m, βCH_2), 1.36 (18H, bs, bulk -CH_2), 0.98-0.95 (3H, t, -CH_3); $^3J_{1,2}$=8.0, $^3J_{2,3}$=9.0 Hz; ^{13}C NMR (100 MHz, CD_3OD): δ 138.4 (*C*H=N-CH), 124.1 (CH=N-*C*H), 124.0 (CH=*C*H-N), 104.3 (C-1), 80.8 (*C*≡CH), 79.7 (C-4), 77.9 (C-3), 76.7 (C-5), 76.4 (C≡*C*H), 75.5 (C-2), 71.2 (2) (∝CH_2, -*C*$H_2CH_2N^+$), 71.1, 70.2 (-OCH_2CH_2O), 69.9 (-*C*H_2CH_2N), 62.1 (C-6), 59.2 (-*C*$H_2C{\equiv}CH$), 51.5 (-CH_2N), 51.0 (-CH_2N^+), 33.2, 30.9, 30.8, 30.7, 30.6, 27.2, 27.0 (bulk CH_2, βCH_2), 23.8 (ω-1), 14.6 (ω). HRDARTMS: Calcd. for $[M]^+$ $[C_{30}H_{53}N_2O_8]^+$ 569.3802; found 569.3807.

2-Hexyl-decyl 4,6-*O*-benzylidene-β-D-glucopyranoside (38a)

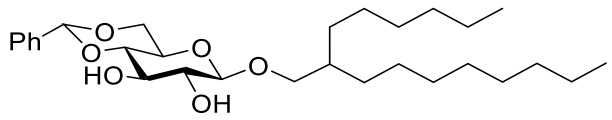

A solution of glucoside **9** (3.8 g, 9.4 mmol), $PhCH(OCH_3)_2$ (3.4 mL, 23 mmol) and *p*-TsOH·H_2O (0.10 g) in CH_2Cl_2 (70 mL) was stirred at room temperature following the general procedure **3.6.8**. Compound **38a** (4.0 g, 87 %) was obtained as a light yellow syrup by column chromatography (EtOAc: hexane = 1:4) with a trace amount of benzaldehyde impurity. $[\propto]_D^{25}$ = -34 (c 0.57, $CHCl_3$); ^{1}H NMR (400 MHz, $CDCl_3$): δ 7.52-7.37 (5H, m, aromatic -CH), 5.55 (1H, s, -CHPh), 4.38-4.34 (2H, m, H-1, H-6eq), 3.86-3.78 (3H, m, H-6ax, H-3, -OC*H*$_2$a-CH), 3.60-3.39 (4H, m, H-5, H-4, H-2, -OC*H*$_2$b-CH), 1.63 (1H, bs, -OCH_2C*H*), 1.28 (24H, m, bulk -CH_2), 0.91-0.88 (6H, t, -CH_3); $^3J_{1,2}$=8.0, $^3J_{2,3}$=10.0, $^3J_{3,4}$=10.0, $^3J_{4,5}$=5.0, $^3J_{5,6ax}$=10.0, $^3J_{5,6eq}$=5.0, $^2J_6$=11.0 Hz; ^{13}C NMR (100 MHz, $CDCl_3$): δ 134.0 (aromatic -C), 129.3, 128.3, 126.3 (aromatic -CH), 103.5 (C-1), 101.9 (-CHPh), 80.6 (C-4), 74.7 (C-2), 73.7 (-O*C*H_2CH), 73.1 (C-3), 68.7 (C-6), 66.4 (C-5), 38.2 (-OCH_2*C*H), 31.90, 31.85/ 31.84, 31.23, 31.15, 30.0, 29.7, 29.60/ 29.58, 29.3, 26.74/ 26.70 (bulk -CH_2), 22.7 (ω-1), 14.1 (ω).

2-Butyl-octyl 4,6-*O*-benzylidene-β-D-glucopyranoside (38b)

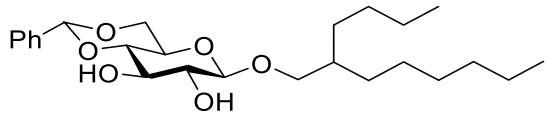

Glucoside **10** (2.7 g, 7.7 mmol) was dissolved in CH_2Cl_2 (50 mL), followed by addition of $PhCH(OCH_3)_2$ (2.8 mL, 19 mmol) and *p*-$TsOH \cdot H_2O$ (0.10 g) according to general procedure **3.6.8**. Compound **38b** (2.4 g, 71 %) was obtained as a light yellow syrup by column chromatography (EtOAc: hexane = 1:4) with a trace amount of benzaldehyde impurity. $[\propto]_D^{25}$ = -37 (c 0.22, $CHCl_3$); ^{1}H NMR (400 MHz, $CDCl_3$): δ 10.04 (1H, s, CHO impurity), 7.91-7.37 (> 5H, m, aromatic -CH), 5.55 (1H, s, -CHPh), 4.38-4.34 (2H, m, H-1, H-6eq), 3.87-3.78 (3H, m, H-3, -OC*H*$_2$a-CH, H-6ax),3.60-3.39 (4H, m, H-4, H-2, -OC*H*$_2$b-CH, H-5), 1.63 (1H, bs, -OCH_2C*H*), 1.28-1.27 (16H, m, bulk -CH_2), 0.91-0.88 (6H, t, -CH_3); $^3J_{1,2}$=8.0, $^3J_{2,3}$=9.5, $^3J_{3,4}$=9.5, $^3J_{4,5}$=9.5, $^3J_{5,6ax}$= 10.0, $^3J_{5,6eq}$= 3.5, $^2J_6$=11.0 Hz; ^{13}C NMR (100 MHz, $CDCl_3$): δ 136.9 (aromatic -C), 129.8, 129.3, 129.0, 128.3, 126.3 (aromatic -CH), 103.5 (C-1), 101.9 (-CHPh), 80.6 (C-4), 74.7 (C-2), 73.7 (-O*C*H_2CH), 73.1 (C-3), 68.7 (C-6), 66.4 (C-5), 38.2 (-OCH_2*C*H), 31.8, 31.2, 31.1, 30.9, 30.8, 29.7, 28.9, 26.69, 26.67, 23.0 (bulk -CH_2), 22.7 (ω-1), 14.1 (CH_3).

2-Hexyl-decyl 2,3,6-tri-*O*-benzyl-β-D-glucopyranoside (40a)

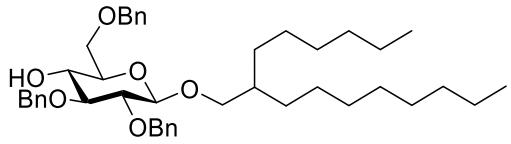

Compound **38a** (3.8 g, 7.7 mmol) was treated with NaH (60 % suspension in paraffin oil) (1.2 g, 30 mmol) in DMF (60 mL), followed by addition of BnBr (2.7 mL, 23 mmol) according to general procedure **3.6.9**. The crude material **39a** was directly subjected to a selective opening of the benzylidene acetal using Et_3SiH (7.5 mL, 46 mmol) and TFA (3.6 mL, 47 mmol) in CH_2Cl_2 (70 mL). Compound **40a** (3.0 g, 58 % over 2 steps) was obtained as a colourless syrup by following the general procedure **3.6.10** and a column chromatography (EtOAc: hexane= 1:7). $[\propto]_D^{25}$ = -22 (c 0.25, $CHCl_3$); ^{1}H NMR (400 MHz, $CDCl_3$): δ 7.37-7.29 (15H, m, aromatic -CH), 4.99-4.92, 4.74-4.70, 4.64-4.57 (6H, 3 dd, -CH_2Ph), 4.40-4.39 (1H, d, H-1), 3.90-3.86 (1H, dd, -OC*H*$_2$a-CH), 3.80-3.77 (1H, dd, H-6a), 3.73-3.69 (1H, dd, H-6b), 3.62-3.58 (1H, dd~t, H-3), 3.49-3.42 (3H, m, -OC*H*$_2$b-CH, H-4, H-5), 3.40-3.36 (1H, dd, H-2), 1.63 (1H, bs, -OCH$_2$C*H*), 1.25 (24H, bs, bulk -CH_2), 0.90-0.87 (6H, t, -CH_3); $^3J_{1,2}$= 8.0, $^3J_{3,4}$= 9.0, $^3J_{4,5}$= 9.0, $^3J_{5,6a}$= 4.0, $^3J_{5,6b}$= 6.0, $^2J_{6a,6b}$= 11.0 Hz; ^{13}C NMR (100 MHz, $CDCl_3$): δ 138.8, 138.7, 138.4, 138.0 (aromatic -C), 128.5, 128.4, 128.3, 128.04, 127.95, 127.8, 127.69, 127.67, 127.6 (aromatic -CH), 103.9 (C-1), 84.1 (C-4), 81.7 (C-2), 75.3, 74.7 (-CH_2Ph), 74.0 (C-5), 73.7 (-CH_2Ph), 73.0 (-O*C*H$_2$CH), 71.4 (C-3), 70.4 (C-6), 38.4 (-OCH$_2$*C*H), 31.9, 31.4, 31.3, 30.1, 29.7, 29.66/ 29.64, 29.4, 27.0, 26.9, 26.8, 26.7 (bulk -CH_2), 22.7 (ω-1), 14.1 (ω).

2-Butyl-octyl 2,3,6-tri-*O*-benzyl--β-D-glucopyranoside (40b)

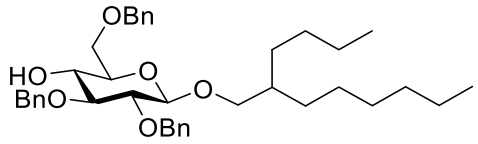

Compound **38b** (2.3 g, 5.3 mmol) was treated with NaH (60 % suspension in paraffin oil) (0.90 g, 23 mmol) in DMF (50 mL) and BnBr (1.9 mL, 16 mmol) afterwards following the general procedure **3.6.9**. The crude **39b** was used for the subsequent selective opening of the benzylidene acetal by treating it with Et_3SiH (5.2 mL, 32 mmol) and TFA (2.5 mL, 32 mmol) in CH_2Cl_2 (50 mL) according to the general procedure **3.6.10**. Compound **40b** (1.4 g, 42 %) was obtained as a colourless solid by column chromatography (EtOAc: hexane= 1:7). $[\propto]_D^{25}$ = -18 (c 0.20, $CHCl_3$); ^{1}H NMR (400 MHz, $CDCl_3$): δ 7.37-7.29 (15H, m, aromatic -CH), 4.99-4.92, 4.74-4.71, 4.64-4.57 (6H, 3 dd, -CH_2Ph), 4.40-4.39 (1H, d, H-1), 3.90-3.87 (1H, dd, -OC*H*$_2$a-CH), 3.80-3.77 (1H, dd, H-6a), 3.73-3.69 (1H, dd, H-6b), 3.62-3.57 (1H, dd, H-3), 3.49-3.36 (4H, m, H-4, H-5, H-2, -OC*H*$_2$b-CH), 1.64-1.61 (1H, m, -OCH$_2$C*H*), 1.29-1.25 (16H, m, bulk -CH_2), 0.88-0.87 (6H, t, -CH_3); $^3J_{1,2}$= 8.0, $^3J_{3,4}$= 9.0, $^3J_{4,5}$= 9.0, $^3J_{5,6a}$= 4.0, $^3J_{5,6b}$= 5.5, $^2J_{6a,6b}$= 11.0 Hz; ^{13}C NMR (100 MHz, $CDCl_3$): δ 138.8, 138.7, 138.4, 138.0 (aromatic -C), 128.5, 128.4, 128.3, 128.1, 127.9, 127.8, 127.68, 127.66, 127.6 (aromatic -CH), 103.9 (C-1), 84.1 (C-4), 81.7 (C-2), 75.2, 74.7 (-CH_2Ph), 74.0 (C-5), 73.7 (-CH_2Ph), 73.0 (-O*C*H$_2$CH), 71.7 (C-3), 70.4 (C-6), 38.3 (-OCH$_2$*C*H), 31.9, 31.37/ 31.31, 31.06/ 30.98, 29.7, 29.16/ 28.96, 26.94/ 26.71, 23.0 (bulk -CH_2), 22.7 (ω-1) 14.1 (ω).

2-Hexyl-decyl 2,3,6-tri-*O*-benzyl-4-*O*-(2-iodoethyl)-β-D-glucopyranoside (43a)

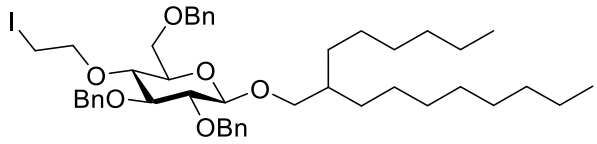

A mixture containing compound **40a** (2.9 g, 4.3 mmol), 50 % NaOH (aq) (40 mL), toluene (60 mL), TBAB (1.4 g, 4.3 mmol) and $BrCH_2COOtBu$ (1.3 mL, 8.7 mmol) was treated according to general procedure **3.6.12**. Crude material **41a** was obtained a yellow syrup and it was subjected to a reduction using $LiAlH_4$ (0.40 g, 11 mmol) in THF (70 mL), according to general procedure **3.6.13** to provide crude **42a** as a yellow syrup. The mixture of crude **42a**, I_2 (1.7 g, 6.7 mmol), PPh_3 (1.6 g, 6.1 mmol) and imidazole (0.90 g, 13 mmol) in toluene (50 mL) was heated to 50 ^{o}C, following general procedure **3.6.14**. Compound **43a** (2.1 g, 59 % over 3 steps) was obtained as a light yellow syrup after chromatography over silica gel (EtOAc: hexane= 1:12). $[\propto]_D^{25}$ = +6 (c 0.42, $CHCl_3$); ^{1}H NMR (400 MHz, $CDCl_3$): δ 7.33-7.27 (15H, m, aromatic -CH), 4.96-4.55 (6H, 3 dd, –CH_2Ph), 4.34-4.32 (1H, d, H-1), 3.97-3.96 (1H, m, -OC*H*$_2$a-CH), 3.88-3.86 (1H, dd,H-6a), 3.75-3.69 (3H, m, -OC*H*$_2$$CH_2$I, -OC*H*$_2$b-CH), 3.57-3.53 (1H, dd~t, H-4), 3.45-3.36 (4H, m, H-6b, H-3, H-2, H-5), 3.05-3.02 (2H, m, -CH_2I), 1.79 (1H, bs, -OCH$_2$C*H*), 1.41-1.23 (24H, m, bulk -CH_2), 0.86 (6H, bs, -CH_3); $^3J_{1,2}$= 7.5, $^3J_{2,3}$= 9.0, $^3J_{3,4}$= 9.0 Hz; ^{13}C NMR (100 MHz, $CDCl_3$): δ 138.6, 138.5, 138.2 (aromatic -C), 128.34, 128.29, 128.0, 127.9, 127.8, 127.6 (aromatic -CH), 103.9 (C-1), 84.4 (C-4), 82.2 (C-5), 77.9 (C-2), 75.5 (-CH_2Ph), 74.69 (C-3), 74.67 (-CH_2Ph), 73.5 (-CH_2Ph), 73.0 (-O*C*H$_2$CH), 72.9 (C-6), 68.7 (O*C*H$_2$$CH_2$I), 38.4 (-OCH$_2$*C*H), 31.9, 31.4, 31.3, 30.1, 29.7, 29.66/ 29.63, 29.3, 26.98, 26.94, 26.8, 26.7 (bulk -CH_2), 22.7 (ω-1), 14.1 (ω), 3.5 (CH_2I).

2-Butyl-octyl 2,3,6-tri-*O*-benzyl-4-*O*-(2-iodoethyl)-β-D-glucopyranoside (43b)

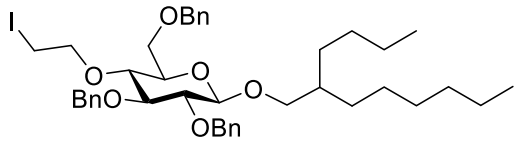

A solution of **40b** (1.3 g, 2.1 mmol) in toluene (30 mL) was treated with 50 % NaOH (aq) (20 mL), TBAB (0.70 g, 2.2 mmol) and $BrCH_2COOtBu$ (0.60 mL, 4.1 mmol) were added slowly following the general procedure **3.6.12**, to furnish a yellow syrup **41b**, which was subjected to a reduction using $LiAlH_4$ (0.16 g, 4.2 mmol) in THF (40 mL), according to general procedure **3.6.13** to provide crude **42b** as a yellow syrup. The mixture of compound **42b**, I_2 (0.80 g, 3.2 mmol), PPh_3 (0.80 g, 3.1 mmol) and imidazole (0.40 g, 5.9 mmol) in toluene (30 mL) was heated to 50 ^{o}C following general procedure **3.6.14**. Compound **43b** (0.90 g, 55 % over 3 steps) was obtained as a light yellow syrup after chromatography over silica gel (EtOAc: hexane= 1:16). $[\propto]_D^{25} = +9$ (c 0.49, $CHCl_3$); ^{1}H NMR (400 MHz, $CDCl_3$): δ 7.33-7.23 (15H, m, aromatic -CH), 4.95-4.54 (6H, m, $-CH_2Ph$), 4.34-4.32 (1H, d, H-1), 3.99-3.93 (1H, m, -OC*H*$_2$a-CH), 3.89-3.85 (1H, dd, H-6a), 3.75-3.68 (3H, m-, -OC*H*$_2$CH$_2$I, -OC*H*$_2$b-CH), 3.57-3.53 (1H, dd~t, H-4), 3.45-3.34 (4H, m, H-6b, H-3, H-2, H-5), 3.08-2.99 (2H, m, CH_2I), 1.60-1.59 (1H, m, -OCH$_2$C*H*), 1.27-1.23 (16H, m, bulk -CH_2), 0.86-0.85 (6H, t~bs, -CH_3); $^3J_{1,2}$=8.0, $^3J_{2,3}$=9.0, $^3J_{3,4}$=9.0, $^3J_{5,6a}$=5.0, $^2J_{6a,6b}$=9.5 Hz; ^{13}C NMR (100 MHz, $CDCl_3$): δ 138.5, 138.4, 138.2 (aromatic-C), 128.33, 128.29, 128.0, 127.9, 127.8, 127.6 (aromatic -CH), 103.9 (C-1), 84.4 (C-4), 82.2 (C-5), 77.8 (C-2), 75.5 (-CH_2Ph), 74.68 (-CH_2Ph), 74.65 (C-3), 73.5 (-CH_2Ph), 73.0 (-O*C*H$_2$CH), 72.8 (C-6), 68.7 (-O*C*H$_2$CH$_2$I), 38.3 (-CH_2I), 31.9, 31.3, 31.05/ 31.00, 29.7, 29.2, 29.0, 26.9, 26.7, 23.0 (bulk -CH_2), 22.7 (ω-1),14.1 (ω), 3.5 (CH_2I).

2-Hexyl-decyl2,3,6-tri-*O*-benzyl-4-*O*-(2-(1*H*-imidazol-1-yl)ethyl)-β-D glucopyranoside (44a)

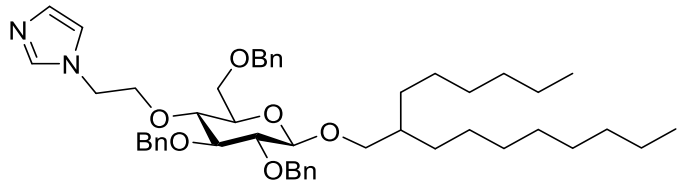

To a mixture of imidazole (0.30 g, 4.4 mmol) and NaH (60 % suspension in paraffin oil) (0.20 g, 5.0 mmol) in THF (25 mL), iodo-compound **43a** (1.9 g, 2.3 mmol) was added according to general procedure **3.6.1**. Compound **44a** (1.2 g, 68 %) was obtained as a light yellow syrup by column chromatography (EtOAc: hexane= 2:3). ^{1}H NMR (400 MHz, $CDCl_3$): δ 7.58 (1H, s, C*H*=N-CH), 7.36-7.20 (15H, m, aromatic -CH), 7.03 (1H, s, CH=N-C*H*), 6.80-6.79 (1H, t, CH=C*H*-N), 4.97-4.40 (6H,3 dd, -CH_2Ph), 4.34-4.32 (1H, d, H-1), 3.98-3.93 (1H, m, -OC*H*$_2$aCH_2), 3.89-3.84 (3H, m, -OC*H*$_2$a-CH, -CH_2N), 3.65-3.60 (1H, m, -OC*H*$_2$bCH_2), 3.55-3.50 (2H, m, H-6a, H-4), 3.45-3.34 (4H, m, H-2, H-3, H-6b, -OC*H*$_2$b-CH), 3.31-3.28 (1H, m, H-5), 1.63-1.60 (1H, m, -OCH_2C*H*), 1.43-1.24 (24H, m, bulk -CH_2), 0.89-0.85 (6H, m, CH_3); $^{3}J_{1,2}$=8.0, $^{3}J_{2,3}$=9.0, $^{3}J_{3,4}$=9.0, $^{3}J_{4,5}$=9.0, $^{3}J_{5,6a}$=2.0, $^{3}J_{5,6b}$=6.0 $^{2}J_{6a,6b}$=12.0 Hz; ^{13}C NMR (100 MHz, $CDCl_3$): δ 138.5, 138.3, 138.1 (aromatic -C), 137.2 (N=CH-N), 128.22, 128.20, 127.9, 127.63, 127.58, 127.5 (aromatic -CH, CH=N-*C*H), 119.2 (CH=*C*H-N), 103.8 (C-1), 84.3 (C-4), 82.0 (C-3), 77.7 (C-2), 75.2, 74.9 (-CH_2Ph), 74.4 (C-5), 73.2 (-CH_2Ph), 72.7 (-O*C*H_2CH), 71.3 (-O*C*H_2CH_2), 68.3 (C-6), 47.3 (-CH_2N), 38.2 (OCH_2*C*H), 31.8, 31.2, 30.0, 29.6, 29.5, 29.2, 26.9, 26.8, 26.7, 26.6 (bulk -CH_2), 22.6 (ω-1), 14.0 (ω).

2-Butyl-octyl 2,3,6-tri-*O*-benzyl-4-*O*-(2-(1*H*-imidazol-1-yl)ethyl)-β-D-glucopyranoside (44b)

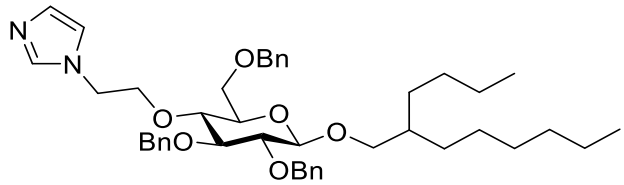

In a mixture containing imidazole (0.13 g, 1.9 mmol) and NaH (60 % suspension in paraffin oil) (0.10 g, 2.5 mmol) in THF (25 mL), iodo-compound **43b** (0.71 g, 0.92 mmol) was added according to general procedure **3.6.1**. Compound **44b** (0.50 g, 76 %) was obtained as a light yellow syrup after column chromatography (EtOAc: hexane= 2:3). ^{1}H NMR (400 MHz, $CDCl_3$): δ 7.56 (1H, s, C*H*=N-CH), 7.37-7.21 (15H, m, aromatic-CH), 7.04-7.03 (1H, t, CH=N-C*H*), 6.80 (1H, t, CH=C*H*-N), 4.98-4.88 (2H, dd, CH_2Ph), 4.70-4.57 (2H, dd, CH_2Ph), 4.52-4.41 (2H, dd, CH_2Ph), 4.35-4.33 (1H, d, H-1), 3.98-3.94 (1H, m, -OC*H*$_2$aCH$_2$), 3.89-3.85 (3H, m, -OC*H*$_2$aCH, -CH_2N), 3.66-3.61 (1H, m, -OC*H*$_2$bCH$_2$), 3.55-3.51 (2H, m, H-6a, H-4), 3.4-3.35 (4H, m, H-2, H-3, H-6b, -OC*H*$_2$CH), 3.32-3.28 (1H, m, H-5), 1.62-1.61 (1H, m, -OCH$_2$C*H*), 1.44-1.25 (16H, m, bulk -CH_2), 0.89-0.85 (6H, m, -CH_3); $^{3}J_{1,2}$=8.0, $^{3}J_{2,3}$=9.0, $^{3}J_{3,4}$=9.0, $^{3}J_{4,5}$=9.0, $^{3}J_{5,6a}$=2.5, $^{3}J_{5,6b}$=5.0 $^{2}J_{6a,6b}$=12.0 Hz; ^{13}C NMR (100 MHz, $CDCl_3$): δ 138.4, 138.2, 138.0 (aromatic -C), 137.2 (*C*H=N-CH), 128.3, 128.2, 128.1, 127.8, 127.6, 127.5, 127.4 (aromatic-CH, CH=N-*C*H), 119.1 (CH=*C*H-N), 103.7 (C-1), 84.2 (C-4), 81.9 (C-3), 77.7 (C-2), 75.2, 74.4 (-CH_2Ph), 74.3 (C-5), 73.2 (-CH_2Ph), 72.6 (-O*C*H$_2$CH), 71.3 (-OCH$_2$*C*H$_2$), 68.2 (C-6), 47.2 (-CH_2N), 38.1 (OCH$_2$*C*H), 31.7, 31.2, 30.88/ 30.84, 29.5, 28.97/ 28.80, 26.76/ 26.54, 22.9 (bulk -CH_2), 22.5 (ω-1), 13.9 (ω).

2-Hexyl-decyl2,3,6-tri-*O*-acetyl-4-*O*-(2-(1*H*-imidazol-1-yl)ethyl)-β-D-glucopyranoside (46a)

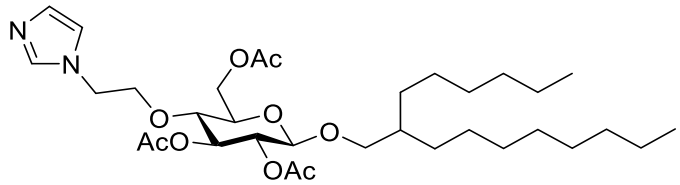

Benzylated compound **44a** (1.0 g, 1.3 mmol) was dissolved in CH_3OH (100 mL). Conc. HCl (1.0 mL) and catalyst Pd/C (10 %, 30 mg) were added and the reaction was under H_2 atmosphere according to general procedure **3.6.11** to furnish crude compound **45a**, which was then dissolved in pyridine (30 mL) and treated with Ac_2O (1.5 mL, 16 mmol) according to general procedure **3.6.7**. Acetylated compound **46a** (0.55 g, 68 % over 2 steps) was obtained as a yellow syrup by column chromatography (EtOAc: acetone 1:8) over silica gel. $[\propto]_D^{25}$ = -24 (c 0.24, $CHCl_3$); ^{1}H NMR (400 MHz, $CDCl_3$): δ 8.27 (< 1H, s, C*H*=N-CH), 7.16 (1H, s, CH=N-C*H*), 7.02 (1H, s, CH=C*H*-N), 5.18-5.13 (1H, dd~t,, H-3), 4.87-4.82 (1H, dd~t, H-2), 4.42-4.40 (1H, d, H-1), 4.29-4.21 (3H, m, H-6a, -CH_2N), 4.10-4.04 (1H, m, H-6b), 3.90-3.75 (3H, m, -OC*H*$_2$CH$_2$, -OC*H*$_2$a-CH), 3.51-3.49 (2H, m, H-4, H-5), 3.29-3.25 (1H, dd, -OC*H*$_2$b-CH), 2.10, 2.01, 1.97 (9H, 3 s, Ac), 1.53 (1H, bs, -OCH$_2$C*H*), 1.25-1.23 (24H, m, bulk -CH_2), 0.90-0.86 (6H, t, -CH_3); $^3J_{1,2}$=8.0, $^3J_{2,3}$=9.0, $^3J_{3,4}$=9.0, $^2J_{6a,6b}$=12.5 Hz; ^{13}C NMR (100 MHz, $CDCl_3$): δ 170.5, 170.0, 169.5 (C=O), 137.0 (*C*H=N-CH), 127.1 (CH=N-*C*H), 119.7 (CH=*C*H-N), 100.8 (C-1), 76.4 (C-4), 74.5 (C-3), 73.1 (-O*C*H$_2$CH), 72.4 (C-5), 71.8 (C-2), 71.3 (-O*C*H$_2$CH$_2$), 62.3 (C-6), 47.7 (-CH_2N), 37.9 (-OCH$_2$*C*H), 31.82, 31.78, 31.0, 30.8, 30.01, 29.97, 29.65/ 29.6, 29.5, 29.28/ 29.26, 26.73/ 26.67, 26.54/ 26.49 (bulk -CH_2), 22.6 (ω-1), 20.8, 20.7, 20.5 (3 Ac), 14.0 (ω).

2-Butyl-octyl 2,3,6-tri-*O*-acetyl-4-*O*-(2-(1*H*-imidazol-1-yl)ethyl)-β-D-glucopyranoside (46b)

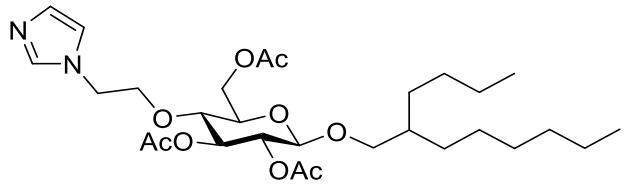

Benzylated compound **44b** (0.30 g, 0.42 mmol) was dissolved in CH_3OH (100 mL). Conc. HCl (1.0 mL) and catalyst Pd/C (10 %, 30 mg) were added. The reaction was under H_2 atmosphere according to general procedure **3.6.11** to furnish a yellow syrup **45b**, which was then dissolved in pyridine (20 mL) and treated with Ac_2O (0.50 mL, 5.3 mmol) according to general procedure **3.6.7**. Acetylated compound **46b** (0.17 g, 71 % over 2 steps) was obtained as a yellow syrup by column chromatography (EtOAc: acetone 1:8) over silica gel. $[\propto]_D^{25}$ = -17 (c 0.05, $CHCl_3$); ^{1}H NMR (400 MHz, $CDCl_3$): δ 7.54 (1H, s, N=CH-N), 7.03 (1H, s, CH=C*H*-N), 6.89 (1H, s, C*H*=CH-N), 5.16-5.11 (1H, dd~t,, H-3), 4.84-4.79 (1H, dd~t, H-2), 4.40-4.38 (1H, d, H-1), 4.25-4.22 (1H, dd~d, H-6a), 4.06-4.04 (2H, t, -CH_2N), 4.02-3.98 (1H, dd, H-6b), 3.82-3.73 (3H, m, CH_2O, -OC*H*$_2$a-CH), 3.48-3.43 (2H, m, H-4, H-5), 3.27-3.23 (1H, dd, -OC*H*$_2$b-CH), 2.07, 1.99, 1.93 (9H, 3 s, Ac), 1.50 (1H, bs, -OCH_2C*H*), 1.27-1.21 (16H, m, bulk -CH_2), 0.87-0.84 (6H, t, CH_3); $^3J_{1,2}$=8.0, $^3J_{2,3}$=9.0, $^3J_{3,4}$=9.0, $^2J_{6a,6b}$=12.5 Hz; ^{13}C NMR (100 MHz, $CDCl_3$): δ 170.5, 170.0, 169.5 (C=O), 137.0 (N=CH-N), 127.1 (*C*H=CH-N), 119.7 (CH=*C*H-N), 100.8 (C-1), 76.4 (C-5), 74.5 (C-3), 73.1 (-O*C*H_2CH), 72.4 (C-4), 71.8 (C-2), 71.3 (CH_2O), 62.3 (C-6), 47.7 (CH_2N), 37.9 (OCH_2*C*H), 31.82, 31.78, 31.0, 30.8, 30.01, 29.97, 29.7, 29.6, 29.5, 29.28, 29.26, 26.73, 26.67, 26.54 (bulk CH_2), 26.49 (γ), 22.6 (ω-1), 20.8, 20.7, 20.5 (3 Ac), 14.0 (ω).

2-Hexyl-Decyl 4-*O*-[[1-(1-propyn-4,7-dioxa-nonyl)-3-ethyl]-imidazolium]-2,3,6-tri-*O*-acetyl-β-D-glucopyranoside iodide (47a)

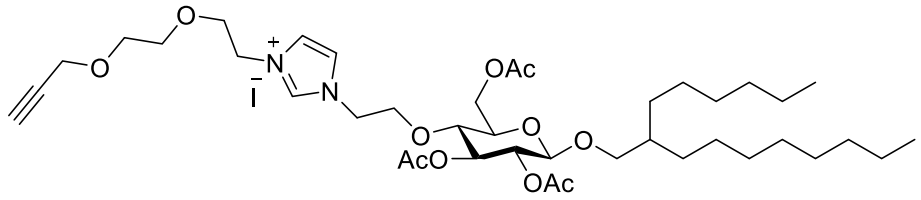

Compounds **46a** (0.50 g, 0.80 mmol) and **6** (0.20 g, 0.80 mmol) were dissolved in toluene (3 mL) and treated according to general procedure **3.6.15**, furnishing compound **47a** (0.60 g, 85 %) as a brown syrup. $[\propto]_D^{25}$ = -15 (c 1.21, $CHCl_3$); ^{1}H NMR (400 MHz, $CDCl_3$): δ 9.39 (1H, s, C*H*=N-CH), 7.63 (1H, s, CH=N-C*H*), 7.55 (1H, s, CH=C*H*-N), 5.06-5.02 (1H, dd~t, H-3), 4.75-4.70 (1H, dd~t, H-2), 4.49-4.48 (2H, m, -CH_2N^+), 4.35-4.33 (1H, d, H-1), 4.17-4.11 (3H, m, H-6a, -CH_2N), 4.04-4.00 (1H, dd, H-6b), 3.92-3.85 (4H, m_c, $N^+CH_2CH_2$, NCH_2CH_2O), 3.69-3.56 (8H, m, -OCH_2a-CH, $OCH_2CH_2OCH_2C{\equiv}C$, H-5), 3.46-3.41 (1H, dd~t, H-4), 3.18-3.14 (1H, dd, -OCH_2b-CH), 2.54 (1H, s, C≡CH), 2.02, 1.92, 1.90 (9H, 3 s, Ac), 1.42 (1H, bs, -OCH_2CH), 1.15-1.13 (24H, m, bulk -CH_2), 0.79-0.76 (6H, t, -CH_3); $^3J_{1,2}$=9.0, $^3J_{2,3}$=9.5, $^3J_{3,4}$=9.5, $^3J_{4,5}$=9.5, $^3J_{5,6b}$=4.0, $^2J_{6a,6b}$=12.0 Hz; ^{13}C NMR (100 MHz, $CDCl_3$): δ 170.5, 169.9, 169.0 (C=O), 136.8 (*C*H=N-CH), 122.8 (CH=N-*C*H), 122.3 (CH=*C*H-N), 100.5 (C-1), 79.2 (*C*≡CH), 75.8 (C-4), 74.9 (C≡*C*H), 74.3 (C-3), 72.8 (-O*C*H_2CH), 72.0 (C-5), 71.4 (C-2), 69.9, 69.8, 68.7, 68.6, 68.3 ($N^+CH_2CH_2$, NCH_2CH_2O, $OCH_2CH_2OCH_2C{\equiv}C$), 62.1 (C-6), 58.1 (NCH_2), 49.6 (CH_2N^+), 37.6 (OCH_2CH), 31.52, 31.48, 30.7, 30.5, 29.71, 29.66, 29.4, 29.3, 29.2, 28.97/ 28.96, 26.42/ 26.36, 26.23 (bulk CH_2), 26.18 (γ), 22.3 (ω-1), 20.9, 20.8, 20.3 (3 Ac), 13.8 (ω).

2-Butyl-octyl 4-*O*-[[1-(1-propyn-4,7-dioxa-nonyl)-3-ethyl]-imidazolium]-2,3,6-tri-*O*-acetyl-β-D-glucopyranoside iodide (47b)

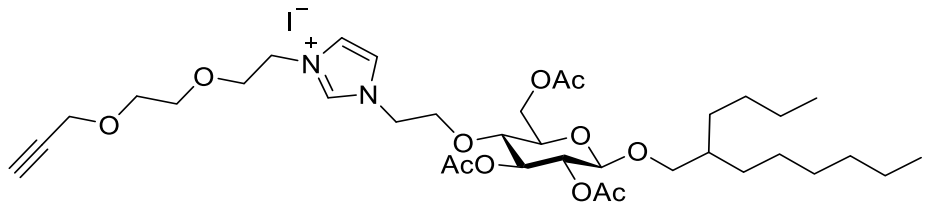

Compounds **46b** (0.13 g, 0.23 mmol) and **6** (58 mg, 0.23 mmol) were dissolved in toluene (5 mL) and treated according to general procedure **3.6.15**, furnishing compound **47b** (0.18 g, 95 %) as a brown syrup. $[\propto]_D^{25}$ = -18 (c 0.16, $CHCl_3$); ^{1}H NMR (400 MHz, $CDCl_3$): δ 9.91 (1H, s, C*H*=N-CH), 7.52 (1H, s, CH=N-C*H*), 7.43 (1H, s, CH=C*H*-N), 5.18-5.13 (1H, dd~t, H-3), 4.87-4.82 (1H, dd~t, H-2), 4.56-4.54 (2H, m, CH_2N^+), 4.45-4.43 (1H, d, H-1), 4.27-4.20 (3H, m, H-6a, -CH_2N), 4.11-4.07 (1H, dd, H-6b), 4.02-3.91 (4H, m, $N^+CH_2CH_2$, NCH_2CH_2O), 3.79-3.69 (7H, m, -OC*H*$_2$a-CH, $OCH_2CH_2OCH_2C{\equiv}C$), 3.66-3.60 (1H, m, H-5) 3.55-3.50 (1H, dd~t, H-4), 3.29-3.25 (1H, m, -OC*H*$_2$b-CH), 2.53-2.51 (1H, t, C≡CH), 2.13, 2.03, 2.00 (9H, 3 s, Ac), 1.52 (1H, bs, -OCH_2C*H*), 1.23 (16H, m, bulk -CH_2), 0.89-0.86 (6H, t, CH_3); $^3J_{1,2}$=8.0, $^3J_{2,3}$=9.5, $^3J_{3,4}$=9.5, $^3J_{4,5}$=9.5, $^3J_{5,6b}$=2.0, $^3J_{5,6b}$=4.0, $^2J_{6a,6b}$=12.0 Hz; ^{13}C NMR (100 MHz, $CDCl_3$): δ 170.9, 170.3, 169.3 (C=O), 137.2 (*C*H=N-CH), 122.9 (CH=N-*C*H), 122.4 (CH=*C*H-N), 100.8 (C-1), 76.3 (C-4), 75.0 (C≡*C*H), 74.6 (C-3), 73.1 (-O*C*H_2CH), 72.4 (C-5), 71.7 (C-2), 70.2, 70.0, 69.1, 68.9, 68.6 ($N^+CH_2CH_2$, NCH_2CH_2O, $OCH_2CH_2OCH_2C{\equiv}C$), 62.3 (C-6), 58.4 (-CH_2N), 50.0 (CH_2N^+), 37.9 (-OCH_2*C*H), 31.8, 31.1, 30.9, 30.7, 30.5, 29.69, 29.66, 28.9, 28.8, 26.7, 26.6, 23.0 (bulk -CH_2), 22.6 (ω-1), 21.2, 21.0, 20.6 (Ac), 14.1 (ω).

2-Hexyl-decyl4-*O*-[[1-(1-propyn-4,7-dioxa-nonyl)-3-ethyl]-imidazolium]-β-D-glucopyranoside iodide (48a)

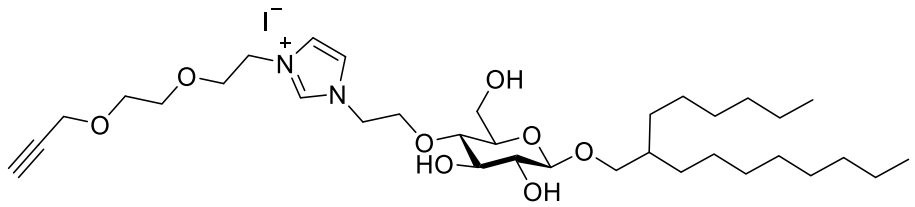

Compound **47a** (0.50 g, 0.57 mmol) was deacetylated according to procedure **3.6.5** in CH_3OH (5 mL) to furnish compound **48a** (0.40 g, 93 %) as a brown syrup. IR [neat] ν/cm^{-1} 3407 (OH), 2924, 2855 (CH), 2114 (C≡C). $[\propto]_D^{25}$ = -10 (c 0.41, CH_3OH); ^{1}H NMR (400 MHz, CD_3OD): δ 8.60 (1H, s, C*H*=N-CH), 7.73 (2H, s, CH=CH-N), 4.55-4.45 (4H, m, -CH_2N^+, -CH_2N), 4.28-4.25 (4H, m, H-1, -C*H*$_2CH_2N^+$, -$CH_2C{\equiv}C$), 4.11-4.07 (1H, m, -C*H*$_2CH_2N^+$), 3.94 (2H, m, -C*H*$_2CH_2N$), 3.86-3.82 (1H, t, -OC*H*$_2$a-CH), 3.75-3.73 (5H, m, H-6a, -OCH_2CH_2O), 3.59-3.51 (2H, m, H-6b, H-3), 3.46-3.42 (1H, t, -OC*H*$_2$b-CH),, 3.40-3.32 (2H, m, H-4, H-5), 3.26-3.22 (1H, dd~t, H-2), 2.96 (1H, s, C≡CH), 1.65 (1H, m, -OCH_2C*H*), 1.46-1.35 (24H, m, bulk -CH_2), 0.97-0.94 (6H, t, -CH_3); $^3J_{1,2}$=9.0, $^3J_{2,3}$=9.0, $^2J_{6a,6b}$=13.0 Hz; ^{13}C NMR (100 MHz, CD_3OD): δ 138.3 (*C*H=N-CH), 124.1 (CH=N-*C*H), 124.0 (N-CH=*C*H), 104.7 (C-1), 80.7 (*C*≡CH), 79.7 (C-4), 77.9 (C-3), 76.7 (C-5), 76.4 (C≡*C*H), 75.5 (C-2), 74.2 (-O*C*H_2CH), 71.22 (-*C*$H_2CH_2N^+$), 71.16, 70.2 (-OCH_2CH_2O), 69.9 (-*C*H_2CH_2N), 62.1 (C-6), 59.2 (-*C*$H_2C{\equiv}CH$), 51.5, 50.9 (-CH_2N, -CH_2N^+), 39.6 (-OCH_2*C*H), 33.1, 32.3, 31.2, 30.9, 30.8, 30.5, 27.9 (bulk -CH_2), 23.8 (ω-1), 14.6 (ω). HRESIMS: Calcd. for M^+ $[C_{34}H_{61}N_2O_8]^+$ 625.4428 (100 %), 626.4462 (37 %), 627.4496 (7 %); found 625.4429 (100 %), 626.4459 (40 %), 627.4490 (5 %).

2-Butyl-octyl 4-*O*-[[1-(1-propyn-4,7-dioxa-nonyl)-3-ethyl]-imidazolium]-β-D-glucopyranoside iodide (48b)

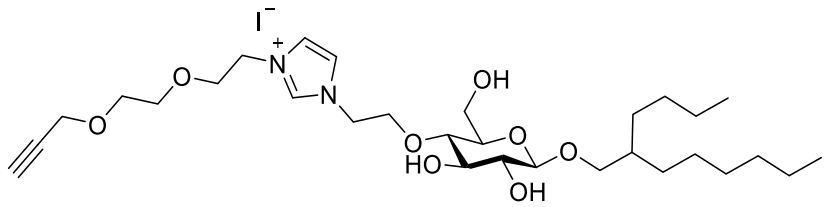

Compound **47b** (0.17 g, 0.21 mmol) was deacetylated according to procedure **3.6.5** in CH_3OH (5 mL) to furnish compound **48b** (0.13 g, 90 %) as a brown syrup. IR [neat] ν/cm^{-1} 3391 (OH), 2955, 2924, 2858 (CH), 2111 (C≡C). $[\propto]_D^{25}$ = -9 (c 0.17, CH_3OH); ^{1}H NMR (400 MHz, CD_3OD): δ 8.58 (1H, s, C*H*=N-CH), 7.71 (2H, d, CH=CH-N), 4.55-4.42 (4H, m, -CH_2N, -CH_2N^+), 4.26-4.23 (4H, m, H-1, -C*H*$_2CH_2N^+$, -C*H*$_2$C≡C), 4.10-4.04 (1H, m, -C*H*$_2CH_2N^+$), 3.93-3.91 (2H, t, -C*H*$_2CH_2$N), 3.84-33.76 (1H, m, -OC*H*$_2$a-CH), 3.72-3.71 (5H, m, H-6a, -OCH_2CH_2O), 3.58-3.49 (2H, m, H-6b, H-3), 3.44-3.32 (3H, m, -OC*H*$_2$b-CH, H-4, H-5), 3.24-3.20 (2H, dd~t, H-2), 2.95-2.94 (1H, t, C≡CH), 1.63 (1H, m, -OCH_2C*H*), 1.44-1.32 (16H, m, bulk -CH_2), 0.94-0.92 (6H, t, -CH_3); $^3J_{1,2}$=8.0, $^3J_{2,3}$=9.5, $^3J_{5,6b}$= 4.0 $^2J_{6a,6b}$=12.0 Hz; ^{13}C NMR (100 MHz, CD_3OD): δ 138.1 (*C*H=N-CH), 124.1 (CH=N-*C*H), 124.0 (CH=*C*H-N), 104.7 (C-1), 80.3 (*C*≡CH) 79.7 (C-4), 77.9 (C-3), 76.7 (C-5), 76.4 (C≡*C*H), 75.5 (C-2), 74.1 (-O*C*H_2CH), 71.22 (-*C*$H_2CH_2N^+$), 71.17, 70.2 (-OCH_2CH_2O), 69.9 (-*C*H_2CH_2N), 62.1 (C-6), 59.2 (-*C*H_2C≡CH) 51.5, 50.9 (-CH_2N, -CH_2N^+), 39.6 (-OCH_2*C*H), 33.1, 32.34, 32.31, 32.01/ 31.99, 30.9, 30.2, 27.9, 24.2 (bulk -CH_2), 23.8 (ω-1), 14.6 (ω). HRESIMS: Calcd. for M^+ $[C_{30}H_{53}N_2O_8]^+$ 569.3802 (100 %), 570.3836 (32 %), 571.3870 (5 %); found 569.3791 (100 %), 570.3831 (46 %), 571.3862 (8%).

Methyl 6-deoxy-6-chloro-2,3,4-tri-*O*-acetyl-∝-D-glucopyranoside (51) (Jiang *et al.*, 2000)

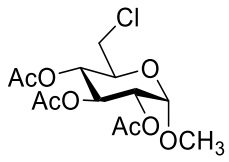

NCS (7.9 g, 59 mmol) was added into a mixture of methyl-∝-D-glucopyranoside (5.7 g, 29 mmol) and PPh_3 (15 g, 57 mmol) in DMF (70 mL) at 0 °C, following the procedure **3.6.6**. Because the crude material is highly water soluble, extraction with $NaHCO_3$ (aq) was avoided and the crude product was directly subjected to an acetylation reaction in pyridine (30 mL) and Ac_2O (28 mL) according to the procedure **3.6.7**. Compound **51** (6.4 g, 66 % over 2 steps) was isolated as a white solid by column chromatography (EtOAc: hexane= 1:4). ^{1}H NMR (400 MHz, $CDCl_3$): δ5.51-5.46 (1H, dd~t, H-3), 5.04-4.98 (2H, m, H-4, H-1), 4.91-4.88 (1H, dd, H-2), 4.05-4.00 (1H, m, H-5), 3.65-3.61 (1H, dd, H-6a), 3.58-3.54 (1H, dd, H-6b), 3.45 (3H, s, CH_3), 2.08, 2.06, 2.01 (9H, 3s, Ac); $^3J_{1,2}$=4.0, $^3J_{2,3}$=10.0, $^3J_{3,4}$=10.0, $^3J_{5,6a}$=3.0, $^3J_{5,6b}$=7.0, $^2J_{6a,6b}$=12.0 Hz; ^{13}C NMR (100 MHz, $CDCl_3$): δ 170.09, 170.06, 169.6 (C=O), 96.6 (C-1), 70.7 (C-2), 70.1 (C-4), 70.0 (C-3), 68.8 (C-5), 55.5 (CH_3), 43.4 (C-6), 20.69, 20.65(2) (Ac).

6-Deoxyl-6-azido-1,2,3,4-tetra-*O*-acetyl-∝-D-glucopyranose (53) (Elchert *et al.*, 2004; Combemale *et al.*, 2014)

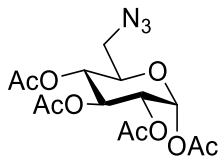

A mixture of compound **51** (6.2 g, 18 mmol) and NaN_3 (1.6 g, 25 mmol) in DMF (60 mL) was treated according to general procedure **3.6.2** to furnish crude compound **52** as a light yellow solid. Crude compound **52** in Ac_2O (60 mL) was added dropwise into an acidic mixture (75 mL) containing Ac_2O, AcOH and H_2SO_4 in ratio of 5:4:1 at 0 °C. The reaction mixture was then warmed to room temperature and continued with stirring for another 4 hours before diluted with EtOAc (30 mL). The mixture was slowly poured into iced water (100 mL), followed by washing the organic layer with saturated $NaHCO_3$ (aq) and H_2O successively. The organic layer was isolated, dried over $MgSO_4$ and concentrated. Compound **53** (3.2 g, 48 % over 2 steps) was successfully crystallized as a white solid from EtOH. $[\propto]_D^{25}$ = +144 (c 0.10, $CHCl_3$); ^{1}H NMR (400 MHz, $CDCl_3$): δ 6.37-6.36 (1H, d, H-1), 5.50-5.45 (1H, dd~t, H-3), 5.13-5.08 (2H, m, H-4, H-2), 4.11-4.06 (1H, m, H-5), 3.43-3.39 (1H, dd, H-6a), 3.33-3.29 (1H, dd, H-6b), 2.20, 2.06, 2.04, 2.03 (12H, 4 s, 4 Ac); $^3J_{1,2}$=4.0, $^3J_{2,,3}$=10.0, $^3J_{3,4}$=10.0, $^3J_{4,5}$=10.0, $^3J_{5,6a}$=3.0, $^3J_{5,6b}$=6.0, $^2J_{6a,6b}$=14.0 Hz; ^{13}C NMR (100 MHz, $CDCl_3$): δ 170.2, 169.6, 169.4, 168.8 (C=O), 88.9 (C-1), 70.9 (C-5), 69.7 (C-3), 69.2, 69.1 (C-2, C-4), 50.8 (C-6), 20.8, 20.63, 20.57, 20.4 (Ac).

2-Chloro-ethyl 6-deoxy-6-azido-2,3,4-tri-*O*-acetyl-∝,β-D-glucopyranoside (56)

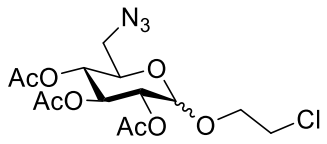

Compound **53** (1.74 g, 4.66 mmol) was subjected to a deacetylation reaction in CH_3OH (30 mL) according to general procedure **3.6.5** to furnish compound **54** (940 mg, 98 %) as a light yellow syrup, which was then used for subsequent reaction without prior purification. A mixture of compound **54** (940 mg, 4.58 mmol), 2-chloroethanol (10 mL) and Amberlite IR120-H^+ form (1.0 g) was heated to 80 °C for 5 hours. The solid was filtered off and the solvent was evaporated. The resulting residue was dried over P_2O_5 overnight to provide crude compound **55** as a brown syrup. The compound was dissolved in pyridine (20 mL) and treated with Ac_2O (7 mL) according to general procedure **3.6.7**. Anomeric mixture of compound **56** (∝: β= 3: 2, 1.10 g, 61 % over 2 steps) was obtained as a light yellow syrup by column chromatography (EtOAc: hexane= 1:4). IR [neat] ν/cm^{-1} 2933 (CH), 2102 (N_3), 1746 (C=O). $[\alpha]_D^{25}$ = +85 (c 0.06, $CHCl_3$). ^{1}H NMR (400 MHz, $CDCl_3$): δ 5.51-5.46 (1H, dd~t, H-3∝), 5.24-5.20 (<1H, dd~t, H-3β), 5.18-5.17 (1H, d, H-1∝), 5.04-4.95 (<2H, m, H-4∝, H-4β), 4.86-4.82 (1H, dd, H-2∝), 4.62-4.60 (<1H, d, H-1β), 4.12-4.08 (<2H, m, -OCH_2aβ, H-5∝), 4.01-3.95 (1H, m, OCH_2a∝), 3.82-3.76 (<2H, m, -OCH_2b∝, -OCH_2bβ), 3.70-3.67 (<3H, m, -CH_2Cl∝, H-5β), 3.64-3.61 (<2H, m, -CH_2Clβ), 3.43-3.38 (<1H, dd, H-6aβ), 3.33-3.31 (2H, m, H-6∝), 3.23-3.19 (<1H, dd, H-6bβ), 2.07, 2.04, 2.02 (9H, 3 s, Ac∝), 2.06, 2.03, 2.01 (<9H, 3 s, Acβ); ∝-anomer:$^3J_{1,2}$= 4.0, $^3J_{2,3}$= 10.0, $^3J_{3,4}$= 10.0 Hz; β-anomer: $^3J_{1,2}$= 8.0, $^3J_{2,,3}$= 10.0, $^3J_{3,4}$= 10.0, $^3J_{5,6a}$= 7.0, $^3J_{5,6b}$= 3.0, $^2J_{6a,6b}$= 14.0 Hz; ^{13}C NMR (100 MHz, $CDCl_3$): δ 170.2, 170.1, 170.0, 169.6, 169.4, 169.3 (C=O), 100.8 (C-1β), 95.7 (C-1∝), 73.6 (C-5β), 72.2 (C-3β), 70.9 (C-4 β), 70.6 (C-2∝), 69.8 (OCH_2β), 69.7 (C-3∝), 69.6 (C-3β), 68.9 (C-5∝), 68.8 (OCH_2β), 51.0 (C-6β), 50.9 (C-6∝), 42.5 (CH_2Cl∝), 42.5 (CH_2Clβ), 20.6, 20.53, 20.47 (Ac).

2-Chloro-ethyl 6-deoxy-6-hexadecanamido-∝-D-glucopyranoside (57)

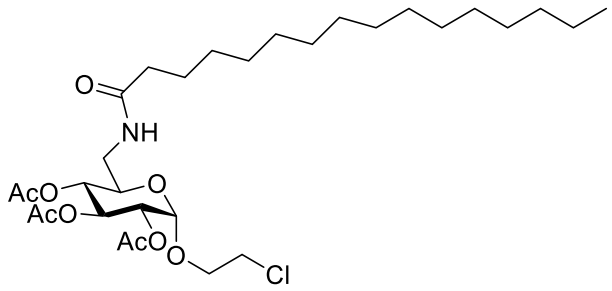

A solution of palmitoyl chloride (1.2 mL, 4.0 mmol) in CH_2Cl_2 (10 mL) was added dropwise into a mixture containing compound **56** (0.80 g, 2.0 mmol) and PPh_3 (0.80 g, 3.1 mmol) in CH_2Cl_2 (10 mL) at 0 °C. The reaction mixture was warmed to room temperature with stirring for overnight. The organic layer was washed with saturated $NaHCO_3$ (aq) and water successively, followed by drying the organic layer over $MgSO_4$. After evaporation of the solvent, the crude was subjected to column chromatography (EtOAc: hexane= 1:1) to obtain compound **57** (0.50 g, 41 % based on an anomeric mixture starting material) as a yellow syrup. $[\propto]_D^{25}$ = +87 (c 0.02, $CHCl_3$). ^{1}H NMR (400 MHz, $CDCl_3$): δ 5.82 (1H, bs, NH), 5.50-5.45 (1H, dd~t, H-3), 5.11 (1H, d, H-1), 4.88-4.83 (1H, dd~t, H-4), 4.80-4.77 (1H, dd, H-2), 4.02-3.98 (1H, m, H-5), 3.92-3.87 (1H, m, -OCH_2a), 3.77-3.71 (1H, m, -OCH_2b), 3.66-3.63 (2H, t, -CH_2Cl), 3.60-3.55 (1H, m, H-6a), 3.37-3.30 (1H, m, H-6b), 2.21-2.13 (2H, m, ∝CH_2), 2.06, 2.05, 2.00 (9H, 3 s, Ac), 1.62-1.59 (2H, m, βCH_2), 1.29-1.24 (26H, m, bulk -CH_2), 0.88-0.85 (3H, t, -CH_3); $^3J_{1,2}$=3.5, $^3J_{2,3}$=10.0, $^3J_{3,4}$=10.0, $^3J_{4,5}$=10.0, $^3J_{5,6a}$=2.5, $^3J_{5,6b}$=6.0, $^2J_{6a,6b}$=12.0, $^3J_{6a,NH}$=6.0, $^3J_{6a,NH}$=6.0, $^3J_{OCH_2,CH_2Cl}$=6.0, $^2J_{OCH_2}$=11.0 Hz; ^{13}C NMR (100 MHz, $CDCl_3$): δ 173.3 (CONH), 170.4, 170.04, 170.00 (C=O), 96.0 (C-1), 70.9 (C-2), 69.8 (C-3), 69.3 (C-4), 68.9 (OCH_2), 68.3 (C-5), 42.5 (CH_2Cl), 38.8 (C-6), 36.7 (∝CH_2), 31.9, 29.7, 29.64/ 29.62, 29.5, 29.34/ 29.31(bulk-CH_2), 25.6 (βCH_2), 22.7 (ω-1), 20.7 (3) (Ac), 14.1 (ω).

2-Iodo-ethyl 6-deoxy-6-hexadecanamido-∝-D-glucopyranoside (58)

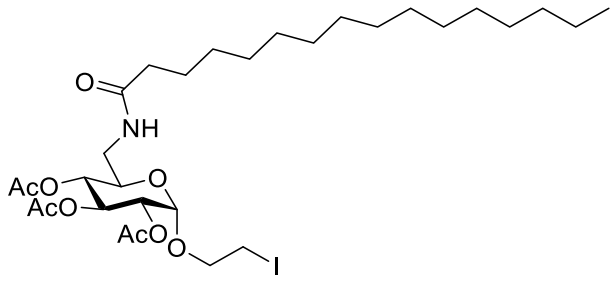

An iodide exchange reaction was done on compound **57** (0.38 g, 0.63 mmol) in acetone (30 mL) using NaI (0.20 g, 1.3 mmol), under reflux condition for 30 hours. The solid was filtered off and excess of acetone was removed under reduced pressure. The residue was taken up in CH_2Cl_2 and water, the organic layer was dried over $MgSO_4$, and concentrated to furnish compound **58** (0.37 g, 84 %) as a yellow syrup. $[\propto]_D^{25}$ = +72 (c 0.09, $CHCl_3$); ^{1}H NMR (400 MHz, $CDCl_3$): δ 5.84-5.81 (1H, dd~t, NH), 5.50-5.45 (1H, dd~t, H-3), 5.11-5.10 (1H, d, H-1), 4.88-4.83 (1H, dd~t, H-4), 4.81-4.77 (1H, dd, H-2), 4.03-3.99 (1H, ddd, H-5), 3.94-3.88 (1H, dt, -OCH_2a), 3.78-3.70 (1H, dt, -OCH_2b), 3.62-3.56 (1H, m, H-6a), 3.36-3.31 (1H, m, H-6b), 3.28-3.25 (2H, t, CH_2I), 2.21-2.17 (2H, m, ∝CH_2), 2.08, 2.06, 2.01 (9H, 3 s, 3 Ac), 1.63-1.60 (2H, m, βCH_2), 1.29-1.25 (26H, m, bulk –CH_2), 0.89-0.86 (3H, t, CH_3); $^3J_{1,2}$=4.0, $^3J_{2,3}$ =10.0, $^3J_{3,4}$=10.0, $^3J_{4,5}$=10.0, $^3J_{5,6a}$=2.5, $^3J_{5,6b}$=6.0, $^3J_{6a,NH}$=6.0, $^3J_{6b,NH}$=6.0, $^2J_{6a,6b}$=12.0, $^3J_{OCH_2,CH_2Cl}$=7.0, $^2J_{OCH_2}$=11.5 Hz; ^{13}C NMR (100 MHz, $CDCl_3$): δ 173.3 (CONH), 170.3, 170.01, 169.95 (C=O), 95.6 (C-1), 70.9 (C-2), 69.7 (C-3), 69.3 (C-4), 69.2 (OCH_2), 68.4 (C-5), 38.8 (C-6), 36.7 (∝CH_2), 31.9, 29.64/ 29.61, 29.5, 29.31, 29.29, (bulk -CH_2), 25.6 (βCH_2), 22.6 (ω-1), 20.7, 20.6 (Ac), 14.1 (ω), 1.6 (CH_2I).

1-[2-(6-Deoxy-6-hexadecanamido-2,3,4-tri-*O*-acetyl-∝-D-glucopyranosyloxy)-ethyl]-3-(8-azido-3,6-dioxa octyl)-imidazolium iodide (59)

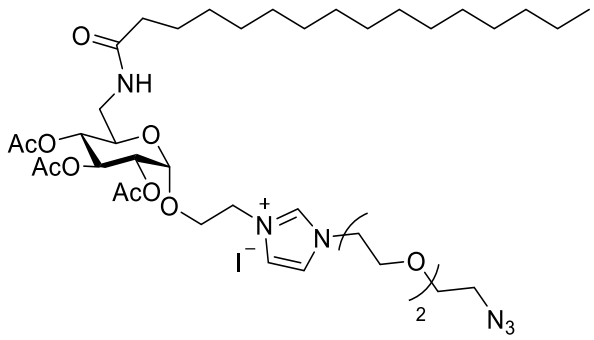

A solution containing compound **58** (80 mg, 0.11 mmol) and **3b** (26 mg, 0.11 mmol) in toluene (3 mL) was treated according to procedure **3.6.15** and it furnished compound **59** (0.10 g, 91 %) appeared as a yellow syrup. $[\propto]_D^{25}$ = +36 (c 0.12, $CHCl_3$). ^{1}H NMR (400 MHz, $CDCl_3$): δ 9.76 (1H, s, C*H*=N-CH), 7.58 (1H, s, CH=N-C*H*), 7.55 (1H, s, CH=C*H*-N), 6.47-6.44 (1H, dd~t, NH), 5.38-5.33 (1H, dd~t, H-3), 5.08-5.07 (1H, d, H-1), 4.88-4.85 (1H, dd, H-2), 4.84-4.79 (1H, dd~t, H-4), 4.72-4.64 (2H, m, CH_2N^+), 4.54-4.52 (2H, t, CH_2N), 4.22-4.17 (1H, m, -OC*H*$_2$a-CH_2N^+), 3.95-3.93 (3H, m, NCH_2CH_2, -OC*H*$_2$b-CH_2N^+), 3.79-3.74 (1H, m, H-5), 3.71-3.64 (6H, m, $OCH_2CH_2OCH_2CH_2N_3$), 3.52-3.46 (1H, m, H-6a), 3.42-3.38 (2H, m, CH_2N_3), 3.35-3.29 (1H, m, H-6b), 2.25-2.22 (2H, t, ∝CH_2), 2.05, 2.04, 1.99 (9H, 3s, Ac), 1.60-1.55 (26H, m, βCH_2), 1.28-1.23 (24H, m, bulk -CH_2), 0.88-0.84 (3H, t, -CH_3); $^3J_{1,2}$=4.0, $^3J_{2,3}$=10.0, $^3J_{3,4}$=10.0, $^3J_{4,5}$=10.0, $^3J_{5,6a}$=3.0, $^3J_{5,6b}$=7.0, $^2J_{6a,6b}$=14.0, $^3J_{NH,6a}$=6.5, $^3J_{NH,6b}$=6.5 Hz; ^{1}C NMR (100 MHz, $CDCl_3$): δ 173.9 (NHCO), 170.3, 169.8, 169.7 (C=O), 137.1 (*C*H=N-CH), 122.8 (CH=N-*C*H), 99.9 (CH=*C*H-N), 95.7 (C-1), 70.9 (C-2), 70.44 (C-3), 70.40, 70.3, 70.0 ($OCH_2CH_2OCH_2CH_2N_3$), 69.6 (C-4), 68.7 ($OCH_2CH_2N^+$), 68.6 (C-5), 50.7 (CH_2N_3), 50.2 (NCH_2CH_2O), 49.7 (CH_2N^+), 39.2 (C-6), 36.7 (∝CH_2), 31.9, 29.7, 29.6, 29.5, 29.4, 29.3 (bulk -CH_2), 25.8 (βCH_2), 22.7 (ω-1), 20.9, 20.69, 20.66 (Ac), 14.1 (ω).

1-[2-(6-Deoxy-6-hexadecanamido-∝-D-glucopyranosyloxy)-ethyl]-3-(8-azido-3,6-dioxa octyl)-imidazolium iodide (60)

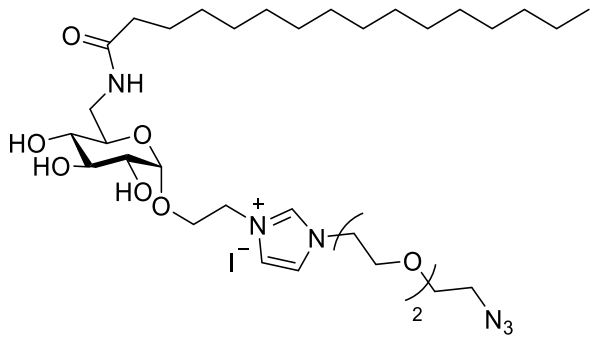

A deactylation was performed on compound **59** (0.25 g, 0.27 mmol) in CH_3OH (10 mL) according to procedure **3.6.5** and successfully produced compound **60** (0.19 g, 89 %) as a yellow syrup. IR [neat] ν/cm^{-1} 3376 (OH), 2923, 2853 (CH), 2106 (N_3), 1639 (C=O). $[\propto]_D^{25}$ = +14 (c 0.03, CH_3OH); ^{1}H NMR (400 MHz, CD_3OD): δ 9.11 (1H, s, C*H*=N-CH), 8.44 (1H, bs, NH), 7.75 (1H, s, CH=N-C*H*), 7.70 (1H, s, CH=C*H*-N), 4.84 (1H, H-1), 4.53-4.45 (4H, m, CH_2N, CH_2N^+), 4.09-4.04 (1H, m, -OC*H*$_2$a-CH_2N^+), 3.94-3.91 (2H, t, -C*H*$_2CH_2N$), 3.84-3.81 (1H, m, -OC*H*$_2$b-CH_2N^+), 3.73-3.66 (6H, m, OC*H*$_2$C*H*$_2$OC*H*$_2CH_2N_3$), 3.63-3.56 (1H, m, H-3), 3.54-3.50 (1H, dd, H-6a), 3.48-3.38 (4H, m, H-6b, CH_2N_3, H-2), 3.30 (1H, H-5), 3.16-3.11 (1H, dd~t, H4), 2.28-2.24 (2H, t, ∝CH_2), 1.65-1.62 (2H, t, βCH_2), 1.32 (26H, m, bulk CH_2), 0.94-0.91 (3H, t, CH_3); $^3J_{3,4}$= 9.5, $^3J_{4,5}$= 9.5, $^3J_{5,6a}$= 3.0, $^3J_{5,6b}$= 4.0, $^2J_{6a,6b}$= 14.0 Hz; ^{13}C NMR (100 MHz, CD_3OD): δ 177.1 (C=O), 138.6 (N=CH-N), 124.4 (N-*C*H=CH), 124.1 (N-CH=*C*H), 100.4 (C-1), 74.6 (C-3), 73.4 (C-2), 73.0 (C-4), 72.4 (C-5), 71.6, 71.2 (O*C*H$_2$*C*H$_2$O*C*H$_2CH_2N_3$), 70.0 (*C*H$_2CH_2N$), 66.9 (O*C*H$_2CH_2N^+$), 52.0 (CH_2N_3), 51.1 (CH_2N), 50.7 (CH_2N^+), 41.5 (C-6), 37.2 (∝CH_2), 33.2, 30.9, 30.8, 30.61/ 30.55 (bulk CH_2), 27.3 (βCH_2), 23.9 (ω-1), 14.6 (ω). HRESIMS: Calcd. for M^+ $[C_{33}H_{61}N_6O_8]^+$ 669.4551(100 %), 670.4585 (36 %), 671.4618 (6 %); found 669.4554 (100 %), 670.4579 (41 %), 671.4605 (7 %).

2-Deoxy-2-[[(4-methoxyphenyl)methylene]amino]-1,3,4,6-tetra-*O*-acetyl-β-D-glucopyranose (64) (Biswas *et al.*, 2017)

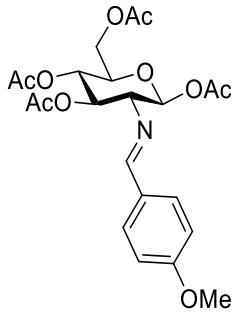

D(+)-glucosamine hydrochloride (3.2 g, 15 mmol) was dissolved in 1 M NaOH (15 mL), followed by dropwise addition of *p*-anisaldehyde (2.0 mL, 17 mmol) at 0 °C. The mixture was stirred at 0 °C for another 1 hour and warmed to room temperature with continued stirring overnight. White precipitate was collected by suction filtration and washed successively with cold H_2O, cold EtOH and Et_2O. Crude compound **63** (3.7 g, 80 %) was obtained as a white solid after being dried under vacuum overnight and used for subsequent reaction without prior purification. A suspension of compound **63** (3.6 g, 12 mmol) in pyridine (20 mL) was stirred at 0 °C for 5 minutes, followed by addition of Ac_2O (6.0 mL, 63 mmol). The mixture was stirred overnight at room temperature. White precipitate was formed after addition of cold H_2O (80 mL). The solid was collected by suction filtration and washed with cold H_2O, furnishing crude compound **64** (4.5 g, 81 %) as a white solid after being dried under vacuum.

2-Deoxy-2-amino-1,3,4,6-tetra-*O*-acetyl-β-D-glucopyranose (66) (Biswas *et al.*, 2017)

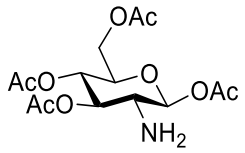

Crude imine **64** (4.5 g, 9.7 mmol) was dissolved in acetone (40 mL), followed by addition of 5 M HCl (2.5 mL). The mixture was stirred for 10 minutes and another one hour after addition of Et_2O (25 mL). The precipitate was collected and washed with cold Et_2O. Crude compound **65** (3.6 g, 97 %) was obtained as a white solid after being dried under vacuum overnight. In a suspension of acetylated glucosamine hydrochloride **65** (3.6 g, 9.4 mmol) in CH_2Cl_2 (60 mL), 1M Na_2CO_3 (aq) (30 mL) was added and the reaction was stirred at room temperature for 30 minutes. The organic layer was separated and the aqueous layer was extracted with CH_2Cl_2 (3 x 20 mL). The combined organic layer was dried over $MgSO_4$ and concentrated to furnish compound **66** (3.0 g, 91 %) as a white solid.

2-Deoxy-2-hexadecanamido-1,3,4,6-tetra-*O*-acetyl-β-D-glucopyranose (67)

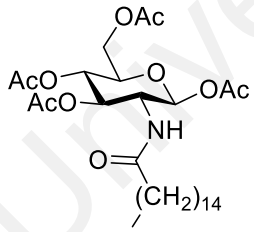

Procedure I (Boullanger *et al.*, 1987): A mixture containing D-(+)-glucosamine hydrochloride (2.0 g, 9.3 mmol), $NaOCH_3$ (0.50 g, 9.3 mmol) in CH_3OH (10 mL) was stirred for 10 minutes at room temperature. The mixture was filtered and the filtrate was treated with Et_3N (1.3 mL, 9.4 mmol) and $ClCOOC_{15}H_{31}$ (3.1 mL, 10 mmol) at 0 °C. The reaction was warmed to room temperature and stirred overnight. The solvent was evaporated under reduced pressure to produce a white solid product. The solid was then

dissolved in pyridine (20 mL), followed by slow addition of Ac_2O (10 mL) according to general procedure **3.6.7** to furnish amide **67** (0.30 g, 5.5 % over 3 steps) was obtained as a white solid by crystallization from Et_2O.

Procedure II: Crude material **66** (3.0 g, 8.6 mmol) was dissolved in CH_2Cl_2 (30 mL) and Et_3N (1.3 mL, 9.4 mmol) was added, followed by addition of $ClCOOC_{15}H_{31}$ (3.1 mL, 10 mmol) dropwise. The mixture was stirred overnight at room temperature. The organic layer was washed successively with 2 N HCl (aq) and saturated NaCl (aq), dried over $MgSO_4$ then concentrated. Amide **67** (3.3 g, 65 %) was obtained as a white solid by crystallization from EtOH. $[\propto]_D^{25}$ = +63 (c 0.02, $CHCl_3$); ^{1}H NMR (400 MHz, $CDCl_3$): δ 5.70-5.68 (1H, d, H-1), 5.53-5.50 (1H, d, NH), 5.17-5.11 (2H, m, H-3, H-4), 4.36-4.41 (1H, m, H-2), 4.30-4.25 (1H, dd, H-6a), 4.15-4.12 (1H, dd, H-6b), 3.82-3.79 (1H, m, H-5), 2.12-2.09 (8H, m, $\propto CH_2$, Ac), 2.05-2.04 (6H, 2 s, Ac), 1.58-1.53 (1H, m, βCH_2), 1.25 (26H, m, bulk -CH_2), 0.90-0.87 (3H, t, -CH_3); $^3J_{1,2}$= 9.0, $^3J_{2,3}$=9.5, $^3J_{3,4}$=9.5, $^3J_{4,5}$=9.5, $^3J_{5,6a}$=5.0, $^3J_{5,6b}$=2.0, $^3J_{2,NH}$=9.5 $^2J_{6a,6b}$=12.5 Hz; ^{13}C NMR (100 MHz, $CDCl_3$): δ 173.1, 171.1, 170.7, 169.5, 169.2 (C=O), 92.7 (C-1), 73.0 (C-5), 72.5 (C-4/ C-3), 67.7 (C-4/ C-3), 61.6 (C-6), 52.8 (C-2), 36.8 ($\propto CH_2$), 31.9, 29.7, 29.63, 29.60, 29.5, 29.33/ 29.29, 29.1 (bulk -CH_2), 25.6 (βCH_2), 22.7 (ω-1), 20.9, 20.7, 20.62, 20.56 (Ac), 14.1 (ω).

2-Hexadecyl-(3,4,6-tri-*O*-acetyl-1,2-dideoxy-∝-D-glucopyranoso)-[1,2-*d*]-2-oxazoline (71)

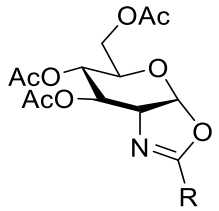

HBr/ AcOH (33 %, 5 mL) was added to a solution containing compound **67** (1.0 g, 1.7 mmol) in AcOH (26 mL) at room temperature. After stirring for 3 hours at room temperature, the mixture was diluted with iced water (200 mL) and extracted with CH_2Cl_2. The combined organic layers were washed successively with saturated $NaHCO_3$ (aq) and saturated NaCl (aq). The organic layer was dried over $MgSO_4$ and concentrated to about 15 mL under vacuum below 30 °C. The reaction mixture was reacted with 2-chloroethanol (0.30 mL, 4.5 mmol), in the presence of 10 % Na_2CO_3 (aq) (13 mL) and TBAB (0.50 g, 1.5 mmol). The reaction was stirred at room temperature and was complete after 2 hours as indicated by TLC. The organic layer was separated and the aqueous phase was extracted with CH_2Cl_2. The combined organic layers were washed with saturated NaCl (aq) and dried over $MgSO_4$ and the solvent was evaporated. The resulting residue was subjected to column chromatography (EtOAc: hexane= 1:3) to furnish compound **71** (0.40 g, 45 % over 2 steps) as a yellow syrup. $[\propto]_D^{25}$ = +22 (c 0.09, $CHCl_3$); ^{1}H NMR (400 MHz, $CDCl_3$): δ 5.34-5.28 (2H, m, H-4, H-1), 5.17-5.12 (1H, dd~t, H-2), 4.35-4.29 (1H, m, H-5), 4.24-4.19 (2H, m, H-3, H-6a), 4.16-4.12 (1H, m, H-6b), 2.19-2.14 (2H, m, $\propto CH_2$), 2.11, 2.05, 2.02 (9H, 3 s, Ac), 1.57 (2H, m, βCH_2), 1.25 (26H, m, bulk CH_2), 0.90-0.87 (3H, t, -CH_3); $^3J_{2,3}$=10.0 $^3J_{3,4}$=10.0, $^3J_{4,5}$=10.0, $^3J_{5,6a}$=7.0, $^3J_{5,6a}$=3.5, $^2J_{6a,6b}$=13.0 Hz; ^{13}C NMR (100 MHz, $CDCl_3$): 173.4, 171.4, 170.9 (C=O), 169.4 (OCN), 91.7 (C-1), 70.8 (C-4), 68.2 (C-2), 67.7 (C-3), 62.1 (C-6), 52.1 (C-5), 36.7 ($\propto CH_2$), 31.9, 29.7, 29.63/ 29.60, 29.33, 29.30, 29.2 (bulk -CH_2), 25.6 (βCH_2), 22.7 (ω-1), 20.8, 20.7, 20.6 (Ac), 14.1 (ω).

1, 2-Bis(2-azidoethoxyl)ethane (Gansow *et al.*, 1981)

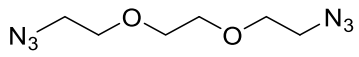

1, 2-Bis(2-chloroethoxy)ethane (3.0 mL, 19 mmol) was dissolved in DMF (50 mL), followed by addition of NaN_3 (3.7 g, 57 mmol). The mixture was heated to 80 °C overnight according to general procedure **3.6.2** to furnish 1,2-bis(2-azidoethoxy)ethane as a colourless liquid (3.7 g, 95 %). ^{1}H NMR (400 MHz, $CDCl_3$): δ 3.68-3.65 (8H, m, 4 -OCH_2), 3.38-3.36 (4H, t, 2x CH_2N_3). ^{13}C NMR (100MHz, $CDCl_3$): δ 70.8 (-OCH_2), 70.22 (-*C*$H_2CH_2N_3$), 50.8 (CH_2N_3).

[Ethane-1,2-diylbis(oxyethane-2,1-diyl-1*H*-1,2,3-triazole-1,4-diyl)]dimethanol

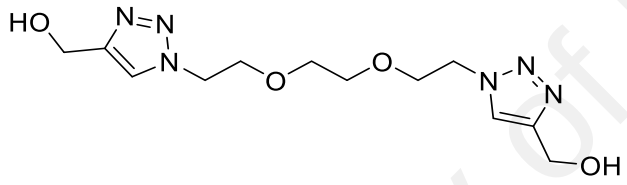

Both 1,2-bis(2-azidoethoxy)ethane (0.50 g, 2.5 mmol) and propargyl alcohol (0.36 mL, 6.2 mmol) was dissolved in CH_3OH (20 mL). Sodium ascorbate (0.22 g, 1.1 mmol) and $Cu(OAc)_2$ (0.07 g, 0.4 mmol) were added under ice bath. The mixture was stirred under an ice bath for 30 minutes and warmed to room temperature with continuous stirring overnight. Methanol was removed under reduced pressure and the residue was distributed between butanol and water. The organic layer was dried over $MgSO_4$ and concentrated under reduced pressure to furnish crude triazole compound as a yellow liquid (0.58 g, 74 %). ^{1}H NMR (400 MHz, CD_3OD): δ 7.93 (2H, s, triazole-CH), 4.68 (4H, s, -CH_2OH), 4.56-4.53 (4H, t, -CH_2N), 3.84-3.82 (4H, t, -C*H*$_2CH_2N$), 3.56 (4H, m, -OCH_2CH_2O-); ^{13}C NMR (100 MHz, CD_3OD): δ 149.1 (triazole –C), 124.9 (triazole –CH), 71.4 (-OCH_2CH_2O-), 70.5 (-*C*H_2CH_2N), 56.6 (-CH_2OH), 51.5 –CH_2N).

HRESIMS: Calcd. for $[M+Na]^+$ $[C_{12}H_{20}N_6O_4Na]^+$ 335.1444 (100 %), 336.1478 (13 %); found 335.1431 (100 %), 336.1457 (14 %).

(1-(2-Butyl-octyl 6-deoxy-6-(3-(11-azido-3,6,9-trioxa-undecyl)-imidazolium)-β-D-glucopyranosyl)-1,2,3-triazol-4-yl)methanol

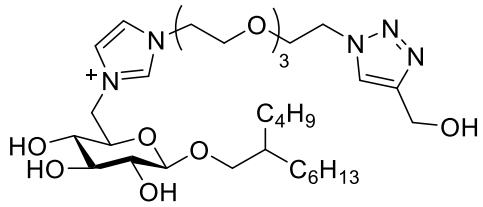

Into a micellar dispersion of glycolipid **16c** (14 mg, 0.02 mmol) in H_2O (1 mL), propargyl alcohol (10 μL, 0.17 mmol), sodium ascorbate (2 mg, 0.01 mmol) and $CuSO_4 \cdot 5H_2O$ (1 mg, 4 μmol) were added. The mixture was stirred at room temperature overnight. Another 5 mL of H_2O was added and the aqueous layer was extracted with 1-butanol (3 x 5 mL). The combined alcohol layer was dried over $MgSO_4$ and concentrated under reduced pressure to give the crude triazole compound (33 mg) as a yellow syrup and its crude ^{1}H NMR spectrum was measured and analyzed. ^{1}H NMR (400 MHz, CD_3OD): δ 8.95 (1H, s, N=CH-N), 7.97 (1H, s, triazole-CH), 7.68 (1H, s, CH=N-C*H*), 7.56 (1H, s, CH=C*H*-N), 4.67 (3H, m, CH_2OH, H-6a), 4.60-4.57 (2H, t, $CH_2N_{triazole}$), 4.40 (3H, m, -NCH_2CH$_2$, H-6b), 4.26-4.24 (1H, d, H-1), 3.93-3.90 (3H, m, H-6a, -NCH$_2$CH_2), 3.66-3.53 (>12H, m, -(OCH_2CH_2)$_2$OCH_2CH$_2$N$_{triazole}$, -OCH_{2a}CH, H-5), 3.40-3.35 (2H, m, H-4, -OCH_{2b}CH), 3.15-3.11 (1H, t, H-2), 3.06-3.02 (1H, t, H-3), 1.55-1.48 (>1H, m, -OCH$_2$C*H*), 1.29 (15H, bs, bulk –CH$_2$), 0.95-0.91 (>6H, m, -CH$_3$). HRESIMS: Calcd. for $[M]^+$ $[C_{32}H_{58}N_5O_9]^+$ 656.4235 (100 %), 657.4269 (35 %); found 656.4231 (100 %), 657.4257 (32 %).

1-Methyl-3-(prop-2-ynyl)-imidazolium bromide (IMI) (Kuang *et al.*, 2012)

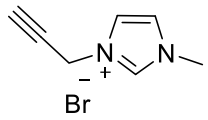

Both 1-methylimidazole (1.8 mL, 23 mmol) and propargyl bromide (80 % in toluene) (2.5 mL, 23 mmol) were dissolved in CH_2Cl_2 (10 mL) and stirred for 4 hours at room temperature. The mixture was washed with CH_2Cl_2, followed by evaporation of the solvent under reduced pressure. The residue was washed thrice with Et_2O and dried using rotary evaporator to furnish **IMI** (2.7 g, 58 %) as a brown liquid. ^{1}H NMR (400 MHz, DMSO-d_6): δ 9.33 (1H, s, N=CH-N), 7.82-7.79 (2H, m, NCHCHN), 5.26 (2H, s, CH_2), 3.89-3.83 (4H, m, CH_3, CCH). ^{13}C NMR (100 MHz, DMSO-d_6): δ 136.6 (NCHN), 124.0 (CH=*C*HN$^+$), 122.1 (*C*H=CHN$^+$), 79.0 (C*C*H), 76.1 (*C*CH), 38.6 (CH_2), 36.1 (CH_3).

2-(Prop-2-ynyloxy)-acetic acid (ACID) (Morimoto *et al.*, 2013)

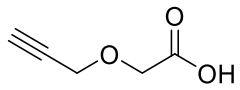

NaH (60 % suspension in paraffin oil) (1.4 g, 35 mmol) was dissolved in THF (40 mL) at 0℃, followed by addition of propargyl alcohol (1.0 mL, 17 mmol). The mixture was stirred for an hour, before tert-butyl bromoacetate (2.3 mL, 16 mmol) was added at 0℃. The mixture was warmed to room temperature and stirred overnight. The reaction mixture was quenched with H_2O (10 mL) and extracted with Et_2O. The organic layer was washed with H_2O, brine successively and dried over $MgSO_4$. The residue obtained after removal of the solvent under reduced pressure, was dissolved in CH_2Cl_2 (20 mL) and TFA (3 mL) was added slowly, followed by stirring for 5 hours at room temperature. The solvents were removed under reduced pressure. The resulting residue was subjected to column chromatography (CH_2Cl_2, 5 % AcOH) to furnish **ACID** (0.50 g, 28 %) as a yellow

liquid. ^{1}H NMR (400 MHz, CD_3OD): δ 4.29-4.27 (2H, m, C*H*$_2$COOH), 4.17-4.16 (2H, m, CH_2C), 2.92-2.90 (1H, m, C≡CH). ^{13}C NMR (100 MHz, CD_3OD): δ 173.7 (C=O), 76.88 (*C*≡CH), 76.87 (C≡*C*H), 66.9 (*C*H$_2$COOH), 59.0 (CH_2C).

Rhodamine-b prop-2-yn-1-yl ester chloride (R3)

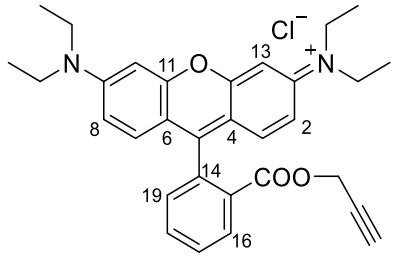

Rhodamine-b (1.0 g, 2.1 mmol) was dissolved in $CHCl_3$ (30 mL) and oxalyl chloride (0.40 mL, 4.7 mmol) was added slowly. The reaction was refluxed for 4 hours before being cooled to room temperature. The solvents were evaporated under reduced pressure to furnish crude **R2** as a red syrup. Into a solution of **R2** in CH_3CN (30 mL), the mixture of propargyl alcohol (0.40 mL, 6.8 mmol) and TEA (0.35 mL, 2.5 mmol) in CH_3CN (20 mL) was added dropwise. The reaction was refluxed overnight. The mixture was cooled to room temperature and the solvent was evaporated. The resulting residue was subjected to column chromatography over silica gel (EtOAc: CH_3OH= 2: 1) to furnish compound **R3** (0.52 g, 48 % over 2 steps) as a metallic dark green syrup. ^{1}H NMR (CD_3OD, 400 MHz): δ 8.35-8.33 (1H, d, H-16), 7.94-7.90 (1H, dd~t, H-18), 7.87-7.83 (1H, dd~t, H-17), 7.50-7.48 (1H, d, H-19), 7.15-7.13 (2H, d, H-3, H-7), 7.07-7.05 (2H, d, H-2, H-8), 7.01 (2H, s, H-10, H-13), 4.63 (2H, s, OCH_2), 3.73-3.68 (8H, q, NCH_2, N^+CH_2), 2.82 (1H, bs, C≡CH), 1.35-1.31 (12H, t, CH_3). $^{3}J_{2,3}$= $^{3}J_{7,8}$= 9.5, $^{3}J_{16,17}$= 8.0, $^{3}J_{17,18}$= 8.0, $^{3}J_{18,19}$= 8.0, $^{3}J_{NCH2,CH3}$= $^{3}J_{=NCH2,CH3}$= 7.0 Hz. ^{13}C NMR (CD_3OD, 100 MHz): δ 166.0 (C=O), 159.8 (C-10, C-13), 159.5 (C-5), 157.3 (C=N^+, C-N), 135.2 (C-14), 134.6 (C-18), 132.5 (C-16/ C-3, C-7), 132.4 (C-16/ C-3, C-7), 131.9 (C-19), 131.7 (C-17), 131.2

(C-15), 115.7 (C-2, C-8), 115.0 (C-4, C-6), 97.5 (C-10, C-13), 76.8 (C≡*C*H) 53.8 (OCH_2), 47.0 (*C*≡CH), 13.0 (CH_3).

1-*C*-(2,3,4,6-tetra-*O*-acetyl-β-D-glucopyranosyl)-propan-2-one (P2) (Riemann *et al.*, 2002)

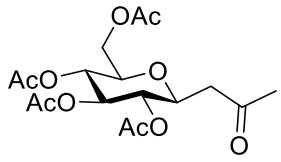

Anhydrous D-(+)-glucose (2.0 g, 11 mmol), $NaHCO_3$ (1.2 g, 14 mmol) and acetylacetone (1.4 mL, 14 mmol) were dissolved in H_2O (30 mL) and heated to 80 °C overnight. The mixture was concentrated under reduced pressure and the resulting crude was dissolved in pyridine (20 mL) and treated with Ac_2O (12 mL) at 0 °C according to general procedure **3.6.7**. The crude was subjected to column chromatography (EtOAc: hexane= 1:1) and furnished compound **P2** as a light yellow solid (3.3 g, 77% over 2 steps). ^{1}H NMR (400 MHz, $CDCl_3$): δ 5.23-5.18 (1H, dd~t, H-3), 5.07-5.02 (1H, dd~t, H-4), 4.92-4.87 (1H, dd~t, H-2), 4.26-4.22 (1H, dd, H-6a), 4.07-3.96 (2H, m, H-6b, H-1), 3.70-3.67 (1H, m, H-5), 2.77-2.71 (1H, dd, CH_2aCO), 2.50-2.46 (1H, d, CH_2bCO), 2.18 (Ac), 2.07 (Ac), 2.03 (6H, s, Ac, CH_3), 2.00 (Ac); $^3J_{1,2}$= 10.0, $^3J_{2,3}$= 10.0, $^3J_{3,4}$= 10.0, $^3J_{4,5}$= 10.0, $^3J_{5,6a}$= 3.0, $^2J_6$= 12.0 Hz; ^{13}C NMR (100 MHz, $CDCl_3$): δ 204.9 (CH_3*C*O), 170.6, 170.2, 169.9, 169.5 (C=O), 75.8 (C-5), 74.1 (C-3), 73.8 (C-1), 71.6 (C-2), 86.5 (C-4), 62.0 (C-6), 45.3 (*C*H_2CO), 31.0 (CH_3), 20.70, 20.65, 20.6 (2) (Ac).

1-*C*-(2,3,4,6-tetra-*O*-benzyl-β-D-glucopyranosyl)-propan-2-one (P6)(Norsikian *et al.*, 2007)

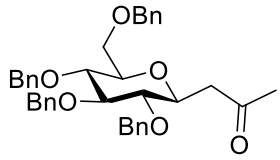

A solution of **P2** (3.1 g, 8.0 mmol) and ethylene glycol (0.90 mL, 16 mmol) in toluene (50 mL) was treated with catalytic amount of PPTS and refluxed with Dean Stark trap to collect H_2O. After 8 hours, toluene was removed under reduced pressure and the residue was diluted with CH_2Cl_2. The organic layer was washed with saturated $NaHCO_3$ (aq) and dried over $MgSO_4$ and concentrated to furnish crude **P3** as a light brown syrup, which was then subjected to deacetylation following general procedure **3.6.5** to provide crude **P4** as a brown syrup. A solution of crude **P4** in DMF (30 mL) was treated with NaH (60 % suspension in paraffin oil) (1.9 g, 48 mmol), followed by addition of BnBr (7.6 mL,64 mmol) according to general procedure **3.6.9** to furnish crude **P5** as a brown syrup. **P5** was treated with TFA (12 mL) and H_2O (1 mL). The reaction was stirred for 30 minutes and poured slowly into iced-cold saturated $NaHCO_3$ (aq) (50 mL). The aqueous layer was extracted with EtOAc (3 x 15 mL) and the combined organic layer was washed with brine, dried over $MgSO_4$ and concentrated. The resulting residue was subjected to column chromatography (EtOAc: hexane= 1: 8) to yield **P6** (2.3 g, 50 % over 4 steps) as a yellow liquid.

(*E*)-1-2(2,3,4,6-tetra-*O*-benzyl-β-D-glucopyranosyl)-4-(1-pyrene)-but-3-ene-2-one (P7) (Nagarajan & Mohan Das, 2009)

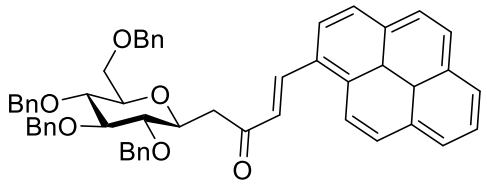

A solution containing **P6** (0.40 g, 0.69 mmol) and 1-pyrenecarboxaldehyde (0.20 g, 0.87 mmol) in CH_2Cl_2 (10 mL) was treated with pyrrolidene (0.02 mL, 0.24 mmol). The reaction was stirred at room temperature overnight. The organic layer was washed with H_2O, dried over $MgSO_4$ and concentrated. The resulting residue was subjected to column chromatography (EtOAc: hexane= 1: 8) to furnish **P7** (0.50 g, 91 %) as a yellow solid. ^{1}H NMR (400 MHz, $CDCl_3$): δ 8.68-8.64 (1H, d, OCCH=C*H*), 8.46-8.04 (9H, m, pyrene aromatic-H), 7.42-7.16 (20H, m, benzyl aromatic-H), 7.08-7.04 (1H, d, OCC*H*=CH), 5.00-4.46 (8H, m, 4 x CH_2Ph), 4.03-3.98 (1H, m, H-5), 3.84-3.72 (4H, m, H-2, H-3, CH_2CO), 3.56-3.47 (2H, m, H-4, H-1), 3.09-3.05 (1H, dd, H-6a), 3.00-2.95 (1H, dd, H-6b); $^3J_{trans}$: 16.0, $^3J_{1,2}$=9.0, $^3J_{2,3}$=9.0, $^3J_{3,4}$=9.0, $^3J_{4,5}$=9.0, $^3J_{5,6a}$=3.5, $^3J_{5,6b}$=8.0, $^2J_{6a,6b}$=15.0 Hz; ^{13}C NMR (100 MHz, $CDCl_3$): δ 197.6 (C=O), 139.3 (OCCH=*C*H), 138.5, 138.2, 138.1, 138.0, 132.8, 131.3, 130.7, 130.1 (aromatic –C), 129.0, 128.64, 128.60, 128.47, 128.45, 128.4 (aromatic –CH), 128.3 (aromatic –C), 128.24, 128.17, 127.87, 127.85, 127.8, 127.72, 127.66, 127.5, 127.3, 126.3, 126.0, 125.9, 125.1 (aromatic –CH), 124.9, 124.6 (aromatic –C), 124.2 (aromatic –CH), 122.5 (aromatic –CH), 87.3 (C-3), 81.2 (C-4), 79.1 (C-1), 78.4 (C-2), 75.9 (C-5), 75.6, 75.0 (2), 73.5 (CH_2Ph), 68.8 (CO*C*H_2), 43.6 (C-6).

(*E*)-1-2(2,3,4,6-tetra-*O*-benzyl-β-D-glucopyranosyl)-4-(1-pyrene)-but-3-ene-2-ol (P8)

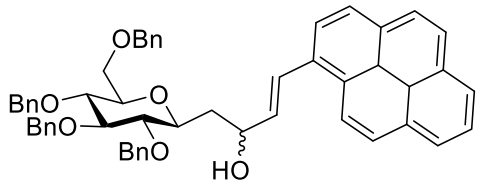

Procedure I: Sugar pyrene **P7** (50 mg, 0.06 mmol) was dissolved in THF (3 mL). $LiAlH_4$ (11 mg, 0.29 mmol) was added according to general procedure **3.6.13**. Compound **P8** (30 mg, 67 %) was obtained as a yellow solid by column chromatography (EtOAc: hexane= 1: 5).

Procedure II: Sugar pyrene **P7** (0.25 g, 0.32 mmol) was dissolved in a solvent mixture containing THF: CH_3OH= 1: 1 (5 mL). $NaBH_4$ (0.05 g, 1.3 mmol) was added slowly. After 4 hours, TLC indicated the reaction was complete. Acetone (3 mL) was added to quench the reaction. The solvents were evaporated and the resulting residue diluted with CH_2Cl_2 and washed with H_2O. The organic layer was dried over $MgSO_4$ and concentrated. Compound **P8** (0.20 g, 78 %) was obtained as a yellow solid by column chromatography (EtOAc: hexane= 1: 5). ^{1}H NMR (400 MHz, $CDCl_3$): δ 8.41-7.99 (9H, m, pyrene aromatic-H), 7.73-7.68 (1H, dd, HOCHCH=C*H*), 7.39-7.17 (20H, m, benzyl aromatic-H), 6.47-6.40 (1H, m, HOCHC*H*=CH), 4.96-4.53 (9H, m, 4x CH_2Ph, C**H*OH), 3.74-3.59 (6H, m, H-6a, H-3, H-6b, H-5 H-1, H-2), 3.41-3.36 (1H, dd~t, H-4), 2.28-2.18 (1H, m, C*H*$_2$a-CHOH), 1.87-1.79 (1H, m, C*H*$_2$b-CHOH); $^3J_{trans}$=15.5, $^3J_{3,4}$=10.0, $^3J_{4,5}$=10.0 Hz; ^{13}C NMR (100 MHz, $CDCl_3$): δ 138.44, 138.41, 138.0, 137.93, 137.89, 137.8 (aromatic-C), 135.58/135.19 (HOCH*C*H=CH), 131.8, 131.7, 131.5, 131.0, 130.7 (aromatic-C), 128.53, 128.47, 128.46, 128.4, 128.1, 127.99, 127.96, 127.90, 127.87, 127.8, 127.74, 127.73, 127.68, 127.44, 127.41, 127.14, 127.11, 126.8 (aromatic-CH), 126.6 (HOCHCH=*C*H), 125.9, 125.1, 125.1, 125.0, 124.92, 124.89, 124.0, 123.30,

123.26 (aromatic-CH), 87.1 (C-3), 82.2 (C-4), 79.8 (C-5), 78.74/78.69 (C-1), 78.59/78.55 (C-2), 75.67/75.62, 75.49/75.28, 75.09/75.00, 73.58/73.54 (4x CH_2Ph), 72.69/70.31 (CHOH), 69.22/69.19 (C-6).

(*E*)-1-2(2,3,4,6-tetra-*O*-benzyl-β-D-glucopyranosyl)-4-(1-pyrene)-but-3-ene-2-hexadodecane (P9)

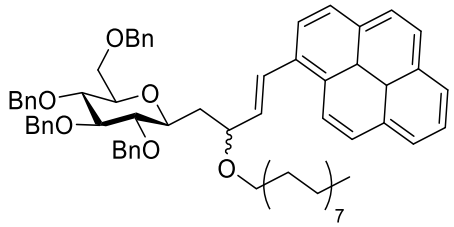

A solution of **P8** (0.12 g, 0.15 mmol) in DMF (10 mL) was treated with NaH (60 % suspension in paraffin oil) (10 mg, 0.25 mmol). After 30 minutes of stirring, 1-bromohexadecane (0.10 mL, 0.33 mmol) was added at 0 °C. The mixture was stirred at room temperature overnight. CH_3OH (3 mL) was added and the solvent was evaporated under reduced pressure. The residue was distributed between CH_2Cl_2 and H_2O, the organic layer was dried over $MgSO_4$ and concentrated. A yellow syrup of compound **P9** (0.10 g, 67 %) was isolated by column chromatography (EtOAc: hexane= 1: 13). ^{1}H NMR ($CDCl_3$, 400 MHz): δ 8.40-7.99 (9H, m, pyrene aromatic-CH), 7.62-7.58 (1H, d, CHOCH=C*H*), 7.42-7.15 (20H, m, benzyl aromatic-CH), 6.40-6.28 (1H, m, CHOC*H*=CH), 4.93-4.53 (8H, m, 4x CH_2Ph), 4.45-434 (1H, m, C*H*OH), 4.16-4.11 (<2H, q, impurity EtOAc), 3.82-3.60 (5H, m, ∝CH_2a, H-6a, H-6b, H-4, H-1), 3.53-3.34 (4H, m, ∝CH_2b, H-5, H-3, H-2), 2.30-2.21 (1H, m, CH_{2a}CHOH), 2.06 (<3H, s, impurity EtOAc), 1.69-1.59 (3H, m, CH_{2a}CHOH, βCH_2), 1.29-1.25 (26H, m, bulk –CH_2; $^3J_{trans}$=15.5 Hz; ^{13}C NMR (100 MHz, $CDCl_3$): δ 138.66/138.57, 138.32/138.23, 138.2 (aromatic-C), 134.88/133.77 (CHO*C*H=CH) 131.6, 131.5, 131.3, 130.93, 130.88, 130.8, 130.7 (aromatic-C), 129.7 (CHOCH=*C*H), 128.42, 128.40, 128.37, 128.34, 128.26 (aromatic-

CH), 128.1 (aromatic-C), 128.0, 127.9, 127.84, 127.81, 127.77, 127.75, 127.7, 127.64, 127.61, 127.59, 127.58, 127.55, 127.48, 127.45, 125.94, 125.91, 125.2, 125.0, 124.94, 124.93, 124.04, 124.01, 123.1, 123.0 (aromatic C-H), 87.40/87.25 (C-2/C-4), 82.7 (C-5/C-3/C-1), 78.97/78.86 (C-5/C-3/C-1), 78.74/78.66 (C-2/C-4), 78.4 (CH_2*C*HO-), 76.36/76.26 (C-5/C-3/C-1), 75.59/75.56, 75.31/75.17, 74.90/74.89, 73.43/73.41 (4x CH_2Ph), 69.30/ 68.97 (∝CH_2), 69.11/69.06 (C-6), 37.6 (*C*H_2CHO-), 31.9, 30.1 (bulk –CH_2), 30. (β CH_2), 29.69, 29.65, 29.6, 29.35, 26.36 (bulk –CH_2), 22.7 (ω-1), 14.2 (ω).

CLICK Reaction in Micellar Dispersion

Using alkyne terminated **TrypEster**: A micellar dispersion of glycolipid **14a** (18 mg, 0.03 mmol) in H_2O (2 mL) above the CAC was subjected to CLICK coupling according to general procedure **3.6.16**, with **TrypEster** (13 mg, 0.03 mmol), in the presence of Cu $(OAc)_2$ (1 mg) and sodium ascorbate (1.7 mg). The mixture was treated with Amberlite 120 (H^+) to remove the cations. The resin was filtered off and the mixture was subjected to freeze-drying to provide a crude brown syrup (30 mg).

Using propargyl alcohol: Into a micellar dispersion of glycolipid **16c** (14 mg, 0.02 mmol) in H_2O (1 mL) above the CAC, propargyl alcohol (10 µL, 0.17 mmol), sodium ascorbate (2 mg, 0.01 mmol) and $CuSO_4 \cdot 5H_2O$ (1 mg, 4 µmol) were added. The mixture was stirred at room temperature overnight. Another 5 mL of H_2O was added and the aqueous layer was extracted with 1-butanol (3 x 5 mL). The combined alcohol layer was dried over $MgSO_4$ and concentrated under reduced pressure to give a yellow syrup (33 mg).

CHAPTER 6: CONCLUSION AND FUTURE OUTLOOK

6.1 Conclusion

A series of glycolipids was successfully synthesized. Owing to the polyfunctionality of the sugar head group, several types of hydroxyl protecting groups were employed throughout the synthesis to achieve regio-selective functionalization. Quaternization of the N-alkylated imidazole gave rise to the cationic character of the resulting imidazolium compound, which precluded classic purification methods. Therefore, the use of any reactants in excess was avoided.

The lyotropic behaviour of the functionalized glycolipids indicated dominance of the hydrophilic domain and their CACs were in good agreement with the base glycolipids of similar chain length. Despite the different linker position, no significant difference was found in terms of their assembly behaviour. Therefore, the use of the C-6 functionalized glycolipid for vesicle preparation is most economic, as it required the lowest number of synthetic step.

Surfactant mixture containing both base glycolipids and functionalized glycolipids showed high affinity for the lyotropic lamellar phase, thereby suggesting suitability for vesicle preparation. Accordingly, uniformly small-sized and stable vesicles, as indicated by their relatively high zeta potential, were produced.

6.2 Future Outlook

In order to quantify the CLICK functionality on the vesicular surface, structural modification on a rhodamine-based probe can be done. This is required to improve the water solubility of the probe. Highly polar functional groups, such as carboxyl and hydroxyl groups, can be targeted. The synthesis of pyrene-bearing glycolipid can be continued, as it provides insight into the glycolipid distribution in vesicular assemblies

that later determines the distribution of the biological recognition sites after CLICK coupling with antigens or receptors.

REFERENCES

Abd-Elbary, A., El-laithy, H. M., & Tadros, M. I. (2008). Sucrose stearate-based proniosome-derived niosomes for the nebulisable delivery of cromolyn sodium. *International Journal of Pharmaceutics, 357*(1-2), 189-198.

Afonso, C. A. M., Santhakumar, V., Lough, A., & Batey, R. A. (2003). An expedient synthesis of cationic rhodamine fluorescent probes suitable for conjugation to amino acids and peptides. *Synthesis, 2003*(17), 2647-2654.

Agharkar, S., Lindenbaum, S., & Higuchi, T. (1976). Enhancement of solubility of drug salts by hydrophilic counterions: Properties of organic salts of an antimalarial drug. *Journal of Pharmaceutical Sciences, 65*(5), 747-749.

Ahmed, S. E., Martins, A. M., & Husseini, G. A. (2015). The use of ultrasound to release chemotherapeutic drugs from micelles and liposomes. *Journal of Drug Targeting, 23*(1), 16-42.

Akbarzadeh, A., Rezaei-Sadabady, R., Davaran, S., Joo, S. W., Zarghami, N., Hanifehpour, Y., . . . Nejati-Koshki, K. (2013). Liposome: Classification, preparation, and applications. *Nanoscale Research Letters, 8*(1), 102.

Akiyama, T., Ibata, C., & Fujihara, H. (2010). Water-soluble palladium and gold nanoparticles functionalized by a new phosphine with zwitterionic liquid based on imidazolium sulfonate linked ethylene glycol moiety. *Heterocycles, 80*(2), 925-931.

Al-Mohammed, N. N., Duali Hussen, R. S., Ali, T. H., Alias, Y., & Abdullah, Z. (2015). Tetrakis-imidazolium and benzimidazolium ionic liquids: A new class of biodegradable surfactants. *RSC Advances, 5*(28), 21865-21876.

Al-Mohammed, N. N., Duali Hussen, R. S., Alias, Y., & Abdullah, Z. (2015). Tris-imidazolium and benzimidazolium ionic liquids: A new class of biodegradable surfactants. *RSC Advances, 5*(4), 2869-2881.

Ali, T. H., Hussen, R. S. D., & Heidelberg, T. (2014). New Y-shaped surfactants from renewable resources. *Colloids and Surfaces B: Biointerfaces, 123*, 981-985.

Ali, T. H., Tajuddin, H. A. B., Hussen, R. S. D., & Heidelberg, T. (2015). Increased emulsion stability for reverse Y-shaped sugar-based surfactants. *Journal of Surfactants and Detergents, 18*(5), 881-886.

Allen, T. M. (1994). The use of glycolipids and hydrophilic polymers in avoiding rapid uptake of liposomes by the mononuclear phagocyte system. *Advanced Drug Delivery Reviews, 13*(3), 285-309.

Allen, T. M., & Cullis, P. R. (2004). Drug delivery systems: Entering the mainstream. *Science, 303*(5665), 1818.

Allen, T. M., & Cullis, P. R. (2013). Liposomal drug delivery systems: From concept to clinical applications. *Advanced Drug Delivery Reviews, 65*(1), 36-48.

Alvarez, R., Velazquez, S., San-Felix, A., Aquaro, S., Clercq, E. D., Perno, C.-F., . . . Camarasa, M. J. (1994). 1,2,3-Triazole-[2,5-bis-*O*-(tert-butyldimethylsilyl)-β-D-ribofuranosyl]-3'-spiro-5"-(4"-amino-1",2"-oxathiole 2",2"-dioxide) (TSAO) analogs: Synthesis and anti-HIV-1 activity. *Journal of Medicinal Chemistry, 37*(24), 4185-4194.

An, J. G., Hina, S., Yang, Y., Xue, M., & Liu, Y. (2016). Characterization of liquid crystals: A literature review. *Reviews on Advanced Materials Science, 44*, 398-406.

Araseki, M., Yamamoto, K., & Miyashita, K. (2002). Oxidative stability of polyunsaturated fatty acid in phosphatidylcholine liposomes. *Bioscience, Biotechnology, and Biochemistry, 66*(12), 2573-2577.

Attwood, D., & Florence, A. T. (2008). *FASTtrack: Physical pharmacy*. London and Chicago: Pharmaceutical Press.

Balme, A., & Lederer, F. (1994). On the rate of proton exchange with solvent of the catalytic histidine in flavocytochrome b2 (yeast L-lactate dehydrogenase). *Protein Science : A Publication of the Protein Society, 3*(1), 109-117.

Bangham, A. D., Standish, M. M., & Watkins, J. C. (1965). Diffusion of univalent ions across the lamellae of swollen phospholipids. *Journal of Molecular Biology, 13*(1), 238-252.

Barney, R., Carroll, J., & Delaet, D. (2006). Surfactant studies of quaternary ammonium compounds: Critical surfactant concentration. *Journal of Surfactants and Detergents, 9*(2), 137-140.

Batzri, S., & Korn, E. D. (1973). Single bilayer liposomes prepared without sonication. *Biochimica et Biophysica Acta (BBA) - Biomembranes, 298*(4), 1015-1019.

Baughman, T. W., Sworen, J. C., & Wagener, K. B. (2004). The facile preparation of alkenyl metathesis synthons. *Tetrahedron, 60*(48), 10943-10948.

Bayach, I., Manickam Achari, V., Wan Iskandar, W. F. N., Sugimura, A., & Hashim, R. (2016). Computational insights into octyl-D-xyloside isomers towards understanding the liquid crystalline structure: Physico-chemical features. *Liquid Crystals, 43*(10), 1503-1513.

Bazito, R. C., & El Seoud, O. A. (2001). Sugar-based cationic surfactants: Synthesis and aggregation of methyl 2-acylamido-6-trimethylammonio-2,6-dideoxy-d-glucopyranoside chlorides. *Journal of Surfactants and Detergents, 4*(4), 395-400.

Bhattacharjee, S. (2016). DLS and zeta potential – what they are and what they are not. *Journal of Controlled Release, 235*, 337-351.

Bibi, S., Kaur, R., Henriksen-Lacey, M., McNeil, S. E., Wilkhu, J., Lattmann, E., . . . Perrie, Y. (2011). Microscopy imaging of liposomes: From coverslips to environmental SEM. *International Journal of Pharmaceutics, 417*(1), 138-150.

Birks, J. B. (1970). *Photophysics of aromatic molecules* London: Wiley-Interscience.

Bishop, C. T., & Cooper, F. P. (1962). Glycosidation of sugars: I. Formation of methyl-D-xylosides. *Canadian Journal of Chemistry, 40*(2), 224-232.

Biswas, N. N., Yu, T. T., Kimyon, Ö., Nizalapur, S., Gardner, C. R., Manefield, M., . . . Kumar, N. (2017). Synthesis of antimicrobial glucosamides as bacterial quorum sensing mechanism inhibitors. *Bioorganic & Medicinal Chemistry, 25*(3), 1183-1194.

Biswas, S., Dodwadkar, N. S., Sawant, R. R., Koshkaryev, A., & Torchilin, V. P. (2011). Surface modification of liposomes with rhodamine-123-conjugated polymer results in enhanced mitochondrial targeting. *Journal of Drug Targeting, 19*(7), 552-561.

Bnyan, R., Khan, I., Ehtezazi, T., Saleem, I., Gordon, S., O'Neill, F., & Roberts, M. (2018). Surfactant effects on lipid-based vesicles properties. *Journal of Pharmaceutical Sciences, 107*(5), 1237-1246.

Bonhôte, P., Dias, A.-P., Papageorgiou, N., Kalyanasundaram, K., & Grätzel, M. (1996). Hydrophobic, highly conductive ambient-temperature molten salts. *Inorganic Chemistry, 35*(5), 1168-1178.

Boschi-Muller, S., & Motorin, Y. (2013). Chemistry enters nuclei acids biology: Enzymatic mechanisms of RNA modification. *Biochemistry (Moscow), 78*(13), 1392-1404.

Botchkarev, V. A. (2003). Molecular mechanisms of chemotherapy-induced hair loss. *Journal of Investigative Dermatology Symposium Proceedings, 8*(1), 72-75.

Boullanger, P., Banoub, J., & Descotes, G. (1987). N-allyloxycarbonyl derivatives of D-glucosamine as promotors of 1,2-trans-glucosylation in Koenigs–Knorr reactions and in Lewis acid catalyzed condensations. *Canadian Journal of Chemistry, 65*(6), 1343-1348.

Boyd, B. J., Drummond, C. J., Krodkiewska, I., & Grieser, F. (2000). How chain length, headgroup polymerization, and anomeric configuration govern the thermotropic and lyotropic liquid crystalline phase behavior and the air−water interfacial adsorption of glucose-based surfactants. *Langmuir, 16*(19), 7359-7367.

Brandenburg, K., & Holst, O. (2015). Glycolipids: Distribution and biological function *eLS*. Chichester: John Wiley & Sons Ltd.

Brandley, B. K., & Schnaar, R. L. (1986). Cell-surface carbohydrates in cell recognition and response. *Journal of Leukocyte Biology, 40*(1), 97-111.

Brito-Arias, M. (2007). *Synthesis and characterization of glycosides*. New York: Springer.

Brooks, N. J., Hamid, H. A. A., Hashim, R., Heidelberg, T., Seddon, J. M., Conn, C. E., . . . Hussen, R. S. D. (2011). Thermotropic and lyotropic liquid crystalline phases of Guerbet branched-chain -D-glucosides. *Liquid Crystals, 38*(11-12), 1725-1734.

Buqui, G. A., Sy, S. K. B., Merino-Sanjuán, M., Gouvea, D. R., Nixdorf, S. L., Kimura, E., . . . Diniz, A. (2015). Characterization of intestinal absorption of *C*-glycoside flavonoid vicenin-2 from Lychnophora ericoides leafs in rats by nonlinear mixed effects modeling. *Revista Brasileira de Farmacognosia, 25*(3), 212-218.

Butt, H.-J., Graf, K., & Kappl, M. (2003). *Physics and chemistry of interfaces*. Weinheim: Wiley-VCH.

Caboi, F., & Monduzzi, M. (1996). Didodecyldimethylammonium bromide vesicles and lamellar liquid crystals. A multinuclear NMR and optical microscopy study. *Langmuir, 12*(15), 3548-3556.

Cai, S., Yang, Q., Bagby, T. R., & Forrest, M. L. (2011). Lymphatic drug delivery using engineered liposomes and solid lipid nanoparticles. *Advanced Drug Delivery Reviews, 63*(10-11), 901-908.

Cevc, G., & Richardsen, H. (1999). Lipid vesicles and membrane fusion. *Advanced Drug Delivery Reviews, 38*(3), 207-232.

Chen, B.-L., Wang, Y.-J., Guo, H., & Zeng, G.-Y. (2016). Design, synthesis, and biological evaluation of crenatoside analogues as novel influenza neuraminidase inhibitors. *European Journal of Medicinal Chemistry, 109*, 199-205.

Chen, L.-J., Lin, S.-Y., & Huang, C.-C. (1998). Effect of hydrophobic chain length of surfactants on enthalpy−entropy compensation of mcellization. *The Journal of Physical Chemistry B, 102*(22), 4350-4356.

Chen, Y., Ma, P., & Gui, S. (2014). Cubic and hexagonal liquid crystals as drug delivery systems. *BioMed Research International, 2014*, 12.

Cheng, H.-T., & London, E. (2011). Preparation and properties of asymmetric large unilamellar vesicles: Interleaflet coupling in asymmetric vesicles is dependent on temperature but not curvature. *Biophysical Journal, 100*(11), 2671-2678.

Claessens, M. M. A. E., van Oort, B. F., Leermakers, F. A. M., Hoekstra, F. A., & Cohen Stuart, M. A. (2004). Charged lipid vesicles: Effects of salts on bending rigidity, stability, and size. *Biophysical Journal, 87*(6), 3882-3893.

Coelho, A. I., Berry, G. T., & Rubio-Gozalbo, M. E. (2015). Galactose metabolism and health. *Current Opinion in Clinical Nutrition & Metabolic Care, 18*(4), 422-427.

Combemale, S., Assam-Evoung, J. N., Houaidji, S., Bibi, R., & Barragan-Montero, V. (2014). Gold nanoparticles decorated with mannose-6-phosphate analogues. *Molecules, 19*(1), 1120-1149.

Combs, E. E., McCloskey, C. M., Sundberg, R. L., & Coleman, G. H. (1949). The alcoholysis of sugar derivatives. *Journal of the American Chemical Society, 71*(1), 276-278.

Coppola, L., Gordano, A., Procopio, A., & Sindona, G. (2002). Phase equilibria and physical-chemical properties of sugar-based surfactants in aqueous solutions.

Colloids and Surfaces A: Physicochemical and Engineering Aspects, 196(2), 175-187.

Corrie, J. E. T., & Craik, J. S. (1994). Synthesis and characterisation of pure isomers of iodoacetamidotetramethylrhodamine. *Journal of the Chemical Society, Perkin Transactions, 1*(20), 2967-2973.

Costerton, J. W., Ingram, J. M., & Cheng, K. J. (1974). Structure and function of the cell envelope of Gram-negative bacteria. *Bacteriological Reviews, 38*(1), 87-110.

Coterón, J. M., Hacket, F., & Schneider, H.-J. (1996). Interactions of hydroxy compounds and sugars with anions. *The Journal of Organic Chemistry, 61*(4), 1429-1435.

Coxon, B. (2009). Developments in the Karplus equation as they relate to the NMR coupling constants of carbohydrates. *Advances in Carbohydrate Chemistry and Biochemistry, 62*, 17-82.

Cristobal Lopez, J., Gomez, A. M., Valverde, S., & Fraser-Reid, B. (1995). Ferrier rearrangement under nonacidic conditions based on iodonium-induced rearrangements of allylic n-pentenyl esters, n-pentenyl glycosides, and phenyl thioglycosides. *The Journal of Organic Chemistry, 60*(12), 3851-3858.

Cullis, P. R., Hope, M. J., & Tilcock, C. P. S. (1986). Lipid polymorphism and the roles of lipids in membranes. *Chemistry and Physics of Lipids, 40*(2), 127-144.

Dahmén, J., Frejd, T., Grönberg, G., Lave, T., Magnusson, G., & Noori, G. (1983). 2-Bromoethyl glycosides: Synthesis and characterisation. *Carbohydrate Research, 116*(2), 303-307.

Danby, S. G., Brown, K., Wigley, A. M., Chittock, J., Pyae, P. K., Flohr, C., & Cork, M. J. (2018). The effect of water hardness on surfactant deposition after washing and subsequent skin irritation in atopic dermatitis patients and healthy control subjects. *Journal of Investigative Dermatology, 138*(1), 68-77.

Das, R., & Mukhopadhyay, B. (2016). Chemical O-Glycosylations: An overview. *Chemistry Open, 5*(5), 401-433.

Davis, B. G., & Fairbanks, A. J. (2002). *Carbohydrate chemistry*. Oxford: Oxford University Press.

Deiters, A., Cropp, T. A., Mukherji, M., Chin, J. W., Anderson, J. C., & Schultz, P. G. (2003). Adding amino acids with novel reactivity to the genetic code of saccharomyces cerevisiae. *Journal of the American Chemical Society, 125*(39), 11782-11783.

Demé, B., Dubois, M., & Zemb, T. (2002). Swelling of a lecithin lamellar phase induced by small carbohydrate solutes. *Biophysical Journal, 82*(1), 215-225.

Demurtas, D., Guichard, P., Martiel, I., Mezzenga, R., Hébert, C., & Sagalowicz, L. (2015). Direct visualization of dispersed lipid bicontinuous cubic phases by cryo-electron tomography. *Nature Communications, 6*, 8915.

Demus, D. (1994). Phase types, structures and chemistry of liquid crystals. In H. Stegemeyer & H. Behret (Eds.), *Liquid crystals* (pp. 1-50). Heidelberg: Steinkopff.

Dimakos, V., & Taylor, M. S. (2018). Site-selective functionalization of hydroxyl groups in carbohydrate derivatives. *Chemical Reviews, 118*(23), 11457-11517.

Diot, J., García-Moreno, M. I., Gouin, S. G., Ortiz Mellet, C., Haupt, K., & Kovensky, J. (2009). Multivalent iminosugars to modulate affinity and selectivity for glycosidases. *Organic & Biomolecular Chemistry, 7*(2), 357-363.

Docherty, K. M., & Kulpa, J. C. F. (2005). Toxicity and antimicrobial activity of imidazolium and pyridinium ionic liquids. *Green Chemistry, 7*(4), 185.

Dou, H. J.-M., Hassanaly, P., & Metzger, J. (1977). Alkylation d'anions ambidents en catalyse par transfert de phase. Cas des hydroxypyridines. *Journal of Heterocyclic Chemistry, 14*(2), 321-323.

Dowhan, W., Bogdanov, M., & Mileykovskaya, E. (2008). Functional roles of lipids in membranes. In J. E. Vance (Ed.), *Biochemistry of Lipids, Lipoproteins and Membranes* (5th ed., pp. 1-37). San Diego: Elsevier.

Draelos, Z. D. (2018). The science behind skin care: Cleansers. *Journal of Cosmetic Dermatology, 17*(1), 8-14.

Drexhage, K. H. (1976). Fluorescence efficiency of laser dyes. *Journal of Research of the Natioanl Bureau of Standards, 80A*(3), 421-428.

Driguez, H. (1998). Thiooligosaccharides in glycobiology. In H. Driguez & J. Thiem (Eds.), *Glycoscience synthesis of substrate analogs and mimetics* (pp. 85-116). Berlin, Heidelberg: Springer Berlin Heidelberg.

Drummond, C. J., & Wells, D. (1998). Nonionic lactose and lactitol based surfactants: Comparison of some physico-chemical properties. *Colloids and Surfaces A: Physicochemical and Engineering Aspects, 141*(1), 131-142.

Duffin, G. F. (1964). The quaternization of heterocyclic compounds. In A. R. Katritzky (Ed.), *Advances in heterocyclic chemistry* (Vol. 3, pp. 1-56): Academic Press.

Duhamel, J. (2012). New insights in the study of pyrene excimer fluorescence to characterize macromolecules and their supramolecular assemblies in solution. *Langmuir, 28*(16), 6527-6538.

Ehrlich, P. (1960). Über moderne chemotherapie [Reprinted from Verh. 10. Kongr. dtsch. derm. Ges., 1908; cf. Bibl. 194.]. In F. Himmelweit (Ed.), *The collected papers of Paul Ehrlich* (pp. 140-149). London: Pergamon Press.

Einstein, A. (1906). Zur Theorie der Brownschen Bewegung. *Annalen der Physik, 324*(2), 371-381.

El-Sukkary, M. M. A., Syed, N. A., Aiad, I., Helmy, S. M., & El-Azab, W. I. M. (2009). Aqueous solution properties, biodegradability, and antimicrobial activity of some alkylpolyglycosides surfactants. *Tenside Surfactants Detergents, 46*(5), 311-316.

Elchert, B., Li, J., Wang, J., Hui, Y., Rai, R., Ptak, R., . . . Chang, C.-W. T. (2004). Application of the synthetic aminosugars for glycodiversification: Synthesis and antimicrobial studies of pyranmycin. *The Journal of Organic Chemistry, 69*(5), 1513-1523.

Elizondo, E., Moreno, E., Cabrera, I., Córdoba, A., Sala, S., Veciana, J., & Ventosa, N. (2011). Liposomes and other vesicular systems: Structural characteristics, methods of preparation, and use in nanomedicine. In A. Villaverde (Ed.), *Progress in molecular biology and translational science* (Vol. 104, pp. 1-52). London: Academic Press.

Esmaeilian, N., Malek, R. M. A., Arami, M., Mazaheri, F. M., & Dabir, B. (2018). Environmentally friendly sugar-based cationic surfactant as a new auxiliary in polyacrylonitrile dyeing. *Colloids and Surfaces A: Physicochemical and Engineering Aspects, 552*, 103-109.

Faivre, V., & Rosilio, V. (2010). Interest of glycolipids in drug delivery: From physicochemical properties to drug targeting. *Expert Opinion on Drug Delivery, 7*(9), 1031-1048.

Farinha, J. P. S., Charreyre, M. T., Martinho, J. M. G., Winnik, M. A., & Pichot, C. (2001). Picosecond fluorescence studies of the surface morphology of charged polystyrene latex particles. *Langmuir, 17*(9), 2617-2623.

Finkelstein, H. (1910). Darstellung organischer Jodide aus den entsprechenden Bromiden und Chloriden. *Berichte der deutschen chemischen Gesellschaft, 43*(2), 1528-1532.

Fischer, E. (1893). Ueber die Glucoside der Alkohole. *Berichte der deutschen chemischen Gesellschaft, 26*(3), 2400-2412.

Fischer, E. (1916). Darstellung der Aceto-bromglucose. *Berichte der deutschen chemischen Gesellschaft, 49*(1), 584-585.

Fischer, E., & Beensch, L. (1894). Ueber einige synthetische Glucoside. *Berichte der deutschen chemischen Gesellschaft, 27*(2), 2478-2486.

Fischer, E., & Helferich, B. (1911). Über neue synthetische Glucoside. *Justus Liebigs Annalen der Chemie, 383*(1), 68-91.

Fraser-Reid, B., Merritt, J. R., Handlon, A. L., & Andrews, C. W. (1993). The chemistry of n-pentenyl glycosides: Synthetic, theoretical, and mechanistic ramifications. *Pure and Applied Chemistry, 65*(4), 779.

Gansow, O. A., Kausar, A. R., & Triplett, K. B. (1981). Synthesis and characterization of some bifunctional 2b:2:1 cryptands. *Journal of Heterocyclic Chemistry, 18*(2), 297-302.

Garg, M., Asthana, A., Agashe, H. B., Agrawal, G. P., & Jain, N. K. (2006). Stavudine-loaded mannosylated liposomes: In-vitro anti-HIV-I activity, tissue distribution and pharmacokinetics. *Journal of Pharmacy Pharmacology, 58*(5), 605-616.

Garidel, P., Kaconis, Y., Heinbockel, L., Wulf, M., Gerber, S., Munk, A., . . . Brandenburg, K. (2015). Self-organisation, thermotropic and lyotropic properties of glycolipids related to their biological implications. *The Open Biochemistry Journal, 9*, 49-72.

Gelardi, G., Mantellato, S., Marchon, D., Palacios, M., Eberhardt, A. B., & Flatt, R. J. (2016). 9-Chemistry of chemical admixtures. In P.-C. Aïtcin & R. J. Flatt (Eds.), *Science and Technology of Concrete Admixtures* (pp. 149-218). Cambridge: Woodhead Publishing.

Gololobov, Y. G., & Kasukhin, L. F. (1992). Recent advances in the Staudinger reaction. *Tetrahedron, 48*(8), 1353-1406.

González-García, E., Helaine, V., Klein, G., Schuermann, M., Sprenger, G. A., Fessner, W.-D., & Reymond, J.-L. (2003). Fluorogenic stereochemical probes for transaldolases. *Chemistry – A European Journal, 9*(4), 893-899.

Goodby, J., Cowling, S., Davis, E., & Queneau, Y. (2014). Liquid crystal glycolipids. *Carbohydrate chemistry* (Vol. 40, pp. 312-340). Cambridge: The Royal Society of Chemistry.

Goodby, J. W., Pfannemüller, B., Welte, W., & Chin, E. (2006). Liquid‐crystalline glycolipids: Towards understanding the roles of liquid crystals in biological and life processes. *Liquid Crystals, 33*(11-12), 1229-1245.

Grit, M., & Crommelin, D. J. A. (1993). Chemical stability of liposomes: Implications for their physical stability. *Chemistry and Physics of Lipids, 64*(1), 3-18.

Guo, J., Xu, B., Wang, Y., Zhuang, L., & Wang, G. (2015). Solubility of 3,3′-(oxidi-2,1-ethanediyl)bis[1-methyl-imidazolium] dihexafluorophosphate in water, methanol, ethanol, acetone, and acetonitrile and binary mixtures (water + DMF) from (283.00 to 323.00) K. *Journal of Chemical & Engineering Data, 60*(4), 1091-1097.

Guthrie, R. D., & McCarthy, J. F. (1967). Acetolysis. In M. L. Wolfrom & R. S. Tipson (Eds.), *Advances in Carbohydrate Chemistry* (Vol. 22, pp. 11-23). London: Academic Press.

Hallett, F. R., Nickel, B., Samuels, C., & Krygsman, P. H. (1991). Determination of vesicle size distributions by freeze-fracture electron microscopy. *Journal of Electron Microscopy Technique, 17*(4), 459-466.

Hamilton, R. L., Goerke, J., Guo, L. S., Williams, M. C., & Havel, R. J. (1980). Unilamellar liposomes made with the French pressure cell: A simple preparative and semiquantitative technique. *Journal of Lipid Research, 21*(8), 981-992.

Hanessian, S., Ducharme, D., Massé, R., & Louise Capmau, M. (1978). A one-flask preparation of methyl 6-azido-6-deoxy-α-d-hexopyranosides. *Carbohydrate Research, 63*, 265-269.

Hanessian, S., Ponpipom, M. M., & Lavallee, P. (1972). Procedures for the direct replacement of primary hydroxyl groups in carbohydrates by halogen. *Carbohydrate Research, 24*(1), 45-56.

Hashim, R., Hashim, H. H. A., Rodzi, N. Z. M., Hussen, R. S. D., & Heidelberg, T. (2006). Branched chain glycosides: Enhanced diversity for phase behavior of easily accessible synthetic glycolipids. *Thin Solid Films, 509*(1), 27-35.

Hashim, R., Zahid, N. I., Velayutham, T. S., Aripin, N. F. K., Ogawa, S., & Sugimura, A. (2018). Dry thermotropic glycolipid self-assembly: A review. *Journal of Oleo Science, 67*(6), 651-668.

Hatakeyama, H., Akita, H., Maruyama, K., Suhara, T., & Harashima, H. (2004). Factors governing the in vivo tissue uptake of transferrin-coupled polyethylene glycol liposomes in vivo. *International Journal of Pharmaceutics, 281*(1), 25-33.

Henry, D. C., & Lapworth, A. (1931). *The cataphoresis of suspended particles. Part I.—The equation of cataphoresis.* Paper presented at the Proceedings of the Royal Society of London.

Herscovici, J., Bennani-Baiti, M. I., Frayssinet, C., & Antonakis, K. (1991). Keto C-glycosides. A new class of antitumor compounds. *Bioorganic & Medicinal Chemistry Letters, 1*(8), 395-398.

Hindi, S. (2016). Birefringence of bio-based liquid crystals. *BioCrystals Journal , 1*, 13-25.

Hoffmann, H., & Poessnecker, G. (1994). The mixing behavior of surfactants. *Langmuir, 10*(2), 381-389.

Huisgen, R. (1963). 1,3-Dipolar cycloadditions. Past and future. *Angewandte Chemie International Edition in English, 2*(10), 565-598.

Hussen, R. S. D. (2010). *Preparation and evaluation of vesicles based on non-ionic branched chain glycolipids.* (Doctoral dissertation), University of Malaya, Kuala Lumpur, Malaysia.

Hussen, R. S. D. (2012). *Niosomes from chain-branched glycolipids for drug delivery. Synthesis, formulation and evaluation*. Saarbrücken: Lambert Academic Publishing.

Ichikawa, Y., Manaka, A., & Kuzuhara, H. (1985). Discrimination between the 2,3- and the 2′,3′-hydroxyl groups of maltose and cellobiose through their specific protection. *Carbohydrate Research, 138*(1), 55-64.

Immordino, M. L., Dosio, F., & Cattel, L. (2006). Stealth liposomes: Review of the basic science, rationale, and clinical applications, existing and potential. *International Journal of Nanomedicine, 1*(3), 297-315.

Inácio, Â. S., Domingues, N. S., Nunes, A., Martins, P. T., Moreno, M. J., Estronca, L. M., . . . Vieira, O. V. (2016). Quaternary ammonium surfactant structure determines selective toxicity towards bacteria: Mechanisms of action and clinical implications in antibacterial prophylaxis. *Journal of Antimicrobial Chemotherapy, 71*(3), 641-654.

Isbell, H. S. (1940). Chemistry of the carbohydrates and glycosides. *Annual Review of Biochemistry, 9*(1), 65-92.

Ishida, Y., Sasaki, D., Miyauchi, H., & Saigo, K. (2004). Design and synthesis of novel imidazolium-based ionic liquids with a pseudo crown-ether moiety: Diastereomeric interaction of a racemic ionic liquid with enantiopure europium complexes. *Tetrahedron Letters, 45*(51), 9455-9459.

Israelachvili, J. (1992). *Intermolecular and surface forces* (2nd ed.). London: Academic Press.

Israelachvili, J. N. (2011). *Intermolecular and surface forces* (3rd ed.). London: Academic Press.

Ito, H., Kamachi, T., & Yashima, E. (2012). Specific surface modification of the acetylene-linked glycolipid vesicle by click chemistry. *Chemical Communications, 48*(45), 5650-5652.

Jaafar-Maalej, C., Diab, R., Andrieu, V., Elaissari, A., & Fessi, H. (2010). Ethanol injection method for hydrophilic and lipophilic drug-loaded liposome preparation. *Journal of Liposome Research, 20*(3), 228-243.

Jackson, P., Bobrow, M. N., & Trometer, J. D. (2005). US20050224354A1. U. S. Patent.

Jain, K. K. (2008). Drug delivery systems- an overview. In K. K. Jain (Ed.), *Drug delivery systems* (pp. 1-50). New York: Humana Press.

Jain, S., Jain, V., & Mahajan, S. C. (2014). Lipid based vesicular drug delivery systems. *Advances in Pharmaceutics, 2014*, 1-13.

Jain, S., Patel, N., & Lin, S. (2015). Solubility and dissolution enhancement strategies: Current understanding and recent trends. *Drug Development and Industrial Pharmacy, 41*(6), 875-887.

Jia, Y., Ma, N., Liu, Z., Bois-Choussy, M., Gonzalez-Zamora, E., Malabarba, A., . . . Zhu, J. (2006). Design and synthesis of simple macrocycles active against vancomycin-resistant *Enterococci* (VRE). *Chemistry – A European Journal, 12*(20), 5334-5351.

Jiang, J., Biggins, J. B., & Thorson, J. S. (2000). A general enzymatic method for the synthesis of natural and "unnatural" UDP- and TDP-nucleotide sugars. *Journal of the American Chemical Society, 122*(28), 6803-6804.

Jiang, W., Kim, B. Y. S., Rutka, J. T., & Chan, W. C. W. (2007). Advances and challenges of nanotechnology-based drug delivery systems. *Expert Opinion on Drug Delivery, 4*(6), 621-633.

Jones, M. N. (1994). Carbohydrate-mediated liposomal targeting and drug delivery. *Advanced Drug Delivery Reviews, 13*(3), 215-249.

Kagawa, Y., & Racker, E. (1966). Partial resolution of the enzymes catalyzing oxidative phosphorylation: VIII. Properties of a factor conferring oligomycin sensitivity on mitochondrial adenosine triphosphatase. *Journal of Biological Chemistry, 241*(10), 2461-2466.

Kalpesh, C., Ashara, K., Paun, J., Soniwala, M., R Chavda, J., V Nathawani, S., . . . P Mendapara, V. (2014). Vesicular drug delivery system: A novel approach. *Mintage Journal of Pharmaceutical & Medical Sciences, 3*(3), 1-14.

Kamboj, R., Singh, S., Bhadani, A., Kataria, H., & Kaur, G. (2012). Gemini imidazolium surfactants: Synthesis and their biophysiochemical study. *Langmuir, 28*(33), 11969-11978.

Kamboj, S., Saini, V., Maggon, N., Bala, S., & Jhawat, V. (2013). Vesicular drug delivery systems: A novel approach for drug targeting. *International Journal of Drug Delivery, 5*, 121-130.

Kasuya, M. C., Ito, A., & Hatanaka, K. (2007). Simple and convenient synthesis of a fluorinated GM4 analogue. *Journal of Fluorine Chemistry, 128*(5), 562-565.

Kasyanenko, N., Unksov, I., Bakulev, V., & Santer, S. (2018). DNA interaction with head-to-tail associates of cationic surfactants prevents formation of compact particles. *Molecules, 23*(7), 1576.

Khan, A., & Marques, E. (1997). Catanionic surfactants. In I. D. Robb (Ed.), *Specialist surfactants* (pp. 37-80). Dordrecht: Springer.

Kiwada, H., Niimura, H., Fujisaki, Y., Yamada, S., & Kato, Y. (1985). Application of synthetic alkyl glycoside vesicles as drug carriers. I. Preparation and physical properties. *Chemical & Pharmaceutical Bulletin, 33*(2), 753-759.

Kiwada, H., Niimura, H., & Kato, Y. (1985). Tissue distribution and pharmacokinetic evaluation of the targeting efficiency of synthetic alkyl glycoside vesicles. *Chemical & Pharmaceutical Bulletin, 33*(6), 2475-2482.

Koenigs, W., & Knorr, E. (1901). Ueber einige Derivate des Traubenzuckers und der Galactose. *Berichte der deutschen chemischen Gesellschaft, 34*(1), 957-981.

Kolb, H. C., Finn, M. G., & Sharpless, K. B. (2001). Click chemistry: Diverse chemical function from a few good reactions. *Angewandte Chemie International Edition, 40*(11), 2004-2021.

Konda, S., Rao, P., & Oruganti, S. (2014). Click chemistry route to tricyclic monosaccharide triazole hybrids: Design and synthesis of substituted hexahydro-4*H*-pyrano[2,3-*f*][1,2,3]triazolo[5,1-*c*][1,4]oxazepines. *RSC Advances, 4*(109), 63962-63965.

Kopitz, J. (2009). Glycolipids. In H.-J. Gabius (Ed.), *The sugar code: Fundamentals of glycosciences* (pp. 177-198). Weinheim: Wiley.

Krag, J., Christiansen, M. S., Petersen, J. G., & Jensen, H. H. (2010). Direct chemical glycosylation with pentenyl- and thioglycoside donors of N-acetylglucosamine. *Carbohydrate Research, 345*(7), 872-879.

Krasnici, S., Werner, A., Eichhorn, M. E., Schmitt-Sody, M., Pahernik, S. A., Sauer, B., . . . Dellian, M. (2003). Effect of the surface charge of liposomes on their uptake by angiogenic tumor vessels. *International Journal of Cancer, 105*(4), 561-567.

Kuang, Y., Wu, B., Hu, D., Zhang, X., & Chen, J. (2012). One-pot of highly dispersed palladium nanoparticles on acetylenic ionic liquid polymer functionalized carbon nanotubes for electrocatalytic oxidation of glucose. *Journal of Solid State Electrochemistry, 16*(2), 759-766.

Kuo, A.-T., Tu, C.-L., Yang, Y.-M., & Chang, C.-H. (2018). Enhanced physical stability of mixed ion pair amphiphile/double-chained cationic surfactant vesicles in the presence of cholesterol. *Journal of Oleo Science, 67*(6), 727-735.

L'Heureux, G. P., & Fragata, M. (1989). Monomeric and aggregated pyrene and 16-(1-pyrenyl)hexadecanoic acid in small, unilamellar phosphatidylcholine vesicles and ethanol—buffer solutions. *Journal of Photochemistry and Photobiology B: Biology, 3*(1), 53-63.

Larsen, R. P., & Kraus, C. A. (1954). The rates of reaction between alkyl halides and tertiary amines as determined conductometrically. *Proceedings of the National Academy of Sciences, 40*(2), 70.

Laughlin, R. G. (1992). The role of swelling methods in surfactant phase science: Past, present, and future. *Advances in Colloid and Interface Science, 41*, 57-79.

Lee, I. C., Zulueta, M. M. L., Shie, C.-R., Arco, S. D., & Hung, S.-C. (2011). Deuterium-isotope study on the reductive ring opening of benzylidene acetals. *Organic & Biomolecular Chemistry, 9*(22), 7655-7658.

Lee, J.-M., Park, K.-M., Lim, S.-J., Lee, M.-K., & Kim, C.-K. (2002). Microemulsion formulation of clonixic acid: Solubility enhancement and pain reduction. *Journal of Pharmacy and Pharmacology, 54*, 43-49.

Lee, M., Choi, U. H., Wi, S., Slebodnick, C., Colby, R. H., & Gibson, H. W. (2011). 1,2-Bis[N-(N′-alkylimidazolium)]ethane salts: A new class of organic ionic plastic crystals. *Journal of Materials Chemistry, 21*(33), 12280-12287.

Lehmann, O. (1889). Über fliessende Krystalle. *Zeitschrift für Physikalische Chemie, 4U*(1), 462-472.

Lemieux, R. U., & Shyluk, W. P. (1953). A new synthesis of β-glucopyranosides. *Canadian Journal of Chemistry, 31*(6), 528-535.

Leytus, S. P., Melhado, L. L., & Mangel, W. F. (1983). Rhodamine-based compounds as fluorogenic substrates for serine proteinases. *Biochemical Journal, 209*(2), 299-307.

Li, J., Wang, X., Zhang, T., Wang, C., Huang, Z., Luo, X., & Deng, Y. (2015). A review on phospholipids and their main applications in drug delivery systems. *Asian Journal of Pharmaceutical Sciences, 10*(2), 81-98.

Li, Y., Zhang, X., Li, Y., Li, C., & Guo, X. (2014). Micellization of glucose-based surfactants with different counter ions and their interaction with DNA. *Colloids and Surfaces A: Physicochemical and Engineering Aspects, 443*, 224-232.

Lianos, P., & Duportail, G. (1992). Reactions in lipid vesicles. Pyrene excimer formation in restricted geometries. Effect of temperature and concentration. *European Biophysics Journal, 21*(1), 29-34.

Lin, Y.-C., Liang, M.-R., Lin, Y.-C., & Chen, C.-T. (2011). Specifically and reversibly immobilizing proteins/enzymes to nitriolotriacetic-acid-modified mesoporous silicas through histidine tags for purification or catalysis. *Chemistry – A European Journal, 17*(46), 13059-13067.

Lindhorst, T. K. (2000). *Essentials of carbohydrate chemistry and biochemistry*. United States: John Wiley.

Lindman, B. (2002). Physico-chemical properties of surfactants. In K. Holmberg (Ed.), *Handbook of applied surface and colloid chemistry* (Vol. 1-2, pp. 421-443). West Sussex: John Wiley & Sons.

Lockman, P. R., Mumper, R. J., Khan, M. A., & Allen, D. D. (2002). Nanoparticle technology for drug delivery across the blood-brain barrier. *Drug Development and Industrial Pharmacy, 28*(1), 1-13.

López, J. C., Uriel, C., Guillamón-Martín, A., Valverde, S., & Gómez, A. M. (2007). IPy2BF4-Mediated transformation of n-pentenyl glycosides to glycosyl fluorides: A new pair of semiorthogonal glycosyl donors. *Organic Letters, 9*(15), 2759-2762.

Lucero, H. A., & Robbins, P. W. (2004). Lipid rafts-protein association and the regulation of protein activity. *Archives of Biochemistry Biophysics, 426*(2), 208-224.

Lukyanov, A. N., Elbayoumi, T. A., Chakilam, A. R., & Torchilin, V. P. (2004). Tumor-targeted liposomes: Doxorubicin-loaded long-circulating liposomes modified with anti-cancer antibody. *Journal of Controlled Release, 100*(1), 135-144.

Luzzati, V., & Husson, F. (1962). The structure of the liquid-crystalline phasis of lipid-water systems. *The Journal of Cell Biology, 12*(2), 207-219.

Macy, R. (1935). Surface tension by the ring method. Applicability of the du Noüy apparatus. *Journal of Chemical Education, 12*(12), 573.

Madunić-Čačić, D., Sak-Bosnar, M., Galović, O., Sakač, N., & Matešić-Puač, R. (2008). Determination of cationic surfactants in pharmaceutical disinfectants using a new sensitive potentiometric sensor. *Talanta, 76*(2), 259-264.

Magde, D., Wong, R., & Seybold, P. G. (2002). Fluorescence quantum yields and their relation to lifetimes of rhodamine 6G and fluorescein in nine solvents: Improved

absolute standards for quantum yields. *Photochemistry and Photobiology, 75*(4), 327-334.

Maibaum, L., Dinner, A. R., & Chandler, D. (2004). Micelle formation and the hydrophobic effect. *The Journal of Physical Chemistry B, 108*(21), 6778-6781.

Maiti, S., & Sen, K. K. (2017). Introductory chapter: Drug delivery concepts. In S. Maiti & K. K. Sen (Eds.), *Advanced Technology for Delivering Therapeutics* (pp. 1-12). Rijeka: Intech Open.

Mak, O. W., Seman, N., Harun, N. H., Hussen, R. S. D., Rodzi, N. M., & Heidelberg, T. (2015). Nanovesicles based on mixtures of a biantennary glycolipid with ionic co-surfactants. *Journal of Surfactants and Detergents, 18*(6), 973-980.

Malhotra, S. V., & Kumar, V. (2010). A profile of the in vitro anti-tumor activity of imidazolium-based ionic liquids. *Bioorganic & Medicinal Chemistry Letters, 20*(2), 581-585.

Manaia, E. B., Kaminski, R. C. K., Oliveira, A. G. d., Corrêa, M. A., & Chiavacci, L. A. (2015). Multifunction hexagonal liquid-crystal containing modified surface TiO2 nanoparticles and terpinen-4-ol for controlled release. *International Journal of Nanomedicine, 10*(1), 811-819.

Marques, E. F. (2000). Size and stability of catanionic vesicles: Effects of formation path, sonication, and aging. *Langmuir, 16*(11), 4798-4807.

Marques, E. F., Regev, O., Khan, A., da Graça Miguel, M., & Lindman, B. (1998). Vesicle formation and general phase behavior in the catanionic mixture SDS−DDAB−Water. The anionic-rich side. *The Journal of Physical Chemistry B, 102*(35), 6746-6758.

Maton, C., Van Hecke, K., & Stevens, C. V. (2015). Peralkylated imidazolium carbonate ionic liquids: Synthesis using dimethyl carbonate, reactivity and structure. *New Journal of Chemistry, 39*(1), 461-468.

Maunier, V., Boullanger, P., Lafont, D., & Chevalier, Y. (1997). Synthesis and surface-active properties of amphiphilic 6-aminocarbonyl derivatives of D-glucose. *Carbohydrate Research, 299*(1), 49-57.

Menchen, S. M., & Fung, S. (1988). EP0272007A2. E. Patent.

Menschutkin, N. (1890a). Beiträge zur Kenntnis der Affinitätskoeffizienten der Alkylhaloide und der organischen Amine. *Zeitschrift für Physikalische Chemie, 5U*(1), 589-600.

Menschutkin, N. (1890b). Über die Affinitätskoeffizienten der Alkylhaloide und der Amine. *Zeitschrift für Physikalische Chemie, 6U*(1), 41-57.

Merrill, A. H., Jr., Wang, M. D., Park, M., & Sullards, M. C. (2007). (Glyco)sphingolipidology: An amazing challenge and opportunity for systems biology. *Trends in Biochemical Sciences, 32*(10), 457-468.

Michael, A. (1881). Ueber die Synthese des Methylarbutins. *Berichte der deutschen chemischen Gesellschaft, 14*(2), 2097-2102.

Milkereit, G., Gerber, S., Brandenburg, K., Morr, M., & Vill, V. (2005). Synthesis and mesomorphic properties of glycosyl dialkyl- and diacyl-glycerols bearing saturated, unsaturated and methyl branched fatty acid and fatty alcohol chains. Part I. Synthesis. *Chemistry and Physics of Lipids, 135*(1), 1-14.

Minamikawa, H., Murakami, T., & Hato, M. (1994). Synthesis of 1,3-di-O-alkyl-2-O-(β-glycosyl)glycerols bearing oligosaccharides as hydrophilic groups. *Chemistry and Physics of Lipids, 72*(2), 111-118.

Mishra, N., Pant, P., Porwal, A., Jaiswal, J., Samad, M. A., & Tiwari, S. (2016). Targeted drug delivery: A review. *American Journal of PharmTech Research, 6*(1), 1-24.

Moody, D. B., & Besra, G. S. (2001). Glycolipid targets of CD1-mediated T-cell responses. *Immunology, 104*(3), 243-251.

Mootoo, D. R., Konradsson, P., Udodong, U., & Fraser-Reid, B. (1988). Armed and disarmed n-pentenyl glycosides in saccharide couplings leading to oligosaccharides. *Journal of the American Chemical Society, 110*(16), 5583-5584.

Morimoto, N., Hirano, S., Takahashi, H., Loethen, S., Thompson, D. H., & Akiyoshi, K. (2013). Self-assembled pH-sensitive cholesteryl pullulan nanogel as a protein delivery vehicle. *Biomacromolecules, 14*(1), 56-63.

Mydock, L. K., & Demchenko, A. V. (2010). Mechanism of chemical O-glycosylation: From early studies to recent discoveries. *Organic & Biomolecular Chemistry, 8*(3), 497-510.

Nagarajan, R. (2003). Theory of micelle formation: Quantitative approach to predicting micellar properties from surfactant molecular structure. In K. Esumo & M. Ueno (Eds.), *Strucutre-performance Relationships in Surfactants* (2nd ed., pp. 14-122). New York: Marcel Dekker, Inc.

Nagarajan, S., & Mohan Das, T. (2009). A sugar–pyrene-based fluorescent gelator: Nanotubular architecture and interaction with SWCNTs. *New Journal of Chemistry, 33*(12), 2391-2396.

Nazaruk, E., Miszta, P., Filipek, S., Górecka, E., Landau, E. M., & Bilewicz, R. (2015). Lyotropic cubic phases for drug delivery: Diffusion and sustained release from the mesophase evaluated by electrochemical methods. *Langmuir, 31*(46), 12753-12761.

Nguyen, T. X., Huang, L., Gauthier, M., Yang, G., & Wang, Q. (2016). Recent advances in liposome surface modification for oral drug delivery. *Nanomedicine, 11*(9), 1169-1185.

Nichols, J. W., & Bae, Y. H. (2014). EPR: Evidence and fallacy. *Journal of Controlled Release, 190*, 451-464.

Nicotra, F., Airoldi, C., & Cardona, F. (2007). Synthesis of C- and S-glycosides. In H. Kamerling (Ed.), *Comprehensive Glycoscience* (pp. 647-683). Oxford: Elsevier.

Nieva, J. L., Alonso, A., Basáñez, G., Goñi, F. M., Gulik, A., Vargas, R., & Luzzati, V. (1995). Topological properties of two cubic phases of a phospholipid: Cholesterol: Diacylglycerol aqueous system and their possible implications in the phospholipase C-induced liposome fusion. *FEBS Letters, 368*(1), 143-147.

Nilsson, F., Söderman, O., & Johansson, I. (1998). Four different C_8G_1alkylglucosides. Anomeric effects and the influence of straight vs branched hydrocarbon chains. *Journal of Colloid and Interface Science, 203*(1), 131-139.

Noack, K., Schulz, P. S., Paape, N., Kiefer, J., Wasserscheid, P., & Leipertz, A. (2010). The role of the C2 position in interionic interactions of imidazolium based ionic liquids: A vibrational and NMR spectroscopic study. *Physical Chemistry Chemical Physics, 12*(42), 14153-14161.

Norsikian, S., Zeitouni, J., Rat, S., Gérard, S., & Lubineau, A. (2007). New and general synthesis of β-C-glycosylformaldehydes from easily available β-C-glycosylpropanones. *Carbohydrate Research, 342*(18), 2716-2728.

Nwe, K., & Brechbiel, M. W. (2009). Growing applications of "Click Chemistry" for bioconjugation in contemporary biomedical research. *Cancer Biotherapy & Radiopharmaceuticals, 24*(3), 289-302.

Obeid, M. A., Khadra, I., Mullen, A. B., Tate, R. J., & Ferro, V. A. (2017). The effects of hydration media on the characteristics of non-ionic surfactant vesicles (NISV) prepared by microfluidics. *International Journal of Pharmaceutics, 516*(1), 52-60.

Ohlin, M., Johnsson, R., & Ellervik, U. (2011). Regioselective reductive openings of 4,6-benzylidene acetals: Synthetic and mechanistic aspects. *Carbohydrate Research, 346*(12), 1358-1370.

Olson, F., Hunt, C. A., Szoka, F. C., Vail, W. J., & Papahadjopoulos, D. (1979). Preparation of liposomes of defined size distribution by extrusion through polycarbonate membranes. *Biochimica et Biophysica Acta (BBA) - Biomembranes, 557*(1), 9-23.

Oshima, A., & Sumitomo, K. (2017). Vesicle fusion with bilayer lipid membrane controlled by electrostatic interaction. *Biochemistry and Biophysics Reports, 11*, 58-63.

Ouchi, M., Inoue, Y., Liu, Y., Nagamune, S., Nakamura, S., Wada, K., & Hakushi, T. (1990). Convenient and efficient tosylation of oligoethylene glycols and the related alcohols in tetrahydrofuran–water in the presence of sodium hydroxide. *Bulletin of the Chemical Society of Japan, 63*(4), 1260-1262.

Patel, H. M., Katherine M, B., & Vaughan-Jones, R. (1984). Assessment of the potential uses of liposomes for lymphoscintigraphy and lymphatic drug delivery. Failure of 99m-technetium marker to represent intact liposomes in lymph nodes. *Biochimica et Biophysica Acta (BBA) - General Subjects, 801*(1), 76-86.

Pencer, J., & Hallett, F. R. (2003). Effects of vesicle size and shape on static and dynamic light scattering measurements. *Langmuir, 19*(18), 7488-7497.

Phillips, W. T., Klipper, R., & Goins, B. (2000). Novel method of greatly enhanced delivery of liposomes to lymph nodes. *Journal of Pharmacology and Experimental Therapeutics, 295*(1), 309-313.

Pick, U. (1981). Liposomes with a large trapping capacity prepared by freezing and thawing of sonicated phospholipid mixtures. *Archives of Biochemistry and Biophysics, 212*(1), 186-194.

Piron, F., Oprea, C., Cismaş, C., Terec, A., Roncali, J., & Grosu, I. (2010). Synthesis of podands with cyanurate or isocyanurate cores and terminal triple bonds. *Synthesis, 2010*(10), 1639-1644.

Porter, M. R. (1991). *Handbook of Surfactants*. New York: Springer US.

Poste, G., & Kirsh, R. (1983). Site–specific (targeted) drug delivery in cancer therapy. *Bio/Technology, 1*, 869-878.

Powel, G. M. (1980). Polyethylene glycol. In R. L. Davidson (Ed.), *Handbook of Water Soluble Gums and Resins* (pp. 1-31). New York: McGraw-Hill.

Qabaja, G., Wilent, J. E., Benavides, A. R., Bullard, G. E., & Petersen, K. S. (2013). Facile synthesis of versatile enantioenriched α-substituted hydroxy esters through a Brønsted Acid catalyzed kinetic resolution. *Organic Letters, 15*(6), 1266-1269.

Ramirez, L. Y., Huestis, S. E., Yap, T. Y., Zyzanski, S., Drotar, D., & Kodish, E. (2009). Potential chemotherapy side effects: What do oncologists tell parents. *Pediatric Blood & Cancer, 52*(4), 497-502.

Rao, K. V., Patil, P. R., Atmakuri, S., & Kartha, K. P. (2010). Iodine-sodium cyanoborohydride-mediated reductive ring opening of 4,6-O-benzylidene acetals of hexopyranosides. *Carbohydrate Research, 345*(18), 2709-2713.

Reinitzer, F. (1888). Beitr ge zur Kenntniss des Cholesterins. *Monatshefte für Chemie, 9*(1), 421-441.

Ren, B., Wang, M., Liu, J., Ge, J., Zhang, X., & Dong, H. (2015). Zemplén transesterification: A name reaction that has misled us for 90 years. *Green Chemistry, 17*(3), 1390-1394.

Riemann, I., Fessner, W.-D., Papadopoulos, M. A., & Knorst, M. (2002). C-glycosides by aqueous condensation of β-dicarbonyl compounds with unprotected sugars. *Australian Journal of Chemistry, 55*(2), 147-154.

Rizwan, S. B., Boyd, B. J., Rades, T., & Hook, S. (2010). Bicontinuous cubic liquid crystals as sustained delivery systems for peptides and proteins. *Expert Opinion on Drug Delivery, 7*(10), 1133-1144.

Röhrling, J., Potthast, A., Lange, T., Rosenau, T., Adorjan, I., Hofinger, A., & Kosma, P. (2002). Synthesis of oxidized methyl 4-O-methyl-β-D-glucopyranoside and

methyl-β-D-glucopyranosyl-(1→4)- β-D-glucopyranoside derivatives as substrates for fluorescence labeling reactions. *Carbohydrate Research, 337*(8), 691-700.

Roos, A., Xu, W., Castellano, G., Nauta, A. J., Garred, P., Daha, M. R., & van Kooten, C. (2004). Mini-review: A pivotal role for innate immunity in the clearance of apoptotic cells. *European Journal of Immunology, 34*(4), 921-929.

Rosen, M. J. (2004). *Surfactants and Interfacial Phenomena* (3rd ed.). New Jersey: John Wiley & Sons.

Rosen, M. J., & Kunjappu, J. T. (2012). *Surfactants and Interfacial Phenomena*. Hoboken: Wiley.

Roux, E., Francis, M., Winnik, F. M., & Leroux, J. (2002). Polymer based pH-sensitive carriers as a means to improve the cytoplasmic delivery of drugs. *International Journal of Pharmaceutics, 242*(1), 25-36.

Roux, E., Stomp, R., Giasson, S., PÉzolet, M., Moreau, P., & Leroux, J. (2002). Steric stabilization of liposomes by pH-responsive N-isopropylacrylamide copolymer. *Journal of Pharmaceutical Sciences, 91*(8), 1795-1802.

Rye, C. S., & Withers, S. G. (2002). Synthesis and evaluation of potential inhibitors of chondroitin AC lyase from *Flavobacterium* heparinum. *Journal of Organic Chemistry, 67*(13), 4505-4512.

Sabah, K., Heidelberg, T., & Hashim, R. (2011). Novel crown ethers on glucose based glycolipids. *Carbohydrate Research, 346*(7), 891-896.

Sakya, P., Seddon, J. M., Templer, R. H., Mirkin, R. J., & Tiddy, G. J. T. (1997). Micellar cubic phases and their structural relationships: The nonionic surfactant system $C_{12}EO_{12}$/water. *Langmuir, 13*(14), 3706-3714.

Salim, M., Abou-Zied, O. K., Kulathunga, H. U., Baskaran, A., Kuppusamy, U. R., & Hashim, R. (2015). Alkyl mono- and di-glucoside sugar vesicles as potential drug delivery vehicles: Detecting drug release using fluorescence. *RSC Advances, 5*(68), 55536-55543.

Salman, A. A., Goh, E. W., Heidelberg, T., Hussen, R. S. D., & Ali, H. M. (2016). Bis-(alkylimidazolium)-glycosides-promising materials for easy vesicle preparation. *Journal of Molecular Liquids, 222*, 609-613.

Salman, A. A., & Heidelberg, T. (2014). In situ functionalized fluorescent nanoparticles for efficient receptor coupling. *Journal of Nanoparticle Research, 16*, 2399.

Salman, S. M., Heidelberg, T., Hussen, R. S. D., & Tajuddin, H. A. B. (2014). Amide-based surfactants from methyl glucoside as potential emulsifiers. *Journal of Surfactants and Detergents, 17*(6), 1141-1149.

Salman, S. M., Heidelberg, T., & Tajuddin, H. A. B. (2013). N-linked glycolipids by Staudinger coupling of glycosylated alkyl diazides with fatty acids. *Carbohydrate Research, 375*, 55-62.

Sánchez-Fernández, E. M., Rísquez-Cuadro, R., Chasseraud, M., Ahidouch, A., Mellet, C. O., Ouadid-Ahidouch, H., & Fernández, J. M. G. (2010). Synthesis of N-, S-, and C-glycoside castanospermine analogues with selective neutral α-glucosidase inhibitory activity as antitumour agents. *Chemical Communications, 46*(29), 5328-5330.

Sani, F. A., Heidelberg, T., Hashim, R., & Farhanullah. (2012). Alkyl triazole glycosides (ATGs)—a new class of bio-related surfactants. *Colloids and Surfaces B: Biointerfaces, 97*, 196-200.

Sankhyan, A., & Pawar, P. K. (2013). Metformin loaded non-ionic surfactant vesicles: optimization of formulation, effect of process variables and characterization. *Daru : Journal of Faculty of Pharmacy, Tehran University of Medical Sciences, 21*(1), 7.

Santra, A., Ghosh, T., & Misra, A. K. (2013). Removal of benzylidene acetal and benzyl ether in carbohydrate derivatives using triethylsilane and Pd/C. *Beilstein Journal of Organic Chemistry, 9*, 74-78.

Sarmoria, C., Puvvada, S., & Blankschtein, D. (1992). Prediction of critical micelle concentrations of nonideal binary surfactant mixtures. *Langmuir, 8*(11), 2690-2697.

Saupe, A. (1977). Textures, deformations, and structural order of liquid crystals. *Journal of Colloid and Interface Science, 58*(3), 549-558.

Schirrmacher, V. (2019). From chemotherapy to biological therapy: A review of novel concepts to reduce the side effects of systemic cancer treatment (Review). *International Journal of Oncology, 54*(2), 407-419.

Schmidt, R. R., & Michel, J. (1980). Facile synthesis of α- and β-*O*-glycosyl imidates; preparation of glycosides and disaccharides. *Angewandte Chemie International Edition in English, 19*(9), 731-732.

Schubert, R. (2003). Liposome preparation by detergent removal. *Methods in Enzymology* (Vol. 367, pp. 46-70): Academic Press.

Schurtenberger, P., Mazer, N., Waldvogel, S., & Känzig, W. (1984). Preparation of monodisperse vesicles with variable size by dilution of mixed micellar solutions of bile salt and phosphatidylcholine. *Biochimica et Biophysica Acta (BBA) - Biomembranes, 775*(1), 111-114.

Seddon, K. R., Stark, A., & Torres, M.-J. (2000). Influence of chloride, water, and organic solvents on the physical properties of ionic liquids. *Pure and Applied Chemistry, 72*(12), 2275-2287.

Senior, J., Delgado, C., Fisher, D., Tilcock, C., & Gregoriadis, G. (1991). Influence of surface hydrophilicity of liposomes on their interaction with plasma protein and clearance from the circulation: Studies with poly(ethylene glycol)-coated vesicles. *Biochimica et Biophysica Acta (BBA) - Biomembranes, 1062*(1), 77-82.

Serajuddin, A. T. (2007). Salt formation to improve drug solubility. *Advanced Drug Delivery Reviews, 59*(7), 603-616.

Shabarova, Z., & Bogdanov, A. (1994). Structure of nucleosides *Advanced Organic Chemistry of Nucleic Acids* (pp. 1-32). New York: VCH.

Shah, J. C., Sadhale, Y., & Chilukuri, D. M. (2001). Cubic phase gels as drug delivery systems. *Advanced Drug Delivery Reviews, 47*(2), 229-250.

Simons, K., & Toomre, D. (2000). Lipid rafts and signal transduction. *Nature Reviews Molecular Cell Biology, 1*, 31-40.

Singh, R. (2016). Chemotaxonomy: A tool for plant classification. *Journal of Medicinal Plants Studies, 4*(2), 90-93.

Singh, S., Vardhan, H., Kotla, N. G., Maddiboyina, B., Sharma, D., & Webster, T. J. (2016). The role of surfactants in the formulation of elastic liposomal gels containing a synthetic opioid analgesic. *International Journal of Nanomedicine, 11*, 1475-1482.

Siu, H., & Duhamel, J. (2004). Global analysis of the fluorescence decays of a pyrene-labeled polymer using a Blob Model. *Macromolecules, 37*(24), 9287-9289.

Sletten, E. M., & Liotta, L. J. (2006). A flexible stereospecific synthesis of polyhydroxylated pyrrolizidines from commercially available pyranosides. *Journal of Organic Chemistry, 71*(4), 1335-1343.

Söderman, O., Herrington, K. L., Kaler, E. W., & Miller, D. D. (1997). Transition from micelles to vesicles in aqueous mixtures of anionic and cationic surfactants. *Langmuir, 13*(21), 5531-5538.

Sohrabi, B., Bazyari, A., & Hashemianzadeh, M. (2010). Effect of ethylene glycol on micellization and surface properties of Gemini surfactant solutions. *Colloids and Surfaces A: Physicochemical and Engineering Aspects, 364*(1), 87-93.

Sohrabi, B., Gharibi, H., Tajik, B., Javadian, S., & Hashemianzadeh, M. (2008). Molecular interactions of cationic and anionic surfactants in mixed monolayers and aggregates. *Journal of Physical Chemistry B, 112*(47), 14869-14876.

Spernath, A., Yaghmur, A., Aserin, A., Hoffman, R. E., & Garti, N. (2002). Food-grade microemulsions based on nonionic emulsifiers: Media to enhance lycopene solubilization. *Journal of Agricultural and Food Chemistry, 50*(23), 6917-6922.

Squier, C. A., Cox, P., & Wertz, P. W. (1991). Lipid content and water permeability of skin and oral mucosa. *Journal of Investigative Dermatology, 96*(1), 123-126.

St. Laurent, J. B., de Buzzaccarini, F., De Clerck, K., Demeyere, H., Labeque, R., Lodewick, R., & van Langenhove, L. (2007). Laundry cleaning of textiles. In I. Johansson & P. Somasundaran (Eds.), *Handbook for Cleaning/Decontamination of Surfaces* (pp. 57-102). Amsterdam: Elsevier Science B.V.

Stanek, J. (1963). *The monosaccharides*. New York: Academic Press.

Starks, C. M., Liotta, C. L., & Halpern, M. E. (1994). *Phase-transfer Catalysis Reaction with Strong Bases*. Dordrecht: Springer Netherlands.

Staudinger, H., & Jules, M. (1919). Über neue organische Phosphorverbindungen III. Phosphinmethylenderivate und Phosphinimine. *Helvetica Chimica Acta, 2*(1), 635-646.

Stuart, M. C., & Boekema, E. J. (2007). Two distinct mechanisms of vesicle-to-micelle and micelle-to-vesicle transition are mediated by the packing parameter of phospholipid-detergent systems. *Biochimica et Biophysica Acta, 1768*(11), 2681-2689.

Sun, D., Kang, S., Liu, C., Lu, Q., Cui, L., & Hu, B. (2016). Effect of zeta potential and particle size on the stability of SiO_2 nanospheres as carrier for ultrasound imaging contrast agents. *International Journal of Electrochemical Science, 11*, 8520-8529.

Sutherland, W. (1905). A dynamical theory of diffusion for non-electrolytes and the molecular mass of albumin. *The London, Edinburgh, and Dublin Philosophical Magazine and Journal of Science, 9*(54), 781-785.

Szabo, P. (1989). Phosphorylated sugars. Part 25. Synthesis and behaviour in acidic media of 2-acetamido-2-deoxy-D-glucose 4- and 6-phosphates and of a 'Lipid A' analogue. *Journal of the Chemical Society, Perkin Transactions 1,* (5), 919-924.

Szoka, F. J., & Papahadjopoulos, D. (1980). Comparative properties and methods of preparation of lipid vesicles (liposomes). *Annual Review of Biophysics and Bioengineering, 9*(1), 467-508.

Tabandeh, M., Goh, E. W., Salman, A. A., Heidelberg, T., & Duali Hussen, R. S. (2018). Functionalized glycolipids for potential bioconjugation of vesicles. *Carbohydrate Research, 469*, 14-22.

Tadros, T. F. (2014). *An Introduction to Surfactants*. Germany: De Gruyter.

Takahashi, H., Hayakawa, T., Murate, M., Greimel, P., Nagatsuka, Y., Kobayashi, T., & Hirabayashi, Y. (2012). Phosphatidylglucoside: Its structure, thermal behavior, and domain formation in plasma membranes. *Chemistry and Physics of Lipids, 165*(2), 197-206.

Takeuchi, H., Ichikawa, T., Yoshio, M., Kato, T., & Ohno, H. (2016). Induction of bicontinuous cubic liquid-crystalline assemblies for polymerizable amphiphiles via tailor-made design of ionic liquids. *Chemical Communications, 52*(96), 13861-13864.

Talalay, P. (1999). The war against cancer: New hope. *Proceedings of the American Philosophical Society, 143*(1), 52-72.

Tamba, Y., Terashima, H., & Yamazaki, M. (2011). A membrane filtering method for the purification of giant unilamellar vesicles. *Chemistry and Physics of Lipids, 164*(5), 351-358.

Tan, S. Y., & Grimes, S. (2010). Paul Ehrlich (1854-1915): Man with the magic bullet. *Singapore Medical Journal, 51*(11), 842-843.

Tang, B., Xing, Y., Li, P., Zhang, N., Yu, F., & Yang, G. (2007). A rhodamine-based fluorescent probe containing a Se−N bond for detecting thiols and its application in living cells. *Journal of the American Chemical Society, 129*(38), 11666-11667.

Taniguchi, T., & Monde, K. (2012). Exciton chirality method in vibrational circular dichroism. *Journal of the American Chemical Society, 134*(8), 3695-3698.

Thar, J., Brehm, M., Seitsonen, A. P., & Kirchner, B. (2009). Unexpected hydrogen bond dynamics in imidazolium-based ionic liquids. *Journal of Physical Chemistry B, 113*(46), 15129-15132.

Tondre, C., & Caillet, C. (2001). Properties of the amphiphilic films in mixed cationic/anionic vesicles: A comprehensive view from a literature analysis. *Advances in Colloid and Interface Science, 93*(1), 115-134.

Torchilin, V. P. (2006). Multifunctional nanocarriers. *Advanced Drug Delivery Reviews, 58*(14), 1532-1555.

Traïkia, M., Warschawski, D. E., Recouvreur, M., Cartaud, J., & Devaux, P. F. (2000). Formation of unilamellar vesicles by repetitive freeze-thaw cycles: Characterization by electron microscopy and ^{31}P-nuclear magnetic resonance. *European Biophysics Journal, 29*(3), 184-195.

Trüeb, R. M. (2007). Shampoos: Ingredients, efficacy and adverse effects. *Journal der Deutschen Dermatologischen Gesellschaft, 5*(5), 356-365.

Tschierske, C. (2002). Amphotropic liquid crystals. *Current Opinion in Colloid & Interface Science, 7*(5), 355-370.

Tsuzuki, S., Tokuda, H., & Mikami, M. (2007). Theoretical analysis of the hydrogen bond of imidazolium C2-H with anions. *Physical Chemistry Chemical Physics, 9*(34), 4780-4784.

Uchegbu, I. F., & Vyas, S. P. (1998). Non-ionic surfactant based vesicles (niosomes) in drug delivery. *International Journal of Pharmaceutics, 172*(1), 33-70.

Unger, E. C., Winokur, T., MacDougall, P., Rosenblum, J., Clair, M., Gatenby, R., & Tilcock, C. (1989). Hepatic metastases: Liposomal Gd-DTPA-enhanced MR imaging. *Radiology, 171*(1), 81-85.

Uzawa, H., Ito, H., Izumi, M., Tokuhisa, H., Taguchi, K., & Minoura, N. (2005). Synthesis of polyanionic glycopolymers for the facile assembly of glycosyl arrays. *Tetrahedron, 61*(24), 5895-5905.

Varshosaz, J., Pardakhty, A., Hajhashemi, V.-i., & Najafabadi, A. R. (2003). Development and physical characterization of sorbitan monoester niosomes for insulin oral delivery. *Drug Delivery, 10*(4), 251-262.

Veeneman, G. H., van Leeuwen, S. H., & van Boom, J. H. (1990). Iodonium ion promoted reactions at the anomeric centre. II An efficient thioglycoside mediated approach toward the formation of 1,2-trans linked glycosides and glycosidic esters. *Tetrahedron Letters, 31*(9), 1331-1334.

Vill, V., & Hashim, R. (2002). Carbohydrate liquid crystals: Structure–property relationship of thermotropic and lyotropic glycolipids. *Current Opinion in Colloid & Interface Science, 7*(5), 395-409.

von Minden, H. M., Brandenburg, K., Seydel, U., Koch, M. H. J., Garamus, V., Willumeit, R., & Vill, V. (2000). Thermotropic and lyotropic properties of long chain alkyl glycopyranosides. Part II. Disaccharide headgroups. *Chemistry and Physics of Lipids, 106*(2), 157-179.

von Rybinski, W., & Hill, K. (1998). Alkyl polyglycosides—properties and applications of a new class of surfactants. *Angewandte Chemie International Edition, 37*(10), 1328-1345.

Wagner, A., & Vorauer-Uhl, K. (2011). Liposome technology for industrial purposes. *Journal of Drug Delivery, 2011*, Article# 591325.

Wang, Q., Chan, T. R., Hilgraf, R., Fokin, V. V., Sharpless, K. B., & Finn, M. G. (2003). Bioconjugation by copper(I)-catalyzed azide-alkyne [3 + 2] cycloaddition. *Journal of the American Chemical Society, 125*(11), 3192-3193.

Wasserscheid, P., Hal, R. v., & Bösmann, A. (2002). 1-n-Butyl-3-methylimidazolium ([bmim]) octylsulfate—an even 'greener' ionic liquid. *Green Chemistry, 4*(4), 400-404.

Waterman, K. C., Adami, R. C., Alsante, K. M., Antipas, A. S., Arenson, D. R., Carrier, R., . . . Wang, H. (2002). Hydrolysis in pharmaceutical formulations. *Pharmaceutical Development and Technology, 7*(2), 113-146.

Winnik, F. M. (1993). Photophysics of preassociated pyrenes in aqueous polymer solutions and in other organized media. *Chemical Reviews, 93*(2), 587-614.

Wong, S. P., Lim, W. H., Cheng, S. F., & Chuah, C. H. (2011). Physico-chemical properties of mixed anionic/ cationic surfactant solution: Mixtures of sodium laurate methyl ester α-sulphonate and tetradecyltrimethylammonium bromide. *Journal of Oil Palm Research, 23*(1), 968-973.

Worrell, B. T., Malik, J. A., & Fokin, V. V. (2013). Direct evidence of a dinuclear copper intermediate in Cu(I)-catalyzed azide-alkyne cycloadditions. *Science, 340*(6131), 457-460.

Xu, X.-W., Wang, X.-L., Wu, A.-M., Zheng, Z.-M., Yi, M.-G., & Xiao, R. (2009). Synthesis and molecular recognition of novel multiimidazole cyclophanes. *Journal of Heterocyclic Chemistry, 46*(6), 1137-1141.

Xu, X., Costa, A., & Burgess, D. J. (2012). Protein encapsulation in unilamellar liposomes: High encapsulation efficiency and a novel technique to assess lipid-protein interaction. *Pharmaceutical Research, 29*(7), 1919-1931.

Yaacob, I. I., & Bose, A. (1996). An investigation of microstructures in cationic/anionic surfactant suspensions by cryogenic transmission electron microscopy. *Journal of Colloid and Interface Science, 178*(2), 638-647.

Yakuphanoglu, F., Okutan, M., Köysal, O., Özder, S., Ocakoğlu, K., & İçli, S. (2005). Dielectric studies of tetraethylene glycol−bis(3-methylimidazolium) dichloride (TEGDC) exhibiting large negative dielectric anisotropy. *The Journal of Physical Chemistry B, 109*(51), 24338-24342.

Yamaoka, T., Tabata, Y., & Ikada, Y. (1994). Distribution and tissue uptake of poly(ethylene glycol) with different molecular weights after intravenous administration to mice. *Journal of Pharmaceutical Sciences, 83*(4), 601-606.

Yan, J. M., Jiang, Z. L., Zhang, L., & Xie, R. G. (1998). A new synthesis of 1-(ω-haloalkyl)-imidazoles. *Chinese Chemical Letters, 9*(6), 519-520.

Yang, J., Bahreman, A., Daudey, G., Bussmann, J., Olsthoorn, R. C. L., & Kros, A. (2016). Drug delivery via cell membrane fusion using lipopeptide modified liposomes. *ACS Central Science, 2*(9), 621-630.

Yang, J., Liu, H., & Zhang, X. (2014). Design, preparation and application of nucleic acid delivery carriers. *Biotechnology Advances, 32*(4), 804-817.

Yoneda, Y., Kawada, T., Rosenau, T., & Kosma, P. (2005). Synthesis of methyl 4'-O-methyl-$^{13}C_{12}$-β-D-cellobioside from $^{13}C_6$-d-glucose. Part 1: Reaction optimization and synthesis. *Carbohydrate Research, 340*(15), 2428-2435.

Zalipsky, S. (1995). Chemistry of polyethylene glycol conjugates with biologically active molecules. *Advanced Drug Delivery Reviews, 16*(2), 157-182.

Zana, R. (2005). Surfactant science series 114 (Novel surfactants: Preparation, application and biodegradability). In K. Holmberg (Ed.), *Surfactant Science Series 114* (2nd ed.). New York, Basel: Marcel Dekker.

Zemplén, G., & Kunz, A. (1924). Studien über Amygdalin, IV: Synthese des natürlichen l-Amygdalins. *Berichte der deutschen chemischen Gesellschaft (A and B Series), 57*(8), 1357-1359.

LIST OF PUBLICATIONS AND PAPERS PRESENTED

PUBLICATIONS:

1. Salman, A. A., **Goh, E. W.**, Heidelberg, T., Hussen, R. S. D., & Ali, H. M. (2016). Bis-(alkylimidazolium)-glycosides- Promising materials for easy vesicle preparation. *Journal of Molecular Liquids, 222*, 609-613.

PAPERS PRESENTED:

1. **Goh Ean Wai** & Thorsten Heidelberg, Bis-(alkylimidazolium)-glycosides, promising materials for easy vesicles preparation, *International Symposium on Pure & Applied Chemistry 2017 (ISPAC 2017)*, (8^{th} – 10^{th} June 2017), Hotel Continental Saigon, Ho Chi Minh City, Vietnam.

2. **Goh Ean Wai**, Mojtaba Tabandeh & Thorsten Heidelberg, Synthesis of Functionalized Glycolipids for Vesicular Delivery System, *UM111-Chemistry Symposium*, (3^{rd} March, 2016), University of Malaya, Kuala Lumpur, Malaysia.